

Properties of Enzymes Involved in Tetrachloroethene Respiration - From Physiology to Protein Function

THÈSE N° 7762 (2017)

PRÉSENTÉE LE 30 JUIN 2017

À LA FACULTÉ DE L'ENVIRONNEMENT NATUREL, ARCHITECTURAL ET CONSTRUIT
LABORATOIRE DE BIOTECHNOLOGIE ENVIRONNEMENTALE
PROGRAMME DOCTORAL EN GÉNIE CIVIL ET ENVIRONNEMENT

ÉCOLE POLYTECHNIQUE FÉDÉRALE DE LAUSANNE

POUR L'OBTENTION DU GRADE DE DOCTEUR ÈS SCIENCES

PAR

Géraldine Florence BUTTET

acceptée sur proposition du jury:

Prof. U. von Gunten, président du jury
Prof. C. Holliger, Dr J. Maillard, directeurs de thèse
Prof. G. Diekert, rapporteuse
Dr H. P. Kohler, rapporteur
Prof. T. I. Battin, rapporteur



ÉCOLE POLYTECHNIQUE
FÉDÉRALE DE LAUSANNE

Suisse
2017

à papa, parti trop tôt. Pour toujours dans mon cœur.

Overview

Remerciements	iii
Résumé	v
Summary	vii
List of abbreviations	ix
<u>CHAPTER 1</u>	
General Introduction	1
<u>CHAPTER 2</u>	
Characterization of an unusual <i>Sulfurospirillum</i> reductive dehalogenase dechlorinating tetrachloroethene to trichloroethene	27
<u>CHAPTER 3</u>	
Dechlorination kinetics governs the competition between two new strains of the genus <i>Sulfurospirillum</i>	57
<u>CHAPTER 4</u>	
Biochemical characterization of the flavin domain of PceC	85
<u>CHAPTER 5</u>	
Concluding remarks and outlook	117
Table of Content	129
List of Figures	133
List of Tables	135
Appendices	137
Curriculum Vitae	155

Remerciements

Arrivée au terme de ces années de recherches, je réalise que la thèse est loin d'être un travail en solitaire. J'éprouve une sincère gratitude envers les nombreuses personnes qui m'ont accompagnée et soutenue tout au long de ce parcours et je tiens à les remercier.

En premier lieu, je tiens à exprimer mes plus vifs remerciements à Christof Holliger, mon directeur de thèse et Julien Maillard, mon co-directeur de thèse pour la confiance qu'ils m'ont accordée en acceptant d'encadrer ce travail doctoral, pour leurs conseils et pour toutes les heures qu'ils ont consacrées à diriger cette recherche. Julien fut pour moi un superviseur attentif et disponible malgré ses nombreuses charges. Sa compétence et sa rigueur scientifique m'ont beaucoup appris.

Je tiens à exprimer mes remerciements à l'ensemble des membres de mon jury qui ont examiné ce travail, Prof. Tom Ian Battin, Prof. Gabriele Diekert et Prof. Hans Peter Kohler, ainsi que le président du jury, Prof. Urs von Gunten.

Un grand merci à Alice Badin, Cindy Kunze, Sebastian Keller, Torsten Schubert, Tobias Goris, Romain Hamelin, Laure Menin, Alex Murray et Marcel Schreier pour leur précieuse collaboration sans qui mon travail n'aurait pas pu être complet.

Je remercie toutes les personnes formidables que j'ai eu la chance de rencontrer grâce au Laboratoire de Biotechnologie Environnementale et qui d'une manière ou d'une autre ont participé au bon déroulement de ma recherche : Marc Deront, Emmanuelle Rohrbach, Jean-Pierre Kradolfer, Stéphane Marquis, Pierre Rossi, Eduardo Gomes, Sonia Tarnawski, Samuel Lochmatter, Jonas Margot, Noam Shani, David Weissbrodt, Magalie Bassan, Aline Adler, Arnaud Gelb, Mathilde Willemin, Laure Prat et sans oublier les apprentis et stagiaires de passage, avec qui j'ai partagé pleins de bon moments : Guy de Bourbon Parme, Julie Luche, Morgane Baumgartner, Emmy Oppliger, Marie Vingerhoets, Vincent Jeannet, Naomi Dumas, Ilham Sbaiti, Corantin Grob et Marta Cerutti. Je tiens aussi à remercier chaleureusement Mme Nevenka Adler pour son implication et ses précieux conseils tout au long de mon passage au LBE. Un grand merci à Filomena Jacquier pour son aide administrative et son amitié. Merci à Mathilde, Gabrielle et Claudia pour la relecture de cette thèse. Je tiens également à remercier sincèrement Christof, Filomena et Morgane pour leur soutien lors d'un moment particulièrement difficile dans ma vie. J'ai beaucoup été touchée par votre présence, votre disponibilité et votre écoute.

Une petite mention spéciale pour Aamani Rupakula Boyanapalli qui m'a accueillie et accompagnée au LBE comme une sœur, pour Gabrielle Hack qui m'a fait découvrir ce qu'était un véritable coup de foudre, pour Clément Descarpentries, une merveilleuse rencontre, et pour Mélissa Burion, pour sa précieuse collaboration, sa grande motivation, son amitié et surtout sa folie ! Merci également à Luma Delaplace qui m'a ouvert de nouveaux horizons et m'a guidé jusqu'au doctorat.

J'adresse tout mon affection à ma famille : Papa, Maman, Valérie et Estella Arnold, Claudia, Saïan et Ellijah Kuratli. Merci d'avoir fait de moi ce que je suis aujourd'hui. A ma précieuse amie qui désespère de me voir un jour quitter les études : Ivana Velijkovic, je te remercie

pour les kilomètres parcourus ensemble et nos moments partagés pleins de fous rires. Un immense MERCI à tous mes fidèles compagnons qui me remplissent chaque jour de bonheur !

And finally but not least, a special thanks to Gina Fiore for your love, your patience, your precious advice and your unconditional support.

Résumé

Le tetrachloroéthène (PCE) est un composé dangereux pour la nature et la santé humaine, à cause de sa toxicité et de son potentiel carcinogène. Due à l'activité industrielle, de larges quantités de ce composé se sont déversées dans l'environnement durant ces dernières décennies, ainsi le PCE représente un des polluants majeurs des eaux souterraines. La respiration des composés organohalogénés (anglais : organohalide respiration, OHR) est un processus de respiration bactérienne anaérobie par lequel des composés halogénés, tels que les chloroéthènes, sont utilisés comme accepteur terminal d'électrons. Ce processus requière la présence d'une chaîne de transport d'électrons située dans la membrane cytoplasmique et permet l'établissement d'une force motrice à travers la membrane. La présence et l'association de protéines redox ainsi que des éléments non-protéiques chargés de transmettre les électrons sont essentiels pour cette chaîne de transport d'électrons. Au sein des bactéries de genre *Desulfitobacterium* et *Dehalobacter*, représentants d'un des groupes majeurs des bactéries OHR, le groupe de gènes *pceABCT* a été identifié comme étant responsable pour la respiration du PCE. Ces bactéries sont considérées comme un système modèle pour étudier la respiration de type OHR. Alors que la fonction de la protéine PceA, l'enzyme catalysant la réaction de réduction du PCE, et celle de la protéine PceT, un chaperon moléculaire dédié au bon repliement de l'enzyme PceA, ont bien été établies, la protéine PceB joue très probablement le rôle d'ancrage de la protéine PceA à la membrane. Le gène restant, *pceC*, est susceptible de coder pour une flavoprotéine liée à la membrane et présentant des motifs conservés à cystéines. Bien que cette protéine a longtemps été considérée comme pouvant jouer le rôle d'un régulateur de transcription, elle présente toutes les caractéristiques pouvant potentiellement remplir le rôle dans le transfert d'électrons entre les ménaquinones et l'enzyme PceA.

Au Laboratoire de Biotechnologie Environnementale (LBE), un consortium bactérien, nommé SL2-PCEb, dérivé lui-même d'un enrichissement provenant de boues activées d'un réacteur déchlorant du PCE, constitue un modèle de consortium bactérien pour la respiration de type OHR. Le consortium SL2-PCEb a été préalablement caractérisé pour sa particularité de déchlorer par étapes le PCE jusqu'au *cis*-dichloroéthène (*cis*-DCE) via une accumulation importante de trichloroéthène (TCE). A partir de ce consortium, deux sous-cultures ont été obtenues (SL2-PCEc et SL2-TCE), chacune d'elles possédant une population bactérienne

distincte du genre *Sulfurospirillum* (souches appelées SL2-1 et SL2-2, respectivement). Ces deux sous-cultures ont montré un potentiel de déchloration différent, la souche SL2-1 est uniquement capable de transformer le PCE en TCE comme produit finale, alors que la souche SL2-2 a gardé le potentiel du consortium parental, c'est-à-dire qu'elle est toujours capable de dégrader le PCE en *cis*-DCE, mais sans accumulation de TCE. L'enzyme-clé dans le consortium SL2-PCEc, connue sous le nom PceA_{TCE}, possède 92% d'identité au niveau de sa séquence d'acides aminés à l'enzyme PceA bien caractérisée issue de *S. multivorans*. Les caractéristiques uniques de l'enzyme PceA_{TCE} ont été étudiées en détail dans le **CHAPITRE 2**. L'enzyme PceA_{TCE} de la souche SL2-1 a été purifiée par chromatographie. Des quantités relativement faibles de protéine purifiée ont été récupérées (0.25 et 1.3 mg). Chacune d'elles montrant un facteur de purification de 127 à 82 fois. L'activité des déshalogénases réductrices purifiées a été mesurée à 2'425 et 1'144 nkat/mg en présence de PCE. Cependant, seulement 8 et 11 % de rendement ont été calculés en comparaison avec les extraits bruts utilisés pour la purification. En outre, à partir d'une préparation enzymatique, le cofacteur de type corrinnoïde a été extrait de la protéine PceA_{TCE} et identifié comme étant une norpseudovitamine B₁₂, identique à celui se trouvant dans l'enzyme PceA de *S. multivorans*. Au niveau physiologique, la croissance de la souche SL2-1 en présence de PCE n'a pas été altérée par l'ajout de 5,6-diméthylbenzimidazole dans la culture, contrairement à ce qui a été observé chez *S. multivorans*. De plus, un modèle du site actif de l'enzyme PceA_{TCE} a été proposé sur la base de la structure cristalline de la protéine PceA de *S. multivorans* qui a été dernièrement caractérisée. Ce modèle a permis de mettre en évidence huit acides aminés uniques à PceA_{TCE}. Ces derniers sont différents mais conservés chez les autres enzymes PceA de *Sulfurospirillum* spp. capables de déchlorer du PCE au *cis*-DCE. Ces différences pourraient ainsi expliquer la capacité restreinte de PceA_{TCE} à dégrader le PCE. Dès lors, ce travail démontre l'importance de continuer à étudier au niveau biochimique les nouvelles déshalogénases réductrices. Afin de comprendre la longue coexistence des deux sous-cultures, SL2-PCEc et SL2-TCE, au sein du consortium parental SL2-PCEb, les caractéristiques particulières liées à chacun des consortia ont été étudiées au niveau génomique et physiologique (**CHAPITRE 3**). Ce chapitre présente une ébauche des génomes obtenus à partir de chacune des souches SL2, qui ont révélé une très grande similitude de séquence. Il a été découvert que seules les séquences de leur gène *pceA* respectif diffèrent de manière significative. Dès lors et suite à la comparaison avec les génomes de

Sulfurospirillum spp., une nouvelle espèce de *Sulfurospirillum* a été proposé pour les souches SL2-1 et SL2-2 : '*Candidatus Sulfurospirillum diekertiae*'. Les paramètres cinétiques de déchloration du PCE par chaque souche ont été évalués par une série de cultures effectuées à différentes concentrations de PCE. Alors que les deux souches possèdent le même taux de croissance maximale ($\sim 0.1 \text{ h}^{-1}$), leur constante d'affinité apparente pour le PCE est significativement différente, avec une valeur autour de $6 \mu\text{M}$ pour la souche SL2-1 et $35 \mu\text{M}$ pour la souche SL2-2. Ces observations ont été validées par la suite par des expériences de compétition où les deux souches ont été mélangées à population égale et cultivées à 6 et $30 \mu\text{M}$ de PCE (concentration en phase aqueuse). Les paramètres cinétiques de ses souches ont permis d'expliquer la coexistence de longue durée des deux souches dans le consortium parental, puisque celui-ci a été cultivé en routine à $20 \mu\text{M}$ de PCE. Cette étude suggère que la compétition, lorsqu'un substrat est limité, est susceptible d'être l'élément qui pousse à la diversification des souches bactériennes impliquées dans la respiration de type OHR.

Les éléments de la chaîne de transfert d'électrons spécifique à la respiration de type OHR sont encore peu connus à ce jour, à l'exception de l'enzyme-clé, la déshalogénase réductrice. Dès lors, la question concernant le rôle de la protéine PceC, issue du groupe de gènes *pceABCT* a fait l'objet de l'étude présentée au **CHAPITRE 4**. En effet, PceC a été détecté dans le protéome membranaire de *Desulfitobacterium hafniense* TCE1 et de *Dehalobacter restrictus*. L'interprétation des résultats protéomiques a montré qu'elle était autant présente que la protéine PceB, et qu'elle contenait un cofacteur FMN lié de manière covalente. Pour caractériser cette protéine, le domaine de PceC qui a été prédit comme liant le FMN (anglais : PceC FMN-binding domain, PceC-FBD) a été produit de manière hétérologue chez *E. coli* sous forme de corps d'inclusion. Après une dénaturation à base d'urée, une stratégie a été développée pour reconstituer la protéine PceC-FBD sous une forme soluble en y insérant le FMN à l'aide de la protéine Ftp1, une flavine transférase de *D. hafniense* qui a également été produite chez *E. coli*. La thréonine prédite pour la liaison du FMN (PceC-Thr₁₆₈) a été clairement identifiée au moyen d'expériences de mutagenèse dirigée et par des analyses de spectrométrie de masse. Ces résultats offrent de nouvelles perspectives dans l'étude du rôle de la protéine PceC dans le métabolisme de respiratoire de type organohalide.

L'objectif général de cette thèse a été d'apporter de nouvelles données aux niveaux physiologique et biochimique des bactéries utilisant le tétrachloroéthène comme accepteur terminal d'électrons. Ainsi sont présentées la caractérisation biochimique d'une nouvelle déshalogénase réductrice provenant d'un consortium bactérien, la détermination des paramètres cinétiques de déchloration des souches présentes dans ce consortium, et également la caractérisation du domaine FMN de la protéine PceC, une flavoprotéine liée à la membrane potentiellement impliquée dans le transfert d'électrons vers la protéine PceA.

Mots-clés: respiration des composés organohalogénés, tétrachloroéthène, *Sulfurospirillum*, consortium bactérien, déshalogénase réductrice, génome, paramètres cinétiques, *Desulfitobacterium*, *Dehalobacter*, enzyme redox, flavine, reconstitution de protéine

Summary

Tetrachloroethene (PCE) pollution threatens nature and human health due to its toxic and carcinogenic potential. Due to industrial activities, large amounts of PCE were discharged into the environment over the last decades and represent one of major groundwater pollutants. Organohalide respiration (OHR) is a bacterial anaerobic respiration in which the halogenated compounds, such as chloroethenes, are used as terminal electron acceptors. This process requires the presence of an electron transport chain located in the cytoplasmic membrane which allows proton translocation and establishes a proton-motive force across the membrane. Redox proteins and other non-protein electron shuttles are usually combined in the membrane to accomplish that task. In members of the genera *Desulfitobacterium* and *Dehalobacter*, which represent a paradigmatic group of organohalide-respiring bacteria (OHRB), the *pceABCT* gene cluster has been identified as responsible for PCE respiration, and can be considered as a model system for studying OHR. While the function of PceA, the key enzyme of this process, and PceT, the dedicated chaperon, are well established, it is very likely that PceB plays the role of membrane anchor for PceA. The remaining gene, *pceC*, codes for a predicted membrane-bound flavoprotein harboring conserved cysteine motifs in the transmembrane domain. Despite the fact that it has been considered as a putative transcriptional regulator, PceC presents all the features that could potentially fulfill the role of electron shuttle between reduced menaquinones and PceA.

In the Laboratory for Environmental Biotechnology, a bacterial consortium (SL2-PCEb) and derived subcultures thereof has been used as a model OHRB community. SL2-PCEb has been previously characterized for its stepwise dechlorination of PCE to *cis*-DCE via a significant accumulation of TCE. Two derived subcultures, named SL2-PCEc and SL2-TCE, harbor a distinct population of *Sulfurospirillum* sp. (SL2-1 and SL2-2, respectively). Both subcultures showed a different pattern of dechlorination, as strain SL2-1 was only able to dechlorinate PCE to trichloroethene (TCE), while strain SL2-2 kept the potential of the parental consortium, namely PCE to *cis*-DCE, however, without TCE accumulation. The key enzyme in the consortium SL2-PCEc is known as PceA_{TCE} and displays 92% amino acid sequence identity with the well-characterized PceA enzyme from *S. multivorans*. The unique features of the PceA_{TCE} enzyme were further explored in **CHAPTER 2**. Briefly the PceA_{TCE} enzyme of strain SL2-

1 was purified by chromatography in two successive attempts. Relatively small amounts of purified proteins were recovered (0.25 and 1.3 mg), each of them displaying 127- and 82-fold purification factor, 2'425 and 1'144 nkat/mg of reductive dehalogenase activity with PCE, but only 8 and 11% of yield in comparison with the crude extracts, respectively. From one enzyme preparation, the corrinoid cofactor of PceA_{TCE} was extracted and identified as norpseudovitamin B₁₂, as in PceA from *S. multivorans*. On a physiological level, re-routing the de novo corrinoid biosynthesis of the consortium SL2-PCEc by adding 5,6-dimethylbenzimidazole did not impact the growth rate of the culture on PCE, in contrast to what has been observed with *S. multivorans*. Based on the recent crystal structure of *S. multivorans* PceA, a structure model of the active site of the PceA_{TCE} enzyme was proposed which highlights eight unique residues in PceA_{TCE} that are different from but consistently conserved in the other *Sulfurospirillum* spp. enzymes catalyzing the dechlorination of PCE to *cis*-DCE. These differences may result in altered structural properties of PceA_{TCE} which could be the basis for the differences in the restricted substrate range of this enzyme. This work demonstrated the importance of pursuing biochemical studies on new reductive dehalogenases. The features of these consortia were investigated here at the genomic and physiological levels in order to understand their long-term coexistence in the parental consortium (**CHAPTER 3**). On one side, this chapter presents the draft genomes that were obtained for each SL2 strain, revealing the very high similarity that they display with each other at the sequence level. Only the sequence of their respective *pceA* gene differs significantly. Based on genome comparison with other *Sulfurospirillum* spp., a new species name, '*Candidatus Sulfurospirillum diekertiae*', was proposed for strains SL2-1 and SL2-2. An extended series of batch cultures of the two strains amended with a large range of PCE concentrations allowed to estimate their respective dechlorination kinetic parameters. While both strains share a similar maximal growth rate around 0.1 h⁻¹, the apparent affinity constant for PCE is significantly different, with values around 6 μM for strain SL2-1 and 35 μM for strain SL2-2. These findings were validated in competition experiments where both populations were mixed at equal population size and cultivate at 6 and 30 μM PCE (aqueous concentration). The kinetic parameters of these strains allow to explain their long-term coexistence in the parental consortium as the latter was routinely cultivated at 20 μM PCE. From an ecological point of view, the results obtained here suggest that competition for a limiting substrate is a possible driving force for strain diversity in organohalide respiration.

Since only little information is available on the composition of the electron transport chain in organohalide respiration (OHR), that feeds electrons to the reductive dehalogenase, the terminal enzyme in the process. The question of resolving the physiological role of PceC, a protein encoded by the *pceABCT* gene cluster was addressed in **CHAPTER 4**. Indeed, it was shown that PceC is present in the membrane proteomes of *Desulfitobacterium hafniense* strain TCE1 and *Dehalobacter restrictus* and proteomic data interpretation suggested that it is as abundant as PceB, and harbors a covalent FMN cofactor. The predicted FMN-binding domain of PceC (PceC-FBD) was heterologously produced in *E. coli* where it formed inclusion bodies. After denaturation with urea, a strategy was developed to reconstitute PceC-FBD in a soluble form by inserting FMN with the help of Ftp1, a flavin-transferase of *D. hafniense* also produced in *E. coli*. The predicted threonine residue in the FMN-binding motif (PceC-Thr₁₆₈) was unambiguously assigned by site-specific mutagenesis and detailed mass spectrometry analysis. These results offer a new way to address the question of the involvement of PceC in the respiratory chain of OHR metabolism.

The overall goal of this thesis was to provide new insights into the physiology and biochemistry of tetrachloroethene-respiring bacteria, to characterize at the biochemical level a new reductive dehalogenase identified from a bacterial consortium, and to assess the kinetic parameters of strains present in this consortium and competing for tetrachloroethene. Finally, the characterization of PceC, a predicted membrane-bound flavoprotein was undertaken.

Keywords: organohalide respiration, tetrachloroethene, *Sulfurospirillum*, bacterial consortium, reductive dehalogenase, genome, kinetic parameters, *Desulfitobacterium*, *Dehalobacter*, redox enzyme, flavin, protein reconstitution.

List of abbreviations

A	Asymptote of the curve
ANI	Average nucleotide identity
BSA	bovine serum albumin
CEs	chlorinated ethenes, chloroethenes
<i>cis</i> -DCE	<i>cis</i> -dichloroethene
CISM	Complex Iron-Sulfur Molybdoenzymes
Cl	chloride
[Cl] _t	chloride concentration in the aqueous phase at time t (in h)
[Cl] ₀	initial chloride concentration
Cl-OHPA	3-chloro-4-hydroxyphenyl acetate
DCEs	dichloroethenes
<i>Dha</i>	<i>Desulfitobacterium hafniense</i>
DMB	5,6-dimethylbenzimidazole
DMSO	dimethyl-sulfoxide
DNA	deoxyribonucleic acid
DNAPL	dense non aqueous phase liquid
dNTPs	nucleoside triphosphates containing deoxyribose
<i>Dre</i>	<i>Dehalobacter restrictus</i>
<i>e</i>	Euler constant
FeS	iron-sulfur cluster
FAD	flavin adenine dinucleotide
FMN	flavin mononucleotide
FPLC	fast protein liquid chromatography
Glu-C	serine protease
β-HCH	β-hexachlorocyclohexane
HPLC	high performance liquid chromatography
IF	insoluble fraction
IPTG	isopropyl-β-D-thiogalactopyranoside
JGI	Joint Genome Institute
<i>K_{HW}</i>	hexadecane-water partition coefficient
<i>K_i</i>	inhibition constant
<i>K_s</i>	affinity constant
λ	lag phase (in h)
LB	Luria-Bertani medium
MBH	membrane-bound hydrogenase
MV	methyl viologen
MS	Mass spectrometry
MQ	menaquinone
μ _{Cl}	dechlorination-based growth rate
μ _{maxCl}	dechlorination-based maximal growth rate
OHR	organohalide respiration (formerly dehalorespiration, halorespiration)
OHRB	organohalide-respiring bacteria
ORFs	open reading frames
PCE	tetrachloroethene, perchloroethene
PCE _{aq}	tetrachloroethene in aqueous phase
PCE _{HD}	tetrachloroethene dissolved in hexadecane
PceC-FBD	FMN-binding domain of PceC
PCF	Protein Core Facility
PCR	polymerase chain reaction
PDB	Protein Data Bank

PVDF	polyvinylidene difluoride membrane
q _{Cl}	dechlorination rate
<i>rdh</i>	reductive dehalogenase gene cluster
RdhA	reductive dehalogenase enzyme
RDase	reductive dehalogenase enzyme
RNA	ribonucleic acid
rRNA	ribosomal ribonucleic acid
RT	room temperature
SDS-PAGE	SDS polyacrylamide gel electrophoresis
SF	soluble fraction
sp., spp.	species (singular, plural)
SSE	Sum of Squares due to Error
Tat	Twin-arginine translocation
TCE	trichloroethene
2,4,6-TBP	2,4,6-tribromophenol
2,4,6-TCP	2,4,6-trichlorophenol
TMAO	trimethylamine- <i>N</i> -oxide
TMH	transmembrane α -helix
qPCR	quantitative PCR
VC	vinyl chloride

Chapter 1

General introduction

1. General introduction

1.1. Chlorinated organic contamination

1.1.1. Natural chloroethenes sources

Today, over five thousands natural halogenated compounds have been identified in the earth biosphere (35). Diverse natural enzymatic and abiotic reactions account for the halogenation and dehalogenation of natural organohalogen metabolites (15, 106, 162). Organohalides are a class of organic molecules that contain one or more covalently bound halogen atoms. Within this class of compounds, chlorinated and brominated organohalides are the most abundant that are naturally produced (49). Chlorinated ethenes (CEs), the halogenated compounds of interest for this thesis, are organohalides with one or more chlorine atoms. Based on the number of chlorine atoms present, the compounds are named tetrachloroethene (PCE, perchloroethene, C_2Cl_4), trichloroethene (TCE, C_2HCl_3), dichloroethene (DCE, $C_2H_2Cl_2$) and vinyl chloride (VC, C_2H_3Cl). PCE and TCE are known to be naturally present in the environment as a result of abiotic reactions like volcanic activities (46, 60) or biological production by marine algae (1, 22).

1.1.2. Anthropogenic chloroethenes sources

Over the last 80 years, the natural cycle of chlorine in the environment has been disrupted by extensive anthropogenic production of CEs. For example, PCE was first synthesized in 1821 by Michael Faraday, however, the commercial use in Europe started in the 1920's. Since then, the production of organohalides has dramatically increased (142). CEs are commonly used for dry cleaning, metal degreasing, and for chemical synthetic processes by numerous industries (34). The mismanagement of the use and elimination of CEs, primarily PCE and TCE, is the direct cause of their spreading and contamination in the environment. These organic solvents can infiltrate from the surface to the groundwater and even down to the bedrock (Fig. 1.1). They belong to the most frequently found organic contaminants posing serious environmental concerns (4, 20, 34). Not only are CEs toxic and potentially carcinogenic, but they remain as liquid solvents in the aquifer thus forming so-called dense non-aqueous phase liquids (DNAPL) that slowly dissolve into the groundwater.

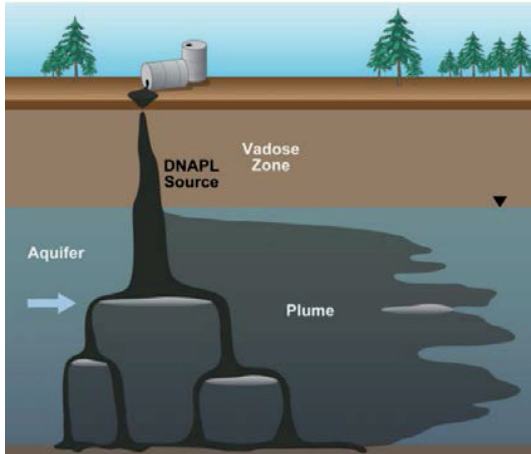


Figure 1.1. Formation of dense non-aqueous phase liquid (DNAPL) and contamination plume following a spillage of chlorinated solvents (taken from (97)).

The development of alternative technologies has reduced the demand for CEs in dry-cleaning (33, 97) and the yearly production of PCE and TCE has dramatically decreased in recent years (Fig. 1.2) (28, 29). Large efforts have also been made in the remediation of CEs-contaminated sites, in particular with the enforcement of environmental protection laws and with the stimulation of *in situ* microbial activity (141).

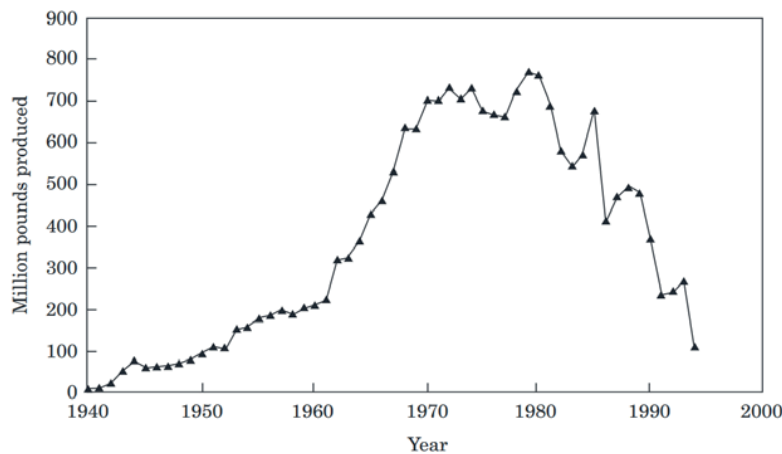


Figure 1.2. Yearly production of PCE in the U.S.A. (taken from (28)).

1.2. Biodegradation of chloroethenes

Biodegradation is known as the chemical breakdown of compounds by organisms and their associated metabolic processes (12). Initially, highly chlorinated CEs were considered as resistant to microbial biodegradation due to their persistence in aerobic environments and their presence in the environment was considered to be entirely anthropogenic (12).

Nowadays, it is known that practically all CEs are degradable when certain chemical and redox conditions are met. CEs biodegradation can also occur in contaminated sites but the success depends on many factors which are usually difficult to understand, thus leading to too slow or incomplete remediation (18). It is known that lower chlorinated compounds can be biologically transformed under aerobic conditions via co-metabolic processes or as sources of carbon and energy (13, 50, 89). DCEs and VC can also be chemically oxidized in the presence of strong oxidizers, such as Fe(III)-oxides (14, 117). Anaerobic biodegradation of highly chlorinated ethenes occurs through reductive dechlorination. CEs are known to be dechlorinated by methanogens and homoacetogens via co-metabolic activities, however, the majority of reductive dechlorination reactions is likely to be catalyzed by bacteria that utilize chloroethenes as a terminal electron acceptor in a process called organohalide respiration (30, 53, 98, 156).

1.3. *Organohalide respiration (OHR)*

In the early 1990's, bacteria capable of using halogenated compounds and conserving energy during reductive dehalogenation have been discovered. This phylogenetically diverse bacterial group is able to utilize organohalides as terminal electron acceptors in a respiration process, referred to as organohalide respiration (OHR). In this process, chlorinated aromatics (e.g., chlorinated phenols, benzoates, benzenes, phenoxyacetates) and aliphatics (e.g., chlorinated alkanes and alkenes) are the two major groups of chlorinated compounds commonly used as terminal electron acceptor (30). The complete anaerobic degradation of CEs is a process during which chlorines are sequentially replaced by hydrogen atoms until completion and the production of the environmentally harmless ethene (Fig. 1.3). PCE and TCE, with their four and three chlorine atoms, respectively, are stronger oxidants than many naturally occurring electron accepting species found in anoxic groundwater systems (158). Indeed, the standard redox potential for the couple R-Cl/R-H lies between approximately +250 and +600 mV (32). Therefore these compounds are thermodynamically favorable electron acceptors in the absence of detectable dissolved oxygen. Due to their high density and their low solubility in water, these two compounds represent the most commonly found groundwater contaminants (12). On the other side, the less chlorinated ethenes (DCEs and VC) are degradable under anaerobic and aerobic conditions (38, 93).

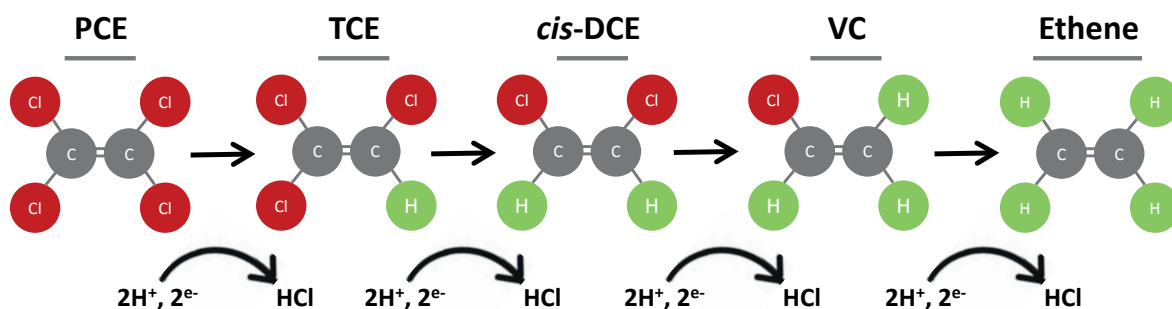


Figure 1.3. Sequential reductive dechlorination of PCE to ethene.

Two electrons and two protons are necessary for the elimination of each chlorine. PCE: tetrachloroethene; TCE: trichloroethene; *cis*-DCE: *cis*-1,2-dichloroethene; VC: vinyl chloride.

The use of the electrons in the respiratory chain of organohalide-respiring bacteria (OHRB) can widely vary depending on the bacterial species (76, 77). For example, *Dehalobacter restrictus* PER-K23 (52) and *Dehalococcoides mccartyi* (95), both exclusively utilize H_2 as electron donor, whereas a broad spectrum of electron donors are used by *Sulfurospirillum* spp. (44) and *Desulfitobacterium* spp. (40).

Over the last two decades, there has been a growing interest in OHR for applications in *in situ* bioremediation of contaminated sites (5, 64, 126, 150, 160), in biotechnological applications (6, 25, 51, 57, 73, 94, 141), as well as in building a fundamental understanding of this particular anaerobic respiration process at the level of molecular biology (69, 71, 115, 137), enzymology (23, 27, 88, 105, 121, 133) and energy conservation processes (30, 78, 134).

1.4. Overview of known organohalide-respiring bacteria: phylogenetic affiliation and chlorinated substrates specificity

Organohalide-respiring bacteria (OHRB) are spread among several phyla comprising *Beta*-, *Delta*- and *Epsilonproteobacteria*, as well as *Firmicutes* and *Chloroflexi* (Fig. 1.4). The first described anaerobic bacterium, which was capable to couple reductive dehalogenation of an organohalide (3-chlorobenzoate) to energy conservation, was *Desulfomonile tiedjei* strain DCB-1 (26). Later, CEs were also shown to be used as terminal electron acceptors by OHRB (54, 67, 95). Nowadays, more than seventy bacterial strains capable of OHR have been isolated from different polluted environments (for a review (3)). The isolates can be divided

into facultative and obligate OHRB based on whether OHR is their only energy-conserving metabolism or whether they have alternative metabolic pathways (91).

Facultative OHRB are also characterized by a more versatile metabolism regarding the electron donor they can oxidize (formate, lactate, pyruvate, acetate, butyrate, fumarate, and more). As electron acceptors, besides organohalides, they can use nitrate, sulfite, thiosulfate, iron, and many more (139). Isolates that belong to the genera *Anaeromyxobacter* (130), *Comamonas* (17), *Desulfitobacterium* (40), *Desulfoluna* (2), *Desulfomonile* (26), *Desulfovibrio* (11, 143), *Desulfuromonas* (67), (146), *Geobacter* (145), *Shewanella* (164), *Sulfurospirillum* (44), and *Trichlorobacter* (24) are such versatile microorganisms.

Another category of OHRB is composed of species which strictly require organohalides as terminal electron acceptor to support their growth. Among them, *Dehalobacter* spp. (86), *Dehalococcoides* spp. (165) and *Dehalogenimonas* spp. (101) are the most important ones.

Dehalobacter spp. from the *Firmicutes* has first been shown to reductively dechlorinate PCE and TCE to *cis*-DCE (86). Cultivation and environmental studies reported that members of this genus are able to grow on several other halogenated compounds such as chlorinated ethanes (48, 144), 2,4,6-trichlorophenol (2,4,6-TCP) (159), 2,4,6-tribromophenol (2,4,6-TBP) (75), chloroform (47), chlorinated benzenes (107, 108), β -hexachlorocyclohexane (β -HCH) (155) and 4,5,6,7-tetrachlorophthalide (144, 163). The *Dehalococcoidia* class from the *Chloroflexi* contains the highest number of obligate OHRB isolates. To date, *Dehalococcoides mccartyi* strain 195 is the only bacterium known that can completely dechlorinate PCE to ethene, although the last step does not conserve energy (95). The range of CEs dechlorination by *Dehalococcoides* spp. is varying considerably depending on the isolates (165). More recently, *Dehalogenimonas lykanthroporepellens* (102) and *Dehalogenimonas alkenigignens* IP3-3T (90), also from the *Chloroflexi*, have been shown to reductively dehalogenate chlorinated alkanes such as 1,2-dichloroethane, 1,2-dichloropropane, and 1,1,2-trichloroethane. *Dehalobium chlorocoercia* DF-1, also related to *Dehalococcoides*, has been reported to reductively dechlorinate PCBs and chlorobenzenes (120).

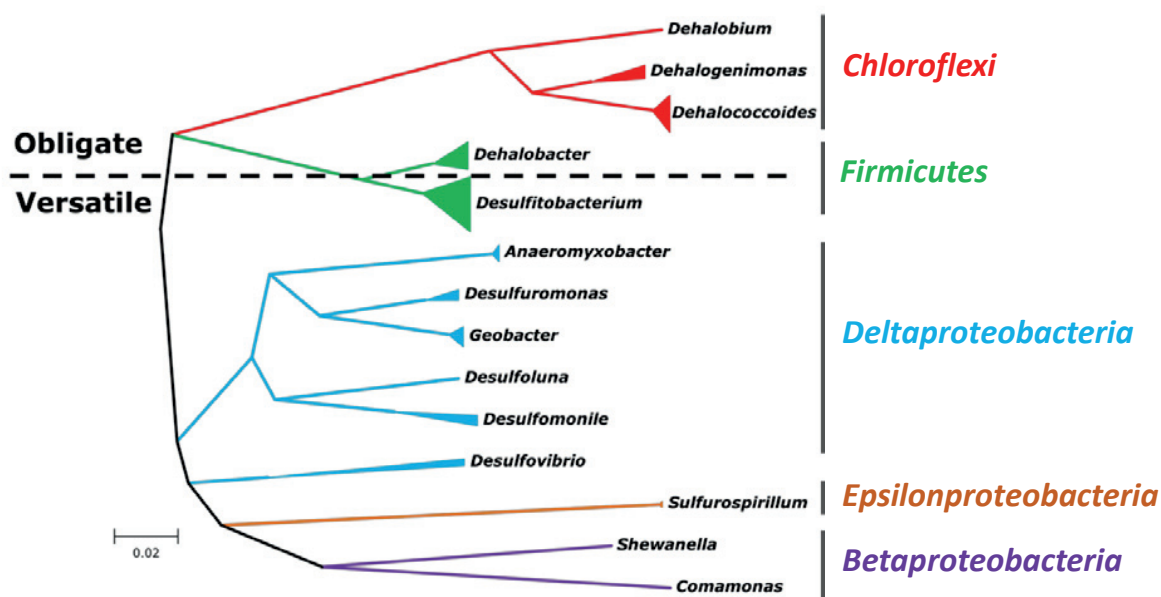


Figure 1.4. Phylogenetic tree of known OHRB based on bacterial 16S rRNA gene sequences.

The reference bar at the bottom indicates the branch length that represents 2% of sequence divergence (taken from (3)).

Sulfurospirillum is the only organohalide-respiring *Epsilonproteobacteria*, and is phylogenetically distinct from other OHRB (Figure 1.4). The genus *Sulfurospirillum*, whose name comes from its ability to reduce and oxidize sulfur compounds, has been proposed twenty-five years ago with the isolation of *Sulfurospirillum deleyianum* (136). Some *Sulfurospirillum* strains but not all can reductively dechlorinate chloroethenes (PCE and TCE) and also dehalogenate brominated ethenes and chloropropenes (44). In contrast to the genera *Dehalobacter* and *Dehalococcoides*, they are metabolically versatile bacteria that can use various non-chlorinated electron acceptors such as fumarate, sulfur, polysulfide, thiosulfate, sulfite, DMSO, TMAO, nitrate, nitrite, arsenate, selenate and manganate (44). The recently published complete genome sequence of *Sulfurospirillum multivorans* strain K (GenBank accession no. CP007201) (45) including a comparison with genome sequences of two related non-dehalogenating species, *Sulfurospirillum deleyianum* and *Sulfurospirillum barnesii*, have enabled to unravel additional aspects of the metabolic versatility of this genus. Indeed a large family of 20 different gene clusters encoding putative molybdopterin-containing oxidoreductases including the periplasmic nitrate reductase (*nap*) have been identified in the genome of strain K. Cultivation experiments of *S. multivorans* with TMAO,

DMSO, polysulfide, perchlorate and tetrathionate as electron acceptors demonstrated that all these compounds support the growth of *S. multivorans* (44).

1.4.1. The SL2 enrichment culture

At the Laboratory for Environmental Biotechnology (LBE), an anaerobic enrichment culture named SL2, which was originally inoculated with a fixed-bed bioreactor sludge treating PCE-contaminated groundwater is under scrutiny since many years. The initial enrichment culture (SL2-PCEa) has been characterized by a particular stepwise dechlorination pattern of PCE with successive accumulations of TCE, *cis*-DCE, VC and ethene (148), and by the presence of mainly two CEs dechlorinating bacterial genera, namely *Sulfurospirillum* (PCE to *cis*-DCE) and *Dehalococcoides* (*cis*-DCE to ethene) (128). Upon rapid transfer, the enrichment culture has given rise to several distinct and successive bacterial consortia. First, SL2-PCEb has been obtained which has only kept the ability to dechlorinate PCE to *cis*-DCE (with transient accumulation of TCE) consistent with the disappearance of *Dehalococcoides* (84). The consortium SL2-PCEb has been shown to harbor two different *Sulfurospirillum* sp. populations each of which catalyzing one step of dechlorination in the consortium. Two further subcultures have been derived from SL2-PCEb, each one harboring one *Sulfurospirillum* sp. population and allowing the identification of distinct dechlorination potential: the consortium SL2-PCEc dechlorinated PCE to TCE only, while the consortium SL2-TCE (originally selected on TCE) kept the potential to dechlorinate both PCE and TCE. A molecular fingerprinting method targeting small differences in the *rdhA* genes of both *Sulfurospirillum* populations has been developed to follow the two populations in the parental consortium. The PCE dechlorination activity measured in cell extracts of both distinct populations have suggested that the PCE reductive dehalogenase (PceA) enzyme produced by the consortium SL2-PCEc had a five-fold higher turnover rate than the one produced by SL2-TCE (16).

1.5. Diversity of reductive dehalogenases and accessory genes

The key enzymes in OHR are reductive dehalogenases (RdhA, RDase). The first reductive dehalogenase was purified in 1995 (113), with the first gene sequence determined in 1998 (112). Today, only eight PCE reductive dehalogenases (PceA) from *Desulfitobacterium hafniense* strains Y51 (147), PCE-S (100), and PCE1 (153), from *Dehalobacter restrictus* strain

PER-K23 (88), *Dehalococcoides mccartyi* strain 195 (83), and *S. multivorans* (111) were characterized on biochemical level.

The genetic structure of the gene clusters encoding RdhA enzymes are rather conserved even though the bacteria harboring them are classified in distant phylogenetic groups. For example, the minimal reductive dehalogenase (*rdh*) gene clusters or operons typically comprise *rdhA*, the gene for the catalytically active enzyme, and *rdhB*, a gene encoding a putative membrane-anchoring protein (112). Whenever investigated, these two genes have always been co-transcribed.

In the case of the chlorophenol reductive dehalogenase (*cpr*) gene cluster from *Desulfitobacterium dehalogenans*, six additional genes surround the *cprA* and *cprB* genes (*cprTKZEBACD*) (140). The genetic environment around the *pceA* gene from *Dehalobacter restrictus* PER-K23 and several *Desulfitobacterium* strains is made of a four-gene cluster, *pceABCT* (31, 39, 87). Interestingly, PCE dechlorinating *Desulfitobacterium* spp. seemed to have acquired the *pceABCT* gene cluster by horizontal gene transfer as it has been found on an active transposon (31).

The majority of the currently known OHRB carry multiple *rdhA* genes, from 1 to 36 depending on the strain (56). Several studies have demonstrated that the presence of multiple non-identical *rdhA* genes is a typical feature of OHRB (55, 127, 129). This suggests that the substrate range of OHRB may be far greater than previously believed (92). However, the substrate specificity has been determined for only about fifteen enzymes among the several hundreds of putative *rdhA* sequences reported in databases (56). It has been previously shown that sequence homology alone cannot be used to determine the substrate specificity of RdhA enzymes, as almost identical enzymes can have distinct substrates and substrate ranges (16, 31) and reversely very distantly related enzymes the same substrate spectrum. Therefore, efforts need to be made in order to associate substrates to newly identified *rdhA* genes.

While the products of *rdhA* genes have been well studied in several cases, there is little knowledge on the other gene products of *rdh* operons. The physiological role of the RdhB proteins has been early predicted to be that of a membrane anchor (2-3 transmembrane α -helices) for the catalytic subunit (RdhA) (112), although no study has yet presented any

evidence on protein level. No physiological data has yet been obtained on any RdhC either. Sequence homology analysis has revealed that CprC (the first identified member of the RdhC family) resembles to the membrane-bound NirI/NosR transcriptional regulator family (140). However, a peripheral domain located in the N-terminal half of RdhC is predicted to bind FMN as cofactor, suggesting that it is possibly involved in electron transfer to RdhA (86). The membrane spanning C-terminal part of RdhC displays similarities to the membrane-bound protein NapH, which is a subunit of the quinol dehydrogenase NapGH involved in electron transfer to the periplasmic nitrate reductase NapA (63). Interestingly, in *Sulfurospirillum* spp. which do not harbor *rdhC* genes, the involvement of a quinol dehydrogenase in the organohalide respiratory chain is also likely to occur (45). Member of the RdhT protein family (more particularly PceT) have been shown to participate in the maturation of PceA possibly acting as molecular chaperones in the folding quality control of RdhA prior to its transport across the cytoplasmic membrane via the Twin-arginine translocation (Tat) system (85, 103). This feature has since been used for the heterologous production of active RdhA enzymes in *Shimwellia blattae* (81). In *Desulfitobacterium* spp., the *cpr* operon is under a tight transcriptional control operated by CprK, a regulatory protein which upon binding of chlorinated phenols recognizes the promoter region of *cpr* genes and activates their transcription (61, 62, 96, 121). The RdhK family seems to be more widespread as previously thought as 24 copies of it are present in the genome of *Dehalobacter restrictus* PER-K23 (129). While CprD and CprE proteins are predicted to be molecular chaperones of the GroEL type, their involvement in the maturation of RdhA has not yet been demonstrated (140).

1.6. Biochemistry of OHR

1.6.1. Reductive dehalogenases

A reductive dehalogenase gene (*rdhA*) is annotated based on some particular properties. Most of the RdhA enzymes have been identified as a 46-65 kDa monomeric proteins. However, the structural analysis of PceA of *S. multivorans* suggested a homodimeric form of this respiratory RdhA under native conditions (9). All RdhA enzymes purified and characterized so far were shown to harbor a cobalt-containing porphyrin-derived corrinoid cofactor (with an exception : the 3-chlorobenzoate RdhA of *Desulfomonile tiedjei*) (133), two iron-sulfur (FeS) clusters (two conserved cysteine motifs: CX₂₋₁₂CX₂CX₃CP) which were

proposed to be essential for catalysis, and a cleavable Twin-arginine translocation (Tat) signal peptide which harbors a conserved twin-arginine motif (RRxFLK) that is usually found in complex redox proteins that are exported to or across the cytoplasmic membrane (7, 8, 38, 116, 131). The 3D-structure of PceA of *S. multivorans* reported that the corrinoid cofactor was found to be non-covalently attached to the enzyme at the active site in the base-off conformation (9). A similar mode of B₁₂-binding was also reported in the structure of the cytoplasmic *ortho*-dibromophenol RDase of the marine alphaproteobacterium *Nitratireductor pacificus* pht-3B (119). The *rdhAs* are located in the exoplasm of bacterial cells (the periplasm in Gram-negative bacteria), and are associated with the cytoplasmic membrane (58, 114, 124).

1.6.2. The corrinoid cofactor of reductive dehalogenases

Initially, the presence of corrinoid in RdhA has been shown by its reversible inactivation by iodopropane (99, 109, 134). Three formal oxidation states are known for the cobalt atom in the corrinoid structure, namely Co(III), Co(II), and Co(I) (74). It has been shown that the super-reduced form of cobalt of corrinoids even in its free form can reductively dechlorinate PCE and other chlorinated ethenes (43), however at much lower rates than the corrinoid-containing RdhA proteins. A mutant strain of *S. multivorans* which had lost the ability to produce a specific form of corrinoid was unable to dechlorinate PCE (138). Extraction and identification of the corrinoid from the wild-type strain from PceA of *S. multivorans* has revealed a new corrinoid, namely norpseudovitamin B₁₂ (66), which has not been found in the RdhA of other OHRB identified so far. The corrinoid-binding consensus sequence (DxHxxG) identified in other classes of corrinoid enzymes (80) is not present in reductive dehalogenases, consistent with the fact that the base-off configuration of the corrinoid has been identified in PceA from *Dehalobacter restrictus* (135) and PceA from *S. multivorans* (9).

It has been reported, that *Desulfitobacterium hafniense* strain TCE1 has the ability to produce its own corrinoid and to grow in the absence of external vitamin B₁₂ in the cultivation medium (19). In contrast, the corrinoid-auxotrophic organism *Dehalobacter restrictus* PER-K23 is expected to recruit an external cobalamin that is added to the growth medium (52, 129).

The redox chemistry of RdhA enzymes has been analyzed by electron paramagnetic resonance (EPR) spectroscopy, revealing a rather high redox potential for the transition between Co(I) and Co(II) (around -350 mV). More contrasting data have been obtained for the nature and redox potential of the FeS clusters (135, 154). The RdhA enzymes are rapidly inactivated by molecular oxygen probably due to irreversible alteration of the FeS clusters.

1.6.3. The OHR electron transport chain

Respiratory metabolism such as OHR requires the presence of an electron transport chain located in the cytoplasmic membrane which allows the establishment of a proton-motive force across the membrane. Redox proteins and other non-protein electron shuttles are usually combined in the membrane to accomplish that task. Several studies have described the OHR process on the biochemical level, but they have mainly considered the reductive dehalogenases (RdhA) as a standalone enzyme (10, 36, 65, 82, 88, 100, 105, 110, 111, 147, 149, 151, 153, 154). The composition of the organohalide respiratory chain remains very poorly characterized, and so are the redox partners of RdhA enzymes (133). For example, the physiological electron donating enzyme to RdhA enzymes has yet to be identified, and it is believed that these donors may differ among OHRB. Generally for obligate OHRB, the implication of two key enzymes have been reported, an electron-donating hydrogenase and the electron-accepting reductive dehalogenase (RdhA) (37, 53). Multiple hydrogenase complexes are predicted in the genomes of obligate OHRB (68, 71, 137) with the membrane-bound periplasmic Hup hydrogenase being the one most likely used in the OHR process (104, 129). Furthermore, *b*-type cytochromes have been shown by optical difference spectra to participate in electron transport in *S. multivorans* (132), *Dehalobacter restrictus* (52) and *D. dehalogenans* (152). In facultative OHRB, many organic and inorganic electron donors can participate in OHR depending on the strains (132, 157). It has been recently reported that a *S. multivorans* genomic survey allowed to identify a gene cluster encoding NiFe hydrogenases, which is presumably periplasmic and membrane-bound (MBH). Generally in anaerobic respiration, electrons are usually transferred to the quinone pool (125). Menaquinones are likely to play that role in the cytoplasmic membrane of *D. restrictus* (134), *S. multivorans* (132), *Desulfitobacterium dehalogenans* (152), *Desulfomonile tiedjei* (78), and *Desulfitobacterium hafniense* strain TCE1 (122). Indeed, the membrane-bound menaquinone was reduced by oxidation of H₂ and re-oxidized by the reduction of PCE, indicating that

menaquinone functions as an electron mediator. Recently, Kublik *et al.*, reported that there is no quinone participation in the respiration of *Dehalococcoides mccartyi*, suggesting a quinone-independent protein-based respiratory electron transfer chain (72). There are some indications that additional redox elements might be involved in transferring electrons from the quinone pool to the terminal enzyme. Since the analogue 2,3-dimethyl-1,4-naphthoquinone failed to directly react with the isolated PCE reductive dehalogenase, menaquinone does not appear to be the direct electron donor to the PCE reductive dehalogenase (134). Membrane-bound c-type cytochromes were observed in *Desulfitobacterium hafniense* strain DCB-2 (21), strain TCE1 (41), in *Desulfitobacterium* sp. strain PCE1 (42), and *Desulfomonile tiedjei* (79), but again no biochemical evidence for their participation in electron transfer has been clearly demonstrated.

Several studies using “omics” technologies aimed to better characterize the nature of enzymatic complexes involved in organohalide respiration (59, 72, 104, 122, 123, 161). However, except for a few ones, these studies have mainly reported on known or predicted proteins that clearly participate to organohalide respiration, and did not report any new redox element so far. One exception has to be mentioned where indications have been obtained that when Cl-OHPA is the terminal electron acceptor, electrons are transferred from menaquinones to the outward-facing CprA, via an unidentified membrane complex, and potentially an extracellular flavoprotein acting as an electron shuttle between the quinol dehydrogenase membrane complex and CprA (69, 70).

1.7. Objectives and outline of the thesis

1.7.1. Objectives of the thesis

The membrane-associated reductive dehalogenase plays the key role in the energy metabolism of OHRB. However, the cultivation and isolation of OHRB is not trivial, and respiratory RdhA enzymes are known to be oxygen-sensitive. Although genetic systems have been developed for heterologous expression of functional reductive dehalogenases (81, 118), it is still very challenging to produce active RdhA enzymes in substantial amount. This is currently representing the major bottleneck for in-depth biochemical characterization of these enzymes. Taken together, these challenges are explaining why many aspects of OHR metabolism are not well understood. Specific questions such as the substrate specificity of newly identified RdhA enzymes and as well as the composition of the OHR electron transport chain need to be addressed.

The overall goal of this thesis was to give new insights into the physiology and biochemistry of tetrachloroethene-respiring bacteria. Specific objectives were (i) to characterize at the biochemical and structural levels a new reductive dehalogenase from the bacterial consortium SL2 harboring *Sulfurospirillum* spp. populations, (ii) to assess the kinetic parameters of *Sulfurospirillum* spp. strains competing for tetrachloroethene, and (iii) to initiate the characterization of PceC from *Desulfitobacterium hafniense*, a membrane-bound flavoprotein suspected to be involved in the electron transfer to PceA.

1.7.2. Outline of the thesis

CHAPTER 1 presents an introductory overview of the OHR process and the key bacterial players in this field.

In **CHAPTER 2**, a new reductive dehalogenase identified in a bacterial consortium harboring *Sulfurospirillum* spp. populations and displaying an unusually restricted substrate range is characterized, and a model of the active site of this enzyme based on the structure of *S. multivorans* PceA is proposed.

CHAPTER 3 presents the results of genomic and kinetic investigations of two *Sulfurospirillum* spp. strains present in a consortium which displays a particular stepwise dechlorination of PCE to TCE and *cis*-DCE.

In **CHAPTER 4**, the characterization of the FMN-binding domain of PceC from *Desulfitobacterium hafniense* is presented for the first time and proposes a new way for further investigations on its involvement in the OHR process.

Finally, the main findings presented in this thesis are discussed and evaluated with respect to the present knowledge on organohalide respiration in **CHAPTER 5**.

1.8. References

1. **Abrahamson, K., Ekdah, J., Collén, J. & Pedersen, K.** 1995. Marine algae—a source of trichloroethylene and perchloroethylene. *Limnol Oceanogr* **40**:1321-1326.
2. **Ahn, Y. B., L. J. Kerkhof, and M. M. Haggblom.** 2009. *Desulfoluna spongiiphila* sp. nov., a dehalogenating bacterium in the *Desulfobacteraceae* from the marine sponge *Aplysina aerophoba*. *Int J Syst Evol Microbiol* **59**:2133-2139.
3. **Atashgahi, S. L., Y. Lu, and H. Smidt.** 2016. Overview of known organohalide-respiring bacteria—phylogenetic diversity and environmental distribution, p.63-105. *In* L. Adrian and F. E. Löffler (ed.), *Organohalide-Respiring Bacteria*. Springer Berlin Heidelberg, Berlin.
4. **Aulenta, F., Canosa, A., Leccese, M., Petrangeli Papini, M., Majone, M., and Viotti, P.** 2007. Field study of *in situ* anaerobic bioremediation of a chlorinated solvent source zone. *Industrial & Engineering Chemistry Research* **46 (21)**:6812–6819.
5. **Aulenta, F., A. Fina, M. Potalivo, M. Petrangeli Papini, S. Rossetti, and M. Majone.** 2005. Anaerobic transformation of tetrachloroethane, perchloroethylene, and their mixtures by mixed-cultures enriched from contaminated soils and sediments. *Water Sci Technol* **52**:357-362.
6. **Aulenta, F., S. Rossetti, B. Matturro, V. Tandoi, R. Verdini, and M. M.** 2016. Redox interactions of Organohalide-Respiring Bacteria (OHRB) with solid-state electrodes: principles and perspectives of microbial electrochemical remediation. *In* L. Adrian and F. E. Löffler (ed.), *Organohalide-Respiring Bacteria*. Springer Berlin Heidelberg, Berlin.
7. **Berks, B. C.** 1996. A common export pathway for proteins binding complex redox cofactors? *Mol Microbiol* **22**:393-404.
8. **Berks, B. C., T. Palmer, and F. Sargent.** 2003. The Tat protein translocation pathway and its role in microbial physiology. *Advances in microbial physiology* **47**:187-254.
9. **Bommer, M., C. Kunze, J. Fessler, T. Schubert, G. Diekert, and H. Dobbek.** 2014. Structural basis for organohalide respiration. *Science* **346**:455-458.
10. **Boyer, A., R. Page-BeLanger, M. Saucier, R. Villemur, F. Lepine, P. Juteau, and R. Beaudet.** 2003. Purification, cloning and sequencing of an enzyme mediating the reductive dechlorination of 2,4,6-trichlorophenol from *Desulfitobacterium frappieri* PCP-1. *Biochem J* **373**:297-303.
11. **Boyle, A. W., C. D. Phelps, and L. Y. Young.** 1999. Isolation from estuarine sediments of a *Desulfovibrio* strain which can grow on lactate coupled to the reductive dehalogenation of 2,4,6-tribromophenol. *Appl Environ Microbiol* **65**:1133-1140.
12. **Bradley, P. M., and F. H. Chapelle.** 2010. Chapter 3, p.39-67. *In* H. F. W. Stroo, C. Herb (Eds.) (ed.), *In situ* remediation of chlorinated solvent plumes. Springer, New York.
13. **Bradley, P. M. C., F.H.** 2000. Aerobic microbial mineralization of dichloroethene as sole carbon substrate. *Environ Sci Technol* **34**:221-223.
14. **Bradley, P. M. C., F.H.** 1996. Anaerobic mineralization of vinyl chloride in Fe(III)-reducing, aquifer sediments. *Environ Sci Technol* **30**:2084-2086.
15. **Butler, A., and M. Sandy.** 2009. Mechanistic considerations of halogenating enzymes. *Nature* **460**:848-854.
16. **Buttet, G. F., C. Holliger, and J. Maillard.** 2013. Functional genotyping of *Sulfurospirillum* spp. in mixed cultures allowed the identification of a new tetrachloroethene reductive dehalogenase. *Appl Environ Microbiol* **79**:6941-6947.
17. **Chen, K., Y. Liu, D. M. Mao, X. M. Liu, S. P. Li, and J. D. Jiang.** 2013. An essential esterase (BroH) for the mineralization of bromoxynil octanoate by a natural consortium of *Sphingopyxis* sp. strain OB-3 and *Comamonas* sp. strain 7D-2. *Journal of agricultural and food chemistry* **61**:11550-11559.
18. **ChloroNet** 2015, posting date. ChloroNet: a national platform for CHC contamination. [Online.]

19. **Choudhary, P. K., A. Duret, E. Rohrbach-Brandt, C. Holliger, R. K. Sigel, and J. Maillard.** 2013. Diversity of cobalamin riboswitches in the corrinoid-producing organohalide respirer *Desulfitobacterium hafniense*. *J Bacteriol* **195**:5186-5195.
20. **Christ, J. A., C. A. Ramsburg, L. M. Abriola, K. D. Pennell, and F. E. Löffler.** 2005. Coupling aggressive mass removal with microbial reductive dechlorination for remediation of DNAPL source zones: a review and assessment. *Environ Health Perspect* **113**:465-477.
21. **Christiansen, N., Kiaer, B.** 1996. *Desulfitobacterium hafniense* sp. nov., an anaerobic reductively dechlorinating bacterium. *Int J Syst Bacteriol.* **46**:442-448.
22. **Collen, J. E., A.; Abrahamsson, K.; Pedersen, M.** 1994. The involvement of hydrogen peroxide in the production of volatile halogenated compounds by *Meristiella gelidium*. *Elsevier* **36**:1197-1202.
23. **Contentin, C., M. Robert, and J. M. Saveant.** 2005. Does catalysis of reductive dechlorination of tetra- and trichloroethylenes by vitamin B₁₂ and corrinoid-based dehalogenases follow an electron transfer mechanism? *J Am Chem Soc* **127**:12154-12155.
24. **De Wever, H., J. R. Cole, M. R. Fettig, D. A. Hogan, and J. M. Tiedje.** 2000. Reductive dehalogenation of trichloroacetic acid by *Trichlorobacter thiogenes* gen. nov., sp. nov. *Appl Environ Microbiol* **66**:2297-2301.
25. **De Wildeman, S., G. Linthout, H. Van Langenhove, and W. Verstraete.** 2004. Complete lab-scale detoxification of groundwater containing 1,2-dichloroethane. *Appl Microbiol Biotechnol* **63**:609-612.
26. **DeWeerd, K. A., Concannon, F. & Suflita, J.M.** 1991. Relationship between hydrogen consumption, dehalogenation, and the reduction of sulfur oxyanions by *Desulfomonile tiedjei*. *Appl Environ Microbiol* **57**:1929-1934.
27. **Dobbek, H. a. L. D.** 2016. Insights into reductive dehalogenase function obtained from crystal structures, p.485-495. *In* L. Adrian and F. E. Löffler (ed.), *Organohalide-Respiring Bacteria*. Springer Berlin Heidelberg.
28. **Doherty.** 2000. A history of the production and use of carbon tetrachloride, tetrachloroethylene, trichloroethylene and 1,1,1-trichloroethane in the United States: Part 1. Historical background; carbon tetrachloride and tetrachloroethylene. *J Environ Forensics* **1**:69-81.
29. **Doherty.** 2000b. A history of the production and use of carbon tetrachloride, tetrachloroethylene, trichloroethylene and 1,1,1-trichloroethane in the United States: Part 2. Trichloroethylene and 1,1,1-trichloroethane. *J Environ Forensics* **1**:83-93.
30. **Dolfing, J.** 2016. Energetic Considerations in Organohalide Respiration, p.31-48. *In* L. Adrian and F. E. Löffler (ed.), *Organohalide-Respiring Bacteria*. Springer Berlin Heidelberg.
31. **Duret, A., C. Holliger, and J. Maillard.** 2012. The physiological opportunism of *Desulfitobacterium hafniense* strain TCE1 towards organohalide respiration with tetrachloroethene. *Appl Environ Microbiol* **78**:6121-6127.
32. **El Fantroussi, S., H. Naveau, and S. N. Agathos.** 1998. Anaerobic dechlorinating bacteria. *Biotechnol Prog* **14**:167-188.
33. **EuroChlor** 2015, posting date. Chlorine Industry Review 2014-2015. [Online.]
34. **Fetzner, S.** 1998. Bacterial dehalogenation. *Appl Microbiol Biotechnol* **50**:633-657.
35. **Field, J. A.** 2016. Natural production of organohalide compounds in the environment, p.7-29. *In* L. Adrian and F. E. Löffler (ed.), *Organohalide-Respiring Bacteria*. Springer Berlin Heidelberg, Berlin.
36. **Furukawa, K., A. Suyama, Y. Tsuboi, T. Futagami, and M. Goto.** 2005. Biochemical and molecular characterization of a tetrachloroethene dechlorinating *Desulfitobacterium* sp. strain Y51: a review. *J Ind Microbiol Biotechnol* **32**:534-541.
37. **Futagami, T., M. Goto, and K. Furukawa.** 2005. Biochemical and genetic bases of chloroethene-dehalorespiring bacteria. *Tanpakushitsu Kakusan Koso* **50**:1548-1554.
38. **Futagami, T., M. Goto, and K. Furukawa.** 2008. Biochemical and genetic bases of dehalorespiration. *Chem Rec* **8**:1-12.

39. **Futagami, T., Y. Tsuboi, A. Suyama, M. Goto, and K. Furukawa.** 2006. Emergence of two types of nondechlorinating variants in the tetrachloroethene-halo-respiring *Desulfitobacterium* sp. strain Y51. *Appl Microbiol Biotechnol* **70**:720-728.
40. **Futagami, T. F., K.** 2016. The Genus *Desulfitobacterium*, p.173-208. In L. Adrian and F. E. Löffler (ed.), *Organohalide-Respiring Bacteria*. Springer, Berlin Heidelberg.
41. **Gerritse, J., O. Drzyzga, G. Kloetstra, M. Keijmel, L. P. Wiersum, R. Hutson, M. D. Collins, and J. C. Gottschal.** 1999. Influence of different electron donors and acceptors on dehalorespiration of tetrachloroethene by *Desulfitobacterium frappieri* TCE1. *Appl Environ Microbiol* **65**:5212-5221.
42. **Gerritse, J., V. Renard, T. M. Pedro Gomes, P. A. Lawson, M. D. Collins, and J. C. Gottschal.** 1996. *Desulfitobacterium* sp. strain PCE1, an anaerobic bacterium that can grow by reductive dechlorination of tetrachloroethene or ortho-chlorinated phenols. *Arch Microbiol* **165**:132-140.
43. **Glod, G., W. Angst, C. Holliger, and R. P. Schwarzenbach.** 1997. Corrinoid-Mediated Reduction of Tetrachloroethene, Trichloroethene, and Trichlorofluoroethene in Homogeneous Aqueous Solution: Reaction Kinetics and Reaction Mechanisms. *Environ Sci Technol* **31**:253-260.
44. **Goris, T., and G. Diekert.** 2016. The Genus *Sulfurospirillum*, p.209-234. In L. Adrian and F. E. Löffler (ed.), *Organohalide-Respiring Bacteria*. Springer Berlin Heidelberg.
45. **Goris, T., T. Schubert, J. Gadkari, T. Wubet, M. Tarkka, F. Buscot, L. Adrian, and G. Diekert.** 2014. Insights into organohalide respiration and the versatile catabolism of *Sulfurospirillum multivorans* gained from comparative genomics and physiological studies. *Environ Microbiol* **16**:3562-3580.
46. **Gribble, G. W.** 1994. The natural production of chlorinated compounds. *Environ Sci Technol* **28**:310A-319A.
47. **Groster, A., M. Duhamel, S. Dworatzek, and E. A. Edwards.** 2010. Chloroform respiration to dichloromethane by a *Dehalobacter* population. *Environ Microbiol* **12**:1053-1060.
48. **Groster, A., and E. A. Edwards.** 2006. Growth of *Dehalobacter* and *Dehalococcoides* spp. during degradation of chlorinated ethanes. *Appl Environ Microbiol* **72**:428-436.
49. **Häggbloom, M. M., and Bossert, I. D.** 2003. Dehalogenation: microbial processes and environmental applications. Springer.
50. **Hartmans, S., and J. A. De Bont.** 1992. Aerobic vinyl chloride metabolism in *Mycobacterium aurum* L1. *Appl Environ Microbiol* **58**:1220-1226.
51. **He, J., and D. L. Bedard.** 2016. The microbiology of anaerobic PCB dechlorination. In L. Adrian and F. E. Löffler (ed.), *Organohalide-Respiring Bacteria*. Springer Berlin Heidelberg, Berlin.
52. **Holliger, C., D. Hahn, H. Harmsen, W. Ludwig, W. Schumacher, B. Tindall, F. Vazquez, N. Weiss, et al.** 1998. *Dehalobacter restrictus* gen. nov. and sp. nov., a strictly anaerobic bacterium that reductively dechlorinates tetra- and trichloroethene in an anaerobic respiration. *Arch Microbiol* **169**:313-321.
53. **Holliger, C., C. Regeard, and G. Diekert.** 2003. Dehalogenation by anaerobic bacteria, p.115-157. In M. M. Häggbloom and I. B. Bossert (ed.), *Dehalogenation: microbial processes and environmental applications*. Kluwer Academic, Boston, Dordrecht, London.
54. **Holliger, C., G. Schraa, A. J. Stams, and A. J. Zehnder.** 1993. A highly purified enrichment culture couples the reductive dechlorination of tetrachloroethene to growth. *Appl Environ Microbiol* **59**:2991-2997.
55. **Holscher, T., R. Krajmalnik-Brown, K. M. Ritalahti, F. Von Wintzingerode, H. Gorisch, F. E. Löffler, and L. Adrian.** 2004. Multiple nonidentical reductive-dehalogenase-homologous genes are common in *Dehalococcoides*. *Appl Environ Microbiol* **70**:5290-5297.
56. **Hug, L. A., F. Maphosa, D. Leys, F. E. Löffler, H. Smidt, E. A. Edwards, and L. Adrian.** 2013. Overview of organohalide-respiring bacteria and a proposal for a classification system for reductive dehalogenases. *Philosophical transactions of the Royal Society of London. Series B, Biological sciences* **368**:20120322.

57. **Hunkeler, D.** 2016. Use of Compound-Specific Isotope Analysis (CSIA) to Assess the Origin and Fate of Chlorinated Hydrocarbons, p.587-617. *In* L. Adrian and F. E. Löffler (ed.), Organohalide-Respiring Bacteria. Springer Berlin Heidelberg, Berlin.
58. **John, M., R. P. Schmitz, M. Westermann, W. Richter, and G. Diekert.** 2006. Growth substrate dependent localization of tetrachloroethene reductive dehalogenase in *Sulfurospirillum multivorans*. *Arch Microbiol* **186**:99-106.
59. **Johnson, D. R., E. L. Brodie, A. E. Hubbard, G. L. Andersen, S. H. Zinder, and L. Alvarez-Cohen.** 2008. Temporal transcriptomic microarray analysis of "*Dehalococcoides ethenogenes*" strain 195 during the transition into stationary phase. *Appl Environ Microbiol* **74**:2864-2872.
60. **Jordan A., H. J., Borchers R., Le Guern F. & Shinohara H.** 2000. Volcanogenic halocarbons. *Environ Sci Technol* **34**:1122-1124.
61. **Joyce, M. G., C. Levy, K. Gabor, S. M. Pop, B. D. Biehl, T. I. Doukov, J. M. Ryter, H. Mazon, et al.** 2006. CprK crystal structures reveal mechanism for transcriptional control of halorespiration. *J Biol Chem* **281**:28318-28325.
62. **Kemp, L. R., M. S. Dunstan, K. Fisher, J. Warwicker, and D. Leys.** 2013. The transcriptional regulator CprK detects chlorination by combining direct and indirect readout mechanisms. *Philosophical transactions of the Royal Society of London. Series B, Biological sciences* **368**:20120323.
63. **Kern, M., and J. Simon.** 2008. Characterization of the NapGH quinol dehydrogenase complex involved in *Wolinella succinogenes* nitrate respiration. *Mol Microbiol* **69**:1137-1152.
64. **Kittelmann, S., and M. W. Friedrich.** 2008. Identification of novel perchloroethene-respiring microorganisms in anoxic river sediment by RNA-based stable isotope probing. *Environ Microbiol* **10**:31-46.
65. **Krasotkina, J., T. Walters, K. A. Maruya, and S. W. Ragsdale.** 2001. Characterization of the B₁₂- and iron-sulfur-containing reductive dehalogenase from *Desulfitobacterium chlororespirans*. *J Biol Chem* **276**:40991-40997.
66. **Kräutler, B., W. Fieber, S. Ostermann, M. Fasching, K. H. Ongania, K. Gruber, C. Kratky, C. Mikl, et al.** 2003. The cofactor of tetrachloroethene reductive dehalogenase of *Dehalospirillum multivorans* is norpseudo-B₁₂, a new type of a natural corrinoid. *Helvetica Chimica Acta* **86**:3698-3716.
67. **Krumholz, L. R.** 1997. *Desulfuromonas chloroethenica* sp. nov. uses tetrachloroethylene and trichloroethylene as electron acceptors. *Int J Syst Bacteriol.* **47**:1262-1263.
68. **Kruse, T., J. Maillard, L. Goodwin, T. Woyke, H. Teshima, D. Bruce, C. Detter, R. Tapia, et al.** 2013. Complete genome sequence of *Dehalobacter restrictus* PER-K23(T.). *Stand Genomic Sci* **8**:375-388.
69. **Kruse, T., H. Smidt, and U. Lechner.** 2016. Comparative genomics and transcriptomics of organohalide-respiring bacteria and regulation of *rdh* gene transcription, p.345-376. *In* L. Adrian and F. E. Löffler (ed.), Organohalide-Respiring Bacteria. Springer Berlin Heidelberg.
70. **Kruse, T., B. A. van de Pas, A. Atteia, K. Krab, W. R. Hagen, L. Goodwin, P. Chain, S. Boeren, et al.** 2015. Genomic, proteomic, and biochemical analysis of the organohalide respiratory pathway in *Desulfitobacterium dehalogenans*. *J Bacteriol* **197**:893-904.
71. **Kube, M., A. Beck, S. H. Zinder, H. Kuhl, R. Reinhardt, and L. Adrian.** 2005. Genome sequence of the chlorinated compound-respiring bacterium *Dehalococcoides* species strain CBDB1. *Nat Biotechnol* **23**:1269-1273.
72. **Kublik, A., D. Deobald, S. Hartwig, C. L. Schiffmann, A. Andrades, M. von Bergen, R. G. Sawers, and L. Adrian.** 2016. Identification of a multi-protein reductive dehalogenase complex in *Dehalococcoides mccartyi* strain CBDB1 suggests a protein-dependent respiratory electron transport chain obviating quinone involvement. *Environ Microbiol* **18**:3044-3056.
73. **Lanthier, M., R. Villemur, F. Lepine, J. G. Bisailon, and R. Beaudet.** 2000. Monitoring of *Desulfitobacterium frappieri* PCP-1 in pentachlorophenol-degrading anaerobic soil slurry reactors. *Environ Microbiol* **2**:703-708.

74. **Lexa, D., and J. M. Saveant.** 1983. The electrochemistry of vitamin B₁₂. *Acc. Chem. Res.* **16**:235–243.
75. **Li, Z., N. Yoshida, A. Wang, J. Nan, B. Liang, C. Zhang, D. Zhang, D. Suzuki, et al.** 2015. Anaerobic mineralization of 2,4,6-tribromophenol to CO₂ by a synthetic microbial community comprising *Clostridium*, *Dehalobacter*, and *Desulfatiglans*. *Bioresource technology* **176**:225-232.
76. **Löffler, F. E., J. R. Cole, K. M. Ritalahti, and J. M. Tiedje.** 2004. Diversity of Dechlorinating Bacteria, p.53-87, *Dehalogenation: Microbial Processes and Environmental Applications*, Kluwer Academic Publishers ed. Springer.
77. **Löffler, F. E., R. A. Sanford, and K. M. Ritalahti.** 2005. Enrichment, cultivation, and detection of reductively dechlorinating bacteria. *Methods in enzymology* **397**:77-111.
78. **Louie, T. M., and W. W. Mohn.** 1999. Evidence for a chemiosmotic model of dehalorespiration in *Desulfomonile tiedjei* DCB-1. *J Bacteriol* **181**:40-46.
79. **Louie, T. M., S. Ni, L. Xun, and W. W. Mohn.** 1997. Purification, characterization and gene sequence analysis of a novel cytochrome c co-induced with reductive dechlorination activity in *Desulfomonile tiedjei* DCB-1. *Arch Microbiol* **168**:520-527.
80. **Ludwig, M. L., and R. G. Matthews.** 1997. Structure-based perspectives on B₁₂-dependent enzymes. *Annual review of biochemistry* **66**:269-313.
81. **Mac Nelly, A., M. Kai, A. Svatos, G. Diekert, and T. Schubert.** 2014. Functional heterologous production of reductive dehalogenases from *Desulfitobacterium hafniense* strains. *Appl Environ Microbiol* **80**:4313-4322.
82. **Magnuson, J. K., M. F. Romine, D. R. Burris, and M. T. Kingsley.** 2000. Trichloroethene reductive dehalogenase from *Dehalococcoides ethenogenes*: sequence of *tceA* and substrate range characterization. *Appl Environ Microbiol* **66**:5141-5147.
83. **Magnuson, J. K., R. V. Stern, J. M. Gossett, S. H. Zinder, and D. R. Burris.** 1998. Reductive dechlorination of tetrachloroethene to ethene by a two-component enzyme pathway. *Appl Environ Microbiol* **64**:1270-1275.
84. **Maillard, J., M. P. Charnay, C. Regeard, E. Rohrbach-Brandt, K. Rouzeau-Szynalski, P. Rossi, and C. Holliger.** 2011. Reductive dechlorination of tetrachloroethene by a stepwise catalysis of different organohalide respiring bacteria and reductive dehalogenases. *Biodegradation* **22**:949-960.
85. **Maillard, J., P. Genevoux, and C. Holliger.** 2011. Redundancy and specificity of multiple trigger factor chaperones in *Desulfitobacteria*. *Microbiology* **157**:2410-2421.
86. **Maillard, J., and C. Holliger.** 2016. The Genus *Dehalobacter*, p.153-171. *In* L. Adrian and F. E. Löffler (ed.), *Organohalide-Respiring Bacteria*. Springer Berlin Heidelberg, Berlin.
87. **Maillard, J., C. Regeard, and C. Holliger.** 2005. Isolation and characterization of *Tn-Dha1*, a transposon containing the tetrachloroethene reductive dehalogenase of *Desulfitobacterium hafniense* strain TCE1. *Environ Microbiol* **7**:107-117.
88. **Maillard, J., W. Schumacher, F. Vazquez, C. Regeard, W. R. Hagen, and C. Holliger.** 2003. Characterization of the corrinoid iron-sulfur protein tetrachloroethene reductive dehalogenase of *Dehalobacter restrictus*. *Appl Environ Microbiol* **69**:4628-4638.
89. **Malachowsky, K. J., T. J. Phelps, A. B. Teboli, D. E. Minnikin, and D. C. White.** 1994. Aerobic mineralization of trichloroethylene, vinyl chloride, and aromatic compounds by *rhodococcus* species. *Appl Environ Microbiol* **60**:542-548.
90. **Maness, A. D., K. S. Bowman, J. Yan, F. A. Rainey, and W. M. Moe.** 2012. *Dehalogenimonas* spp. can reductively dehalogenate high concentrations of 1,2-dichloroethane, 1,2-dichloropropane, and 1,1,2-trichloroethane. *AMB Express* **2**:54.
91. **Maphosa, F., W. M. de Vos, and H. Smidt.** 2010. Exploiting the ecogenomics toolbox for environmental diagnostics of organohalide-respiring bacteria. *Trends Biotechnol* **28**:308-316.
92. **Maphosa, F., S. H. Lieten, I. Dinkla, A. J. Stams, H. Smidt, and D. E. Fennell.** 2012. Ecogenomics of microbial communities in bioremediation of chlorinated contaminated sites. *Front Microbiol* **3**:351.

93. **Mattes, T. E., A. K. Alexander, and N. V. Coleman.** 2010. Aerobic biodegradation of the chloroethenes: pathways, enzymes, ecology, and evolution. *FEMS Microbiol Rev* **34**:445-475.
94. **May, H. D., and S. K. R.** 2016. "*Dehalobium chlorocoercia*" DF-1—from discovery to application, p.563-586. *In* L. Adrian and F. E. Löffler (ed.), *Organohalide-Respiring Bacteria* Springer Berlin Heidelberg, Berlin.
95. **Maymó-Gatell, X., Chien, Y., Gossett, J. M., and Zinder, S. H.** 1997. Isolation of a bacterium that reductively dechlorinates tetrachloroethene to ethene. *Science* **276**:1568–1571.
96. **Mazon, H., K. Gabor, D. Leys, A. J. Heck, J. van der Oost, and R. H. van den Heuvel.** 2007. Transcriptional activation by CprK1 is regulated by protein structural changes induced by effector binding and redox state. *J Biol Chem* **282**:11281-11290.
97. **McCarty, P. L.** 2010. Groundwater Contamination by Chlorinated Solvents: History, Remediation Technologies and Strategies. SERDP/ESTCP Environmental Remediation Technology:1-28.
98. **McCarty, P. L.** 1994. An overview of anaerobic transformation of chlorinated solvents. *In* EPA symposium on intrinsic bioremediation of ground water:135-142.
99. **Miller, E., G. Wohlfarth, and G. Diekert.** 1997. Comparative studies on tetrachloroethene reductive dechlorination mediated by *Desulfitobacterium* sp. strain PCE-S. *Arch Microbiol* **168**:513-519.
100. **Miller, E., G. Wohlfarth, and G. Diekert.** 1998. Purification and characterization of the tetrachloroethene reductive dehalogenase of strain PCE-S. *Arch Microbiol* **169**:497-502.
101. **Moe, W. M., F. A. Rainey, and J. Yan.** 2016. The genus *Dehalogenimonas*, p.137-152. *In* L. Adrian and F. E. Löffler (ed.), *Organohalide-Respiring Bacteria*. Springer Berlin Heidelberg, Berlin.
102. **Moe, W. M., J. Yan, M. F. Nobre, M. S. da Costa, and F. A. Rainey.** 2009. *Dehalogenimonas lykanthroporepellens* gen. nov., sp. nov., a reductively dehalogenating bacterium isolated from chlorinated solvent-contaminated groundwater. *Int J Syst Evol Microbiol* **59**:2692-2697.
103. **Morita, Y., T. Futagami, M. Goto, and K. Furukawa.** 2009. Functional characterization of the trigger factor protein PceT of tetrachloroethene-dechlorinating *Desulfitobacterium hafniense* Y51. *Appl Microbiol Biotechnol* **83**:775-781.
104. **Morris, R. M., S. Sowell, D. Barofsky, S. Zinder, and R. Richardson.** 2006. Transcription and mass-spectroscopic proteomic studies of electron transport oxidoreductases in *Dehalococcoides ethenogenes*. *Environ Microbiol* **8**:1499-1509.
105. **Müller, J. A., B. M. Rosner, G. Von Abendroth, G. Meshulam-Simon, P. L. McCarty, and A. M. Spormann.** 2004. Molecular identification of the catabolic vinyl chloride reductase from *Dehalococcoides* sp. strain VS and its environmental distribution. *Appl Environ Microbiol* **70**:4880-4888.
106. **Murphy, C. D.** 2003. New frontiers in biological halogenation. *Journal of applied microbiology* **94**:539-548.
107. **Nelson, J. L., J. M. Fung, H. Cadillo-Quiroz, X. Cheng, and S. H. Zinder.** 2011. A role for *Dehalobacter* spp. in the reductive dehalogenation of dichlorobenzenes and monochlorobenzene. *Environ Sci Technol* **45**:6806-6813.
108. **Nelson, J. L., J. Jiang, and S. H. Zinder.** 2014. Dehalogenation of chlorobenzenes, dichlorotoluenes, and tetrachloroethene by three *Dehalobacter* spp. *Environ Sci Technol* **48**:3776-3782.
109. **Neumann, A., H. Scholz-Muramatsu, and G. Diekert.** 1994. Tetrachloroethene metabolism of *Dehalospirillum multivorans*. *Arch Microbiol* **162**:295-301.
110. **Neumann, A., A. Siebert, T. Trescher, S. Reinhardt, G. Wohlfarth, and G. Diekert.** 2002. Tetrachloroethene reductive dehalogenase of *Dehalospirillum multivorans*: substrate specificity of the native enzyme and its corrinoid cofactor. *Arch Microbiol* **177**:420-426.
111. **Neumann, A., G. Wohlfarth, and G. Diekert.** 1996. Purification and characterization of tetrachloroethene reductive dehalogenase from *Dehalospirillum multivorans*. *J Biol Chem* **271**:16515-16519.

112. **Neumann, A., G. Wohlfarth, and G. Diekert.** 1998. Tetrachloroethene dehalogenase from *Dehalospirillum multivorans*: cloning, sequencing of the encoding genes, and expression of the *pceA* gene in *Escherichia coli*. *J Bacteriol* **180**:4140-4145.
113. **Ni, S., J. K. Fredrickson, and L. Xun.** 1995. Purification and characterization of a novel 3-chlorobenzoate-reductive dehalogenase from the cytoplasmic membrane of *Desulfomonile tiedjei* DCB-1. *J Bacteriol* **177**:5135-5139.
114. **Nijenhuis, I., and S. H. Zinder.** 2005. Characterization of hydrogenase and reductive dehalogenase activities of *Dehalococcoides ethenogenes* strain 195. *Appl Environ Microbiol* **71**:1664-1667.
115. **Nonaka, H., G. Keresztes, Y. Shinoda, Y. Ikenaga, M. Abe, K. Naito, K. Inatomi, K. Furukawa, et al.** 2006. Complete genome sequence of the dehalorespiring bacterium *Desulfitobacterium hafniense* Y51 and comparison with *Dehalococcoides ethenogenes* 195. *J Bacteriol* **188**:2262-2274.
116. **Palmer, T., F. Sargent, and B. C. Berks.** 2005. Export of complex cofactor-containing proteins by the bacterial Tat pathway. *Trends in microbiology* **13**:175-180.
117. **Pant, P., and S. Pant.** 2010. A review: advances in microbial remediation of trichloroethylene (TCE). *Journal of environmental sciences* **22**:116-126.
118. **Parthasarathy, A., T. A. Stich, S. T. Lohner, A. Lesnefsky, R. D. Britt, and A. M. Spormann.** 2015. Biochemical and EPR-spectroscopic investigation into heterologously expressed vinyl chloride reductive dehalogenase (VcrA) from *Dehalococcoides mccartyi* strain VS. *J Am Chem Soc* **137**:3525-3532.
119. **Payne, K. A., C. P. Quezada, K. Fisher, M. S. Dunstan, F. A. Collins, H. Sjuts, C. Levy, S. Hay, et al.** 2015. Reductive dehalogenase structure suggests a mechanism for B₁₂-dependent dehalogenation. *Nature* **517**:513-516.
120. **Payne, R. B., H. D. May, and K. R. Sowers.** 2011. Enhanced reductive dechlorination of polychlorinated biphenyl impacted sediment by bioaugmentation with a dehalorespiring bacterium. *Environ Sci Technol* **45**:8772-8779.
121. **Pop, S. M., R. J. Kolarik, and S. W. Ragsdale.** 2004. Regulation of anaerobic dehalorespiration by the transcriptional activator CprK. *J Biol Chem* **279**:49910-49918.
122. **Prat, L.** 2009. Identification and characterization of proteins supporting dehalorespiration in *Desulfitobacterium hafniense* strain TCE1. PhD Thesis. EPFL, Lausanne.
123. **Rahm, B. G., and R. E. Richardson.** 2008. *Dehalococcoides*' gene transcripts as quantitative bioindicators of tetrachloroethene, trichloroethene, and *cis*-1,2-dichloroethene dehalorespiration rates. *Environ Sci Technol* **42**:5099-5105.
124. **Reinhold, A., M. Westermann, J. Seifert, M. von Bergen, T. Schubert, and G. Diekert.** 2012. Impact of vitamin B₁₂ on formation of the tetrachloroethene reductive dehalogenase in *Desulfitobacterium hafniense* strain Y51. *Appl Environ Microbiol* **78**:8025-8032.
125. **Richardson, D. J.** 2000. Bacterial respiration: a flexible process for a changing environment. *Microbiology* **146**:551-571.
126. **Richardson, R.** 2016. Organohalide-Respiring Bacteria as Members of Microbial Communities: Catabolic Food Webs and Biochemical Interactions, p.309-341. In L. Adrian and F. E. Löffler (ed.), *Organohalide-Respiring Bacteria*. Springer Berlin Heidelberg, Berlin.
127. **Ritalahti, K. M., B. K. Amos, Y. Sung, Q. Wu, S. S. Koenigsberg, and F. E. Löffler.** 2006. Quantitative PCR targeting 16S rRNA and reductive dehalogenase genes simultaneously monitors multiple *Dehalococcoides* strains. *Appl Environ Microbiol* **72**:2765-2774.
128. **Rouzeau-Szynalski, K., J. Maillard, and C. Holliger.** 2011. Frequent concomitant presence of *Desulfitobacterium* spp. and "*Dehalococcoides*" spp. in chloroethene-dechlorinating microbial communities. *Appl Microbiol Biotechnol* **90**:361-368.
129. **Rupakula, A., T. Kruse, S. Boeren, C. Holliger, H. Smidt, and J. Maillard.** 2013. The restricted metabolism of the obligate organohalide respiring bacterium *Dehalobacter restrictus*: lessons from tiered functional genomics. *Philosophical transactions of the Royal Society of London. Series B, Biological sciences* **368**:20120325.

130. **Sanford, R. A., J. R. Cole, and J. M. Tiedje.** 2002. Characterization and description of *Anaeromyxobacter dehalogenans* gen. nov., sp. nov., an aryl-halo-respiring facultative anaerobic myxobacterium. *Appl Environ Microbiol* **68**:893-900.
131. **Sargent, F., B. C. Berks, and T. Palmer.** 2006. Pathfinders and trailblazers: a prokaryotic targeting system for transport of folded proteins. *FEMS Microbiol Lett* **254**:198-207.
132. **Scholz-Muramatsu, H., A. Neumann, M. Messmer, E. Moore, and G. Diekert.** 1995. Isolation and characterization of *Dehalospirillum multivorans* gen. nov., sp. nov., a tetrachloroethene-utilizing, strictly anaerobic bacterium. *Arch Microbiol* **163**:48-56.
133. **Schubert, T., and G. Diekert.** 2016. Comparative biochemistry of organohalide respiration, p.397-427. *In* L. Adrian and F. E. Löffler (ed.), *Organohalide-Respiring Bacteria*. Springer-Verlag Berlin Heidelberg.
134. **Schumacher, W., and C. Holliger.** 1996. The proton/electron ration of the menaquinone-dependent electron transport from dihydrogen to tetrachloroethene in "*Dehalobacter restrictus*". *J Bacteriol* **178**:2328-2333.
135. **Schumacher, W., C. Holliger, A. J. Zehnder, and W. R. Hagen.** 1997. Redox chemistry of cobalamin and iron-sulfur cofactors in the tetrachloroethene reductase of *Dehalobacter restrictus*. *FEBS Lett* **409**:421-425.
136. **Schumacher, W., P. M. H. Kroneck, and N. Pfennig.** 1992. Comparative systematic study on '*Spirillum*' 5175, *Campylobacter* and *Wolinella* species. Description of '*Spirillum*' 5175 as *Sulfurospirillum deleyianum* gen. nov., spec. nov. *Arch Microbiol* **158**:287-293.
137. **Seshadri, R., L. Adrian, D. E. Fouts, J. A. Eisen, A. M. Phillippy, B. A. Methe, N. L. Ward, W. C. Nelson, et al.** 2005. Genome sequence of the PCE-dechlorinating bacterium *Dehalococcoides ethenogenes*. *Science* **307**:105-108.
138. **Siebert, A., A. Neumann, T. Schubert, and G. Diekert.** 2002. A non-dechlorinating strain of *Dehalospirillum multivorans*: evidence for a key role of the corrinoid cofactor in the synthesis of an active tetrachloroethene dehalogenase. *Arch Microbiol* **178**:443-449.
139. **Smidt, H., and W. M. de Vos.** 2004. Anaerobic microbial dehalogenation. *Annu Rev Microbiol* **58**:43-73.
140. **Smidt, H., M. van Leest, J. van der Oost, and W. M. de Vos.** 2000. Transcriptional regulation of the *cpr* gene cluster in *ortho*-chlorophenol-respiring *Desulfitobacterium dehalogenans*. *J Bacteriol* **182**:5683-5691.
141. **Steffan, R. J. S. C. E.** 2016. Current and future bioremediation applications : bioremediation from a practical and regulatory perspective, p.517-540. *In* L. Adrian and F. E. Löffler (ed.), *Organohalide-Respiring Bacteria*. Springer Berlin Heidelberg.
142. **Stringer, R., and P. Johnston.** 2001. Chlorine and the environment: an overview of the chlorine industry. Springer Science+Business Media B.V., Netherlands.
143. **Sun, B., J. R. Cole, R. A. Sanford, and J. M. Tiedje.** 2000. Isolation and characterization of *Desulfovibrio dechloracetivorans* sp. nov., a marine dechlorinating bacterium growing by coupling the oxidation of acetate to the reductive dechlorination of 2-chlorophenol. *Appl Environ Microbiol* **66**:2408-2413.
144. **Sun, B., B. M. Griffin, H. L. Ayala-del-Rio, S. A. Hashsham, and J. M. Tiedje.** 2002. Microbial dehalorespiration with 1,1,1-trichloroethane. *Science* **298**:1023-1025.
145. **Sung, Y., K. E. Fletcher, K. M. Ritalahti, R. P. Apkarian, N. Ramos-Hernandez, R. A. Sanford, N. M. Mesbah, and F. E. Löffler.** 2006. *Geobacter lovleyi* sp. nov. strain SZ, a novel metal-reducing and tetrachloroethene-dechlorinating bacterium. *Appl Environ Microbiol* **72**:2775-2782.
146. **Sung, Y., K. M. Ritalahti, R. A. Sanford, J. W. Urbance, S. J. Flynn, J. M. Tiedje, and F. E. Löffler.** 2003. Characterization of two tetrachloroethene-reducing, acetate-oxidizing anaerobic bacteria and their description as *Desulfuromonas michiganensis* sp. nov. *Appl Environ Microbiol* **69**:2964-2974.

147. **Suyama, A., M. Yamashita, S. Yoshino, and K. Furukawa.** 2002. Molecular characterization of the PceA reductive dehalogenase of *Desulfitobacterium* sp. strain Y51. *J Bacteriol* **184**:3419-3425.
148. **Szynalski, K.** 2003. Ecophysiology and molecular identification of microbial populations involved in the reductive dechlorination of chloroethenes. PhD Thesis. EPFL, Lausanne.
149. **Tang, S., W. W. Chan, K. E. Fletcher, J. Seifert, X. Liang, F. E. Löffler, E. A. Edwards, and L. Adrian.** 2013. Functional characterization of reductive dehalogenases by using blue native polyacrylamide gel electrophoresis. *Appl Environ Microbiol* **79**:974-981.
150. **Tarnawski, S.-E., P. Rossi, M. V. Brennerova, M. Stavelova, and C. Holliger.** 2016. Validation of an Integrative Methodology to Assess and Monitor Reductive Dechlorination of Chlorinated Ethenes in Contaminated Aquifers. *Frontiers in Environmental Science*:4:7.
151. **Thibodeau, J., A. Gauthier, M. Duguay, R. Villemur, F. Lepine, P. Juteau, and R. Beaudet.** 2004. Purification, cloning, and sequencing of a 3,5-dichlorophenol reductive dehalogenase from *Desulfitobacterium frappieri* PCP-1. *Appl Environ Microbiol* **70**:4532-4537.
152. **Van de Pas, B. A.** 2000. Biochemistry and physiology of halo-respiration by *Desulfitobacterium dehalogenans*. Wageningen Institute for Environment and Climate Research, Wageningen.
153. **van de Pas, B. A., J. Gerritse, W. M. de Vos, G. Schraa, and A. J. Stams.** 2001. Two distinct enzyme systems are responsible for tetrachloroethene and chlorophenol reductive dehalogenation in *Desulfitobacterium* strain PCE1. *Arch Microbiol* **176**:165-169.
154. **van de Pas, B. A., H. Smidt, W. R. Hagen, J. van der Oost, G. Schraa, A. J. Stams, and W. M. de Vos.** 1999. Purification and molecular characterization of *ortho*-chlorophenol reductive dehalogenase, a key enzyme of halo-respiration in *Desulfitobacterium dehalogenans*. *J Biol Chem* **274**:20287-20292.
155. **van Doesburg, W., M. H. van Eekert, P. J. Middelorp, M. Balk, G. Schraa, and A. J. Stams.** 2005. Reductive dechlorination of beta-hexachlorocyclohexane (beta-HCH) by a *Dehalobacter* species in coculture with a *Sedimentibacter* sp. *FEMS Microbiol Ecol* **54**:87-95.
156. **van Eekert, M. H. A., A. J. M. Stams, J. A. Field, and G. Schraa.** 1999. Gratuitous dechlorination of chloroethanes by methanogenic granular sludge. *Applied Microbiology and Biotechnology* **51**:46-52.
157. **Villemur, R., M. Lanthier, R. Beaudet, and F. Lepine.** 2006. The *Desulfitobacterium* genus. *FEMS Microbiol Rev* **30**:706-733.
158. **Vogel, T. M., C. S. Criddle, and P. L. McCarty.** 1987. ES Critical Reviews: Transformations of halogenated aliphatic compounds. *Environ Sci Technol* **21**:722-736.
159. **Wang, S., W. Zhang, K. L. Yang, and J. He.** 2014. Isolation and characterization of a novel *Dehalobacter* species strain TCP1 that reductively dechlorinates 2,4,6-trichlorophenol. *Biodegradation* **25**:313-323.
160. **Wei K., G. A., Chan W. W.M., Richardson R. E., Edwards E. A.** 2016. Electron acceptor interactions between organohalide-respiring bacteria: cross-feeding, competition, and inhibition, p.283-308. *In* L. Adrian and F. E. Löffler (ed.), *Organohalide-Respiring Bacteria*. Springer Berlin Heidelberg.
161. **Werner, J. J., A. C. Ptak, B. G. Rahm, S. Zhang, and R. E. Richardson.** 2009. Absolute quantification of *Dehalococcoides* proteins: enzyme bioindicators of chlorinated ethene dehalorespiration. *Environ Microbiol* **11**:2687-2697.
162. **Wever R, v. d. H. M.** 2013. The role of vanadium haloperoxidases in the formation of volatile brominated compounds and their impact on the environment. *Dalton Trans* **42**:11778-11786.
163. **Yoshida, N., L. Ye, D. Baba, and A. Katayama.** 2009. A novel *Dehalobacter* species is involved in extensive 4,5,6,7-tetrachlorophthalide dechlorination. *Appl Environ Microbiol* **75**:2400-2405.
164. **Zhao, J. S., D. Manno, C. Beaulieu, L. Paquet, and J. Hawari.** 2005. *Shewanella sediminis* sp. nov., a novel Na⁺-requiring and hexahydro-1,3,5-trinitro-1,3,5-triazine-degrading bacterium from marine sediment. *Int J Syst Evol Microbiol* **55**:1511-1520.

165. **Zinder, S.** 2016. The genus *Dehalococcoides*, p.107-136. In L. Adrian and F. E. Löffler (ed.), Organohalide-Respiring Bacteria. Springer Berlin Heidelberg, Berlin.

Chapter 2

Characterization of an unusual
Sulfurospirillum reductive
dehalogenase dechlorinating
tetrachloroethene to
trichloroethene

2. Characterization of an unusual *Sulfurospirillum* reductive dehalogenase dechlorinating tetrachloroethene to trichloroethene

2.1. Abstract

Tetrachloroethene (PCE) represents a major groundwater pollutant. Some bacteria are able to use PCE as electron acceptor in an anaerobic respiration process called organohalide respiration (OHR). A bacterial consortium (SL2-PCEc) containing *Sulfurospirillum diekertiae* strain SL2-1 is known to catalyze the dechlorination of PCE to trichloroethene (TCE) as end-product. The key enzyme, named PceA_{TCE}, displays 92% amino acid sequence identity with PceA from *S. multivorans*. The unique features of the PceA_{TCE} enzyme were explored further in this chapter.

In this work, PceA_{TCE} of *S. diekertiae* SL2-1 was purified by chromatography which resulted in two successive enzyme preparations displayed the following properties. Relatively small amount of purified proteins were recovered (0.25 and 1.3 mg), each of them displaying 127- and 82-fold purification factor, 2'425 and 1'144 nkat/mg of reductive dehalogenase activity with PCE, but only 8 and 11% of yield in comparison with the crude extracts, respectively. From one enzyme preparation, the corrinoid cofactor of PceA_{TCE} was extracted and was identified as norpseudovitamin B₁₂, as in PceA from *S. multivorans*. On physiological level, re-routing the *de novo* corrinoid biosynthesis of the SL2-PCEc consortium by adding DMB did not impact the growth rate of the culture on PCE, in contrast to what has been observed with *S. multivorans*. Based on the recent crystal structure of *S. multivorans* PceA, a structure model of the active site of the PceA_{TCE} enzyme was proposed which highlighted eight unique residues in PceA_{TCE} that are different from but consistently conserved in the other *Sulfurospirillum* spp. enzymes catalyzing PCE to *cis*-DCE dechlorination. These differences might result in altered structural properties of PceA_{TCE} which could be the basis for the differences in the restricted substrate range of this enzyme. This study clearly demonstrated the importance of pursuing biochemical studies on new reductive dehalogenases.

2.2. Introduction

Sulfurospirillum multivorans represents one of the first isolated bacteria growing with tetrachloroethene (PCE) as electron acceptor (24). Over the years, it became a model organism of organohalide-respiring bacteria (OHRB). The key enzyme in this process, the PCE reductive dehalogenase (PceA) catalyzing the dechlorination of tetrachloroethene (PCE) to *cis*-dichloroethene (*cis*-DCE), and its corresponding gene were the first to be identified (26, 27). As essential cofactor present in reductive dehalogenases, corrinoids are responsible for their catalytic activity (22, 24, 31). One can distinguish corrinoids from one another based on the structure of the lower axial ligand which can be 5,6-dimethylbenzimidazole (DMB), a purine, or a phenolic compound (28) (Figure 2.1). Siebert *et al.* reported that the corrinoid cofactor of PceA is synthesized *de novo* in *S. multivorans* (32). In addition, the identification of the corrinoid present in PceA of *S. multivorans* has revealed a new corrinoid structure, namely norpseudovitamin B₁₂ which differs from the classical cobalamin by two aspects: an adenine group instead of DMB is found as base of the lower ligand, and the nucleotide loop of norpseudovitamin B₁₂ lacks a methyl group at position 176 of the corrinoid (15). In a recent study, the specificity of *S. multivorans* PceA enzyme for norpseudovitamin B₁₂ cofactor was assessed by re-routing the *de novo* corrinoid biosynthesis. The presence of exogenous DMB resulted in the formation of norvitamin B₁₂ and affected PCE-dependent growth of the bacterium (14). Furthermore, the crystal structure of PceA of *S. multivorans* has been solved recently, showing for the first time, in comparison with the sequence of other RdhA enzymes, how the corrinoid supports the reductive dechlorination by exploiting a conserved corrinoid-binding protein scaffold capped by a highly variable substrate-binding region (5).

In an earlier study, a bacterial consortium (SL2-PCEc) containing *Sulfurospirillum* sp. strain SL2-1, was shown to catalyze the dechlorination of PCE to trichloroethene (TCE) as end-product. The key enzyme, named PceA_{TCE}, displays 92% amino acid sequence identity with *S. multivorans* PceA (7). Due to its incapacity to dechlorinate TCE, it was already used in another study as a model OHR culture for one-step PCE dechlorination (3). This feature further raised interest in the properties of the enzyme responsible for the restricted substrate range. Therefore the characterization of PceA_{TCE} was undertaken here.

In this chapter, PceA_{TCE} of *Sulfurospirillum* sp. strain SL2-1 (named as *S. diekertiae* strain SL2-1, see CHAPTER 3) was purified by chromatography and characterized on biochemical levels. The corrinoid of PceA_{TCE} was extracted and revealed norpseudovitamin B₁₂ as in *S. multivorans* PceA. Rerouting the *de novo* corrinoid biosynthesis of the SL2-PCEc consortium by adding DMB did not impact the growth rate of the culture on PCE. Finally, a structure model of the active site of PceA_{TCE} was established and compared to the structure of *S. multivorans* PceA.

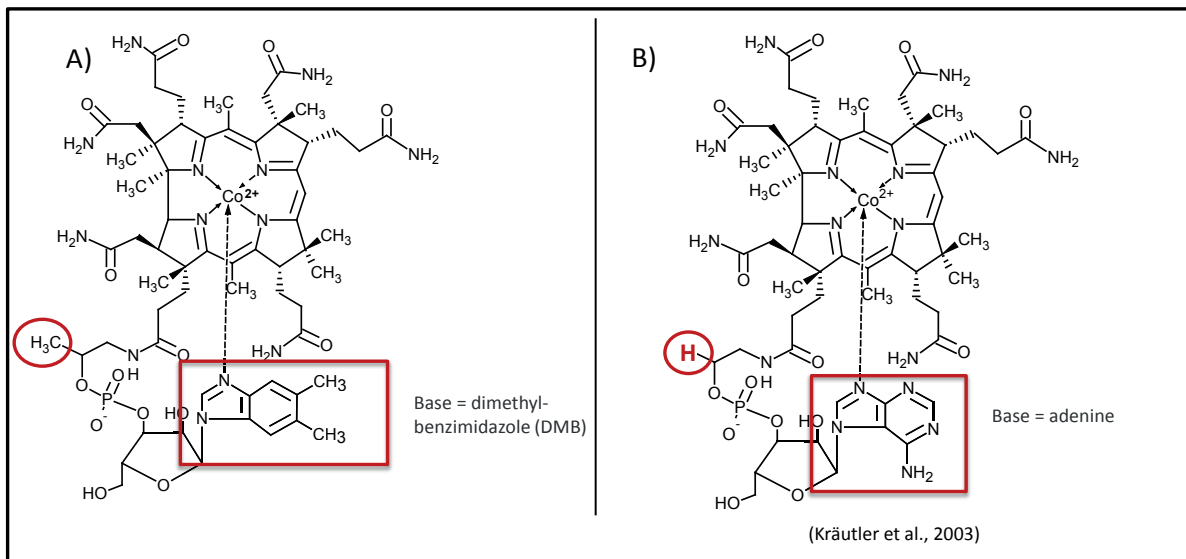


Figure 2.1. Structure of cobamides.

Structure of (A) cobalamin with 5,6-dimethylbenzimidazole as the base of the lower ligand (red box), and of (B) norpseudovitamin B₁₂, where adenine replaces DMB (red box) and a methyl group is missing in the nucleotide loop (red circle).

2.3. Material and methods

All chemicals were analytical grade and used without purification. The gases (N₂, CO₂, H₂) were purchased from SLGas.

2.3.1. Bacterial strains and growth conditions

This work investigated the SL2-PCEc bacterial consortium which is dominated by *Sulfurospirillum diekertiae* strain SL2-1. The original enrichment culture (SL2) has been established at LBE from the biomass of a fixed-bed bioreactor treating PCE-contaminated groundwater (18, 29). The cultivation of the SL2 derived consortia was carried out in serum bottles of 100, 500 or 1000 mL (VWR international) containing 50, 200, 300 or 800 mL of anaerobic medium as described previously (18), with the following few modifications: cyanocobalamin was omitted in some experiments; either formate or pyruvate was added as electron donor to a final concentration of 20 mM, in the case of formate, 2 mM acetate was added as carbon source; as terminal electron acceptor, the medium was amended with 10% (v/v) of 100 mM PCE or TCE dissolved in hexadecane so that the nominal PCE concentration in the aqueous phase was 20 μM for a total available substrate concentration of 10 mM.

Escherichia coli DH5α (genotype: *F endA1 glnV44 thi-1 recA1 relA1 gyrA96 deoR nupG* Φ 80*dlacZ*Δ*M15* Δ(*lacZYA-argF*)*U169*, *hsdR17*(*r_K⁻ m_K⁺*), λ-) was used as a host for molecular cloning. *E. coli* competent cells were prepared using the standard CaCl₂ method (30). The strain was cultivated at 37°C in Luria-Bertani (LB) liquid medium or agar plates containing 100 μg/mL of ampicillin when needed.

2.3.2. Purification of the PceA_{TCE} reductive dehalogenase

The PceA_{TCE} enzyme was purified by a procedure described elsewhere (14). The bacteria were harvested by centrifugation at 5'000 × *g* and 4°C for 20 min, frozen in liquid nitrogen, and stored at -80°C. Cell pellets were resuspended in 50 mM Tris-HCl (pH 7.5) containing 0.5 mM dithiothreitol and protease inhibitor (SigmaFAST™ Protease Inhibitor Cocktail Tablet, Sigma-Aldrich). Cell debris and membranes were removed by centrifugation for 45 min at 100'000 × *g* and 4°C. All steps were performed in an anaerobic chamber with N₂/H₂ (95/5%) as the gas phase. The purification procedure comprised three successive chromatography steps with a Q-Sepharose, a Phenyl Superose and a Mono Q column. For each step, elution

fractions were assessed for the presence of PceA_{TCE} by the measurement of enzymatic activity (see below). Briefly, the cell-free extract was loaded on a Q-Sepharose HP column pre-equilibrated with basic buffer (50 mM Tris-HCl, pH 7.5, containing 0.5 mM dithiothreitol). The reductive dehalogenase was eluted with a linear gradient from 0 to 1 M KCl in basic buffer. Fractions of interest were pooled, and 3.2 M ammonium sulfate dissolved in basic buffer was added to reach a final concentration of 0.4 M. The sample was then applied to a Phenyl-Superose HR column pre-equilibrated with 0.4 M ammonium sulfate in basic buffer. The PceA_{TCE} enzyme was eluted with a linear gradient from 0.4 to 0.0 M ammonium sulfate in basic buffer. Fractions of interest were pooled and diluted 7x in basic buffer. The sample was finally purified on a Mono Q10/10 column pre-equilibrated with HEPES basal buffer (50 mM, pH 7.5) containing 0.5 mM dithiothreitol. The reductive dehalogenase was eluted with a linear gradient from 0.0 to 0.5 M NaCl in basic buffer. Fractions of interest were pooled.

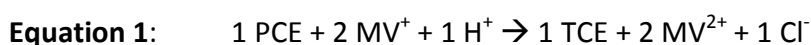
2.3.3. SDS-PAGE and Western blot analysis

Crude extracts of SL2-PCEc biomass (5 µg protein/lane) or purified PceA_{TCE} enzyme (1 or 10 µg protein/lane) were subjected to sodium dodecyl sulfate polyacrylamide gel electrophoresis (SDS-PAGE) with 12.5% acrylamide in the resolving gel (30). Gels were either stained for total proteins with Coomassie R250 brilliant blue, or blotted onto polyvinylidene difluoride (PVDF) membrane (2) using the Transblot Semi-Dry apparatus according to manufacturer's instructions (Bio-Rad Laboratories) at 200 mA for 1 h using the 3-buffers system as recommended by the membrane supplier. Western blot analyses were conducted as described earlier (12). Briefly, the PVDF membrane was blocked for 1 h in PBST (140 mM NaCl, 10 mM KCl, 6.4 mM Na₂HPO₄, 2 mM KH₂PO₄, 0.05% [v/v] Tween 20) containing 1% blocking reagent (Roche). After the PVDF membrane was washed 3× 10 min with PBST, the antiserum raised against *S. multivorans* PceA diluted 50'000-fold in PBST was applied at room temperature for 1 h. Subsequently, the membrane was washed 2× 10 min with PBST and incubated for 2 h with the secondary antibody (goat anti-rabbit antibody-alkaline phosphatase conjugate, Sigma-Aldrich), diluted 20'000-fold in PBST. After washing of the PVDF membrane 3× 10 min with PBST, the reaction mixture for the alkaline phosphatase activity was added (0.34 mg nitroblue tetrazolium and 0.175 mg 5-bromo-4-chloro-3-indolyl

phosphate per mL of developing buffer containing 100 mM Tris-HCl, pH 9.5, 100 mM NaCl and 50 mM MgCl₂). The reaction was stopped after 10 min with 10 mM Tris-HCl, pH 7.5, containing 1 mM EDTA.

2.3.4. Reductive dehalogenase activity assay

The reductive dehalogenase activity was measured spectrophotometrically at 25°C in rubber-stoppered glass cuvettes filled with nitrogen as described elsewhere (26). The reduction of one molecule of PCE was measured as the oxidation of two molecules of reduced methyl viologen according to Equation 1. Alternatively, TCE or 1,1,3-trichloropropene were used in the assay. The assay was conducted in 100 mM Tris-HCl buffer (pH 7.5) containing 0.5 mM methyl viologen (with coefficient $\epsilon_{578} = 9.7 \text{ mM}^{-1} \text{ cm}^{-1}$) and 4 mM ammonium sulfate. Methyl viologen was chemically reduced up to an absorbance value of 3.0 ($A_{578 \text{ nm}}$) by the addition of titanium(III) citrate solution (40). PceA_{TCE} enzyme was then added. The absorbance was again monitored until a stable signal was reached, and then the substrate was added from 80 mM stock solution in ethanol.



The absorbance was monitored for 2-3 min and the absolute value of the initial reaction rate ($\Delta A/\Delta t$) was used to calculate the enzymatic RDH activity according to Equation 2.

Equation 2: $activity \text{ [nkat]} = \frac{1}{2} \times \left\{ \frac{\Delta A}{\Delta t} / \epsilon \times l \right\} / V_R$

where nkat (nanokatal) is in 10^{-9} mol/s , ϵ is the extinction coefficient, l is the path length (1 cm), V_R is the reaction volume (1.8 mL). Finally, the specific activity (nkat/mg protein) was calculated with the estimated protein concentration (see below).

2.3.5. Cobamide extraction

Cobamide extraction and purification was performed according to the protocol originally described by Stupperich and colleagues (33). The pH of a purified fraction of PceA_{TCE} was lowered to a value ≤ 5 with acetic acid. Subsequently, 0.1 M potassium cyanide was added and the sample was boiled for 15 min. After centrifugation for 10 min at $6'700 \times g$, the supernatant containing the cobamides was kept at room temperature, and the pellet was

resuspended in 1 mL milliQ water. The resuspended pellet was subjected to the same extraction procedure a second time. The pooled supernatants from successive extractions were mixed with 0.25 g Amberlite XAD4 per ml extract (Sigma-Aldrich) and incubated on a shaker overnight. After sedimentation of the cobamide-loaded XAD4 material, the supernatant was removed. The XAD4 material was washed with 10 vol. of milliQ water. Subsequently, the cobamides were eluted with one volume of methanol (1 h incubation on a shaker). The elution was repeated a second time. The cobamide-containing eluates were dried completely using a vacuum concentrator. The dry sample was resuspended in 2 mL milliQ water and transferred to a column containing 3 g aluminum oxide. The cobamides were recovered from the column by eluting with 40 mL milliQ water. The eluate was dried as above and the pellet was resuspended in 100 μ L milliQ water.

2.3.6. Molecular methods

2.3.6.1. SL2 consortium biomass sampling for DNA extraction

A volume of 50-100 mL of the SL2-PCEc culture was collected by centrifugation at $3'300 \times g$ for 10 min at 4°C. Cell pellets were washed in a 1 mL of 50 mM Tris-HCl buffer (pH 8.0) and transferred to a 1.5 mL microcentrifuge tube. The cells were centrifuged at $8'800 \times g$ for 5 min at 4°C and biomass pellets were flash-frozen in liquid N₂ and stored at -80°C until further use.

2.3.6.2. DNA Extraction

Biomass pellets were resuspended and lyzed in lysis buffer containing 20 mM Tris-HCl (pH 8.0), 2 mM sodium-EDTA, 1.2% Triton[®] X-100 and 20 mg/mL lysozyme. The DNA extraction kit DNeasy[®] Blood & Tissue (Qiagen) was used for genomic DNA extraction according to manufacturer's instructions. Finally 200 μ L DNA samples were recovered. The extracted DNA was quantified with the NanoDrop spectrophotometer (ND-1000, Thermo Fisher Scientific), and the DNA concentration was normalized to 5 ng/ μ L for all samples.

2.3.6.3. DNA amplification by polymerase chain reaction (PCR)

Standard PCR was performed under the following conditions: a 50 μL PCR mixture contained 5 μL of Taq DNA Polymerase 10 \times buffer, 6 μL of 2.5 mM dNTPs, 0.4 μL of 25 mM MgCl_2 , 2.5 μL of 10 μM each primer (purchased at Microsynth) (Table 1), 0.25 μL of Taq DNA Polymerase (PEQLAB Biotechnologie), and 5 μL of DNA template at 5 ng/ μL . The DNA was amplified in a T3 Thermocycler (Biometra), with the following program: 5 min initial denaturation at 94°C, 30 cycles of 1 min denaturation at 94°C, 1 min of primer annealing at 53°C (for *rdhA* genes) or 56°C (for 16S rRNA genes), 1-4 min of elongation at 72°C, depending of the target size. A final extension step of 10 min at 72°C was included.

2.3.6.4. Agarose gel electrophoresis

Agarose gel electrophoresis was performed to visualize PCR products. Agarose gels were prepared fresh in 0.5 \times TAE buffer (containing 20 mM Tris-acetate, 0.5 mM EDTA, pH 8.3). GelRed (Biotium) was added at 1:10'000 dilution before casting the gels. The gels were then loaded with 6 \times loading buffer (Promega) along with the DNA sample and electrophoresis was run at 100 V for 45 min. DNA was visualized using the Syngene gel imaging system (Syngene).

2.3.6.5. Cloning of PCR products

For cloning, PCR products were purified with the QIAquick PCR Purification Kit (Qiagen) according to manufacturer's instructions, and then treated for A-tailing according to the pGEM-T manual (Promega). For ligation, a volume of 10 μL contained 5 μL of 2 \times ligation buffer, 1 μL of pGEM[®]-T Easy vector (50 ng), 1 μL of T4 DNA ligase provided in the cloning kit and a volume of PCR product determined by Equation 3 following a 1:3 vector:insert ratio. Ligated products were transformed into 50 μL of CaCl_2 -competent *E. coli* DH5 α cells by the heat shock procedure. Briefly, after 20 min on ice, the sample is incubated 1 min at 42°C and then 3 min on ice (30). A volume of 950 μL of LB medium was added to the cells which were incubated 1 h at 37°C and 180 rpm before plating them onto LB plates containing 100 $\mu\text{g}/\text{mL}$ of ampicillin. Plates were incubated overnight at 37°C.

Equation 3: $\text{ng of insert} = \frac{\text{ng of vector} \times \text{kb size of insert}}{\text{kb size of vector}} \times \frac{\text{insert}}{\text{vector}}$ molar ratio

2.3.6.6. Colony PCR and plasmid preparation

E. coli transformants were resuspended in 10 μL of sterile H_2O , lysed for 5 min at 95°C and briefly centrifuged. One μL of supernatant was used as template in a 10 μL standard PCR reaction with T7 and SP6 primers targeting the insertion site in the cloning vector. The PCR products were analyzed by agarose gel electrophoresis. Colonies containing DNA fragments of expected length were selected and cultivated overnight in 10 mL of LB medium containing 100 $\mu\text{g}/\text{mL}$ ampicillin. The next day, plasmid isolation was performed with the Plasmid Miniprep kit (Qiagen) according to manufacturer's instructions.

2.3.6.7. DNA sequencing and sequence analysis

Cycle sequencing reactions were performed with our in-house sequencing equipment using the BigDye Terminator v3.1 Ready Reaction Kit (Applied Biosystems) under the following conditions: a 10 μL sequencing mixture contained 2 μL of mix v3.1, 1.6 μL of 1 μM T7 or SP6 primer, 100-200 ng of plasmid DNA and the remaining volume of H_2O . The DNA was amplified with the following program: 2 min initial denaturation at 94°C , 24 cycles of 30 s denaturation at 94°C , 30 s of primer annealing at 50°C , 4 min of elongation at 60°C . A final extension step of 10 min at 72°C was included. For the precipitation of sequencing products, a volume of 64 μL of 100% ethanol and 26 μL of H_2O were added to the 10 μL of sequencing reaction products. The sample was incubated in the dark at room temperature for 20 min, and then centrifuged for 20 min at full speed in a tabletop centrifuge. After removing the supernatant, the pellets were washed with 250 μL of 70% ethanol and centrifuged again for 10 min. After removing the supernatant, samples were centrifuged again for 1 min and the rest of liquid was removed. Then the DNA pellet was air-dried for 5-10 min and resuspended in 10 μL of formamide. The sample was incubated 2 min at 95°C , then 3 min on ice. Samples were run on the ABI Prism 3130XL Genetic Analyzer (Applied Biosystems). Sequences were analyzed with the software SeqMan (DNASar, Inc) and aligned with ClustalX (36). The sequences were compared with databases using the online software BLAST (1).

2.3.6.8. Quantitative PCR (qPCR)

For qPCR, a plasmid containing the *pceA_{TCE}* sequence was obtained as described above. It was linearized by digestion for 2 h at 37°C under the following conditions: 10 U of *ScaI* restriction enzyme (Promega), 1 µL of 10× buffer, 0.2 µL of BSA, 1 µg of plasmid DNA and the remaining volume of H₂O to a final volume of 10 µL. The plasmid was finally purified with the Qiagen PCR purification kit and eluted in 30 µL according to the instructions. The DNA was quantified and gene copy number per microliter was calculated from the size of the plasmid (in base pairs), the average molecular weight of a base pair in double-stranded DNA (650 g/mol) and the obtained plasmid concentration according to Equation 4. The qPCR standards were diluted from 10⁷ down to 10¹ copies/µL.

Equation 4:
$$\text{copie}/\mu\text{L} = \frac{\text{DNA concentration (ng}/\mu\text{L)}}{\frac{10^9}{\text{Molecular Weight}}} \times \text{Avogadro's number}$$

Reactions for qPCR were prepared as follows: per 10 µL reaction volume, 5.0 µL of KAPA SYBR® FAST qPCR mix (KAPABiosystems), 0.2 µL of each primer (Table 2.1) and 2.1 µL of milliQ water. A volume of 2.5 µL DNA template (qPCR standards or cell suspension pretreated by heating them in boiled water at 100°C for 5 min) was added as template to each tube. Samples and standards were always analyzed in triplicates.

Quantitative PCR was performed in a RotorGene RG3000 real-time PCR machine (Corbett Research) using the 72-well rotor. The program for qPCR was as follows: 15 min 94°C initial denaturation, followed by 40 cycles of 30 s at 94°C, 20 s at 60°C, and 30 s at 72°C, after which acquisition took place using the SYBR detection channel. Finally, a melting curve ranging from 50 to 99°C was performed with 1°C steps and a hold of 5 s. For each run standards were included and the gene copy number of samples were calculated with the calibration established from the standards.

The Rotor-Gene Analysis Software V6.0 was used for the analysis of qPCR data. Threshold fluorescence levels were set at a value of 0.1 in order to compare runs. Slopes values of semi-logarithmic regression of the standards were routinely around -3.6 ± 0.4 . Run performances are given in Table 2.2 for each run. The obtained data were expressed as copy number per µL ($\text{cn} \cdot \mu\text{L}^{-1}$) of initial DNA samples.

2.3.7. Additional analytical procedures

The dechlorination activity of the cultures was followed by measuring the concentration of chloride in the aqueous phase by silver ion titration with a Chlor-o-counter (Flohr Instrument) (29). Chloroethenes were analyzed by gas chromatography as previously described (35).

Protein concentrations were determined with the method described by Bradford (6) using the Roti-Nanoquant reagent (Carl Roth GmbH). A standard curve using BSA was established.

DNA samples were quantified using the Nanodrop apparatus (Nanodrop ND-1000). DNA purity was verified using absorbance ratios of 260 nm/280 nm and 260 nm/230 nm.

The extracted cobamides were analyzed using HPLC (Knauer GmbH) combined with a diode array detector. A reverse phase column was used (Chromolith Performance, RP-18e, 100-4.6 mm, Merck) with a flow rate of 1 mL/min at 30°C. Mobile phases used were 18% methanol/0.2% acetic acid in water (solvent A) and 99.8% methanol/0.2% acetic acid (solvent B). The cobamides were separated by running 10 min with solvent A, followed by a gradient to 100% solvent B within 4 min, and finally 100% solvent B for 3 min. To ensure reproducibility a set of cobamide mix standards (10 µM each) containing norpseudovitamin B₁₂, norvitamin B₁₂ (both purified from *S. multivorans*), pseudovitamin B₁₂ (purified from *Propionibacterium acidipropionici* according to (9) and vitamin B₁₂ (Sigma-Aldrich) was included in a series of HPLC analyses. In a first run, mixture of standard cobamides was analyzed and in subsequent runs unknown samples were analyzed.

Table 2.1. Oligonucleotides used in the work.

Primer name	Target gene	Primer sequence 5' → 3'	Reference
T1-PTQ-f	<i>pceA_{TCE}</i>	CTTTGGAGGTAACCTTTGGAGGTTA	(7)
T1-PTQ-r		CTTTAGGCCAAGATTGTTTCATCT	(7)
SP6	pGEM-T Easy MCS	ATTTAGGTGACACTATAGAA	Promega
T7		TAATACGACTCACTATAGGG	Promega

Table 2.2. Parameters of the quantitative PCR runs targeting the *pceA_{TCE}* gene

Run #	1	2	3	4
Efficiency	0.903	0.898	0.901	0.887
R ²	0.9995	0.9997	0.9994	0.9995

2.4. Results and discussion

Sulfurospirillum diekertiae strain SL2-1 from the SL2-PCEc bacterial consortium harbors a PCE reductive dehalogenase, here referred to as PceA_{TCE}, which shares 92% of amino acid sequence identity with the well characterized PceA of *S. multivorans*. While the majority of RdhA designated as PceA dechlorinate PCE to *cis*-DCE, this new reductive dehalogenase catalyzes exclusively the first step in PCE dechlorination with a 5-fold higher rate than PceA of *S. multivorans* and PceA_{DCE} from *S. diekertiae* strain SL2-2 (from the SL2-TCE consortium) as measured in crude extracts (7). Therefore, it is of great interest to investigate the sequence-substrate relationships of *Sulfurospirillum* reductive dehalogenases.

Purification and characterization of the native PceA_{TCE} reductive dehalogenase was performed in order to study the kinetic parameters of this rather peculiar reductive dehalogenase and to compare with PceA of *S. multivorans*. The identification of the corrinoid associated with PceA_{TCE} was also undertaken, as well as the effect of rerouting the *de novo* corrinoid biosynthesis on the culture harboring PceA_{TCE}. Finally, a structure model for PceA_{TCE} was obtained in an attempt to identify specific amino acids involved in the substrate spectrum definition. The work presented in this chapter was performed in collaboration with the laboratory of Prof. G. Diekert (Friedrich-Schiller University, Jena, Germany).

2.4.1. Purification and kinetic parameters of the PceA_{TCE} enzyme

The SL2-PCEc consortium expressing the *pceA_{TCE}* gene was cultivated using pyruvate and fumarate as electron donor and acceptor, respectively. Two purification experiments were carried out from biomass samples of 6.8 g and 12 g (wet biomass), respectively. After cell disruption and fractionation, the PceA_{TCE} enzyme was purified by using a protocol specifically developed for the purification of *S. multivorans* PceA, starting from the soluble extract using three successive chromatography columns: Q-Sepharose, Phenyl-Superose and Mono-Q (26). At each chromatography step, PceA_{TCE}-containing fractions were identified by performing the reductive dehalogenase assay, pooled together and loaded on the next column.

To illustrate the procedure, the purification of PceA_{TCE} is described for the first biomass sample (6.8 g). Fractions 14-18 eluted from the Q-Sepharose column were pooled and

loaded on a Phenyl-Superose column (see chromatogram in Figure 2.2). Subsequently, fractions 17-20 and 22-25 were collected and loaded onto the Mono-Q column (fraction 21 was used for the corrinoid extraction, see below). Fractions 20 and 21 that displayed reductive dehalogenase activity, were pooled, and showed a specific activity of 2'425 nkat/mg. For the purification from the second biomass sample, a specific activity of 1'144 nkat/mg was obtained. The results of both purifications are summarized in Table 2.3.

Table 2.3. Purification runs of PceA_{TCE}

	Purification step	Total activity (nkat^a)	Yield (%)	Total protein content (mg)	Specific activity (nkat/mg)	Purif. factor (-fold)
1 st purification (6.8 g of wet biomass)	Crude extract	7'554	100	391	19	1
	Q-Sepharose	5'360	71	47	113	6
	Phenyl-Superose	786	10	0.6	1'376	72
	Mono Q	607	8	0.25	2'425	127
2 nd purification (12 g of wet biomass)	Crude extract	13'919	100	981	14	1
	Q-Sepharose	7'061	51	174	41	3
	Phenyl-Superose	4'253	31	10	412	29
	Mono Q	1'535	11	1.3	1'144	82

^a 1 nkat is defined as 1 nmol of PCE reduced to TCE or 2 nmol of methyl viologen oxidized per second.

During the Phenyl-Superose chromatography, the total activity decreased dramatically for the first purification attempt, while in the case of the second attempt, most of activity was lost during the Q-Sepharose and Mono-Q chromatography steps. Nevertheless, the purification factors of both attempts were relatively high, 127- and 82-fold, respectively (Table 2.3). The reason for the lower purification factor of the second attempt is probably due to some oxidative damage during protein purification which is likely leading to protein degradation due to the position of the [4Fe-4S] cluster nearest the enzyme surface (11).

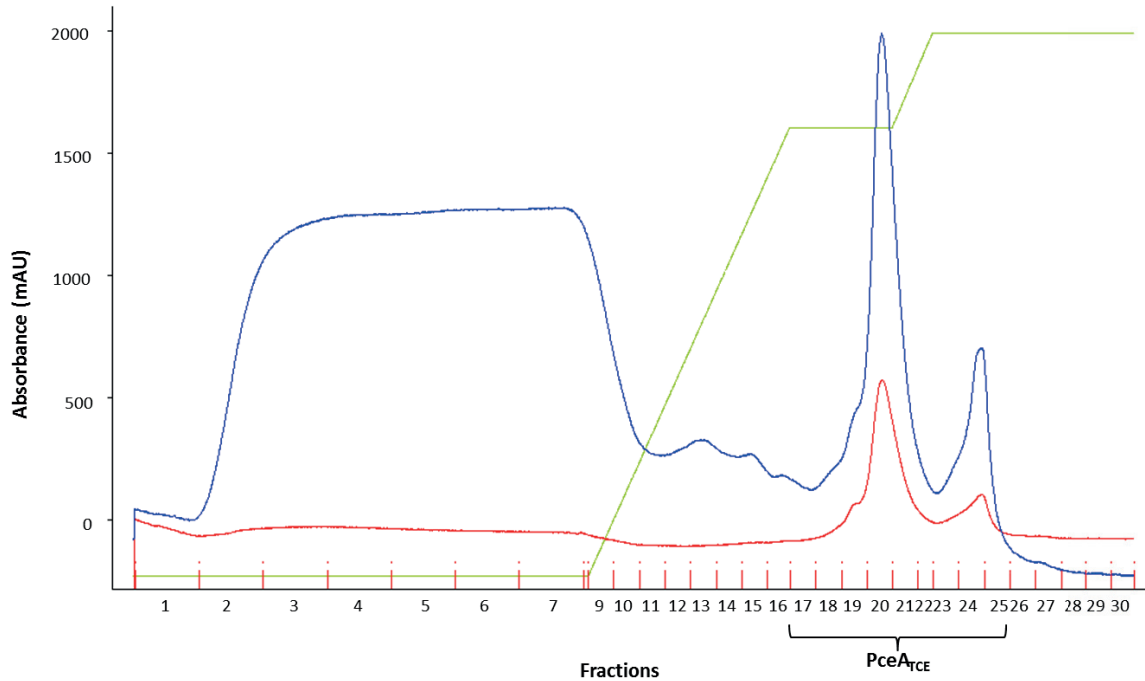


Figure 2.2. Chromatogram of PceA_{TCE} purification on Phenyl-Superose column.

The absorbance (blue curve) was monitored at 280 nm and represents the elution profile of proteins. The red curve was monitored at 400 nm and represents the elution profile of iron-sulfur cluster containing proteins. The green curve indicates the KCl gradient applied for the elution of proteins from the column.

RdhA enzymes are characterized by the presence of a Twin-arginine translocation (Tat) signal peptide which harbors a conserved twin-arginine motif (RRxFLK), a feature that is found in complex redox proteins that are exported to or across the cytoplasmic membrane (4). In certain case, the two forms (processed and unprocessed protein) were reported to be co-purified (17, 26, 34, 37) corresponding to the pre- (with Tat signal peptide) and mature protein, whereas, only one form was purified in other work (19, 23). It has been reported that while the mature form is not visible in all fractions, enzyme activity was still detected (37). It is therefore likely that the unprocessed pre-PceA enzyme is active in the cytoplasm, as protein folding and cofactor assembly occur prior to translocation. Based on that, the molecular mass of mature PceA_{TCE} (lacking the N-terminal Tat signal peptide) was theoretically calculated from the amino acid sequence (55.54 kDa), which is similar to the calculated molecular mass of the mature PceA (55.89 kDa) enzyme of *S. multivorans* (26). SDS-PAGE as well as Western blot using an anti-PceA serum revealed a molecular mass

corresponding to the theoretical processed protein mass of PceA_{TCE} (Figure 2.3). It is interesting to note that the PceA_{TCE} enzyme was purified mainly as mature form, which is contrasting with the two forms observed for *S. multivorans* PceA. One reason of the missing unprocessed form could be the routine growth conditions on formate and tetrachloroethene as electron donor and acceptor, respectively. And after only one transfer on pyruvate and fumarate as electron donor and acceptor, respectively, the biomass of SL2-PCEc was collected to purify the enzyme. As already shown in (13), the localization of the enzyme is dependent on the electron acceptor utilized.

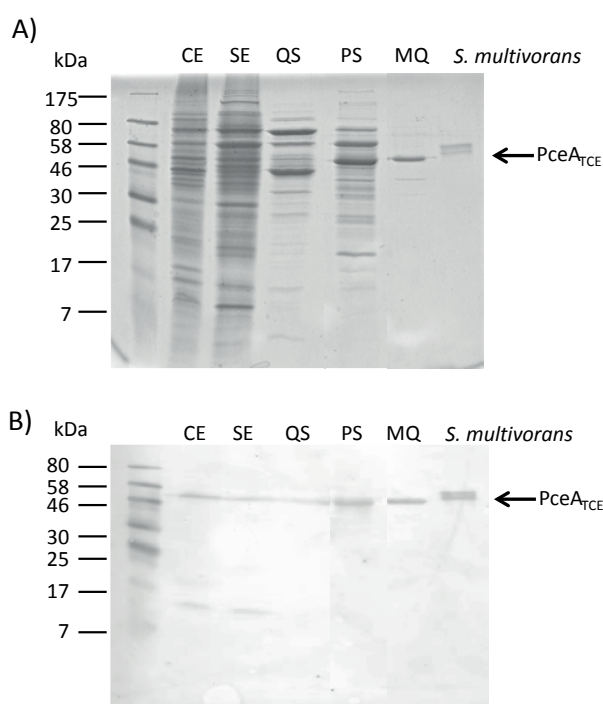


Figure 2.3. PceA_{TCE} purification protein analysis.

Purification analyzed by A) SDS-PAGE and Coomassie staining and by B) Western blot using anti-PceA serum raised against *S. multivorans* PceA. CE, cell extract; SE: soluble extract; QS, Q-Sepharose column, PS, Phenyl-Superose column; MQ, Mono-Q column.

As the SL2-PCEc culture is known to produce exclusively TCE from PCE and not *cis*-DCE (7), the purified PceA_{TCE} enzyme was tested for the dechlorination of TCE. A low specific activity of 2.25 nkat/mg for TCE, around 3 orders of magnitude lower than the activity, was measured for PCE. This confirms why TCE dechlorination may not be physiologically relevant for *Sulfurospirillum diekertiae* SL2-1. Published data showed that the PceA enzyme of *S. multivorans* is able to dechlorinate other halogenated compounds, such as chlorinated propenes (25). Therefore, as an example of those compounds, PceA_{TCE} was tested for its

ability to dechlorinate 1,1,3-trichloropropene. This substrate was not reduced by PceA_{TCE}, suggesting an overall narrower substrate range for PceA_{TCE} in comparison to PceA of *S. multivorans*.

2.4.2. PceA_{TCE} harbors norpseudovitamin B₁₂ as corrinoid cofactor

The type of corrinoid cofactor inserted in PceA_{TCE} was identified after extraction of the fraction 21 eluted from the Phenyl-Superose column obtained in the first purification attempt. The corrinoid extraction revealed a dominating peak at the elution time of 5 min, corresponding to a norpseudovitamin B₁₂ (Figure 2.4), as previously observed for PceA of *S. multivorans* (15). A different type of corrinoid could have explained the restricted substrate range, as it has been shown for *D. mccartyi* (39).

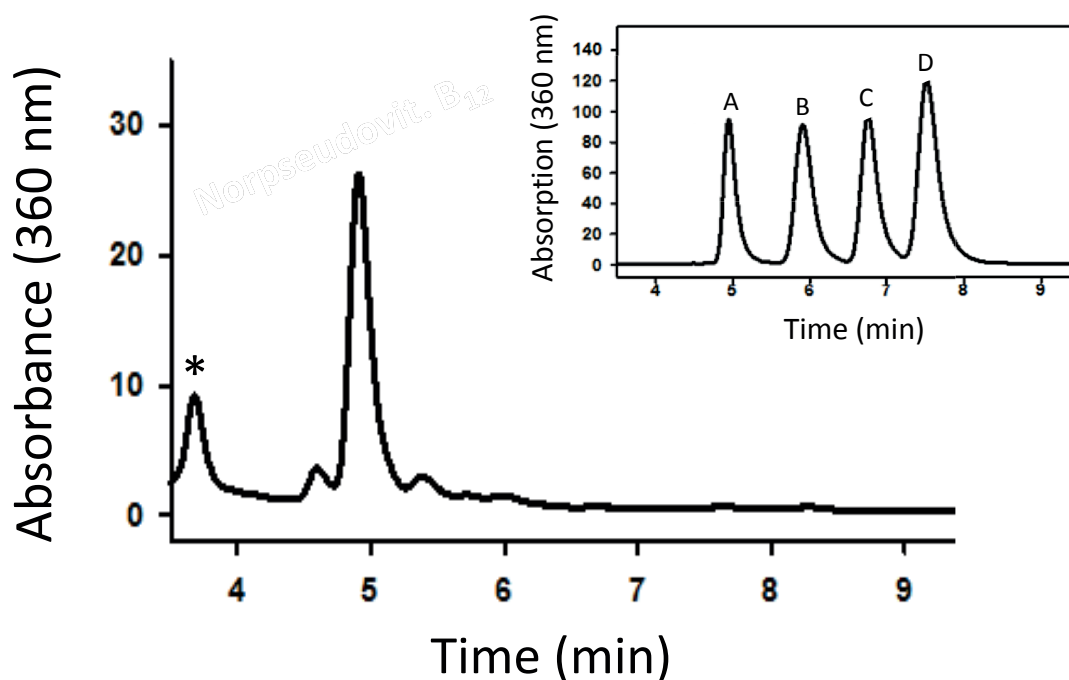


Figure 2.4. HPLC analysis of corrinoid extracts from purified PceA_{TCE}.

The analysis revealed norpseudovitamin B₁₂ as the corrinoid cofactor present in PceA_{TCE}. The asterisk indicates impurities in the corrinoid extract that did not display the typical cobamide absorption spectrum. The inset displays the HPLC profile of corrinoid standards : A, Norpseudovitamin B₁₂; B, Norvitamin B₁₂; C, Pseudovitamin B₁₂; D, Vitamin B₁₂.

2.4.3. Re-routing *de novo* corrinoid biosynthesis with DMB in the SL2-PCEc consortium

In a recent work, the dependence of the PceA enzyme in *S. multivorans* for the norpseudovitamin B₁₂ cofactor, which harbors an adenine moiety as lower ligand, was tested by re-routing the *de novo* corrinoid biosynthesis. This work has initially shown that replacing norpseudovitamin B₁₂ by norvitamin B₁₂ significantly affected dechlorination by *S. multivorans* (14). Therefore, to test the ability of *Sulfurospirillum diekertiae* to incorporate DMB instead of adenine in the corrinoid cofactor of PceA_{TCE}, exogenous DMB was added to SL2-PCEc cultures. The effect of increasing DMB concentrations (0, 25, 50 and 100 μM DMB final concentrations) was investigated by following the PCE dechlorination and growth of the cultures. The *pceA_{TCE}* gene copy number was taken as proxy for growth in this case (Figure 2.5).

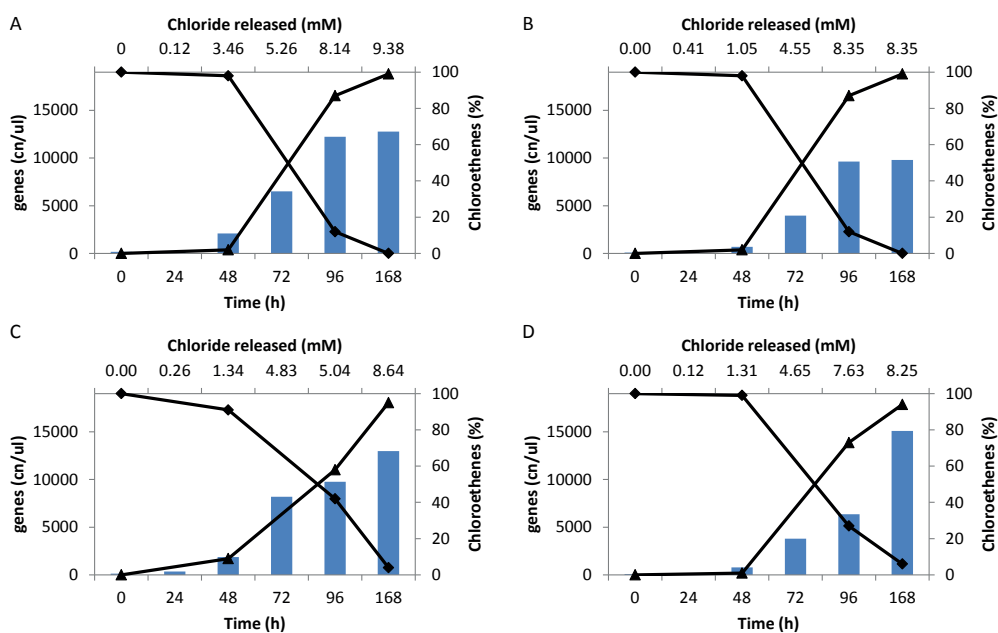


Figure 2.5. Effect of DMB addition on growth and PCE dechlorination of SL2-PCEc cultures.

No DMB (A), 25 μM DMB (B), 50 μM DMB (C), and 100 μM DMB (D) was added to the growth medium of SL2-PCEc cultures. Blue bars indicate *pceA_{TCE}* gene copy numbers as analyzed by qPCR. Chloroethenes are represented by diamonds for PCE and triangles for TCE. The corresponding chloride release is indicated above each time point in the graphs.

To confirm that DMB addition was re-routing corrinoid biosynthesis to norvitamin B₁₂, corrinoid extraction was performed from SL2-PCEc cells cultivated in presence of 100 μM DMB (Figure 2.6). Without amendment of DMB in the medium, a dominating peak eluted at 4.8 min in the HPLC elution profile which confirms the presence of norpseudovitamin B₁₂. When adding DMB, a peak at 5.7 min was observed corresponding to norvitamin B₁₂. These results support the fact that DMB is incorporated during *de novo* corrinoid biosynthesis in *Sulfurospirillum diekertiae* SL2-1.

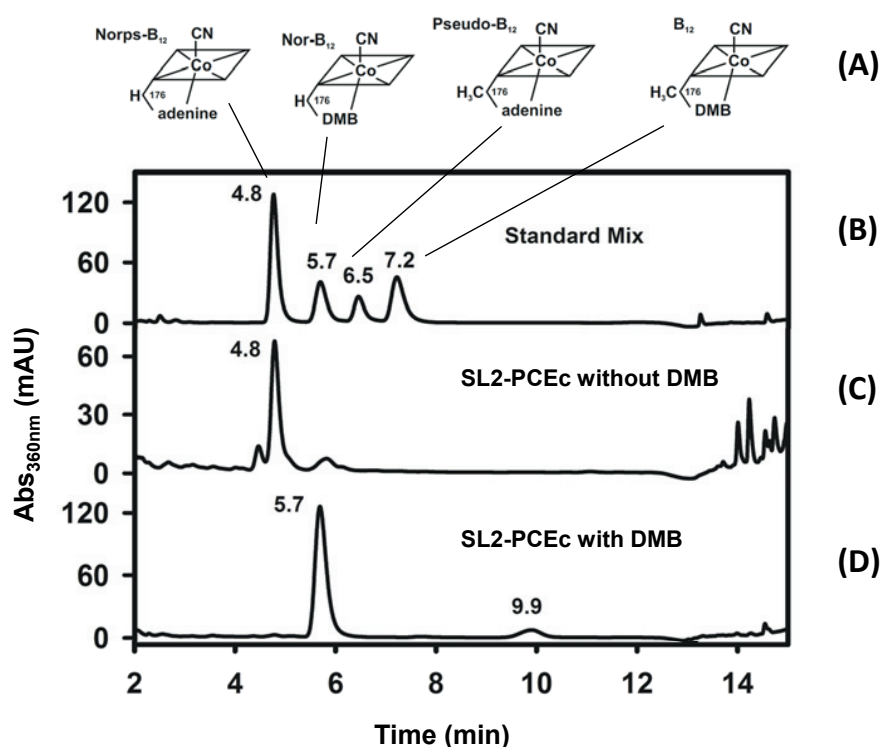


Figure 2.6. HPLC analysis of cobamide extracts from SL2-PCEc cells cultivated without or with amendment of DMB in the medium.

(A) Standard corrinoids used in HPLC analysis. (B) Elution profile of standard corrinoids. (C) Elution profile of corrinoids from SL2-PCEc cultivated without DMB. (D) Elution profile of corrinoids from SL2-PCEc cultivated with 100 μM DMB.

The cobamide lower ligand seems to determine whether OHRB can or cannot use organohalides as electron acceptors (39). In *S. multivorans*, however, it is not expected that the lower ligand affects the substrate specificity of PceA, but it may influence the incorporation of the corrinoid cofactor in the enzyme. However, and in contrast to what has

been observed in the work of Keller and coworkers (14), the formation of norvitamin B₁₂ did not affect PCE-dependent growth of the SL2-PCEc cultures. However, this difference has to be considered carefully as unpublished data have suggested that after some adaptation time, dechlorination resumed for cultures of *S. multivorans* supplemented with DMB (Torsten Schubert, personal communication). A previous study has shown that *D. mccartyi* strain 195 is capable of remodeling non-functional corrinoids into cobalamin in the presence of DMB, thus demonstrating that the nature of the lower ligand is important (38).

2.4.4. Sequence alignments and structure models of *Sulfurospirillum* PceA enzymes

Until now, RdhA encoding genes have been identified in a wide variety of OHRB. However, only few of these enzymes have been biochemically characterized. Analysis of a curated set of reductive dehalogenases reveals that sequence similarity and substrate specificity are not correlated, making functional prediction from sequence information at present impossible (10). Indeed, little knowledge exists today on the substrate spectrum of RdhA present in sequence databases. The divergence of highly similar reductive dehalogenase sequences toward specific substrates has already been highlighted for PceA of *Dehalobacter restrictus* and the closely related DcaA enzyme in *Desulfitobacterium dichloroeliminans* that dechlorinates 1,2-dichloroethane (8, 20, 21).

Although PceA enzymes that display exclusive dechlorination of PCE to TCE have previously been detected in *Desulfitobacterium* sp. PCE1 (Genbank WP_019849102, (37)) and *Dehalococcoides mccartyi* 195 (17), PceA_{TCE} represents the first RDase identified in the genus *Sulfurospirillum* which displays this feature. As PceA of *Desulfitobacterium* strain PCE1 only displays 31% amino acid identity with PceA_{TCE} (data not shown), it is virtually impossible to point out common residues as possible determinants for the restricted substrate spectrum. The comparison at the sequence level of PceA enzymes belonging to the genus *Sulfurospirillum*, however, reveals valuable information about the potential role of specific amino acids in defining the substrate spectrum (Figure 2.7). To this respect, PceA_{TCE} harbors eight unique residues that are different from but consistently conserved in the other three enzymes, suggesting that these amino acids participate in defining the restricted substrate

spectrum of PceA_{TCE}. Additional residues are unique to PceA_{TCE}, however not uniformly conserved in the other three sequences (Table 2.4).

<i>Smu</i> -PceA	1	AEKEKNAAEIRQQFAMTAGSPIIVNDKLERYAEVRTAFTHPTS E FKPNYKGEVKPWFLSA
<i>Sdi</i> -PceA _{DCE}	1	AEKEKNAAEIRQQFAMTAGSPIIVNDKLERYAEVRTAFTHPT S MFKPNYKGEVKPWFLSA
<i>Sdi</i> -PceA _{TCE}	1	AEKEKNAAEIRQQFAMTAGSPIIVNDKLERYAEVRTA T THPTSMFKPNYKGEVKPWFLSG
<i>Sha</i> -PceA	1	AEKEKNAAEIRQQFAMTAGSPIIVNDKLERYA Q VRTAFTHPTSMFKPNYKGEV H WFLSS
consensus		-----e----- fT ----- m -----p WF ---a
<i>Smu</i> -PceA	61	YDEKVRQIENGENGPKMKAKNVGEARAGRALEAAGWTL D IN Y G----NIYPNRF F MLWSG
<i>Sdi</i> -PceA _{DCE}	61	YDEKVRQIENGENGPKMKAKNVGEARAGRALEAAGWTL D IN Y G----NIYPNRF F MLWSG
<i>Sdi</i> -PceA _{TCE}	61	FDEKVRQIENGENGPKMKAKNVGEARAGRALEAAGWTL D NN F GN F GG-YPNRF S MLWSG
<i>Sha</i> -PceA	61	CDEKVRQIENGENGPKMKAKNVGEARAGRALEAAGWTL D X N F G GS F GS Y YPNRF S MLWSG
consensus		y----- w ---i Nx -gxxgn iY -----s-----
<i>Smu</i> -PceA	117	ETMT N T Q LWAPVGLDRRPPD T DPVELTNYVKFAARMAGADLVGVARLNRN W VYSEAV T I
<i>Sdi</i> -PceA _{DCE}	117	ETMP N T Q LWAPVGLDRRPPD T DPVELTNYVKFAARMAGADLVGVARLNRN W VYSEAV T I
<i>Sdi</i> -PceA _{TCE}	120	ETM H N T Q L WAPVGLDRRPPD T DPVELTNYVKFAARMAGADLVGVARLNRN W VYSEAV T I
<i>Sha</i> -PceA	121	ETM L N T Q M W A T V GLDRRPPD T DPVELTNYVKFAARMAGADLVGVARLNRN W VY S CAV T I
consensus		---x---x-p-----e-----
<i>Smu</i> -PceA	177	PADVPY E Q S L H K E IEKPIVFKDVPLPIETDDELIIPNTCENVIVAGIAMNREM Q TAP N S
<i>Sdi</i> -PceA _{DCE}	177	PADVPY E Q S L H K H IEKPIVFKDVPLPIETDDELIIPNTCENVIVAGIAMNREM Q TAP T S
<i>Sdi</i> -PceA _{TCE}	180	PD---- E Q S W H KEIEKPIVFKDVPLPIETDDELIIPNTCENVIVAGIAMNREM Q TAP S
<i>Sha</i> -PceA	181	PD---- E Q S W H KEIEKPIVFKDVPLPIETDDELIIPNTC D N V I S GIAMNREM Q TAP T S
consensus		-xdvpy--- xh - e -----e-----a-----m---t-
<i>Smu</i> -PceA	237	MACAT T A F C Y SRMCMFDMWLCQFIRYMGYYA I PC N GVGQ S V A FAVEAGLQASRMG A C I
<i>Sdi</i> -PceA _{DCE}	237	MACA A A A F C YSRMCMFDMWLCQFIRYMGYYA I PC N GVGQ S V F FAVEAGLQASRMG L C I
<i>Sdi</i> -PceA _{TCE}	236	M S CA A A A F C YSRMCMFDMWLCQFIRYMGYYA I PC N T L GQ S V F FAVEAGLQASRMG L C I
<i>Sha</i> -PceA	237	MACAT V A F C Y SRM G V F DMWLCQFIRYMGYYA I PC N T V GQ S V A FAVEAGLQASRMG A C I
consensus		-a--x x -- CY --cm-----xc N xv---xf-----x--
<i>Smu</i> -PceA	297	TPEFGPNVRLTKVFTNMPLVPDKPIDFGVTEFCETCKKCARECPSK A I T EGPRTFEGRS I
<i>Sdi</i> -PceA _{DCE}	297	TPEFGPNVRLTKVFTNMPLVPDKPIDFGVTEFCETCKKCARECPSK A I S EGPRTFEGRS I
<i>Sdi</i> -PceA _{TCE}	296	TPEFGPNVRLTKVFTNMPLVPDKPIDFGVTEFCETCKKCARECPSK A I S EGPRTFEGRS I
<i>Sha</i> -PceA	297	TPEFGPNVRLTKVFTNMPLVPDKPIDFGVTEFCETCKKCARECPSK A I T EGPRTFEGRS I
consensus		----- R -----x-----
<i>Smu</i> -PceA	357	HNQSGKLQWQNDY N K C L G YWPESGGY C GV C VAVCPFTKGN I W I HDGVEW L DN T R F LD P L
<i>Sdi</i> -PceA _{DCE}	357	HNQSGKLQWQND H N K C L D Y W P K S S GY C G I CVAVCPFTKGN I W I HDGVEW L DN T R F LD P L
<i>Sdi</i> -PceA _{TCE}	356	HNQSGKLQWQND H S K C L D Y W V ESGGY C G I CVAVCPFTKGN I W I HDGVEW L DN T R F LD P L
<i>Sha</i> -PceA	357	HNQSGKLQWQND H S K C L D Y W P ESGG N C G T C FVAVCPFTKGN I W I HDGVEW L DN T R F LD P L
consensus		-----hx---x w pe-g- v ---i-v-----t-----
<i>Smu</i> -PceA	417	MLGMDDALGYGAKRNI T EVWDGK I NTYGLDAD H FRD T VSFRKDR V K S
<i>Sdi</i> -PceA _{DCE}	417	MLGMDDALGYGAKRNI T EVWDGK I NTYGLDAD H FRD A VSFRKDR V K S
<i>Sdi</i> -PceA _{TCE}	416	MLGMDDALGYGAKRNI T EVWDGK I NTYGLDAD H FRD A VSFRKDR V K S
<i>Sha</i> -PceA	417	MLGMDDALGYGAKRNI T E I WDGK I NTYGLDAD H FRD T VSFRKDR V K S
consensus		-----v-----x-----

Figure 2.7, see next page for the legend.

Figure 2.7. Sequence alignment of *Sulfurospirillum* spp. PceA enzymes.

The N-terminal Tat signal peptide (first 37 amino acids) was trimmed, showing sequences corresponding to the processed and active part of PceA enzymes. In the consensus line, residues highlighted in green show amino acids likely involved in the substrate binding pocket, and those in yellow residues likely participating to the substrate channel, as reported by (5). Leu38 of *Sdi*-PceA_{TCE} which possibly accounts for the substrate restriction is indicated in red. Other unique residues identified in *Sdi*-PceA_{TCE} but consistently conserved in the other three sequences are shown in pink. Blue residues indicate conserved amino acids in both PceA sequences from *S. diekertiae*, suggesting a common ancestor. Legend: *Smu*-PceA: PceA of *Sulfurospirillum multivorans* (Genbank AHJ12791); *Sha*-PceA: PceA of *Sulfurospirillum halorespirans* (AAG46194); *Sdi*-PceA_{DCE}: PceA_{DCE} of *S. diekertiae* (AGW23613); *Sdi*-PceA_{TCE}: PceA_{TCE} of *S. diekertiae* (AGW23615).

Table 2.4. Amino acid substitutions observed in *S. diekertiae* PceA_{TCE} in comparison to *S. multivorans* PceA

<i>S. multivorans</i> PceA	<i>S. diekertiae</i> PceA _{TCE}
Phe38	Leu38*
Ala60	Gly60
Tyr61	Phe61
Ile100	Asn100
Ile105	Gly108
Thr120	His123
His187	Pro186*
Asn235	Ala234
Ala238	Ser237*
Cys245	Gly244*
Cys271	Ser270*
Val274	Leu273*
Pro377	Val376*
Thr410	Ile409*

* Amino acid substitutions uniquely found in PceA_{TCE} but consistently conserved in other PceA enzymes.

In PceA of *S. multivorans*, two sets of amino acids have been identified as part of the substrate binding pocket (active site) and the hydrophobic substrate channel (including the 'letter-box' entry) (Table 2.5) (5). A structure model of PceA_{TCE} active site and substrate channel was built based on the structure of *S. multivorans* PceA (PDB 4UR0) and on the sequence alignment between the two sequences (Figure 2.8).

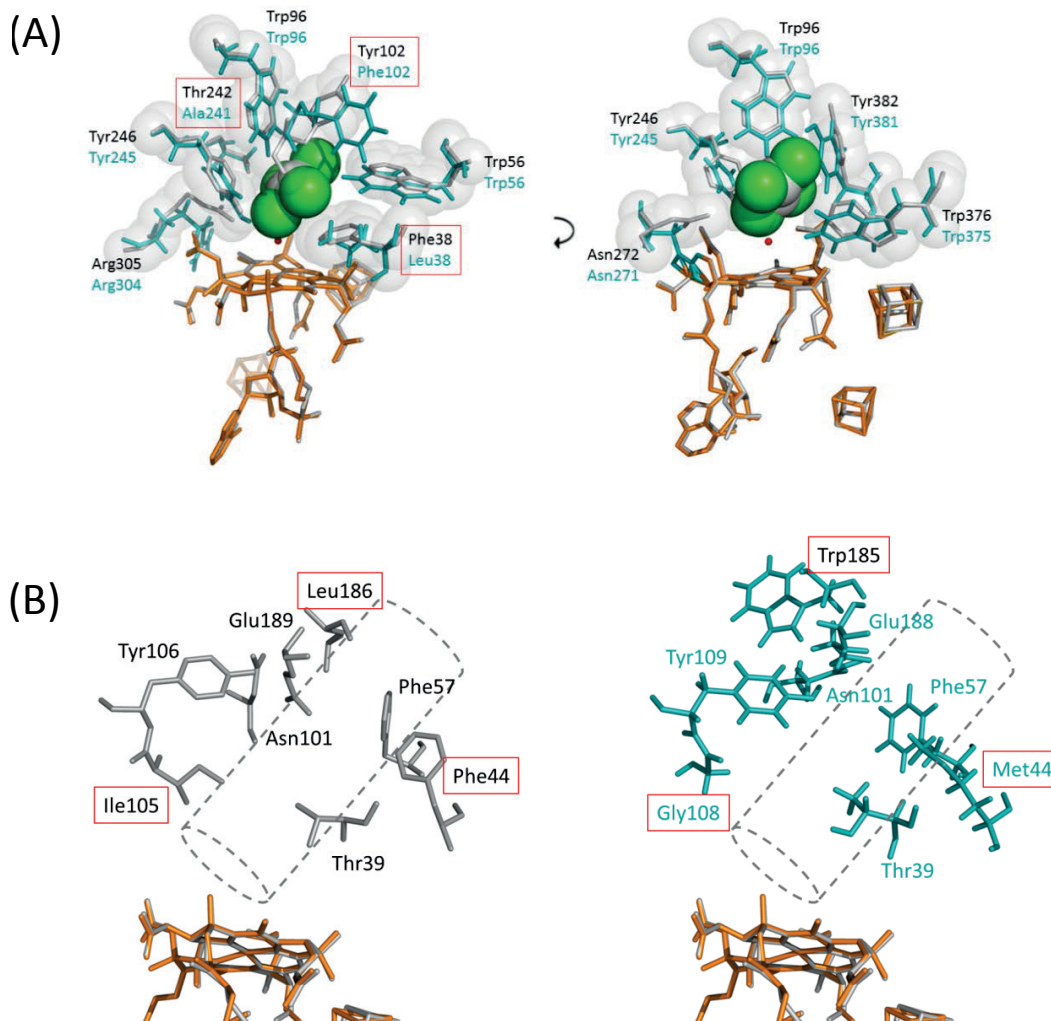


Figure 2.8. Model of the active site PceA_{TCE}.

A model of (A) the active site and (B) the substrate channel of *S. diekertiae* PceA_{TCE} was built based on the structure of *S. multivorans* PceA (PDB 4UR0). PceA_{TCE} is indicated in cyan, PceA of *S. multivorans* is in grey. The key residues in the substrate channel (panel B) are indicated in grey for *S. multivorans* PceA (left panel) and in cyan for PceA_{TCE} (right panel). The corrinoid cofactor is indicated in grey and orange for PceA and PceA_{TCE}, respectively. Amino acid substitutions are indicated in red boxes.

While no drastic conformational change can be observed in the structure model, three residues of the active site are substituted in PceA_{TCE} (Phe38→Leu38; Tyr102→Phe102; Thr242→Ala241), as well as three residues of the substrate channel (Phe44→Met44; Ile105→Gly108; Leu186→Trp185) (Table 2.1, in bold). Among these substitutions, most of them can be seen as important changes in the nature and size of their side chains (except maybe Tyr102→Phe102).

Table 2.5. Amino acids involved in forming the substrate binding pocket and the substrate channel in *S. multivorans* PceA and *S. diekertiae* PceA_{TCE} (substitutions indicated in bold)

<i>S. multivorans</i> PceA	<i>S. diekertiae</i> PceA _{TCE}
Amino acids of the substrate binding pocket	
Phe38	Leu38
Trp56	Trp56
Trp96	Trp96
Tyr102	Phe102
Thr242	Ala241
Tyr246	Tyr245
Asn272	Asn271
Arg305	Arg304
Trp376	Trp375
Tyr382	Tyr381
Amino acids of the substrate channel	
Thr39	Thr39
Phe44	Met44
Phe57	Phe57
Asn101	Asn101
Ile105	Gly108
Tyr106	Tyr109
Leu186	Trp185
Glu189	Glu188

However, from these six relevant substitutions, only Leu38 is unique to PceA_{TCE} and consistently conserved in the three other PceA enzymes (Phe38), strongly suggesting that this substitution might play an important role in preventing PceA_{TCE} to use TCE as substrate. In the structure of PceA, the side chain of Phe38 is located directly between the corrinoid and one of the chlorine atoms of TCE (Figure 2.9). Thus, a replacement by leucine might destabilize TCE in the active site, therefore preventing its further dechlorination to *cis*-DCE. It is not to exclude that other unique substitutions (Table 2.4) may also contribute to the substrate restriction of PceA_{TCE} since some of them are closely located to amino acids of the substrate binding pocket and substrate channel. Nevertheless, one would need to produce variants of PceA and PceA_{TCE} to fully demonstrate the role of single amino acid substitutions.

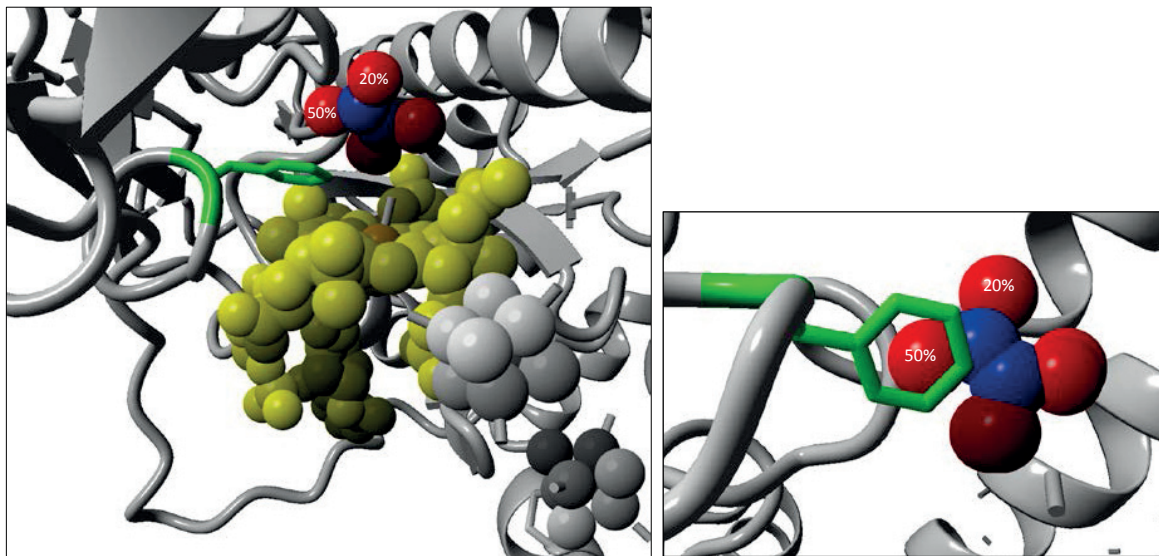


Figure 2.9. Detail of the active site of *S. multivorans* PceA with TCE (PDB 4UR0).

The residue Phe38 (in green) is positioned between the corrinoid (in yellow) and the substrate. TCE (carbon in blue, chlorine in red) has been detected in two conformations where different occupancy levels were observed. The right panel shows the alignment of the phenyl ring of Phe38 with one of the chlorine atoms. (These pictures were produced using YASARA, (16))

2.5. Conclusions

The tetrachloroethene reductive dehalogenase PceA_{TCE} of *Sulfurospirillum diekertiae* strain SL2-1 has a particular narrow substrate range dechlorinating PCE to TCE exclusively. Comparative biochemical analyses of PceA_{TCE} and *S. multivorans* PceA showed that in both cases the same corrinoid cofactor, norpseudovitamin B₁₂, is utilized. Nonetheless, results from the sequence alignments and structure models of *Sulfurospirillum* PceA enzymes revealed eight unique residues in PceA_{TCE} that are different from but consistently conserved in the other three enzymes bringing different structural properties which might explain their physiological differences and the lack of delay of strain SL2-1 in dechlorination upon integration of DMB during *de novo* corrinoid biosynthesis. Heterologous production of catalytically active PceA, PceA_{TCE}, and variants thereof will hopefully allow demonstrating the proposed roles of these amino acids and identifying the determinants for the substrate specificity of *Sulfurospirillum* RDases.

2.6. References

1. **Altschul, S. F., W. Gish, W. Miller, E. W. Myers, and D. J. Lipman.** 1990. Basic local alignment search tool. *J Mol Biol* **215**:403-410.
2. **Ausubel, F. M., R. Brent, R. E. Kingston, D. D. Moore, J. G. Seidman, J. A. Smith, and K. Struhl.** 2012. *Current Protocols in Molecular Biology*. Wiley Online Library vol. 98:iii–v.
3. **Badin, A., G. Buttet, J. Maillard, C. Holliger, and D. Hunkeler.** 2014. Multiple dual C-Cl isotope patterns associated with reductive dechlorination of tetrachloroethene. *Environ Sci Technol* **48**:9179-9186.
4. **Berks, B. C.** 2015. The twin-arginine protein translocation pathway. *Annual review of biochemistry* **84**:843-864.
5. **Bommer, M., C. Kunze, J. Fessler, T. Schubert, G. Diekert, and H. Dobbek.** 2014. Structural basis for organohalide respiration. *Science* **346**:455-458.
6. **Bradford, M. M.** 1976. A rapid and sensitive method for the quantitation of microgram quantities of protein utilizing the principle of protein-dye binding. *Analytical biochemistry* **72**:248-254.
7. **Buttet, G. F., C. Holliger, and J. Maillard.** 2013. Functional genotyping of *Sulfurospirillum* spp. in mixed cultures allowed the identification of a new tetrachloroethene reductive dehalogenase. *Appl Environ Microbiol* **79**:6941-6947.
8. **Duret, A., C. Holliger, and J. Maillard.** 2012. The physiological opportunism of *Desulfitobacterium hafniense* strain TCE1 towards organohalide respiration with tetrachloroethene. *Appl Environ Microbiol* **78**:6121-6127.
9. **Hoffmann, B., M. Oberhuber, E. Stupperich, H. Bothe, W. Buckel, R. Konrat, and B. Krautler.** 2000. Native corrinoids from *Clostridium cochlearium* are adeninylcobamides: spectroscopic analysis and identification of pseudovitamin B₁₂ and factor A. *J Bacteriol* **182**:4773-4782.
10. **Hug, L. A., F. Maphosa, D. Leys, F. E. Löffler, H. Smidt, E. A. Edwards, and L. Adrian.** 2013. Overview of organohalide-respiring bacteria and a proposal for a classification system for reductive dehalogenases. *Philosophical transactions of the Royal Society of London. Series B, Biological sciences* **368**:20120322.
11. **Imlay, J. A.** 2006. Iron-sulphur clusters and the problem with oxygen. *Mol Microbiol* **59**:1073-1082.
12. **John, M., R. Rubick, R. P. Schmitz, J. Rakoczy, T. Schubert, and G. Diekert.** 2009. Retentive memory of bacteria: Long-term regulation of dehalorespiration in *Sulfurospirillum multivorans*. *J Bacteriol* **191**:1650-1655.
13. **John, M., R. P. Schmitz, M. Westermann, W. Richter, and G. Diekert.** 2006. Growth substrate dependent localization of tetrachloroethene reductive dehalogenase in *Sulfurospirillum multivorans*. *Arch Microbiol* **186**:99-106.
14. **Keller, S., M. Ruetz, C. Kunze, B. Krautler, G. Diekert, and T. Schubert.** 2014. Exogenous 5,6-dimethylbenzimidazole caused production of a non-functional tetrachloroethene reductive dehalogenase in *Sulfurospirillum multivorans*. *Environ Microbiol* **16**:3361-3369.
15. **Kräutler, B., W. Fieber, S. Ostermann, M. Fasching, K. H. Ongania, K. Gruber, C. Kratky, C. Mikl, A. Siebert, and G. Diekert.** 2003. The cofactor of tetrachloroethene reductive dehalogenase of *Dehalospirillum multivorans* is norpseudob₁₂, a new type of a natural corrinoid. *Helvetica Chimica Acta* **86**:3698-3716.
16. **Krieger, E., and G. Vriend.** 2014. YASARA View - molecular graphics for all devices - from smartphones to workstations. *Bioinformatics* **30**:2981-2982.
17. **Magnuson, J. K., R. V. Stern, J. M. Gossett, S. H. Zinder, and D. R. Burris.** 1998. Reductive dechlorination of tetrachloroethene to ethene by a two-component enzyme pathway. *Appl Environ Microbiol* **64**:1270-1275.

18. **Maillard, J., M. P. Charnay, C. Regeard, E. Rohrbach-Brandt, K. Rouzeau-Szynalski, P. Rossi, and C. Holliger.** 2011. Reductive dechlorination of tetrachloroethene by a stepwise catalysis of different organohalide respiring bacteria and reductive dehalogenases. *Biodegradation* **22**:949-960.
19. **Maillard, J., W. Schumacher, F. Vazquez, C. Regeard, W. R. Hagen, and C. Holliger.** 2003. Characterization of the corrinoid iron-sulfur protein tetrachloroethene reductive dehalogenase of *Dehalobacter restrictus*. *Appl Environ Microbiol* **69**:4628-4638.
20. **Marzorati, M., A. Balloi, F. de Ferra, L. Corallo, G. Carpani, L. Wittebolle, W. Verstraete, and D. Daffonchio.** 2010. Bacterial diversity and reductive dehalogenase redundancy in a 1,2-dichloroethane-degrading bacterial consortium enriched from a contaminated aquifer. *Microb Cell Fact* **9**:12.
21. **Marzorati, M., F. de Ferra, H. Van Raemdonck, S. Borin, E. Alliffranchini, G. Carpani, L. Serbolisca, W. Verstraete, N. Boon, and D. Daffonchio.** 2007. A novel reductive dehalogenase, identified in a contaminated groundwater enrichment culture and in *Desulfitobacterium dichloroeliminans* strain DCA1, is linked to dehalogenation of 1,2-dichloroethane. *Appl Environ Microbiol* **73**:2990-2999.
22. **Miller, E., G. Wohlfarth, and G. Diekert.** 1997. Comparative studies on tetrachloroethene reductive dechlorination mediated by *Desulfitobacterium* sp. strain PCE-S. *Arch Microbiol* **168**:513-519.
23. **Miller, E., G. Wohlfarth, and G. Diekert.** 1998. Purification and characterization of the tetrachloroethene reductive dehalogenase of strain PCE-S. *Arch Microbiol* **169**:497-502.
24. **Neumann, A., H. Scholz-Muramatsu, and G. Diekert.** 1994. Tetrachloroethene metabolism of *Dehalospirillum multivorans*. *Arch Microbiol* **162**:295-301.
25. **Neumann, A., A. Siebert, T. Trescher, S. Reinhardt, G. Wohlfarth, and G. Diekert.** 2002. Tetrachloroethene reductive dehalogenase of *Dehalospirillum multivorans*: substrate specificity of the native enzyme and its corrinoid cofactor. *Arch Microbiol* **177**:420-426.
26. **Neumann, A., G. Wohlfarth, and G. Diekert.** 1996. Purification and characterization of tetrachloroethene reductive dehalogenase from *Dehalospirillum multivorans*. *J Biol Chem* **271**:16515-16519.
27. **Neumann, A., G. Wohlfarth, and G. Diekert.** 1998. Tetrachloroethene dehalogenase from *Dehalospirillum multivorans*: cloning, sequencing of the encoding genes, and expression of the *pceA* gene in *Escherichia coli*. *J Bacteriol* **180**:4140-4145.
28. **Renz, P.** 1999. Biosynthesis of the 5,6-dimethylbenzimidazole moiety of cobalamin and of the other bases found in natural corrinoids. Wiley, New York.
29. **Rouzeau-Szynalski, K., J. Maillard, and C. Holliger.** 2011. Frequent concomitant presence of *Desulfitobacterium* spp. and "*Dehalococcoides*" spp. in chloroethene-dechlorinating microbial communities. *Appl Microbiol Biotechnol* **90**:361-368.
30. **Sambrook, J., E. F. Fritsch, and T. Maniatis.** 1989. Molecular cloning : a laboratory manual, 2nd ed. Cold Spring Harbor Laboratory, New York.
31. **Schumacher, W., and C. Holliger.** 1996. The proton/electron ration of the menaquinone-dependent electron transport from dihydrogen to tetrachloroethene in "*Dehalobacter restrictus*". *J Bacteriol* **178**:2328-2333.
32. **Siebert, A., A. Neumann, T. Schubert, and G. Diekert.** 2002. A non-dechlorinating strain of *Dehalospirillum multivorans*: evidence for a key role of the corrinoid cofactor in the synthesis of an active tetrachloroethene dehalogenase. *Arch Microbiol* **178**:443-449.
33. **Stupperich, E., I. Steiner, and M. Ruhlemann.** 1986. Isolation and analysis of bacterial cobamides by high-performance liquid chromatography. *Anal Biochem* **155**:365-370.
34. **Suyama, A., M. Yamashita, S. Yoshino, and K. Furukawa.** 2002. Molecular characterization of the PceA reductive dehalogenase of *Desulfitobacterium* sp. strain Y51. *J Bacteriol* **184**:3419-3425.

35. **Szynalski, K.** 2003. Ecophysiology and molecular identification of microbial populations involved in the reductive dechlorination of chloroethenes. PhD Thesis. EPFL, Lausanne.
36. **Thompson, J. D., T. J. Gibson, F. Plewniak, F. Jeanmougin, and D. G. Higgins.** 1997. The CLUSTAL_X windows interface: flexible strategies for multiple sequence alignment aided by quality analysis tools. *Nucleic Acids Res* **25**:4876-4882.
37. **van de Pas, B. A., J. Gerritse, W. M. de Vos, G. Schraa, and A. J. Stams.** 2001. Two distinct enzyme systems are responsible for tetrachloroethene and chlorophenol reductive dehalogenation in *Desulfitobacterium* strain PCE1. *Arch Microbiol* **176**:165-169.
38. **Yan, J., K. M. Ritalahti, D. D. Wagner, and F. E. Löffler.** 2012. Unexpected specificity of interspecies cobamide transfer from *Geobacter* spp. to organohalide-respiring *Dehalococcoides mccartyi* strains. *Appl Environ Microbiol* **78**:6630-6636.
39. **Yan, J., B. Simsir, A. T. Farmer, M. Bi, Y. Yang, S. R. Campagna, and F. E. Löffler.** 2016. The corrinoid cofactor of reductive dehalogenases affects dechlorination rates and extents in organohalide-respiring *Dehalococcoides mccartyi*. *ISME J* **10**:1092-1101.
40. **Zehnder, A. J., and K. Wuhrmann.** 1976. Titanium (III) citrate as a nontoxic oxidation-reduction buffering system for the culture of obligate anaerobes. *Science* **194**:1165-1166.

Chapter 3

Dechlorination kinetics govern
the competition between two
new strains of the genus
Sulfurospirillum

3. Dechlorination kinetics govern the competition between two new strains of the genus *Sulfurospirillum*

3.1. Abstract

Two anaerobic bacterial consortia (SL2-PCEc and SL2-TCE), each of them harboring a distinct *Sulfurospirillum* sp. population (SL2-1 and SL2-2, respectively), were derived from a long-lived parental consortium (SL2-PCEb) which has been previously characterized for its stepwise dechlorination of PCE to *cis*-DCE via a significant accumulation of TCE. Both subcultures showed a different pattern of dechlorination, as strain SL2-1 was only able to dechlorinate PCE to TCE, while strain SL2-2 kept the potential of the parental consortium, however, without TCE accumulation. The features of these consortia were investigated here at the genomic and physiological levels in order to understand their long-term coexistence in the parental consortium.

On one side, this chapter presents the draft genomes that were obtained for each SL2 strain, revealing the very high similarity they display with each other at the sequence level. Only the sequence of their respective *pceA* gene differs significantly, a feature that was already used to distinguish them. Based on genome comparison with other *Sulfurospirillum* spp., a new species name, '*Candidatus Sulfurospirillum diekertiae*', was proposed for strain SL2-1 and SL2-2. On the other side, an extended series of batch cultures with the two strains amended with a large range of PCE concentrations allowed to estimate their respective dechlorination kinetic parameters. While both strains share a similar maximal growth rate around 0.1 h^{-1} , their apparent affinity constant for PCE is significantly different, with values around $6 \mu\text{M}$ for strain SL2-1 and $35 \mu\text{M}$ for strain SL2-2. These findings were validated in competition experiments where both populations were mixed at equal population size and cultivate at 6 and $30 \mu\text{M}$ PCE (aqueous concentration). The kinetic parameters of these strains allow to explain the long-term coexistence of both strains in the parental consortium as the latter was routinely cultivated at $20 \mu\text{M}$ PCE. These results further suggest that competition for a limiting substrate is a possible driving force for strain diversity in organohalide respiration.

3.2. Introduction

An anaerobic bacterial consortium (named SL2-PCEb) consisting mainly of two different *Sulfurospirillum* populations, named here SL2-1 and SL2-2, was obtained from a fixed-bed bioreactor treating tetrachloroethene (PCE) contaminated groundwater (23). The peculiarity of this consortium resides in the stepwise dechlorination of PCE to trichloroethene (TCE) and *cis*-dichloroethene (*cis*-DCE), which is catalyzed by two populations (19). Two subcultures were derived from SL2-PCEb, each one harboring a unique *Sulfurospirillum* population and showing distinct dechlorination potential: SL2-PCEc containing the SL2-1 population dechlorinates PCE to TCE only, while SL2-TCE (SL2-2) which has been selected on TCE kept the potential to dechlorinate both PCE and TCE to *cis*-DCE (4). A molecular fingerprinting method targeting small differences in their *pceA* genes has been developed to follow the dynamics of both populations. Moreover, *in vitro* PCE dechlorination activity measured in cell extracts of both populations suggested that the reductive dehalogenase (RDase) produced by SL2-1 has a higher specific dechlorination rate than the one produced by SL2-2 (4). Furthermore, sequence alignments and structure models of *Sulfurospirillum* PceA enzymes, described in CHAPTER 2, revealed eight unique residues in PceA_{TCE} that are different from but consistently conserved in the three enzymes catalyzing PCE to *cis*-DCE dechlorination. These differences might result in altered structural properties of PceA_{TCE} which could be the basis for the physiological differences between both populations. To our knowledge, the presence of multiple *Sulfurospirillum* strains in a mixed culture has not yet been reported. However, similar occurrences have been observed in chlorinated ethenes- or ethanes-degrading cultures containing multiple strains of *Dehalobacter* or *Dehalococcoides* (9, 13, 22, 26, 28). Motivated by these observations and the will to identify the factors allowing the long-term coexistence of the two populations in SL2-PCEb, the present work examined population-specific properties which could explain their different physiological behavior. First, a draft genome was obtained for each population in order to identify genetic features possibly responsible for the differences observed. Then, the dechlorination kinetics of both populations were determined in order to understand the competition. Finally, competition experiments were performed by mixing both *Sulfurospirillum* populations to validate the kinetic data and correlate population-specific growth with PCE dechlorination.

3.3. Material and methods

3.3.1. Bacterial strains and growth conditions

The bacterial consortia SL2-PCEc and SL2-TCE were cultivated anaerobically in serum bottles sealed with rubber-stoppers as described in CHAPTER 2. Formate was added as electron donor to a final concentration of 20 mM. In order to avoid exposing the bacterial cells to toxic concentrations of PCE, hexadecane was used to dilute PCE (14). Hexadecane is non-miscible in water and has a lower density, making a two-liquid-phase system with an aqueous phase containing a phosphate/bicarbonate-buffered medium and an organic phase containing PCE (10 mM to 1 M). In this system, PCE diffuses from the organic to the aqueous phase and reaches equilibrium with an estimated partition coefficient between hexadecane and water ($\log K_{HW}$) of 3.7 (~5000 part in hexadecane for 1 part in the aqueous phase) (15). It allows the addition of substantial amounts of chlorinated compounds to a batch system without affecting growth. For the sake of simplicity, the corresponding aqueous PCE concentrations $[PCE_{aq}]$ were used in this work (Table 3.1). By varying both the volume of added organic phase and the PCE concentration in hexadecane $[PCE_{HD}]$, the total available amount of PCE in all culture flasks was kept at 500 μmol . The cultures were incubated at 30°C in the dark and set on a rotary shaker at 100 rpm after an initial static incubation of 1 h.

Table 3.1. PCE concentrations used in this work.

$[PCE_{HD}]^1$ in hexadecane stock solution (mM)	Corresponding $[PCE_{aq}]^2$ in aqueous phase (μM)
10	2
20	4
30	6
40	8
50	10
100	20
150	30
200	40
250	50
300	60
400	80
500	100
750	150
1000	200

¹ $[PCE_{HD}]$, PCE concentration in hexadecane.

² $[PCE_{aq}]$, aqueous PCE concentration.

Escherichia coli DH5 α was used as a host for molecular cloning (Table 3.2). *E. coli* competent cells were prepared using the standard CaCl₂ method (24). *E. coli* was cultivated at 37°C in Luria-Bertani (LB) liquid medium or agar plates containing 100 μ g/mL of ampicillin when needed.

Table 3.2. Bacterial strains and consortia, and plasmids used in this work.

Bacteria	Description	References
SL2-PCEc	Bacterial consortium selected from SL2-PCEb containing a <i>Sulfurospirillum</i> population displaying PCE to TCE dechlorination	(4, 19, 23)
SL2-TCE	Bacterial consortium selected on TCE from SL2-PCEb containing a <i>Sulfurospirillum</i> population displaying PCE to <i>cis</i> -DCE dechlorination	(4, 19, 23)
<i>E. coli</i> DH5 α	F ⁻ <i>endA1 glnV44 thi-1 recA1 relA1 gyrA96 deoR nupG</i> Φ 80 <i>lacZ</i> Δ M15 Δ (<i>lacZYA-argF</i>)U169, <i>hsdR17</i> (r _K ⁻ m _K ⁺), λ -	Invitrogen
Plasmids	Description	References
pT1P-T _Q	pGEM-T harboring a fragment of <i>pceA</i> _{TCE}	(4)
pT1P-D _Q	pGEM-T harboring a fragment of <i>pceA</i> _{DCE}	(4)
pRPOB	pGEM-T harboring a fragment of <i>Sulfurospirillum rpoB</i>	This study

3.3.2. Molecular methods

3.3.2.1. Quantitative PCR (qPCR)

For qPCR, plasmids containing fragments of the target genes (*rpoB*, *pceA*_{TCE} and *pceA*_{DCE}) were used as standards (Table 3.2). Primers to clone the *rpoB* gene, encoding the B subunit of the RNA polymerase, were designed based on the genomes of *S. multivorans* (Genbank CP007201.1), *S. deleyianum* (CP001816.1) and *S. halorespirans* (CP017111.1) (Table 3.3). The cloning procedure and preparation of qPCR standards were done as previously described (CHAPTER 2).

Table 3.3. Oligonucleotides used in this study.

Name	Target gene	Sequence (5' → 3')	Reference
T1-PTQ-f	<i>pceA_{TCE}</i>	CTTTGGAGGTAACCTTTGGAGGTTA	(4)
T1-PTQ-r		CTTTAGGCCAAGATTGTTTCATCT	
T1-PDQ-f	<i>pceA_{DCE}</i>	GTAAC TATA ACCAGCTGACGTACC	(4)
T1-PDQ-r		CATAGCGATACCTGCAACGA	
rpoB-f	<i>rpoB</i>	GATGCTAGGAATTTTATTGA	This study
rpoB-r		AACTCTTCAACGTTAACAC	

For this work, qPCR was performed in a MIC apparatus (Bio Molecular Systems). The thermocycling program for qPCR was as follows: an initial denaturation of 2 min at 95°C, then 45 cycles including three steps, 10 s at 95°C, followed by 30 s at 55°C (*rpoB*) or 60°C (*pceA_{TCE}* and *pceA_{DCE}*) and finally 20 s at 72°C, after which the acquisition of fluorescence took place using the SYBR detection channel. A melting curve ranging from 72°C to 95°C was performed with at 0.1°C/s. For each run, triplicates of samples and standards were run alongside and the concentration of samples was calculated from the derived standard curve. The MicPCR v1.6.0 software was used for data analysis. Average run performances are given in Table 3.4 for each considered gene target. The threshold fluorescence level was fixed to 5% for all runs. Replicates displaying standard deviation of below 15% of the average value were kept for analysis.

Table 3.4. Parameters of the quantitative PCR runs.

	<i>rpoB</i>		<i>pceA_{TCE}</i> ¹	<i>pceA_{DCE}</i> ¹
	SL2-1	SL2-2		
Efficiency	0.84	0.82	0.93 ±0.01	0.85 ±0.02
R ²	0.998	0.998	0.995 ±0.001	0.998 ±0.001

¹ Efficiency and R² average of culture batches, standard deviations are indicated on the right.

3.3.2.2. Genomic DNA extraction and library preparation

Two 200 mL batches of each SL2 consortium were cultivated and the biomass collected by centrifugation at 3,300 × *g* for 10 min at 4°C. Biomass pellets were washed in 1 mL of 50 mM Tris-HCl buffer (pH 8.0) and centrifuged in microcentrifuge tubes at 8,800 × *g* for 5 min. Biomass pellets (18.6 mg and 19.7 mg for SL2-PCEc and SL2-TCE, respectively) were flash-frozen in liquid N₂ and stored at -80°C. DNA extraction was performed with the DNeasy Blood & Tissue kit (Qiagen). As the DNA quality is crucial for library preparation, the DNA samples were verified by agarose gel electrophoresis according to the JGI protocol (Genomic

DNA Sample QC v4.0) using Lambda DNA standards (Thermo Fischer Scientific) and Lambda DNA/*Hind*III ladder (Promega), allowing DNA concentration estimation. Agarose gels were prepared as described in CHAPTER 2. Genomic libraries preparation was carried out according to (8). Briefly, DNA samples were purified with magnetic beads (AxyPrep Mag PCR Clean-Up, Axygen) and fragmented using the enzyme mix provided in the Ion Xpress Plus Fragment Library Kit according to the manufacturer instructions (Life Technologies). Size selection (max. 370 bp) was carried out on commercial agarose gels (E-Gel System, Life Technologies). Quantification and size analysis of the selected fragments was carried out using the BioAnalyzer 2100 and the High Sensitivity DNA kit (Agilent Technologies).

3.3.2.3. *Semiconductor sequencing with Ion Torrent PGM*

Emulsion PCR was prepared using the Ion Xpress Template Kit (Life Technologies) as described in the user guide provided by the manufacturer. Sequencing was carried out on the Ion Torrent Personal Genome Machine (PGM) using the Ion Sequencing 300 bp kit (Life Technologies) equipped with a 316 chip following the corresponding protocol. This work was done in collaboration with P. Rossi (CEMBL, EPFL).

3.3.2.4. *Sequence recovery, bioinformatics and statistical analysis*

Numerical treatment of the data gained by semiconductor sequencing was done according to (8). Primary base calling was first performed using the Torrent Suite v3.0 software (Life Technologies). Sequencing reads were then downloaded as .sff files from the Torrent Server and processed on a Linux Ubuntu platform (BioLinux 7, Ubuntu 12.04 LTS) running on a local Dell Precision T3600 2 GHz bench top computer, equipped with a 12 core processor array and 32 GB of RAM. Reads were initially processed on Mothur so as to provide the necessary .fasta and .qual files (25).

3.3.2.5. *Genome annotation and analysis*

The sequencing datasets were then assembled, analyzed and annotated in collaboration with T. Goris (Friedrich-Schiller University, Jena, Germany). Sequencing of strain SL2-1 resulted in 1'580'331 reads and 426'621'911 initial bases, 346'913'840 of them with a score ≥ 20 . The mean read length was 269 bp. The assembly was done with IonGAP (3), which relies on the assembler MIRA (Version 4.0rc4), using standard settings. The genome of *S.*

multivorans (CP007201.1) was used as reference. The assembly resulted in 25 contigs with an average total coverage based on the contigs larger than 5 kbp of 125×. The largest contig has a size of 911'840 bp and N50 contig size of 798'805 bp. Automatic annotation was done via RAST (2), the organohalide-respiration region was checked manually by comparison with those of *S. multivorans* (12) and *S. halorespirans*. The draft genome of strain SL2-1 is 2'895'759 bp large. Assembly of strain SL2-2 resulted in a draft genome with 42 contigs and a coverage of 91×. The draft genome size is 2'899'756 bp.

3.3.3. Additional analytical procedures

Chloride concentration was monitored in batch cultures. One mL of the aqueous phase of cultures were taken and filtered (0.2 µm) and stored at -20°C at the start of cultivation, after 8 h (latency period allowing the culture to start dechlorinating), and every 2 h from that time. Chloride concentration was analyzed with ion chromatography (ICS-90, IonPac AS14A-5 µm /3 x 150 mm column, blower; ACRS 500 2 mm, Dionex) with a mix of 8 mmol/L of Na₂CO₃ and 1 mmol/L of NaHCO₃ as eluent and 50 mmol/L of H₂SO₄ as regenerant.

Chloroethenes were analyzed by gas chromatography with Agilent Technologies 7890B equipped with Optima 624 LB (30m by 0.32 mm; M&N GmnbH & Co. KG) coupled to a flame ionization detector. The carrier gas utilized is helium at a flow rate of 1.8 mL/min. The initial temperature was 30°C; the column was kept at 30°C for 5 min, and then the temperature was raised to 60°C at a rate of 10°C/min and then until 200°C at a rate a 40°C/min and finally kept at 200°C for 5 min. Each culture was analyzed by taking 1.5 mL of the gas phase from the culture flask in sterile conditions.

Chloride release was assumed to follow Monod kinetics (6, 10, 18). The equation selected (**Equation 1**) for fitting the data was based on the Gompertz model (11) and modified to include parameters with biological meaning (32). Initially used on the chloride release concentration to calculate dechlorination rates (q_{Cl}), the equation was then applied on the natural log of chloride ratio ($\ln[Cl_t]/[Cl_0]$), where $[Cl_t]$ (in mM) is the chloride concentration in the aqueous phase at time t (in h) and $[Cl_0]$, the initial chloride concentration. In this way, the dechlorination rate is converted to an apparent growth rate (μ_{Cl}) which is based on dechlorination data.

Equation 1: Gompertz model

$$\ln\left(\frac{[Cl_t]}{[Cl_0]}\right) = A \cdot \exp\left(-\exp\left(\frac{\mu_{Cl} \cdot e}{A}\right)(\lambda - t) + 1\right)$$

With the following parameters: A is the asymptote of the curve which corresponds to the maximum chloride concentration, μ_{Cl} (in h^{-1}), the apparent growth rate based on dechlorination, and λ (in h), the lag phase; e stands for the Euler constant. The parameters were fit to the data using the FITTYPE and FIT functions in Matlab (version R2015a). The fit type method used was nonlinear least squares, and all data points were weighted equally. The goodness of fit for each time series was evaluated by the Sum of Squares due to Error (SSE) fitting output parameter (16). SSE values for all the time series ranged from 0.0001 and 0.1700. Based on visual inspection of each dataset, it was determined that the elements of four time series, those with an $SSE > 0.1$, were too erratic to be fit adequately, and they were omitted from further calculations. The fitted parameter values for sets of replicates were then averaged to yield one set of parameters for every combination of each *Sulfurospirillum diekertiae* strain and initial PCE concentration.

Estimation of PCE affinity constants (K_S) and dechlorination-based maximal growth rates ($\mu_{max_{Cl}}$) was performed with Lineweaver-Burk and Hanes-Woolf linearization procedures according to **Equations 2 and 3**.

Equation 2: Lineweaver-Burk linearization

Adapted from Monod equation: $\mu_{Cl} = \frac{\mu_{max_{Cl}}[S]}{K_S + [S]}$

Taking the reciprocal gives $\frac{1}{\mu_{Cl}} = \frac{K_S}{\mu_{max_{Cl}}[S]} + \frac{1}{\mu_{max_{Cl}}}$

According to the Lineweaver-Burk plot: $y = \left(\frac{K_S}{\mu_{max_{Cl}}}\right)x + \frac{1}{\mu_{max_{Cl}}}$

Graphical interpretation: the y intercept is $\frac{1}{\mu_{max_{Cl}}}$, the slope is $\frac{K_S}{\mu_{max_{Cl}}}$

Equation 3: Hanes-Woolf linearization

Adapted from Monod equation: $\mu_{Cl} = \frac{\mu_{\max Cl} [S]}{K_s + [S]}$

Taking the reciprocal gives $\frac{[S]}{\mu_{Cl}} = \frac{1}{\mu_{\max Cl}} [S] + \frac{K_s}{\mu_{\max Cl}}$

According to the Hanes-Woolf plot: $y = \left(\frac{1}{\mu_{\max Cl}}\right) x + \left(\frac{K_s}{\mu_{\max Cl}}\right)$

Graphical interpretation: the y intercept is $\frac{K_s}{\mu_{\max Cl}}$, the slope is $\frac{1}{\mu_{\max Cl}}$

3.4. Results and discussion

This study aimed at building a better understanding of the long-term coexistence (more than 10 years of uninterrupted culture transfers) of two very closely related strains of *Sulfurospirillum* sp. enriched in the consortium SL2-PCEb, despite the fact that both strains are known to dechlorinate PCE and therefore compete for this electron acceptor. Based on partially assembled genomes of the two strains, a new species is proposed that is clearly distinct for other members within the genus *Sulfurospirillum*, including the ones known as organohalide-respiring bacteria (OHRB). A series of experiments was designed and performed with the separate consortia SL2-PCEc and SL2-TCE, each harboring one of the two *Sulfurospirillum* strains, in order to determine their apparent substrate affinity (K_S) for PCE and maximal growth rate based on dechlorination (μ_{maxCl}). In a second phase, competition experiments were performed by mixing the two consortia to validate the observations made on the individual cultures.

3.4.1. Draft genomes of *Sulfurospirillum* sp. strains SL2-1 and SL2-2 and designation of a new species

The biomass of the consortia SL2-PCEc and SL2-TCE was obtained from 200 mL cultures in standard medium amended with formate and PCE and subjected to genomic DNA extraction. The DNA concentration of both samples was estimated using recommendations of the Joint Genome Institute (JGI) at 17.4 and 28.7 ng/ μ L, respectively, as illustrated for SL2-PCEc (Figure 3.1). Two separate DNA libraries were prepared and sequenced with Ion Torrent PGM.

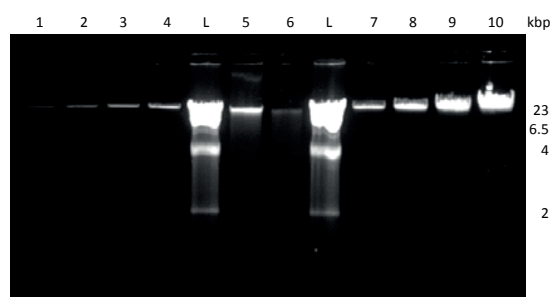


Figure 3.1. Quality control and quantification of genomic DNA from the SL2-PCEc consortium.

Lanes 1-4 and 7-10 show the Lambda DNA standards (48.5 kbp), with increasing quantity: 4.7, 9.4, 18.8, 37.5, 75, 150, 300 and 600 ng, respectively. L: Lambda/*Hind*III ladder from which the corresponding fragment sizes are indicated on the right. Lanes 5 and 6 display genomic DNA extracted from the SL2-PCEc consortium.

The draft genomes of strains SL2-1 and SL2-2 were obtained with the collaboration of T. Goris (Jena, Germany) and deposited in the RAST draft genome database under the identification numbers 6666666.242242 and 6666666.242160, respectively. In Table 3.5, general features of the draft genomes were compared to the available genomes of *Sulfurospirillum* spp.. Average nucleotide identity (ANI) analysis of both strains, and with the genome of available *Sulfurospirillum* strains was performed using the on-line ANI calculator tool (Figure 3.2 for the comparison with *S. multivorans*). While strains SL2-1 and SL2-2 share most of their DNA (ANI: 99.98%), both strains share only 78-83% identity of their sequence with the genomes of *Sulfurospirillum* spp. It is therefore proposed that strains SL2-1 and SL2-2 present in the consortia SL2-PCEb and SL2-TCE, respectively, form a new species of *Sulfurospirillum* that we propose to name '*Candidatus Sulfurospirillum diekertiae*' (or short *S. diekertiae*).

Table 3.5. Features of the draft genomes of *S. diekertiae* strains SL2-1 and SL2-2 in comparison with available *Sulfurospirillum* spp. genomes.

Code	Strain	Reference	Size (bp)	# rRNA	# tRNA	GC (%)	# proteins
<i>Sdi</i> -SL2-1	<i>S. diekertiae</i> SL2-1	6666666.242242 ^a	2895759	2 ^b	54	38.7	3222
<i>Sdi</i> -SL2-2	<i>S. diekertiae</i> SL2-2	6666666.242160 ^a	2899756	1	53	38.7	2986
<i>Smu</i>	<i>S. multivorans</i> DSM 12446	NZ_CP007201.1	3175729	2	45	40.9	3184
<i>Sha</i>	<i>S. halorespirans</i> DSM 13726	NZ_CP017111.1	3029840	2	44	41.3	2965
<i>Sde</i>	<i>S. deleyianum</i> DSM 6946	NZ_013512.1	2306351	3	42	39.0	2258
<i>Sca</i>	<i>S. cavolei</i> UCH003	NZ_AP014724.1	2698323	3	45	43.9	2640
<i>Sba</i>	<i>S. barnesii</i> SES-3	NC_018002.1	2510109	2	41	38.8	2478
<i>Sars</i>	<i>S. arsenophilum</i> NBRC 109478	NZ_BBQF00000000.1	2629984	1	39	39.2	2622
<i>Sarc</i>	<i>S. arcachonense</i> DSM 9755	NZ_JFBL00000000.1	2656384	1	33	30.4	2664

^a RAST identity number (<http://rast.nmpdr.org>).

^b One 16S rRNA copy was detected in two contigs.

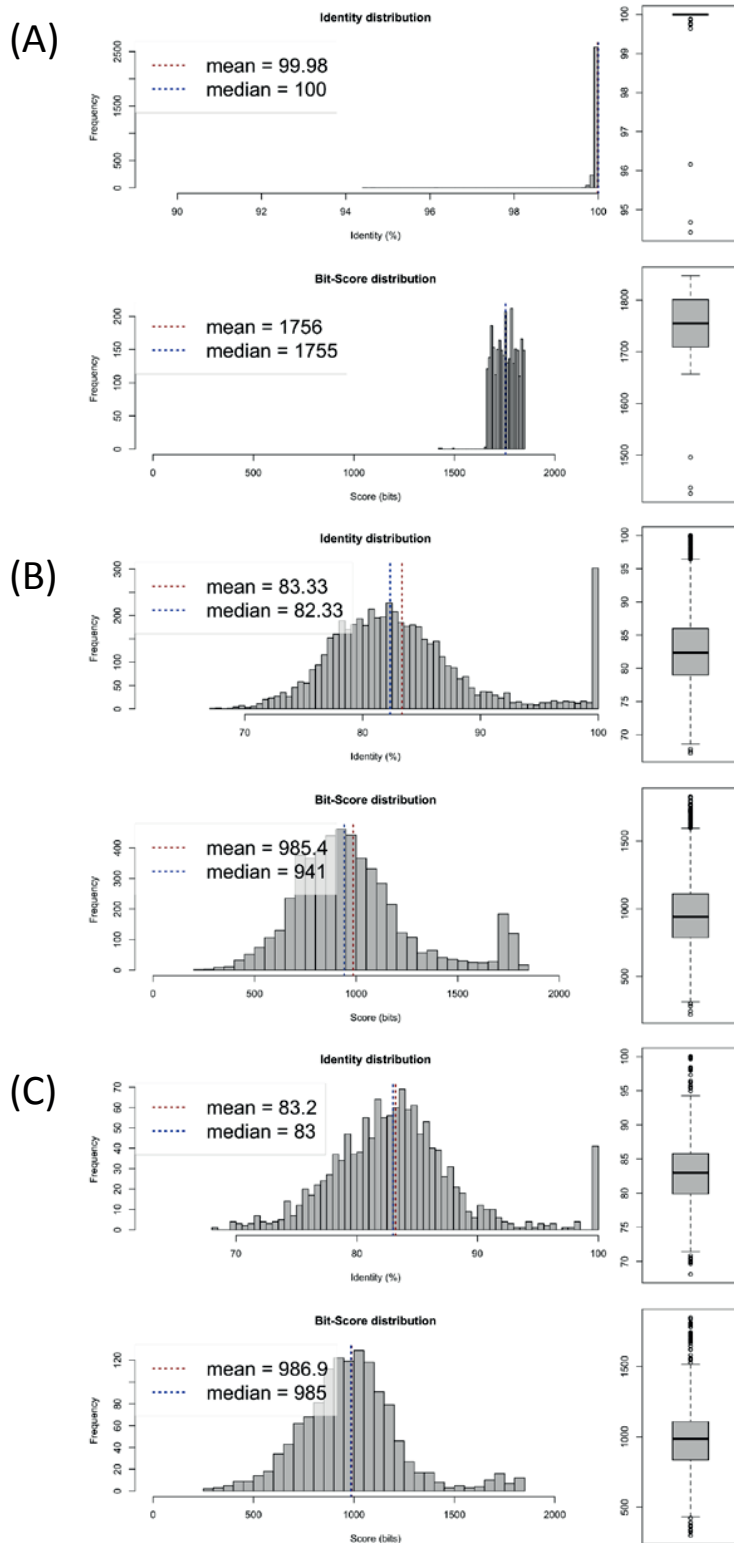


Figure 3.2. Average nucleotide identity (ANI) of the draft genomes of strains SL2-1 and SL2-2 in comparison with *S. multivorans*.

The draft genomes of both strains were compared to each other and to *S. multivorans* using the ANI calculator tool at (<http://enve-omics.ce.gatech.edu>). (A) SL2-1 vs. SL2-2; (B) SL2-1 vs. *S. multivorans*; (C) SL2-2 vs. *S. multivorans*.

Although not completely assembled (25 and 42 contigs for strain SL2-1 and SL2-2, respectively), the draft genomes of SL2 strains seem to be slightly smaller than the ones of other OHRB belonging to *Sulfurospirillum*, and larger than non-OHRB members of this genus. A phylogenetic analysis of *Sulfurospirillum* spp. based on the 16S rRNA genes identified in the genomes is presented in Figure 3.3, revealing that *S. diekertiae* strains cluster nicely with other OHRB, suggesting that *S. multivorans*, *S. halorespirans* and *S. diekertiae* evolved from a common ancestor and that their PCE dechlorination capability was inherited before strain divergence.

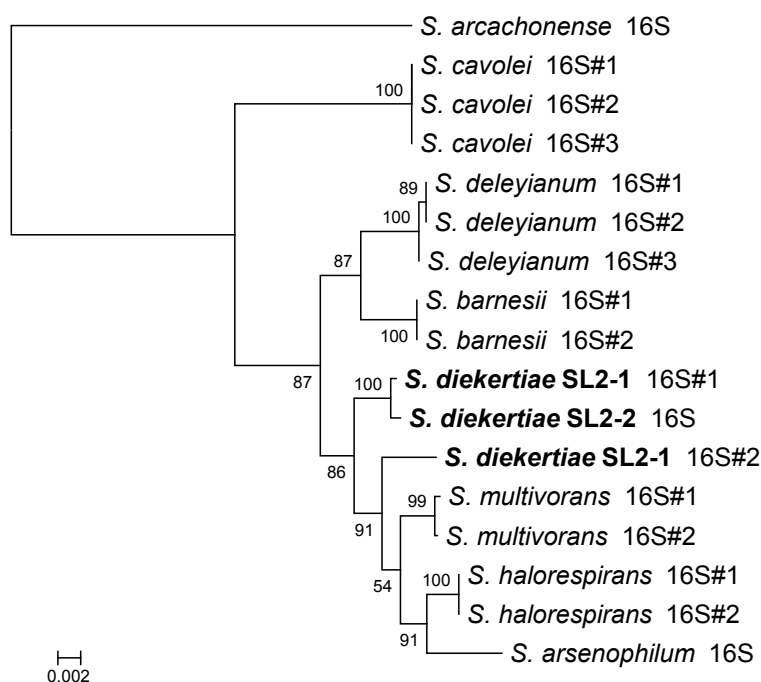


Figure 3.3. Phylogenetic tree based on the 16S rRNA genes from *Sulfurospirillum* spp. genomes. The 16S rRNA genes were taken from available *Sulfurospirillum* spp. genomes, aligned with ClustalX2.0 (17) and the tree was drawn using MEGA (version 6) (27).

The OHR region of the genome of *S. multivorans* is made of genes coding for PceA and other related proteins as well as the gene cluster responsible for the biosynthesis of corrinoids (12). This region is fully missing in non-OHRB *Sulfurospirillum* spp. and displays a GC skew different from the flanking genomic regions in *S. multivorans* (12). The comparison of part of the OHR region (~14 kb containing the essential *rdh* genes, transcriptional regulators and the *napGH*-like genes) between *S. diekertiae* SL2 strains and *S. multivorans* revealed the following differences (Figure 3.4). While the overall DNA sequence alignment showed a very

high degree of sequence identity (pairwise alignments with 99.34-99.69%), a 106-bp fragment is inserted in both SL2 genomes (and absent in *S. multivorans*) in the intergenic region between the *napH*-like gene and *cbiB*, the consequence of which remains unknown. Furthermore, in both SL2 genomes, a *tetR* transcriptional regulatory gene downstream of the corrinoid biosynthesis cluster appears to be functional in contrast to *S. multivorans* in the genome of which the *tetR* gene is disrupted by a transposase (12). An intact *tetR* gene has also been shown in the genome of *S. halorespirans* (T. Goris, personal communication), suggesting that it is not a specific feature of *S. diekertiae*. As previously identified (4), the nucleotide sequence identity of *pceA* genes in OHR members of *Sulfurospirillum* spp. clearly indicates that it is a hotspot for mutations, and represents most likely the driving force for the divergence of *Sulfurospirillum* OHR metabolism. The second reductive dehalogenase gene (*rdhA*), however, has not diverged between the three strains (100% sequence identity), an observation in line with the lack of expression observed so far for this gene (4, 12).

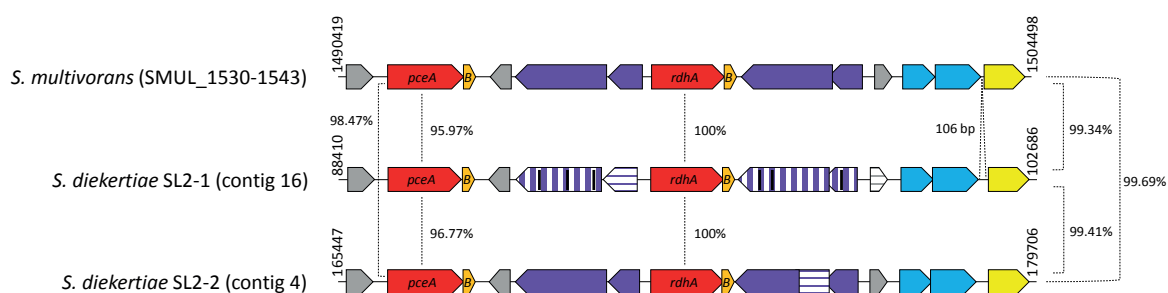


Figure 3.4. OHR region (partial) comparison of *S. diekertiae* strains SL2-1 and SL2-2 with *S. multivorans*.

The OHR region of *S. multivorans* (without the corrinoid biosynthesis gene cluster, (12)) was aligned with the corresponding region in the draft genomes of *S. diekertiae* strains SL2-1 and SL2-2. The coordinates are indicated at the beginning and end of each region. The DNA sequences were analyzed with ORFfinder to detect coding sequences and color-coded: red: reductive dehalogenases; orange: membrane anchor B subunit; purple: transcriptional regulators; blue: *napGH*-like genes; yellow: *cbiB*, the first gene of the corrinoid biosynthesis pathway; grey: unassigned function. Vertically striped arrows indicate genes likely interrupted by sequencing errors; horizontally striped arrows indicate genes or gene parts undetected by ORFfinder, the sequence of which being mostly matching with the one of *S. multivorans*.

3.4.2. Dechlorination as a measure for growth with SL2 consortia

An initial experiment was done to test whether the quantification of the chloride formed in SL2 cultures could be used as a measure for growth. Therefore, it was evaluated if there was

a direct correlation between the chloride release upon PCE dechlorination and the increase in *Sulfurospirillum rpoB* gene copy number, an indicator of the increase in the number of cells. Results showed that the evolution of the *rpoB* copy number of both SL2 strains is relatively well in line with the chloride release (Figure 3.5). This observation has already been demonstrated earlier for *D. restrictus* PER-K23 (15). Concentration of the released chloride reached 10 and 20 mmol/L for cultures of strain SL2-1 and SL2-2, respectively, as strain SL2-1 dechlorinates PCE to TCE exclusively, while strain SL2-2 can dechlorinate PCE and TCE to *cis*-DCE. From there on and in sake of simplicity, the quantification of chloride release was chosen as a good proxy to follow growth of the large number of SL2 cultures.

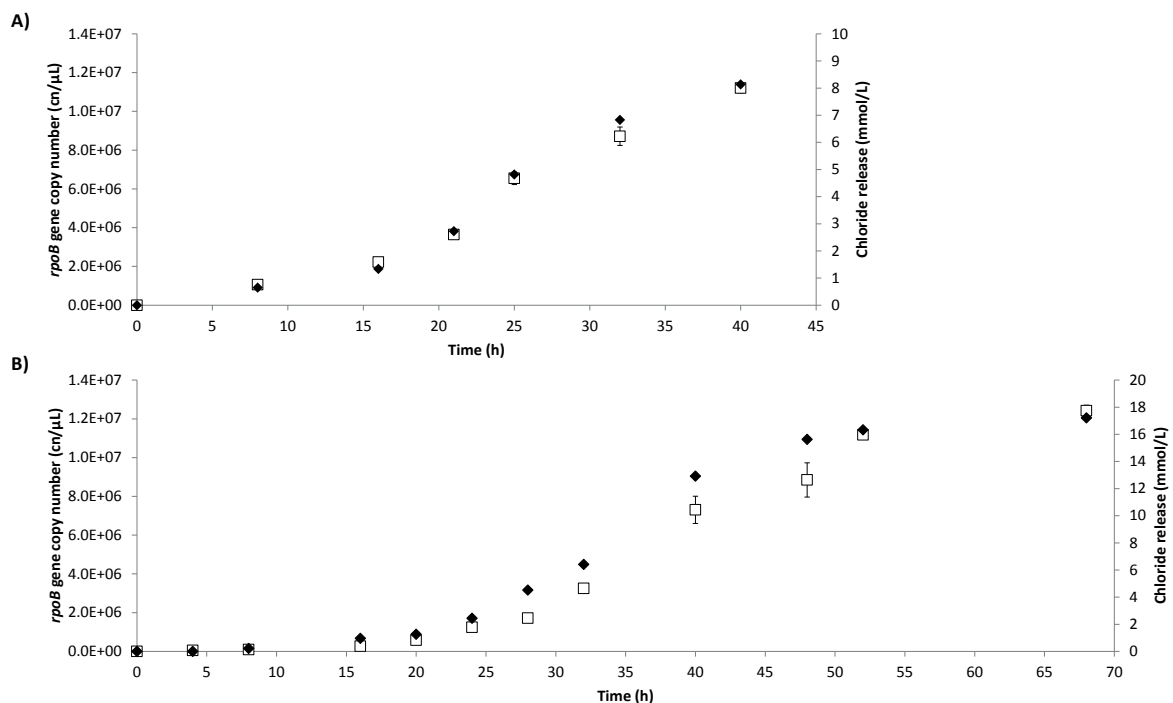


Figure 3.5. Direct correlation between chloride release and the *Sulfurospirillum rpoB* gene copy number in the SL2 consortia.

A) SL2-PCEc consortium (strain SL2-1); B) SL2-TCE consortium (strain SL2-2). Chloride release is represented by black diamonds and the *rpoB* gene copy number by white squares. Error bars refer to the replicate of qPCR runs. The same trend was observed for all culture replicates.

3.4.3. Tetrachloroethene dechlorination kinetic parameters of individual *S. diekertiae* SL2 strains

Since the gene content of *S. diekertiae* strains is extremely similar (Figure 3.2), one reason for their long-term coexistence in the mixed culture could be the result of the kinetic

parameters of their respective PceA enzyme. Previous data obtained from activity measurement in cell extracts (4) or with purified enzyme (CHAPTER 2) are not fully coherent and difficult to interpret. Therefore, it was decided to estimate the kinetic parameters of dechlorination for the two SL2 strains at the culture level.

3.4.3.1. Preliminary study

In a first attempt to see the effect of initial PCE concentration on the dechlorination rate, batch cultures of both SL2 consortia (each harboring one SL2 strain) have been performed with different PCE concentrations. Since preliminary data suggested that both strains have different dechlorination rates depending on the concentration (data not shown), strain SL2-1 was initially cultivated with a range of 2 to 20 μM $[\text{PCE}_{\text{aq}}]$, while SL2-2 was tested at 20, 80 and 100 μM $[\text{PCE}_{\text{aq}}]$ (Figure 3.6). Chloride concentration in the medium was measured over time and used as proxy for growth of the individual SL2 strains. From these data, several interesting features were observed. Firstly, the measured dechlorination rate was found to be dependent on the initial PCE concentration, suggesting that the chosen concentrations were indeed the limiting factor. At low PCE concentration, such as 2 μM $[\text{PCE}_{\text{aq}}]$, the time for complete dechlorination of the available substrate by strain SL2-1 is higher than at 20 μM $[\text{PCE}_{\text{aq}}]$, where it takes less than 50 hours (Figure 3.6 A). The same observation was made for strain SL2-2 and at 80 μM $[\text{PCE}_{\text{aq}}]$, this strain seemed to reach its maximum dechlorination rate, suggesting that PCE might become toxic at a certain concentration (Figure 3.6 B).

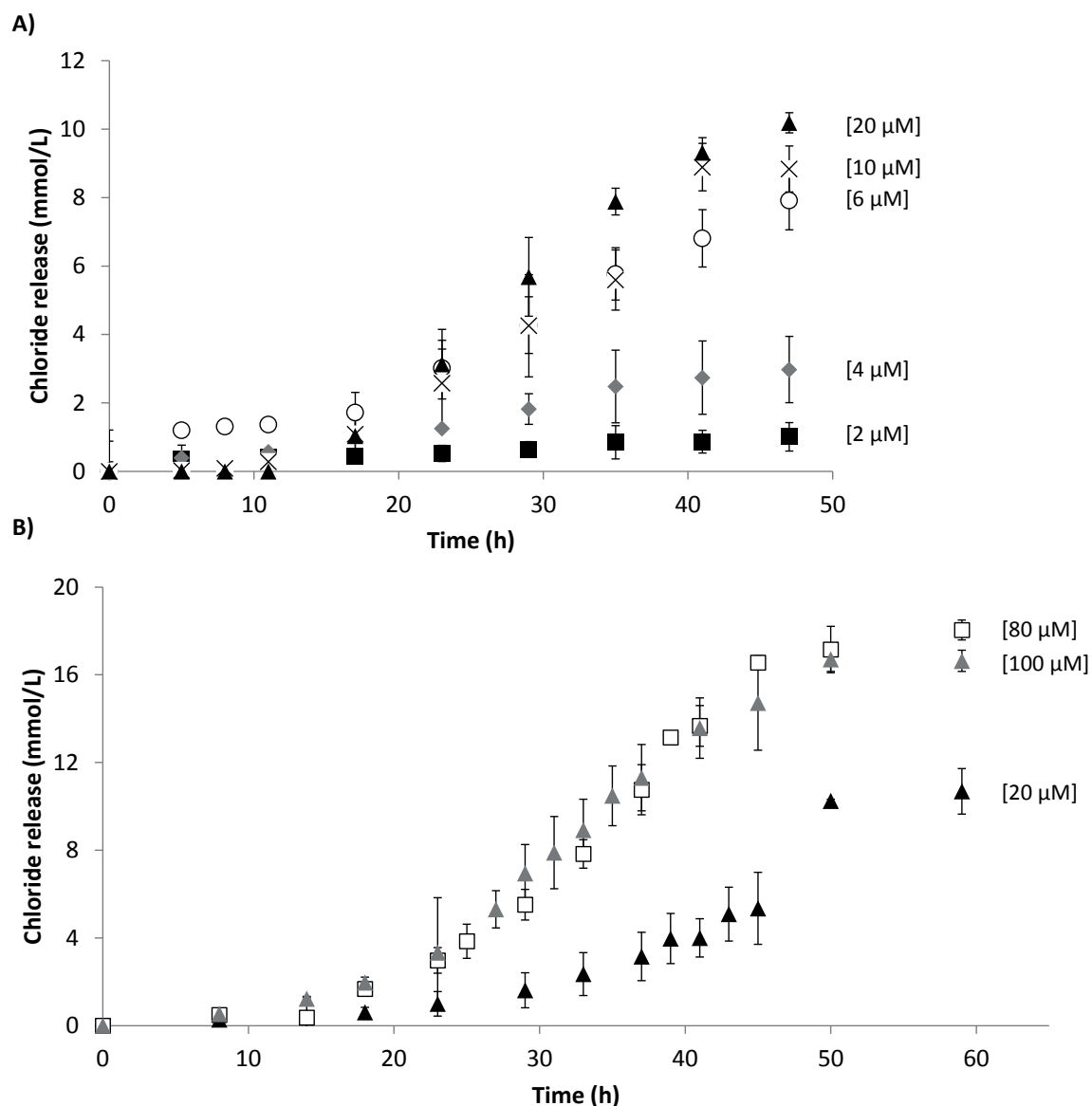


Figure 3.6. Dechlorination of *S. diekertiae* strains at various initial concentrations of PCE.

The graphs show the chloride release (mean of triplicate cultures) for strain SL2-1 (A) and SL2-2 (B). The aqueous initial concentration of PCE applied ($[PCE_{aq}]$) is indicated in brackets next to each dataset. Vertical bars indicate the standard deviation of the replicates.

3.4.3.2. Dechlorination behavior at a large range of PCE concentrations

Next, an extended dechlorination study with the strains SL2-1 and SL2-2 was performed in a range of PCE concentrations from 2 to 200 μM $[PCE_{aq}]$ in order to estimate their specific kinetic parameters. In a first analysis of the obtained chloride data, the growth rates (μ_{Cl} in h^{-1}) were estimated for all batch cultures by using visual inspection of the graphs (data not

shown). For each strain, the average of growth rate values obtained at given initial PCE concentrations was calculated and graphically represented (Figure 3.7). Despite some variability among replicates, a clear trend can be seen. For strain SL2-1, partial dechlorination inhibition seems to occur above 50 μM $[\text{PCE}_{\text{aq}}]$, while strain SL2-2 is inhibited above 80 μM $[\text{PCE}_{\text{aq}}]$. Both populations were severely inhibited at 200 μM $[\text{PCE}_{\text{aq}}]$. These observations are in accordance with what was reported previously for *S. multivorans* which can dechlorinate PCE at concentrations ≤ 330 μM but did not dechlorinate PCE at concentrations ≥ 540 μM (1). The observed dechlorination inhibition could be due to the toxicity of PCE itself or due to its transformation products, namely TCE or *cis*-DCE, as both compounds show higher solubility in water (8 mM and 79 mM, respectively) than PCE (1 mM) (5). Moreover, in previous studies, it has been reported that the highly chlorinated ethenes can competitively inhibit the reductive dechlorination of the less chlorinated ethenes and vice versa to a lesser extent (7, 30, 31). Therefore, in order to evaluate the nature and extent of dechlorination inhibition in SL2 consortia, additional experiments would need to be conducted with, for example, adding given amounts of TCE or *cis*-DCE to batch cultures amended with non-inhibiting concentrations of PCE.

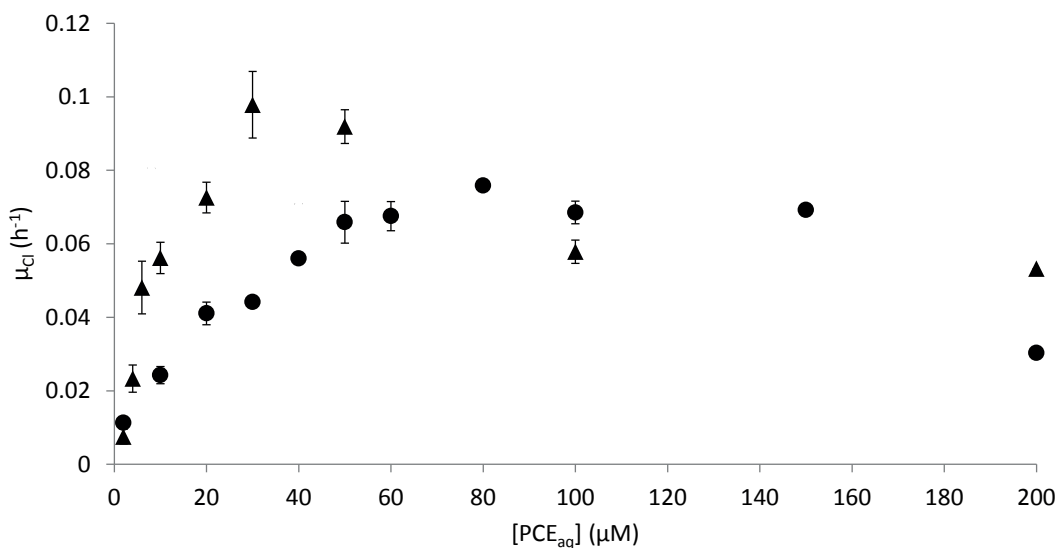


Figure 3.7. Growth rate of *S. diekertiae* SL2 strains as function of aqueous PCE concentration.

Inhibition was observed above 50 and 80 μM $[\text{PCE}_{\text{aq}}]$ for strains SL2-1 and SL2-2, respectively. Black triangles: strain SL2-1; black circles: strain SL2-2. For strain SL2-1 at $[\text{PCE}_{\text{aq}}]$ of 8 and 200 μM and strain SL2-2 at $[\text{PCE}_{\text{aq}}]$ of 2, 150 and 200 μM , the dechlorination rates were only determined in single culture replicates.

3.4.3.3. Estimation of kinetic parameters of both SL2 strains

A second and more thorough analysis of the dechlorination data was undertaken by using the Gompertz model for the description of the dynamics of bacterial cultures (11, 32). To this purpose, the chloride release at any time point t was expressed as the natural log of the ratio of chloride concentrations at time t and at time 0 ($\ln[Cl_t/Cl_0]$). This allowed considering the dechlorination-based kinetics independently of the concentration and mimics the typical behavior of bacterial growth. This way the dechlorination rate (q_{Cl} , in mmol/Lh) is converted into an apparent growth rate (μ_{Cl} , in h^{-1}). The apparent growth rates of all 75 batch cultures were obtained by fitting the data on the Gompertz equation (Annex 3.1). From a selection of the data (cultures with non-inhibiting PCE concentrations and those with SSE < 0.1) two linearization procedures were applied: Lineweaver-Burk and Hanes-Woolf (Figure 3.8). Table 3.6 compiles the dechlorination kinetic parameters for both SL2 strains. While $\mu_{max_{Cl}}$ values seem similar for both strains, $0.097 h^{-1}$ for strain SL2-1 and between 0.103 and $0.115 h^{-1}$ for strain SL2-2, strain SL2-1 has a 5- to 6-fold higher affinity for PCE than strain SL2-2, with K_S of $6.4 \mu M$ and between 32.4 and $37.5 \mu M$, respectively.

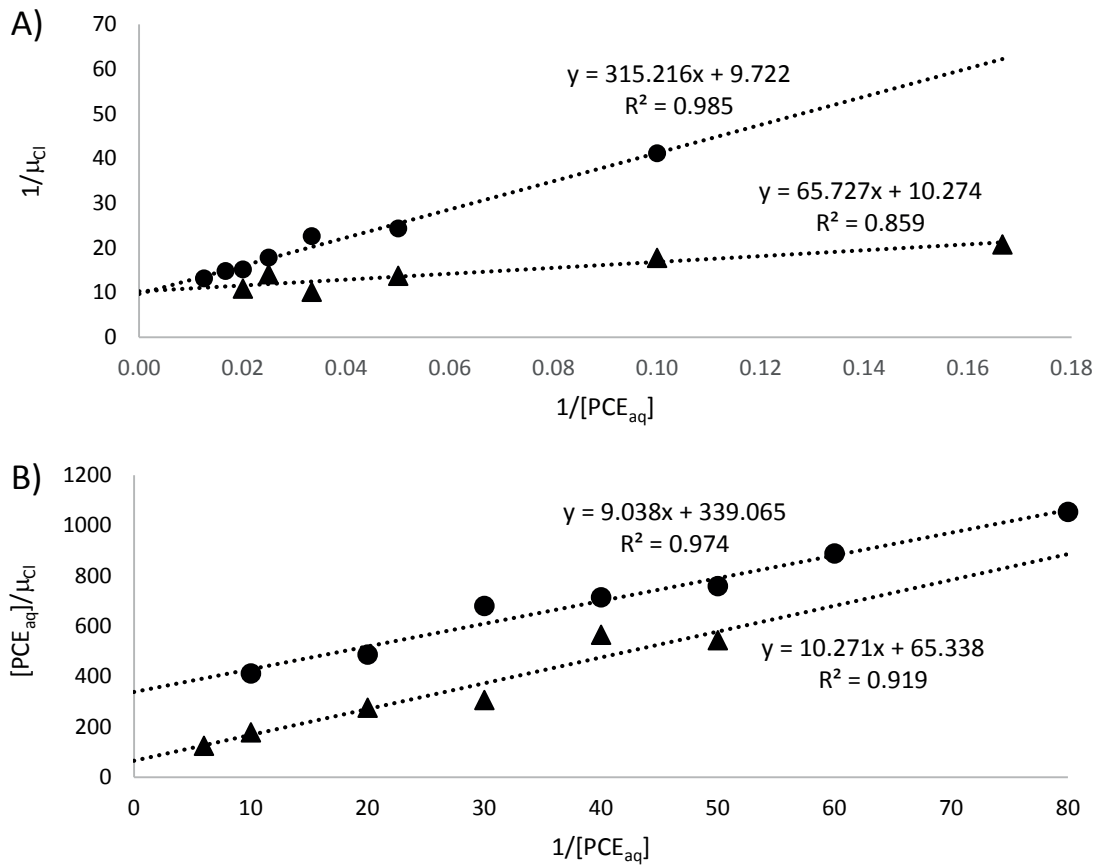


Figure 3.8. Estimation of dechlorination-based kinetic parameters of SL2 strains.

(A) Lineweaver-Burk and (B) Hanes-Woolf linearization procedures were used to estimate the affinity constants for PCE and the dechlorination-based maximal growth rates. Triangles: strain SL2-1; circles: strain SL2-2.

Table 3.6. Dechlorination-based kinetic parameters of SL2 strains.

	Strain SL2-1		Strain SL2-2	
	LB ¹	HW ²	LB ¹	HW ²
$\mu_{max_{Cl}} (h^{-1})$	0.097	0.097	0.103	0.111
$K_S (\mu M)$	6.4	6.4	32.4	37.5

¹ LB: Lineweaver-Burk linearization

² HW: Hanes-Woolf linearization

3.4.4. Competition experiments with *S. diekertiae* strains SL2-1 and SL2-2

Two competition experiments were performed in order to confirm the difference in dechlorination kinetics of the two SL2 strains. The two separate consortia were cultivated at 6 and 30 μM [PCE_{aq}], mixed at equal population size and used as inoculum to start cultures amended with the same concentrations of PCE. A PCE concentration of 30 μM should provide a suitable environment where no inhibition should play a role and both competing strains could coexist, while at 6 μM [PCE_{aq}], strain SL2-2 should be outcompeted by strain SL2-1 during dechlorination of PCE to TCE due to its lower affinity for PCE. The cultures were monitored for chlorinated ethenes (Figure 3.9, A and B), the chloride release and the abundance of strain-specific *pceA* genes (Figure 3.9, C and D).

At 30 μM [PCE_{aq}], both strains grew at approximately the same rate during the first dechlorination step (PCE to TCE) (Figure 3.9 C). After 35 h of incubation, *cis*-DCE started to appear (Figure 3.9 A) and was accompanied by a significant increase in the population size of strain SL2-2. In this culture, TCE did not significantly accumulate, thus reflecting the simultaneous action of both strains. At 6 μM [PCE_{aq}], strain SL2-1 initially grew at a faster rate than SL2-2 (Figure 3.9 D), which corresponds to a clear accumulation of TCE between 48 and 96 h (Figure 3.9 B). In this time window, growth of strain SL2-1 stalled and then started to decrease, while strain SL2-2 took over and was responsible for TCE dechlorination. At low PCE concentration, SL2-1 strain shows a clearly growth advantage over SL2-2, suggesting that the former has a higher affinity for PCE than the latter. This observation is well in line with K_s value for both strains (Table 3.6).

The application of Gompertz equation to the chloride data obtained in the competition batch cultures revealed μ_{Cl} values of 0.051 ± 0.008 and $0.042 \pm 0.007 \text{ h}^{-1}$ for the cultures at 30 and 6 μM [PCE_{aq}], respectively. The overall growth rates of the mixed cultures are the results of the interplay of both strains in PCE dechlorination. Since the affinity for PCE of both strains is different, the growth rate estimated for the cultures at 6 μM [PCE_{aq}] is likely to reflect the activity of strain SL2-1 mainly, while both strains contribute more equally to PCE dechlorination at 30 μM .

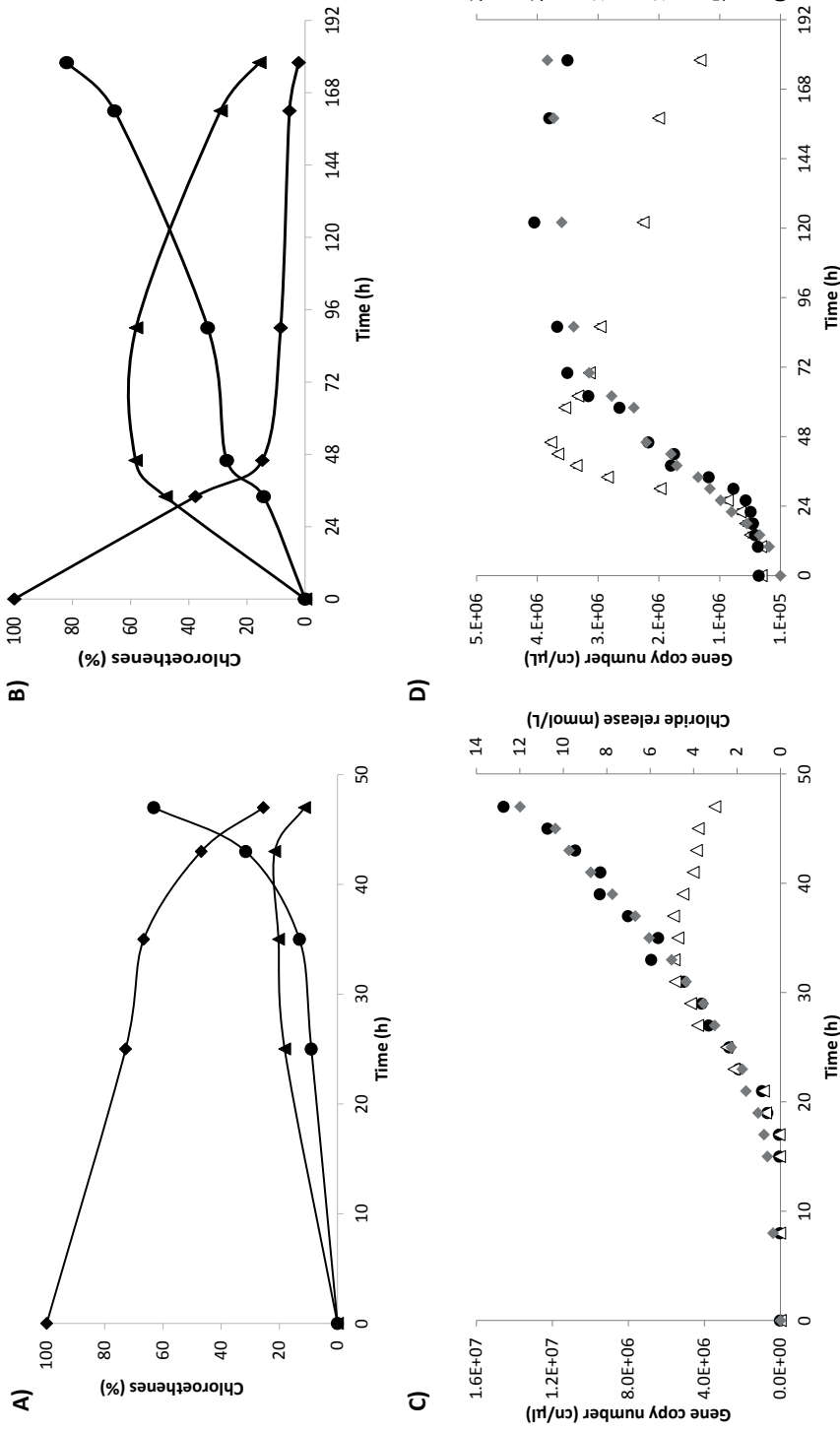


Figure 3.9. Competition of *S. diekertiæ* strains SL2-1 and SL2-2 for PCE.

The strains were cultivated at 30 μM [PCE_{aq}] (A and C) or 6 μM [PCE_{aq}] (B and D). The dechlorination of PCE (diamonds) to TCE (triangles) and *cis*-DCE (dots) is shown in (A and B). The gene copy number of *pceA_{TCE}* (strain SL2-1, white triangles), *pceA_{DCE}* (strain SL2-2, black dots), alongside with the chloride release (grey diamonds) are presented in graphs (C and D). Please note the different time scale of experiments in both cultures. The other replicate cultures followed the same trend (data not shown).

3.5. Concluding remarks and perspectives

The competition for nutrients among organisms can alter the ratio of species in a mixed culture. This is in close relation to the affinity of an organism for the limiting substrate and to its growth rate. If two strains in a mixed population (the simplest model of a bacterial community) have a similar affinity for PCE, the competition can result in the exclusion of the least fit organism from the system. However, after several years of cultivation the SL2-PCEb consortium harboring the strains SL2-1 and SL2-2 of *S. diekertiae*, the two populations were still coexisting. Such coexistence raised questions behind the nature and details of the interplay between these two closely related bacteria. As demonstrated in the first part of this study, *S. diekertiae* strains cluster nicely with other OHRB members of *Sulfurospirillum* spp., suggesting that *S. multivorans*, *S. halorespirans* and *S. diekertiae* evolved from a common ancestor and that their PCE dechlorination capability was inherited before species divergence. The nucleotide sequence identity of their *pceA* genes in *Sulfurospirillum* spp. strongly suggests that it is a hotspot for mutations, which likely represents the driving force for the evolution of *Sulfurospirillum* OHR metabolism. This could be one the reasons for the specialization of strain SL2-1 in the exclusive dechlorination of PCE to TCE. First indications showed that both SL2 strains behaved differently in the range of tested PCE concentrations. Strain SL2-1 has an apparent K_S value lower than strain SL2-2, while they display a similar maximal growth rate. The dechlorination kinetic parameters observed here likely explain the maintenance of strain SL2-1 in SL2-PCEb, as the bacterial consortium was continuously cultivated at 20 μM [PCE_{aq}], a concentration favorable to strain SL2-1.

As mentioned in a previous section of this work, both SL2 populations were severely inhibited at 200 μM [PCE_{aq}]. This observation is in line with work on *S. multivorans*, where substrate inhibition by PCE has been already observed. For example, it has been reported that *S. multivorans* can grow with either PCE or TCE as electron acceptor up to concentrations of 300 μM . At concentrations higher than 540 μM , however, PCE was not dechlorinated (1, 6, 20). In another work, it has been reported that the purified PCE dehalogenase is inhibited by high concentrations of PCE (K_i of 18 mM), TCE (K_i : 39 mM) and *cis*-DCE (K_i : 14 mM) (21). Although it is difficult to compare with the dechlorination kinetics of strains SL2, this reflects the possibility that PCE, but also the transformation products are

likely to affect the activity of the key enzyme in the OHR process, therefore also at the culture level. Moreover, the transformation products of PCE (TCE and *cis*-DCE) display a higher solubility in water, suggesting that inhibition could increase along with the extent of PCE dechlorination. The concept of self-inhibition (by the substrate and its transformation products) has been proposed to play an important role in OHR (29), but remains difficult to fully understand. In order to evaluate the nature and extent of dechlorination inhibition in SL2 cultures, additional experiments should be conducted with, for example, PceA enzymatic assays where inhibition by the final dechlorination product can be tested at the enzyme level. The type of inhibition could be also identified.

In conclusion, the major factor allowing the long-term coexistence of the two *S. dijkertiae* strains in the consortium SL2-PCEb is the relatively low PCE concentration that was amended to the culture throughout the years. Ecological implications of these findings remain to be investigated, but one could imagine that the interplay of OHRB is very likely to occur in environments that display PCE gradients, and that such ecological niches might represent a driving force to generate diversity at the strain and enzyme levels.

3.6. References

1. **Amos, B. K., J. A. Christ, L. M. Abriola, K. D. Pennell, and F. E. Loffler.** 2007. Experimental evaluation and mathematical modeling of microbially enhanced tetrachloroethene (PCE) dissolution. *Environ Sci Technol* **41**:963-970.
2. **Aziz, R. K., D. Bartels, A. A. Best, M. DeJongh, T. Disz, R. A. Edwards, K. Formis, S. Gerdes, et al.** 2008. The RAST Server: rapid annotations using subsystems technology. *BMC genomics* **9**:75.
3. **Baez-Ortega, A., F. Lorenzo-Diaz, M. Hernandez, C. I. Gonzalez-Vila, J. L. Roda-Garcia, M. Colebrook, and C. Flores.** 2015. IonGAP: integrative bacterial genome analysis for Ion Torrent sequence data. *Bioinformatics* **31**:2870-2873.
4. **Buttet, G. F., C. Holliger, and J. Maillard.** 2013. Functional genotyping of *Sulfurospirillum* spp. in mixed cultures allowed the identification of a new tetrachloroethene reductive dehalogenase. *Appl Environ Microbiol* **79**:6941-6947.
5. **Chambon, J. C., P. L. Bjerg, C. Scheutz, J. Baelum, R. Jakobsen, and P. J. Binning.** 2013. Review of reactive kinetic models describing reductive dechlorination of chlorinated ethenes in soil and groundwater. *Biotechnol Bioeng* **110**:1-23.
6. **Christ, J. A., and L. M. Abriola.** 2006. Modeling metabolic reductive dechlorination in dense non-aqueous phase liquid source-zones. *Adv. Water Resour.* **30**:1547-1561.
7. **Cupples, A. M., A. M. Spormann, and P. L. McCarty.** 2004. Comparative evaluation of chloroethene dechlorination to ethene by *Dehalococcoides*-like microorganisms. *Environ Sci Technol* **38**:4768-4774.
8. **Diaby, N., B. Dold, E. Rohrbach, C. Holliger, and P. Rossi.** 2015. Temporal evolution of bacterial communities associated with the *in situ* wetland-based remediation of a marine shore porphyry copper tailings deposit. *Sci Total Environ* **533**:110-121.
9. **Duhamel, M., K. Mo, and E. A. Edwards.** 2004. Characterization of a highly enriched *Dehalococcoides*-containing culture that grows on vinyl chloride and trichloroethene. *Appl Environ Microbiol* **70**:5538-5545.
10. **Fennell, D. E., Gossett, J. M.** 1998. Modeling the production of and competition for hydrogen in a dechlorinating culture. *Environ. Sci. Technol.* **32**:2450-2460.
11. **Gompertz, B.** 1825. On the nature of the function expressive of the law of human mortality, and on a new mode of determining the value of life contingencies. *Phil. Trans. R. Soc.*:513-583.
12. **Goris, T., T. Schubert, J. Gadkari, T. Wubet, M. Tarkka, F. Buscot, L. Adrian, and G. Diekert.** 2014. Insights into organohalide respiration and the versatile catabolism of *Sulfurospirillum multivorans* gained from comparative genomics and physiological studies. *Environ Microbiol* **16**:3562-3580.
13. **Groster, A., and E. A. Edwards.** 2006. Growth of *Dehalobacter* and *Dehalococcoides* spp. during degradation of chlorinated ethanes. *Appl Environ Microbiol* **72**:428-436.
14. **Holliger, C., D. Hahn, H. Harmsen, W. Ludwig, W. Schumacher, B. Tindall, F. Vazquez, N. Weiss, et al.** 1998. *Dehalobacter restrictus* gen. nov. and sp. nov., a strictly anaerobic bacterium that reductively dechlorinates tetra- and trichloroethene in an anaerobic respiration. *Arch Microbiol* **169**:313-321.
15. **Holliger, C., G. Schraa, A. J. Stams, and A. J. Zehnder.** 1993. A highly purified enrichment culture couples the reductive dechlorination of tetrachloroethene to growth. *Appl Environ Microbiol* **59**:2991-2997.
16. **Huang, D., and J. G. Becker.** 2011. Dehalorespiration model that incorporates the self-inhibition and biomass inactivation effects of high tetrachloroethene concentrations. *Environ Sci Technol* **45**:1093-1099.
17. **Larkin, M. A., G. Blackshields, N. P. Brown, R. Chenna, P. A. McGettigan, H. McWilliam, F. Valentin, I. M. Wallace, et al.** 2007. Clustal W and Clustal X version 2.0. *Bioinformatics* **23**:2947-2948.

18. **Lee, I. S., J. H. Bae, Y. Yang, and P. L. McCarty.** 2004. Simulated and experimental evaluation of factors affecting the rate and extent of reductive dehalogenation of chloroethenes with glucose. *J Contam Hydrol* **74**:313-331.
19. **Maillard, J., M. P. Charnay, C. Regeard, E. Rohrbach-Brandt, K. Rouzeau-Szynalski, P. Rossi, and C. Holliger.** 2011. Reductive dechlorination of tetrachloroethene by a stepwise catalysis of different organohalide respiring bacteria and reductive dehalogenases. *Biodegradation* **22**:949-960.
20. **Neumann, A., T. Engelmann, R. Schmitz, Y. Greiser, A. Orthaus, and G. Diekert.** 2004. Phenyl methyl ethers: novel electron donors for respiratory growth of *Desulfitobacterium hafniense* and *Desulfitobacterium* sp. strain PCE-S. *Arch Microbiol* **181**:245-249.
21. **Neumann, A., G. Wohlfarth, and G. Diekert.** 1996. Purification and characterization of tetrachloroethene reductive dehalogenase from *Dehalospirillum multivorans*. *J Biol Chem* **271**:16515-16519.
22. **Ritalahti, K. M., B. K. Amos, Y. Sung, Q. Wu, S. S. Koenigsberg, and F. E. Löffler.** 2006. Quantitative PCR targeting 16S rRNA and reductive dehalogenase genes simultaneously monitors multiple *Dehalococcoides* strains. *Appl Environ Microbiol* **72**:2765-2774.
23. **Rouzeau-Szynalski, K., J. Maillard, and C. Holliger.** 2011. Frequent concomitant presence of *Desulfitobacterium* spp. and "*Dehalococcoides*" spp. in chloroethene-dechlorinating microbial communities. *Appl Microbiol Biotechnol* **90**:361-368.
24. **Sambrook, J., E. F. Fritsch, and T. Maniatis.** 1989. *Molecular cloning : a laboratory manual*, 2nd ed. Cold Spring Harbor Laboratory, New York.
25. **Schloss, P. D., S. L. Westcott, T. Ryabin, J. R. Hall, M. Hartmann, E. B. Hollister, R. A. Lesniewski, B. B. Oakley, et al.** 2009. Introducing mothur: open-source, platform-independent, community-supported software for describing and comparing microbial communities. *Appl Environ Microbiol* **75**:7537-7541.
26. **Sung, Y., K. E. Fletcher, K. M. Ritalahti, R. P. Apkarian, N. Ramos-Hernandez, R. A. Sanford, N. M. Mesbah, and F. E. Löffler.** 2006. *Geobacter lovleyi* sp. nov. strain SZ, a novel metal-reducing and tetrachloroethene-dechlorinating bacterium. *Appl Environ Microbiol* **72**:2775-2782.
27. **Tamura, K., G. Stecher, D. Peterson, A. Filipski, and S. Kumar.** 2013. MEGA6: Molecular Evolutionary Genetics Analysis version 6.0. *Molecular biology and evolution* **30**:2725-2729.
28. **Waller, A. S., R. Krajmalnik-Brown, F. E. Löffler, and E. A. Edwards.** 2005. Multiple reductive-dehalogenase-homologous genes are simultaneously transcribed during dechlorination by *Dehalococcoides*-containing cultures. *Appl Environ Microbiol* **71**:8257-8264.
29. **Wei K., G. A., Chan W. W.M., Richardson R. E., Edwards E. A.** 2016. Electron acceptor interactions between organohalide-respiring bacteria: cross-feeding, competition, and inhibition, p.283-308. *In* L. Adrian and F. E. Löffler (ed.), *Organohalide-Respiring Bacteria*. Springer Berlin Heidelberg.
30. **Yu, S., M. E. Dolan, and L. Semprini.** 2005. Kinetics and inhibition of reductive dechlorination of chlorinated ethylenes by two different mixed cultures. *Environ Sci Technol* **39**:195-205.
31. **Yu, S., and L. Semprini.** 2004. Kinetics and modeling of reductive dechlorination at high PCE and TCE concentrations. *Biotechnol Bioeng* **88**:451-464.
32. **Zwietering, M. H., I. Jongenburger, F. M. Rombouts, and K. van 't Riet.** 1990. Modeling of the bacterial growth curve. *Appl Environ Microbiol* **56**:1875-1881.

Chapter 4

Biochemical characterization
of the flavin domain of PceC

4. Biochemical characterization of the flavin domain of PceC

4.1. Abstract

In organohalide respiration (OHR), only little information is available on the composition of the electron transport chain that feeds electrons to the reductive dehalogenase, the terminal enzyme in the process. The *pceABCT* gene operon involved in PCE respiration can be found in members of the genera *Desulfitobacterium* and *Dehalobacter*, and can be considered as a model system for studying OHR. While the function of PceA and PceT is well established, it is very likely that PceB plays the role of membrane anchor for PceA. The remaining gene, *pceC*, codes for a predicted membrane-bound flavoprotein with additional conserved cysteine motifs. Despite the fact that it has been considered as putative transcriptional regulator, it presents all the features that could potentially fulfill the role of electron shuttle between reduced menaquinones and PceA. This question was addressed in the present chapter.

It was shown that PceC is present in the membrane proteomes of *Desulfitobacterium hafniense* strain TCE1 and *Dehalobacter restrictus* and proteomic data interpretation suggested that it is as abundant as PceB, and harbors a covalent FMN cofactor. The predicted FMN-binding domain of PceC (PceC-FBD) was heterologously produced in *E. coli* where it formed inclusion bodies. After denaturation with urea, a strategy was developed to reconstitute PceC-FBD in a soluble form by inserting FMN with the help of Ftp1, a flavin-transferase of *D. hafniense* also produced in *E. coli*. The predicted threonine residue in the FMN-binding motif (PceC-Thr₁₆₈) was unambiguously assigned by site-specific mutagenesis and detailed mass spectrometry analysis. These results offer a new way to address the question of the involvement of PceC in the respiratory chain of OHR metabolism.

4.2. Introduction

At present, little is known about the composition of the electron transport chain in organohalide-respiring bacteria (OHRB) and the nature of electron-transferring components from the cytoplasmic membrane involved in delivering electrons to the reductive dehalogenase (RdhA). The relatively low redox potential measured for RdhA cofactors, the peripheral location of RdhA on the outside of the cytoplasmic membrane, and the presence of multiple open reading frames (ORFs) within *rdh* gene clusters strongly invite to look for additional redox partners in the OHR process. In *Dehalobacter* spp. and *Desulfitobacterium* spp., the characterization of the genetic context around the tetrachloroethene (PCE) *rdhA* (*pceA*) resulted in the identification of the *pceABCT* gene cluster (12, 21). Besides *pceA*, the other gene products are likely to play a direct or indirect role in the catalytic electron transfer to the chlorinated substrate. While PceB, a small hydrophobic protein, has always been speculatively considered as the membrane anchor of PceA in the cytoplasmic membrane, PceT acts as a dedicated molecular chaperone in PceA maturation (19, 20, 22). The physiological role of gene product of *pceC*, however, remains unclear. PceC is encoded in *pce* gene clusters of *Dehalobacter* and *Desulfitobacterium* isolates and is homologous to CprC of *D. dehalogenans* which has been postulated as a membrane-bound regulatory protein due to its sequence similarity with the NosR/NirI family of regulators (26). These latter proteins have been shown to play a role in a signal transduction pathway that eventually controls the transcription of the nitrous oxide (*nos*) and nitrite reductase (*nir*) gene clusters of *Paracoccus denitrificans* and *Pseudomonas stutzeri*, respectively (25, 29). The sequence similarity is mostly pronounced in the N-terminal region (one transmembrane α -helix (TMH) and a predicted flavin mononucleotide (FMN) binding domain) and a domain with 5 TMHs including two CXXXCP conserved motifs. However, both PceC and CprC (and in a larger spectrum, all members of the RdhC family) are significantly smaller than NosR/NirI proteins, as they lack the C-terminal cytoplasmic domain containing two additional [4Fe-4S] binding motifs present in NosR and NirI.

It was therefore decided to reconsider the function of PceC as it could possibly represent the missing link between the menaquinone pool of the respiratory chain and PceA. However, until now because of the high hydrophobicity of the protein, attempts in expressing the *pceC*

gene in a soluble form have failed (23). A new strategy was applied here based on a recent report where two subunits (NqrB and NqrC) involved in Na⁺-translocating NADH:quinone oxidoreductase (Na⁺-NQR) and containing a covalently attached FMN have been produced by using a flavin-transferase (4).

Using a flavin-transferase of *D. hafniense* strain TCE1, the FMN-binding domain of PceC (PceC-FBD) could be produced in a soluble form and different properties of PceC-FBD were characterized.

4.3. Material and methods

4.3.1. Bacterial strains and growth conditions

E. coli strains were cultivated aerobically at 37°C in Luria Bertani (LB) medium. Cells containing various expression plasmids were cultivated in the presence of 100 µg/mL ampicillin, or 50 µg/mL kanamycin. *E. coli* strains and plasmids used are listed in Table 4.1.

Table 4.1. Bacterial strains and plasmids used in this work.

Strain/Plasmid	Description	Reference or source
Strain		
<i>E. coli</i> DH5α	F ⁻ endA1 glnV44 thi-1 recA1 relA1 gyrA96 deoR nupG purB20 φ80dlacZΔM15 Δ(lacZYA-argF)U169, hsdR17(r _K ⁻ m _K ⁺), λ ⁻	Lifetechnologies
<i>E. coli</i> BL21 (DE3)	F ⁻ ompT gal dcm lon hsdSB (Rb-mB-) λ (DE3 [santi lacUV5-T7 gene 1 ind1 sam7 nin5])	Biolabs
<i>Desulfitobacterium hafniense</i> TCE1	DSM 12704	DSMZ, (13)
Plasmids		
pETDuet-1	Expression vector for two gene targets (2 MCS), IPTG-inducible T7 promoter, Amp ^R , MCS1 with C-terminal His•Tag [®] and MCS2 with C-terminal S•Tag [™]	Novagen
pET24d	Expression vector, IPTG-inducible T7 promoter, Kan ^R , with a C-terminal His•Tag [®] sequence	Novagen
pFTP1	Modified version of <i>ftp1</i> gene from <i>D. hafniense</i> TCE1 cloned into MCS2 of pETDuet-1 with C-terminal S•tag [™]	This work
pFTP2	Modified version of <i>ftp2</i> gene from <i>D. hafniense</i> TCE1 cloned into MCS2 of pETDuet-1 with C-terminal S•tag [™]	This work
pPCH	FMN-binding domain coding gene fragment of <i>pceC</i> (PceC ₄₁₋₂₀₀) from <i>D. hafniense</i> TCE1 cloned into pET24d with C-terminal histidine tag	This work
pPCH-T168V	as pPCH with site-specific mutation for T168V variant (original position in full-length PceC)	This work

4.3.2. DNA work

4.3.2.1. DNA extraction and quantification

Biomass pellets were resuspended in lysis buffer containing 20 mM Tris-HCl (pH 8), 2 mM sodium-EDTA, 1.2% Triton[®] X-100 and 20 mg/mL lysozyme. The DNA extraction kit DNeasy[®] Blood & Tissue (Qiagen, Hilden) was used for genomic DNA extraction according to manufacturer's instructions. Finally 200 µL DNA samples were recovered. The extracted DNA

was quantified with the NanoDrop spectrophotometer (ND-1000, Thermo Fisher Scientific, Wohlen AG).

4.3.2.2. Competent *E. coli* cells preparation

Escherichia coli DH5 α was used as a host for molecular cloning as described in CHAPTER 2 and CHAPTER 3 with the following modifications: competent cells were made in an ice cold TFB-I solution (30 mM potassium acetate, 10 mM CaCl₂, 100 mM RbCl, 15% (v/v) of glycerol, corrected to pH 5.8 with 1 M acetic acid and an ice cold TFB-II solution (10 mM MOPS buffer pH 6.5, 75 mM CaCl₂, 10 mM RbCl, 15 % (v/v) glycerol) (15).

4.3.2.3. Molecular cloning

The *ftp1*, *ftp2* genes from *D. hafniense* strain TCE1 were cloned into the 2nd MCS of the pETDuet-1 (Novagen), conferring a S•tagTM fused at the C-terminal end of the recombinant Ftp1 and Ftp2 in order to make the protein more soluble (Table 4.1). The sequence coding for the initial transmembrane α -helix of both Ftp proteins was excluded in order to make them soluble (Appendix 4.1).

The DNA fragment coding for the FMN-binding domain (FBD) of PceC (PceC-FBD, PceC₄₁₋₂₀₀) of *D. hafniense* strain TCE1 was cloned in the expression vector pET24d (Novagen), conferring a His-tag[®] at the C-terminal end of the recombinant protein (Table 4.2).

Oligonucleotides (purchased at Microsynth, Balgach) and restriction enzymes (Promega) used in this study are listed in Table 4.2. Standard PCR reactions were performed with the following 50 μ L reaction mixture: 5 μ L Pfu DNA Polymerase 10 \times Buffer, 0.075 mM dNTPs, 0.5 μ M each primer, 0.5 μ L of Pfu DNA polymerase (3 units/ μ L) (Promega). The DNA was amplified in T3 Thermocycler (Biometra, Labgene, Châtel-St-Denis) with the following steps: 2 min initial denaturation at 95°C, 30 cycles of 1 min denaturation at 95°C, 1 min of primer annealing at 52°C, 1 min of elongation at 72°C, 10 min of final extension step at 72°C. For cloning, PCR products, pETDuet-1 and pET24d plasmids were digested with appropriate digestion enzymes (Table 4.2), purified using the PCR purification kit (Qiagen). Ligation was then performed with the T4 DNA ligase (Roche) at 16°C o/n (as described in CHAPTER 2), and half of the ligation mixture was transformed into RbCl competent *E. coli* DH5 α cells following a 1 min heat shock at 42°C. Cells were incubated 1 h in 1 mL LB at 37°C before plating onto

LB plates containing the appropriate antibiotics (50 µg/mL ampicillin for pETDuet-1 derivatives and 100 µg/mL kanamycin for pET24d derivatives). To select positive clones, colony PCR was applied as described in CHAPTER 2. Plasmid extraction and sequencing was also performed as described in CHAPTER 2.

Table 4.2. Oligonucleotides used in this study.

Primer name	Target	Sequence (5'→3') ¹	Restriction site
<i>pceC160-24-F</i>	<i>pceC-FBD</i>	GCGCCCATGGGACAATCGGTTGATTACAAGGGAATC	<i>NcoI</i>
<i>pceC160-24-R</i>		GCGCCTCGAGTAAATCGTAAGGGTTGGCCCATTG	<i>XhoI</i>
<i>pceC-T168V-QC-F</i>	<i>pceC-FBD</i> variant	ACGGTAACAGGTTCA GT AGTGTGTCGTACATGCT	-
<i>pceC-T168V-QC-R</i>		AGCATGTGACGACAC TACT GAACTGTTACCGT	-
<i>Dha-Ftp1-F</i>	<i>ftp1</i>	GCGCCATATGAATGGGAAACCTGTACAACAG	<i>NdeI</i>
<i>Dha-Ftp1-R</i>		GCGCCTCGAGATCTTTGACGAATTCGTACTC	<i>XhoI</i>
<i>Dha-Ftp2-F</i>	<i>ftp2</i>	GCGCCATATGTTGTCTGCAGAGACCAAGG	<i>NdeI</i>
<i>Dha-Ftp2-R</i>		GCGCCTCGAGTTTGCTTTCTGGGGAAGGTGTC	<i>XhoI</i>
pET24d-F2	pET24d	GGTGATGTCGGCGATATAGG	-
pET24d-R2		CGTTTAGAGGCCCAAGG	-
Duet-MCS2-F	MCS2	TTGTACACGGCCGCATAATC	-
Duet-MCS2-R		GCTAGTTATTGCTCAGCGG	-

¹ The respective restriction enzymes sites are underlined in the sequence of the primers. The site-specific mutation is indicated in red.

4.3.2.4. Site-directed mutagenesis

To produce the threonine-to-valine (T168V) variant of PceC-FBD, the procedure was adapted from the QuikChange® Site-Directed Mutagenesis protocol (Stratagene). Two primers complementary to each other were designed to contain the site-specific mutation located in the middle of the primer sequence (Table 4.2). The reaction mixture for the PCR was the following: 5 µL of Pfu Turbo polymerase 10× buffer, 12.5 µM each primer, 2.5 mM dNTPs, 1 µL of Pfu Turbo Polymerase (Agilent Technologies). The pPCH plasmid (1 µL) was used as template DNA. Plasmid DNA was amplified in T3 Thermocycler (Biometra, Labgene, Châtel-St-Denis) with the following steps: 30 sec initial denaturation at 95°C, 30 cycles of 30 sec denaturation at 95°C, 60 sec of primer annealing at 55°C, 10 min of elongation at 68°C, 7 min of a final extension step at 68°C. The PCR product was then treated with *DpnI* endonuclease to digest the parental methylated plasmid template and to select for mutation-containing unmethylated plasmid amplified DNA. Linear plasmids were transformed in RbCl competent *E. coli* DH5α cells as describe above. Plasmid extraction and sequencing were performed as explained above.

4.3.3. Production of recombinant Ftp1 and Ftp2 proteins

E. coli BL21 cells harboring plasmids from pFTP1 and pFTP2 were initially cultivated in 50 mL pre-culture in LB medium supplemented with ampicillin at 37°C. The overnight pre-culture served as inoculum for 3 x 1 L culture. Incubation was performed at 37°C under agitation (180 rpm) until the absorbance at 600 nm reached 0.5. At this point, protein expression was induced by the addition of isopropyl- β -D-thiogalactopyranoside (IPTG) to a final concentration of 100 μ M. After 3 h of incubation at 30°C, cells were harvested by centrifugation at 12,000 x *g* for 20 min at 4°C. The cell pellet was washed in 50 mM Tris-HCl buffer (pH 7.5), flash-frozen in liquid N₂, and stored at -80°C. When processed, the cell pellet was resuspended (5 ml/g biomass wet weight) in Tris buffer containing a protease inhibitors cocktail (Sigmafast, Sigma-Aldrich) and a few DNaseI crystals. Cells were lysed by three passages through a French Pressure cell at 1000 psi. Unbroken cells and cell debris were removed by centrifugation at 4,500 x *g* at 4°C for 15 min and the supernatant was collected. *E. coli* soluble extract containing Ftp1 and Ftp2 were used for the reconstitution experiments.

4.3.4. Production of recombinant PceC-FBD and variant

E. coli BL21 cells harboring the pPCH plasmid and derivative thereof were initially cultivated in 5 mL pre-culture in LB medium supplemented with kanamycin. After 4-5 h of incubation at 37°C, 0.5 mL of the pre-culture served as inoculum for 500 mL culture in auto-inducing media as described in (27). Briefly, ZYM-5052 was prepared as follows: 480 mL ZY (10 g N-Z-amine AS, 5 g yeast extract, 1 L H₂O), 1 mL 1 M MgSO₄, 10 mL 50x 5052 (25 g glycerol, 73 mL H₂O, 2.5 g glucose, 10 g α -lactose monohydrate and 10 mL 50x M (17.75 g Na₂HPO₄, 17 g KH₂PO₄, 13.4 g NH₄Cl, 3.55 g Na₂SO₄, pH 6.7). Incubation was performed overnight at 20°C under agitation (250 rpm). After 16 h, cells were harvested by centrifugation at 12,000 x *g* for 20 min at 4°C. The cell pellet was washed in 50 mM Tris-HCl buffer (pH 7.5), flash-frozen in liquid N₂, and stored at -80°C.

4.3.5. Fractionation of cell containing PceC-FBD inclusion bodies

The biomass pellet was resuspended (5 mL/g biomass wet weight) in 50 mM Tris-HCl buffer (pH 7.5) containing a protease inhibitors cocktail (Sigma) and a few crystals of DNaseI

(Roche). Cells were lysed by four passages through a French Pressure cell (1000 psi). Soluble and insoluble fractions (containing PceC-FBD inclusion bodies) were obtained by centrifugation at 4,500 x *g* at 4°C for 15 min and the supernatant was removed. The inclusion bodies were resuspended in a wash buffer (50 mM Tris-HCl (pH 7.5) containing 1% Triton X-100 and the protease inhibitors) and stirred for 15 min at RT. Inclusion bodies were recovered by centrifugation as before. Inclusion bodies were resuspended in denaturing buffer (50 mM Tris-HCl (pH 7.5), 150 mM NaCl, 1 mM dithiothreitol and 4 or 8 M urea) and stirred for 30 min at RT. As before, it was centrifuged once again. The supernatant containing urea-solubilized inclusion bodies was collected and filtered at 0.45 µm.

4.3.6. Reconstitution of PceC-FBD proteins

Reconstitution of PceC-FBD proteins with the flavin-transferase Ftp1 was attempted by using different strategies, as presented below.

4.3.6.1. PceC-FBD reconstitution in solution

In the first strategy, the 4 M urea-denatured PceC-FBD protein displaying a C-terminal His-tag[®] was purified by fast protein liquid chromatography (FPLC) using the ÄKTAprime plus apparatus (GE Healthcare). First the cell extract was loaded onto a Ni-NTA affinity column (HisTrap™ HP, GE Healthcare), equilibrated with urea-containing buffer (150 mM NaCl, 50 mM Tris-HCl buffer (pH 7.5), 10 mM imidazole, 1 mM DTT and 4M urea). Proteins were eluted with 10 mL gradient of 0-1 M imidazole in urea-containing buffer with addition of 1 M imidazole. One mL fractions were collected. Eluted fractions were analyzed by SDS-PAGE stained with Coomassie blue and fractions containing purified urea-solubilized PceC-FBD were pooled. Then, the fraction displaying the purified urea-solubilized PceC-FBD (10 µL) was incubated in 600 µL of a reconstitution buffer containing 100 mM NaCl, 0.1 mM FAD, 10 mM Tris-HCl (pH 8.0), 5 mM MgSO₄, in the presence or absence of 50 µL of Ftp1 or Ftp2 containing extracts (0.22 mg/mL), and the mixture is then diluted with H₂O (340 µL or 390 µL, respectively) to a total volume of 1 mL. The reaction mixture was then stirred at RT for 45 min. After incubation, aliquots of the samples were loaded on SDS-PAGE. The FMN-containing proteins were detected under UV illumination, and the gel was then stained with Coomassie as described below.

4.3.6.2. PceC-FBD reconstitution on column

A second strategy for PceC-FBD refolding and FMN insertion was performed on a 5-mL Ni-NTA column using the ÄKTAprime plus apparatus (GE Healthcare). Inclusion bodies of PceC-FBD were recovered, washed, and urea-denatured as explained above. Unfolded PceC-FBD protein was loaded onto the column in presence of urea-containing binding buffer (4 M urea, 150 mM NaCl, 50 mM Tris-HCl, 25 mM imidazole, 1mM DTT), unbound proteins were removed by rinsing the column with binding buffer. The column was then detached from the purification system and manual injections were applied. Ten-mL mixtures containing various volumes of basic buffer (as binding buffer without urea), basic buffer containing decreasing concentrations of urea, and 0.5 mL of reconstitution buffer (containing 50 mM MgSO₄, 10 mM FAD and 0.18 mg/mL of Ftp1-containing extracts) were successively injected on the column in a reverse urea step gradient, as indicated in Table 4.3. Fifteen column volumes (75 mL) of urea-free buffer was applied to rinse the column prior to elution. Five column volumes (25 mL) of the reconstituted PceC-FBD was eluted in elution buffer (150 mM NaCl, 50 mM Tris-HCl, 600 mM imidazole, 1 mM DTT). Eluted fractions were then analyzed by SDS-PAGE, UV illumination. Protein content was analyzed with the BCA protein quantification kit (Thermo Scientific) with BSA standards prepared in the same buffer.

Table 4.3. Stepwise reconstitution mixtures.

4 M urea buffer (mL)	Urea free buffer (mL)	Reconstitution buffer (mL)	Incubation time (min)
4.5	0	0.5	0
4.0	0.5	0.5	5
3.5	1.0	0.5	5
3.0	1.5	0.5	5
2.5	2.0	0.5	5
2.0	2.5	0.5	10
1.5	3.0	0.5	10
1.0	3.5	0.5	15
0.5	4.0	0.5	15
0	4.5	0.5	30

4.3.6.3. *PceC-FBD reconstitution with dialysis*

The third strategy was performed using successive dialysis baths with decreasing concentrations of urea as following. 20 mL of the urea-denatured PceC-FBD protein was dialyzed at RT for 2 h in 200 mL of dialysis buffer 1 (4 M urea, 50 mM Tris-HCl, pH 7.5, 150 mM NaCl, protease inhibitors). The protein was recovered from the dialysis tube, an aliquot was taken for testing solubility and the following reconstitution elements were added to the rest of the sample: 1.4 mL of reconstitution buffer (5 mM MgSO₄ (final concentration) and 1 mM FAD) and 4 mL of Ftp1-containing cell extract (0.35 mg/mL). The reaction mix was incubated 20 min at RT with stirring. The reaction mix was then dialyzed at RT for 2 h in 200 mL of dialysis buffer 2 (as buffer 1 but with only 2 M urea). The protein was recovered from the dialysis tube, an aliquot taken for testing solubility, and the remaining was mixed with reconstitution elements once again and incubated 20 min at RT with stirring. The protein was dialyzed for 2 h at RT in 200 mL of dialysis buffer 3 (as buffer 1 but without urea). The PceC-FBD protein was collected from the dialysis tube, an aliquot taken for analysis, and the rest of sample was subjected to centrifugation at 15,000 x *g* for 20 min at 4°C. The supernatant was further dialyzed overnight into dialysis buffer 4 (50 mM Tris-HCl (pH 7.5), 150 mM NaCl). Soluble protein was again recovered by centrifugation. A total volume of 25 mL at a protein concentration of 3.93 mg/mL was obtained. Aliquots taken during the complete procedure were loaded on SDS-PAGE. FMN-containing proteins were detected under UV illumination, and the gel was stained with Coomassie as described below.

4.3.7. SDS-PAGE gel staining and image analysis

SDS-PAGE gels were done as described in CHAPTER 2, with some modifications. Firstly the gels were revealed by staining them in Coomassie staining solution (10% acetic acid, 40% ethanol, 0.1 % Coomassie Blue R-250) by heating for 2 min in a microwave (until the solution boils), then incubated for 10 min on a rocking table. The gel was incubated in destaining solution (10% acetic acid, 40% ethanol) by heating again, then incubated for 10 min on a rocking table and finally rinsed in water. Pictures of stained gels were taken on an illuminating plate. In case of in-gel detection of flavin-containing proteins (1), the gels were exposed to UV light on a UV transilluminator (Bio Imaging system, Syngene) prior to Coomassie staining.

4.3.8. Sample preparation for proteome analysis

D. hafniense strain TCE1 cultures (50 mL) were harvested in exponential phase by centrifugation at 3,300 x *g* for 10 min at 4°C. Cell pellets were washed in 50 mM Tris-HCl buffer (pH 7.5) and transferred to a 1.5 mL microcentrifuge tube. The biomass was centrifuged at 8,800 x *g* for 5 min and the pellets were flash-frozen in liquid N₂ and conserved at -20°C. Cell pellets were resuspended in Tris buffer (50 mM Tris-HCl (pH 7.5), 50 mM NaCl, and protease inhibitors), and disrupted by 5 cycles of 10× 1 s sonication (Vibracell 72405, Bioblock Scientific) at 60% of amplitude with 30 s pause on ice in between cycles. Urea solutions (6 M) were added to the cell extracts in order to extract membrane proteins. A sample was also treated without urea for comparison (Tris buffer was added instead of urea). The lysate was incubated on ice for 1 h with stirring, and then clarified by centrifugation at 15,000 x *g* for 20 min at 4°C. The soluble fraction (SF) was transferred to a new 1.5 mL microcentrifuge tube and the insoluble fraction (IF) containing the membranes were resuspended in an identical volume Tris buffer. Protein concentration was determined and integrity of the samples was checked by SDS-PAGE followed by Coomassie staining. Proteomic analysis of the samples was performed by R. Hamelin from the Protein Core Facility (PCF) platform at EPFL. Further details on the procedure are described in Appendix 4.2.

The same proteomic approach was applied to a protein sample of *D. restrictus* prepared as follows. The biomass from 1-L culture was lysed by 3 rounds of French press in presence of DNaseI and protease inhibitor. The insoluble fraction was pelleted by 20 min of centrifugation at 100,000 x *g* and 4°C. The pellet was resuspended in 300 µL of 50 mM Tris-HCl buffer (pH 7.5). The sample was split in 20 µL aliquots. To one aliquot, 5 µL of maltose-neopentyl glycol (0.35 mg/mL) was added and the sample was stirred for 15 min on ice. The sample was finally loaded on a 12% SDS-PAGE. The gel was cut according to the protein ladder into 3 pieces: 1: 55-40 kDa; 2: 40-35 kDa; 3: 35-25 KDa. The proteomic data obtained from the first piece were considered here.

4.3.9. Mass spectrometry analyses of PceC-FBD

All mass spectrometry analyses of PceC-FBD proteins were carried out by Laure Menin (ISIC Mass spectrometry facility, EPFL). A complete detail of the procedure is described in Appendix 4.3.

4.3.10. Additional analytical procedures

Protein concentrations were determined with the method described by Bradford (7). A standard curve using BSA was established in the different buffers used in this study. Table 4.4 lists software used in this study.

Table 4.4. Software and websites used for bioinformatics analysis.

Analysis	Software	Website
MS data analysis	Scaffold2	http://www.proteomesoftware.com/
Multiple sequence alignment	ClustalX v.2.0 ¹	http://www.clustal.org/
Tree analysis	MEGA5 ²	http://mega.software.informer.com/5.0/
Transmembrane α -helix prediction	HMMTOP	http://www.enzim.hu/hmmtop/
Transmembrane protein representation	TOPO2	http://www.sacs.ucsf.edu/cgi-bin/open-topo2.py
Protein sequence homology search	BlastP	http://blast.ncbi.nlm.nih.gov/Blast.cgi

¹ (18)

² (28)

4.4. Results and discussion

4.4.1. Detection of the membrane-bound redox protein PceC in proteomic analysis

A preliminary analysis of the proteome of *D. hafniense* strain TCE1 targeting soluble and membrane-associated proteins from cell that were cultivated on H₂ as electron donor and PCE as electron acceptor has allowed for the first time the detection of the membrane-bound PceC protein.

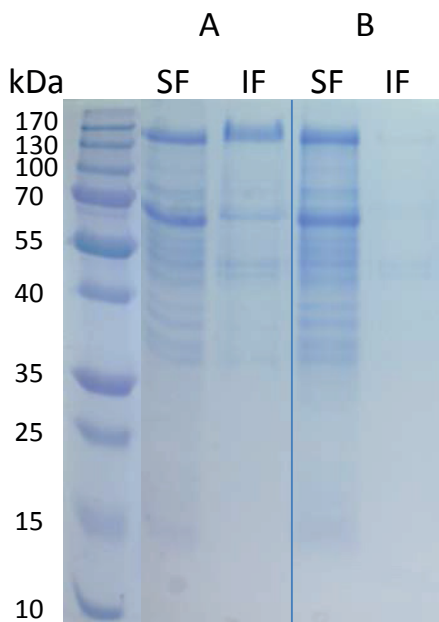


Figure 4.1. SDS-PAGE of *D. hafniense* strain TCE1 protein samples used for proteomic analysis.

Strain TCE1 biomass samples were first lysed by sonication, then cell-free protein extracts were incubated in A) Tris buffer or B) 6 M urea and finally separated into soluble (SF) and insoluble (IF) fractions by centrifugation.

Both soluble and membrane-bound protein samples were first qualitatively verified by SDS-PAGE (Figure 4.1), where it can be seen that urea treatment allowed a better membrane protein extraction. In the proteomic analysis, in total 1'500 different proteins (from the soluble and insoluble fractions) were identified out of the 5'452 proteins, as predicted from the genome of strain TCE1. For many predicted membrane-bound enzyme complexes, it was the non-membrane components which were mainly detected (data not shown). Focusing on the gene products of the *pceABCT* gene cluster, however, nine tryptic peptides of PceC (30%

coverage) and two peptides of PceB (26% coverage) were detected. Figure 4.2 shows the predicted topology of PceC and PceB highlighting the detected peptides.

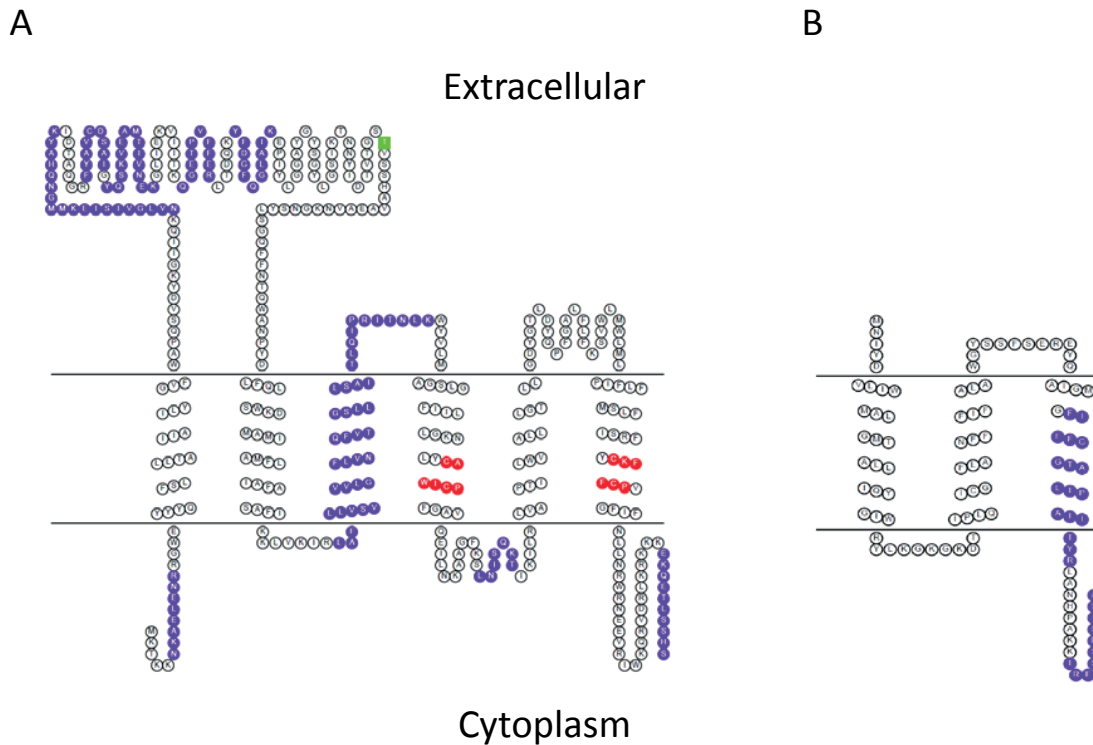


Figure 4.2. Representation of the predicted membrane topology of PceC and PceB proteins of *D. hafniense* strain TCE1.

The prediction was done with HMMTOP server and drawn with TOPO2 online tool. (A) PceC, (B) PceB. For PceC, the predicted FMN-binding threonine residue is shown in green and the conserved cysteine motifs in red. For PceC and PceB, purple amino acid stretches indicate the peptides detected in proteomic analysis.

Both PceA and the molecular chaperone PceT which are rather soluble proteins were also detected. An interesting feature of this proteomic analysis resides in the quantity of PceB and PceC proteins detected in the insoluble fraction of the urea-treated sample (Table 4.5). While largely underrepresented in comparison to the loosely membrane-bound PceA which was 15-times more abundant in this protein fraction, PceC and PceB were detected at similar level, suggesting that PceC is as abundant as PceB, the predicted membrane anchor for PceA (Table 4.5). The apparent stoichiometry of both membrane proteins suggests that PceC has not only a regulatory function but might play a catalytic role in OHR. Extracting and detecting membrane proteins in proteomic analysis remains a challenging task and this result has to be

considered cautiously but represents a first hint for a possible catalytic role of PceC. In another proteomic study on *D. dehalogenans* using 3-chloro-4-hydroxyphenyl acetate (Cl-OHPA) as electron acceptor, CprC, a protein homologous to PceC, has been detected in cells cultivated on Cl-OHPA, but not in cells obtained without chlorinated compounds (17).

Table 4.5. Detection of specific proteins involved in OHR metabolic pathways of *D. hafniense* strain TCE1.

Locus ¹	Protein	TMD	Annotation	SF ²	IF ²
2412	PceA	0	PCE reductive dehalogenase	7.7E+10	1.0E+11
2413	PceB	3	Putative membrane anchor	-	7.2E+09
2414	PceC	6	FMN-binding membrane protein	6.7E+08	6.6E+09
2415	PceT	0	Molecular chaperone	1.3E+09	2.8E+10

¹ Locus number of genes in the draft genome of *D. hafniense* strain TCE1 (JGI project ID 1078214).

² LFQ, identification and quantification of proteins were performed using the MaxLFQ algorithm (8), searching against a database containing the full predicted proteome of *D. hafniense* TCE1.

4.4.2. Detection of the FMN-binding peptide of PceC in *Dehalobacter restrictus*

Another evidence for the presence of PceC was obtained from a SDS solubilized membrane fraction obtained from *D. restrictus* biomass (in collaboration with M. Willemin, LBE, EPFL). A dedicated proteomic analysis of this fraction targeting the tryptic peptide of *D. restrictus* PceC predicted to display the covalently attached FMN (V₁₆₄TGSTVSSHAVA₁₈₀EAVNK) was performed. A peptide mass of 2093.95 Da was detected which nicely matched with the theoretical mass of the corresponding peptide carrying the FMN on a threonine residue (monoisotopic mass of 2094.15 Da), most likely on Thr₁₆₈ (see Appendix 4.4). Various diagnostic ions of protonated FMN forms with masses 457 (FMNH⁺), 439 (-H₂O) and 359 Da (-H₃PO₄) are also indicated, consistent with previous MS analysis of free FMN (14). This result further indicated that PceC can be detected in membrane proteome of OHRB harboring the *pceABCT* gene cluster and that FMN is covalently attached to the native form of the protein.

4.4.3. Sequence analysis of PceC and diversity of the RdhC family

Since PceC (and earlier CprC) have been identified, sequence databases increased exponentially, giving the opportunity to study in greater details the feature and diversity of

the RdhC enzyme family (generic name for the C subunit encoded in reductive dehalogenase gene clusters).

So far, PceC and other members of the RdhC protein family have been considered to be essentially present in the OHR bacterial genera *Dehalobacter* and *Desulfitobacterium*. Besides its sequence similarity to NosR/NirI family, the domain architecture of RdhC proteins (six transmembrane α -helices, a FMN-binding domain and two conserved CXXXCP motifs) also shows partial similarity to the electron-transferring protein NapH involved in nitrate respiration (Figure 4.3). Members of the NapH family have been shown to build with NapG an alternative membrane-bound electron-transferring complex to the periplasmic nitrate reductase NapA (16), further suggesting that RdhC may be part of the electron transport chain of OHR. The FMN-binding domain (FBD) of RdhC raised our interest, since flavins and flavoproteins are known to transfer electrons in redox reactions. A detailed analysis of the alignment of PceC-FBD with characterized flavoproteins harboring covalently-attached FMN cofactors allowed to predict threonine-168 as the conserved amino acid potentially binding FMN in PceC (Figure 4.4). It has been shown that NqrC binds FMN covalently as phosphoester to the hydroxyl group of a threonine residue (4). This detailed sequence comparison also helped defining the edges of FBD in PceC (data not shown).

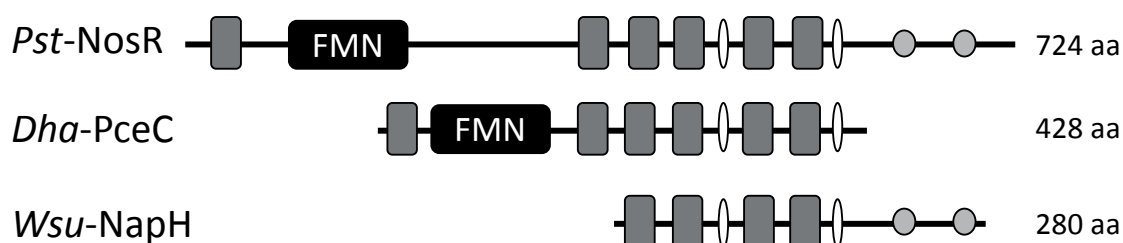


Figure 4.3. Protein domain architecture comparison of PceC with NosR and NapH.

The FMN-binding domain is indicated in black. Grey boxes indicate predicted transmembrane α -helices. White ovals represent the conserved CXXXCP motifs and the light grey circles FeS clusters. *Pst*-NosR: *Pseudomonas stutzeri* NosR (accession CAA78383.1); *Dha*-PceC: *D. hafniense* TCE1 PceC (accession WP_015043728.1); *Wsu*-NapH: *Wolinella succinogenes* NapH (accession CAD55549.1).

More generally, a survey of RdhC sequences in general protein databases revealed a much higher diversity and broader phylogenetic distribution of the protein family. Indeed, RdhC candidates are found in diverse bacteria and not only as initially thought in *Dehalobacter* and *Desulfitobacterium*. Moreover, this analysis has allowed detecting RdhC sequences in

bacteria not yet considered as OHRB, with most of them being encoded in putative *rdh* gene clusters. Among them, 40 of the putative RdhC were found to be related to *Dehalobacter* spp. and 10 specifically to *Dehalobacter restrictus* PER-K23 (24), 36 were found in *Desulfitobacterium* spp., 44 in *Dehalococcoides* spp., and 7 in *Dehalogenimonas* spp. (Appendix 4.5).

<i>Dha</i> TCE1_PceC	156	KTNNYIDTVTGS	TVSSHAV
<i>Mac</i> _RnfG	154	KNGGQVDAISGAT	ISSQAV
<i>Vha</i> _NqrC	217	GSEHGVDGLISGAT	LTGNGV
<i>Vch</i> _NqrC	213	GSEHGVDGLISGAT	LTSNGV
<i>Vch</i> _RnfG	163	KDGGQFDQFTGAT	LTPRAV

Figure 4.4. Sequence alignment of the FMN-binding motif in several flavoproteins biochemically characterized for covalent FMN-binding.

The threonine predicted to bind FMN covalently is indicated in red. *Dha*TCE1_PceC: *D. hafniense* TCE1 PceC (accession number CAG70351); *Mac*_RnfG: *M. acetivorans* RnfG (MA0661); *Vha*_NqrC: *V. harveyi* NqrC (Q9RFV9); *Vch*_NqrC: *V. cholera* NqrC (A5F5Y7); *Vch*_RnfG: *V. cholera* RnfG (ACP09040).

4.4.4. Production of the FMN-binding domain of PceC (PceC-FBD)

Preliminary work has been done in characterizing PceC (23), but attempts to produce a soluble protein in *E. coli* have failed. Since then, the domain architecture was refined revealing the following features. The secondary structure prediction suggests the presence of 6 transmembrane α -helices (TMH), one at the N-terminal end and five at the C-terminal domain. Two cysteine-rich motifs of the type CXXXCP were identified in the 4th and 6th TMH. In-between the 1st and the 2nd TMH, a putative FMN-binding domain was predicted with a threonine at position 168 (Thr₁₆₈) being responsible for covalent attachment of FMN. The overall domain architecture of PceC is shown in Figure 4.2 and Figure 4.5. The sequence coding for PceC-FBD (as newly defined, PceC amino acids 41 to 200) (Figure 4.5 A, indicated in yellow) was cloned into an expression vector and produced in *E. coli*. TMH coding sequences were excluded from the selection in order to prevent protein aggregation (Figure 4.5 B). Nevertheless, PceC-FBD production in *E. coli* always delivered insoluble protein suggesting that it does not fold correctly and form inclusion bodies.

A

```

1  MKTKKNKAELENRRGWEYYQFSLLLTAIIAILYGVFWAPQSVDYKGIIIQ
51  KNVLGVISIEKMMGNQHAYKIDTAQGRFYAVCDSAIGYQSKVEAMTIVNE
101 KGLIEKVIITKQGETPVFFERLTDQKYFDGFGQGLAIKEPIYLGGAYGYSG
151 YLGSIKTNNYIDTVTGSTVSSHAVAEAVNKGNSYLSGQFFNTQWANPYDL
201 FQLSWKDMAMIAMFLIAFASAFIKKLVKIRLAFLLVSVVVLGFLVNQFVT
251 GSLLLSAITLQIPRITNLKQYVLMAGSLGFIILLGKNLYCAWICPFFGAVQ
301 EILNKAAGFKSLNISQKTIKILRLVAPTILWVALLLGTLLGDYGTLDYQP
351 FGALFLFKSVLMLWMLPIFLFMSLFISRFYCKFFCPVGFIFNLLNRWRN
401 EEVRIWKQRVDRLKRKKKEKQETLSSH

```

B

```

1  MGQSVDYKGIIQKNVLGVISIEKMMGNQHAYKIDTAQGRFYAVCDSAIGY
51  QSKVEAMTIVNEKGLIEKVIITKQGETPVFFERLTDQKYFDGFGQGLAIKE
101 PIYLGGAYGYSGYLSIKTNNYIDTVTGSTVSSHAVAEAVNKGNSYLSGQ
151 FFNTQWANPYDLLEHHHHHHH

```

Figure 4.5. Features of the native PceC protein and the recombinant PceC-FBD protein.

(A) From the sequence of the native PceC protein 6 transmembrane α -helices are predicted (underlined), the FMN-binding domain (PceC₄₁₋₂₀₀) as newly defined is indicated in yellow, the putative FMN-binding residue (threonine-168) is in green, and the two CXXXCP conserved motifs are indicated in red (see also Figure 4.2 A). (B) The sequence of the recombinant PceC-FBD protein is given with the threonine-130 (168 in the native protein) indicated in green, and the additional N-terminal and C-terminal residues in blue.

4.4.5. Identification and sequence analysis of flavin-trafficking proteins in *D. hafniense* TCE1 and *D. restrictus* PER-K23

A recent study has shown that flavinylation of *Vibrio harveyi* NqrC in *E. coli* cells occurred only with the co-expression of *apbE*, a gene located in the *nqr* gene cluster (4), the function of which was originally considered as part of thiamine biosynthesis (3). ApbE has been later renamed as flavin-trafficking proteins (Ftp) as it appeared to bind FAD (6) and to play a role in hydrolyzing FAD to AMP and FMN in the periplasm of bacteria and transferring the FMN to a specific threonine residue of FMN-binding redox enzymes (9). The role of Ftp/ApbE in the flavinylation of flavoproteins has been demonstrated in several additional studies (5, 9-11, 30). Two classes of Ftp proteins have been defined depending on their activity, namely class I enzymes with Mg²⁺-dependent FAD pyrophosphatase activity and class II enzymes that only bind FAD (10). Using sequence homology, two putative Ftp proteins were identified in the draft genome of *D. hafniense* TCE1 encoded by the gene loci DeshaDRAFT_4346 and _4351. Both genes are present in an uncharacterized gene cluster (Figure 4.6 A). In the genome of *D. restrictus* PER-K23, one Ftp protein was also identified (locus DEHRE_04230) within the *tat*

operon, coding for the Twin-arginine translocation pathway and in close vicinity to some *rdh* gene clusters (Figure 4.6 B). Sequence alignment of the active site of *D. hafniense* and *D. restrictus* Ftp proteins revealed that the three proteins belong to the class I of Ftp enzymes harboring Mg²⁺-dependent FAD pyrophosphatase activity (Appendix 4.6). While both Ftp enzymes from *D. hafniense* strain TCE1 appeared as putative lipoproteins (see Appendix 4.1), as in the case of ApbE1 of *Klebsiella pneumoniae* (5), no clear N-terminal lipoprotein signal peptide could be found for Ftp from *D. restrictus* (data not shown).

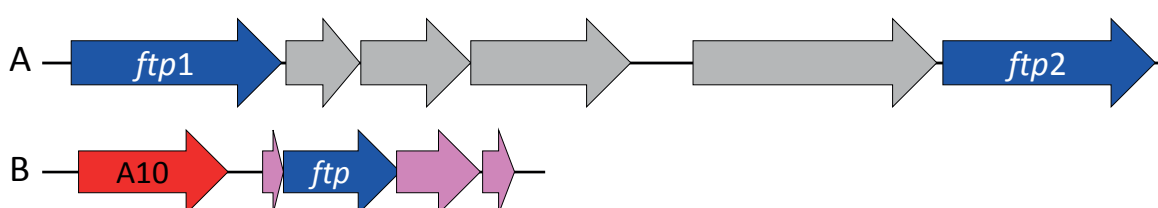


Figure 4.6. Genetic environment of *ftp* genes in *D. hafniense* strain TCE1 and *D. restrictus*. Ftp coding genes (in blue) are shown in the genetic context of (A) *D. hafniense* strain TCE1 and (B) *D. restrictus* PER-K23 genomes. In the genome of *D. restrictus*, the red arrow indicates *rdhA10* and the pink arrows represent the genes coding for the Tat components (24). Grey arrows represent genes without annotated function.

4.4.6. The flavin-transferases of *D. hafniense* can flavinylate PceC-FBD *in vitro*

In order to reconstitute PceC-FBD from inclusion bodies, it was chosen to use Ftp proteins of *D. hafniense* strain TCE1. The *ftp1* and *ftp2* genes were cloned and expressed. The region coding for the hydrophobic N-terminal part of Ftp1 and Ftp2 were not included in order to promote solubility of the recombinant proteins. Consequently, the recombinant Ftp1 and Ftp2 proteins start at positions 51 and 29, respectively, replacing the lipid-binding cysteine by the starting methionine (Appendix 4.1). Cell extract of *E. coli* expressing the *ftp1* and *ftp2* genes were used for the *in vitro* flavinylation of PceC-FBD.

Three different strategies were explored for the reconstitution of PceC-FBD: (1) reconstitution in solution with Ftp1 and Ftp2; (2) on-column reconstitution with Ftp1; and (3) reconstitution with Ftp1 by dialysis. In all three cases, reconstitution was performed *in vitro* using urea-denatured PceC-FBD and *E. coli* soluble extract containing the Ftp enzymes.

4.4.6.1. PceC-FBD reconstitution in solution

The first strategy involved the incubation and stirring of the denatured PceC-FBD protein in a solution containing FAD, Mg^{2+} and Ftp1-containing *E. coli* extract (0.35 mg/ml). This resulted in the appearance of a ~19 kDa fluorescent band under UV illumination (Appendix 4.7), indicative for covalent bond formation between PceC-FBD and a flavin. However, a volume of 10 mL of flavinylated protein with a low concentration (0.05 mg/mL) was recovered. Due to this, the fraction of 10 mL was concentrated with an Amicon® Ultra 10K filters (Sigma-Aldrich) to a final volume of 100 μ L. The filtered reaction mixtures were then loaded onto a SDS-PAGE, the increased amount of sample resulted in an overcrowded signal on the gel (Figure 4.7). In order to verify if the flavinylation reaction required the presence of Ftp, a series of tests was performed with the reconstitution in solution. As shown in Figure 4.7, Ftp1 was required to flavinylate PceC-FBD in the presence of FAD and Mg^{2+} (Lanes A1 and B1), while no band was detected by UV when Ftp (or PceC-FBD) was absent (Lanes A3 and B3). This is in line with previous finding that covalent flavinylation of proteins is not an autocatalytic process, as demonstrated for *E. coli* RnfG (9).

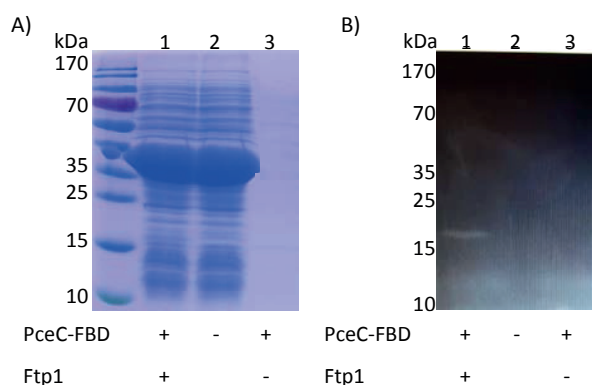


Figure 4.7. *In vitro* flavinylation attempts of PceC-FBD with and without Ftp1.

The reconstitution was done by incubation in a solution. Graphs (A) show Coomassie-stained gels, graphs (B) show FMN-containing protein detection under UV illumination of the same gels. All samples contained FAD and Mg^{2+} . Addition of Ftp1 cell extracts and PceC-FBD is indicated at the bottom of the figure.

4.4.6.2. PceC-FBD reconstitution on-column

To increase the yield of reconstituted PceC-FBD protein, refolding and cofactor assembly was performed on-column after binding urea-denatured PceC-FBD onto a Ni-NTA column. After loading and rinsing unbound protein, a step gradient of decreasing urea concentration in the

presence of FAD, Mg^{2+} and Ftp1 was applied (see Table 4.3 in Material & Methods). PceC-FBD was finally eluted from the column and analyzed. The complete process is illustrated in Figure 4.8. It resulted in the appearance of a ~19 kDa fluorescent band with significantly higher intensity than in-solution reconstitution (Figure 4.8, Lane 19). From this fraction, a volume of 5 mL of soluble PceC-FBD protein at 0.37 mg/mL was recovered.

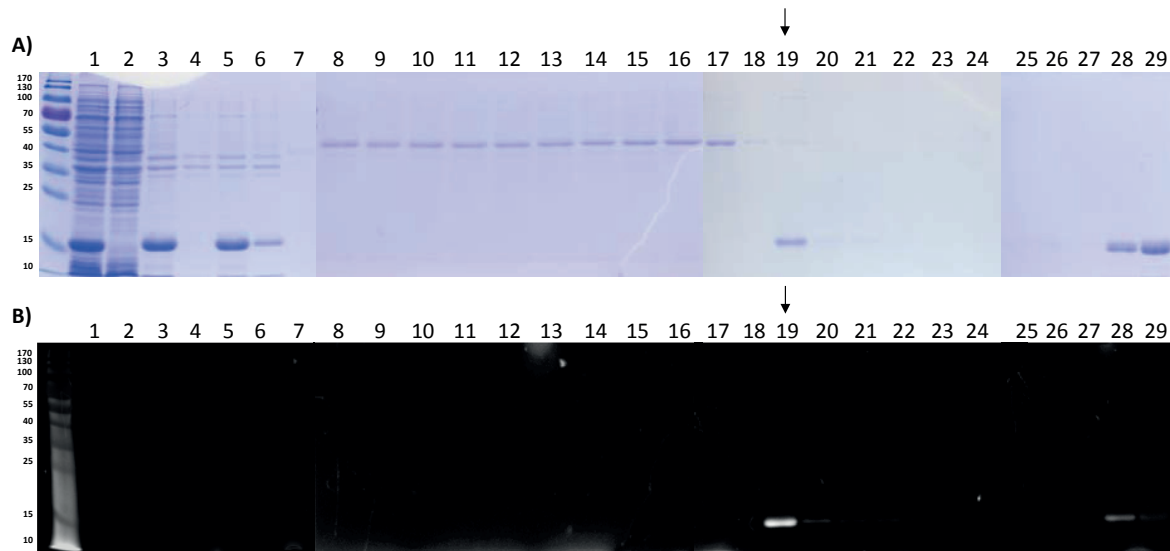


Figure 4.8. PceC-FBD *in vitro* reconstitution following on-column strategy.

The samples collected during the complete procedure were analyzed by SDS-PAGE followed by A) Coomassie staining, and B) UV illumination. Samples list: 1: PceC-FBD producing *E. coli* cell extract; 2: soluble fraction of the cell extract (devoid of PceC-FBD); 3: inclusion bodies after wash; 4: inclusion bodies wash fraction; 5: urea-denatured PceC-FBD; 6: Ni-NTA column flow-through; 7-16: reverse urea step gradient; 17-18: column wash fractions; 19-27: successive elution fractions; 28-29: PceC-FBD fraction eluted with urea. The black arrows indicate the fraction containing flavinylated PceC-FBD.

4.4.6.3. PceC-FBD reconstitution with dialysis

Reconstitution on-column showed that a relative large fraction of PceC-FBD was lost in the flow-through of the column (Figure 4.8, Lane 6) (limited binding capacity) and even more in the last fractions where urea was used to elute the remaining protein from the column (Figure 4.8, Lanes 28-29). Therefore, a third strategy was explored with the use of successive dialysis baths with an inverse gradient of urea concentration (Figure 4.9). Incubation of PceC-FBD with reconstitution solution in-between dialysis baths improved the overall process, resulting in the production of significantly larger amount of flavinylated PceC-FBD (25 mL at 3.93 mg/mL) (Figure 4.9, Lane 12).

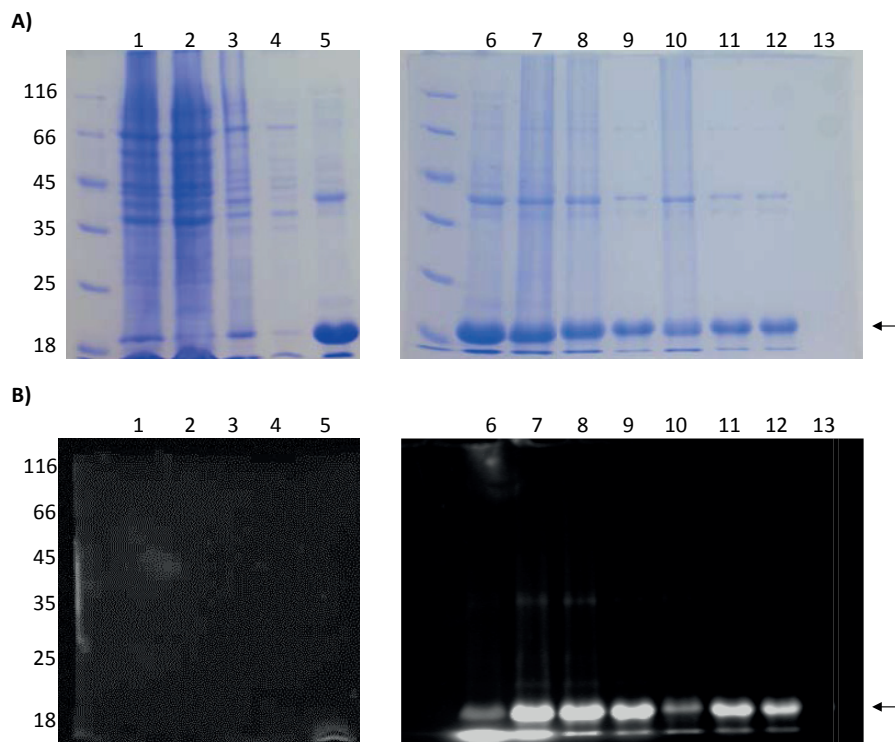


Figure 4.9. *In vitro* reconstitution of PceC-FBD by dialysis.

Urea-denatured PceC-FBD was reconstituted following successive dialysis baths with decreasing urea concentrations in presence of FAD, Mg^{2+} and Ftp1. The samples were analyzed by SDS-PAGE followed by A) Coomassie staining and B) UV illumination. The sample list is given in Table 4.6. The additional fluorescent signal present at the very bottom of the picture likely represents free FAD. The black arrows indicate the fraction containing flavinylated PceC-FBD.

Table 4.6. List of samples collected during PceC-FBD reconstitution by dialysis (see Fig. 4.9).

Lane	Sample description (see Material & Methods for details)
1	<i>E. coli</i> cell extract producing PceC-FBD
2	Cell extract soluble fraction
3	Cell extract insoluble fraction (with PceC-FBD inclusion bodies)
4	Inclusion bodies wash fraction
5	Urea-denatured PceC-FBD
6	Insoluble fraction after dialysis in buffer 1 (4 M urea) (aliquot)
7	Insoluble fraction after dialysis in buffer 2 (2 M urea) (aliquot)
8	Sample after dialysis in buffer 3 (no urea)
9	Soluble fraction after dialysis in buffer 3 (no urea)
10	Insoluble fraction after dialysis in buffer 3 (no urea)
11	Sample after overnight dialysis in buffer 4 (no urea)
12	Soluble fraction after dialysis in buffer 4 (no urea)
13	Insoluble fraction after dialysis in buffer 4 (no urea)

4.4.6.4. Absorption spectra of reconstituted PceC-FBD

The UV-visible absorption spectra of the reconstituted PceC-FBD protein obtained with the dialysis strategy exhibits two peaks with maxima 379 nm and 457 nm, typical for the oxidized form of flavin, whereas, the spectrum of the remaining insoluble fraction showed no signal in the same wavelength range (Figure 4.10).

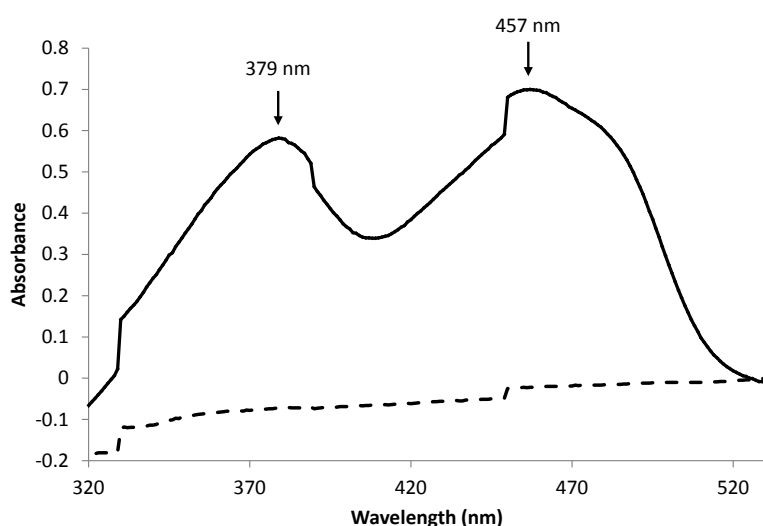


Figure 4.10. UV-visible absorption spectrophotometry of the flavinylated PceC-FBD as isolated.

The solid line represents the UV-visible spectrum of the final soluble PceC-FBD sample, as isolated (see Figure 4.9, Lane 12), while the dashed line is the spectrum of the remaining insoluble fraction which was resuspended in buffer 4 (see Figure 4.9, Lane 13).

4.4.7. Threonine-168 is the site for covalent binding of FMN

In the flavinylation reaction of covalently-bound FMN proteins, the side-chain hydroxyl group of threonine usually serves as the catalytic nucleophile that attacks and cleaves the diphosphate of FAD and binds to the released FMN as phosphoester-threonyl-FMN. To validate the predicted FMN-binding threonine of PceC (Thr₁₆₈), a valine variant of PceC-FBD (T130V, corresponding to T168V in native PceC) was generated by site-directed mutagenesis. Valine was chosen as it is the most similar amino acid to threonine only lacking the hydroxyl group involved in FMN-binding (2). The valine variant was produced and subjected to reconstitution by dialysis as for the wild-type sequence. The PceC-FBD T168V variant initially produced as inclusion bodies, and denatured with urea, completely failed to refold in a reconstitution attempt in the presence of Ftp1 (Figure 4.11). This result clearly indicated that PceC-Thr₁₆₈ is the site for covalent binding of FMN.

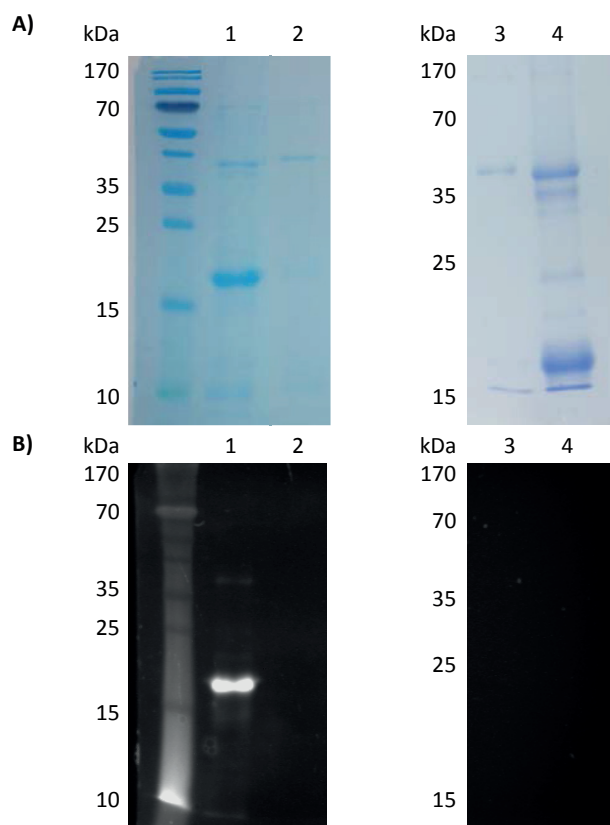


Figure 4.11. *In vitro* flavinylation of PceC-FBD and the T130V variant.

Both proteins were subjected to reconstitution by Ftp1. A) Coomassie-stained SDS-PAGE gel, B) FMN-containing protein detection under UV illumination. Lane 1: PceC-FBD soluble fraction; lane 2: PceC-FBD remaining insoluble fraction; lane 3: T130V variant, soluble fraction; lane 4: T130V variant, insoluble fraction. The bar with number on the left size refers to the molecular masses of the ladder.

4.4.8. Mass spectrometry analysis of reconstituted PceC-FBD

4.4.8.1. Mass spectrometry analysis of intact PceC-FBD

Mass spectrometry analysis of the mass of PceC-FBD gave further evidence for the presence of covalently bound FMN. Initially, the mass of PceC-FBD linked with a FMN was analyzed by mass spectrometry (Appendix 4.8). A clearly dominating mass of 19'212.4 Da was detected for PceC-FBD (wild-type), which corresponds to the theoretical mass of PceC-FBD (18'905.3 Da), from which the initial methionine was cleaved off (18'774.1 Da), that contains one FMN (456.3 Da) and where H₂O was released upon flavinylation of a threonine residue (-18 Da). All this results in a calculated mass of 19'212.4 Da, fully matching with the detected mass. It is also worth noting that, although the analysis was not quantitative, no mass corresponding to non-flavinylated PceC-FBD was detected, suggesting that the yield of flavinylation was nearly 100%. Considering the fact that PceC-FBD loses the starting methionine upon production in *E. coli*, the predicted FMN-binding Thr₁₆₈ becomes Thr₁₂₉ in the recombinant protein.

4.4.8.2. Unambiguous identification of Threonine-129 as FMN-binding residue in PceC-FBD

In order to get additional evidence that FMN was indeed bound to Thr₁₆₈ in PceC (Thr₁₂₉ in PceC-FBD), a first bottom-up MS analysis was performed with the use of two different proteases (Glu-C and trypsin). Although relatively convincing, the results obtained could not completely exclude that FMN was not bound to any other threonine of the reconstituted PceC-FBD protein sample. Indeed, ten threonine residues are present in PceC-FBD and four of them (including Thr₁₂₉) in the predicted FMN-binding motif in PceC (see Appendix 4.9).

Therefore, a more advanced method of protein fragmentation (top-down MS analysis) was finally applied in order to unambiguously assign Thr₁₂₉ as the unique FMN-binding site of PceC-FBD (see Appendix 4.10 for more details). Briefly, the fragment map showing the position of FMN is displayed in Figure 4.12. The localization of the FMN-binding site on PceC-FBD was restricted to a string of 4 residues GST₁₂₉V, fully excluding neighbor threonine residues as possible ligands.

N G Q S V|D|Y|K G I I Q|K|N|V|L|G|V|I|S|I E|K M M G 25
 26 N Q H|A Y K I D|T A Q G R F Y|A|V|C|D S A I G Y Q 50
 51 S K V E A M T|I V N E K G L I E K V I I T K Q G E 75
 76 T P V F F E R L T D|Q K Y F D G F Q G L|A|I|K E|P 100
 101 |I|Y|L|G|G|A|Y|G|Y|S|G Y L|G S I K T N N|Y|I|D T V 125
 126 |T|G S T V|S S H A V|A E A V N K G N S Y|L|S|G|Q|F 150
 151 |F|N|T|Q|W|A|N|P|Y|D|L|L E H|H H|H H H C

Figure 4.12. Fragment map of PceC-FBD showing the unambiguous assignment of Thr129 as the unique FMN-binding residue.

The blue bars pointing to the top left represent the detected N-terminal fragments, without FMN ligand. The blue bars pointing to the bottom right located after the predicted threonine (red box) represent all the detected C-terminal fragments without FMN ligand, while for the other C-terminal fragments FMN was detected. This resulted in a unique possible peptide of four residues (GST₁₂₉V, red box) harboring the FMN ligand.

4.5. Concluding remarks and perspectives

Although the *pceABCT* gene clusters of *Dehalobacter* and *Desulfitobacterium* spp. represents one of paradigmatic genetic systems for the establishment of organohalide respiration, only scarce biochemical knowledge is available on gene products with the exception of PceA. This work intended to shed light on PceC, the most enigmatic protein encoded by the *pceABCT* gene cluster.

After a few unsuccessful attempts in heterologous production of PceC or parts of it, the key to success was to realize that a helper protein was necessary for adding the flavin into the FMN-binding domain of PceC. The recent literature on flavin-trafficking proteins was a good inspiration and allowed to produce a fully soluble PceC FMN-binding domain loaded with FMN on the predicted threonine residue starting from inclusion bodies of the apoprotein. The recombinant Ftp1 protein of *D. hafniense* was demonstrated to insert FMN in PceC-FBD from FAD, thus allowing the protein to fold around the cofactor. A schematic model of PceC maturation is presented in Figure 4.13 A, proposing that FMN transfer and insertion is likely to occur on the outside of the cytoplasmic membrane after PceC has adopted its predicted topology. This is also supported by the fact that Ftp are often lipoproteins facing the outside of the membrane (11). It is uncertain that it occurs in the same way in *D. restrictus* as the unique Ftp protein does not show any recognized motif for lipoproteins.

First experiments for determining the redox potential of the reconstituted PceC-FBD protein were carried out using cyclic voltammetry (see Appendix 4.11). Although the voltammograms obtained for PceC-FBD and free FMN showed differences in the oxidation-reduction waves, it is too preliminary to conclude on relevant redox properties of the reconstituted protein.

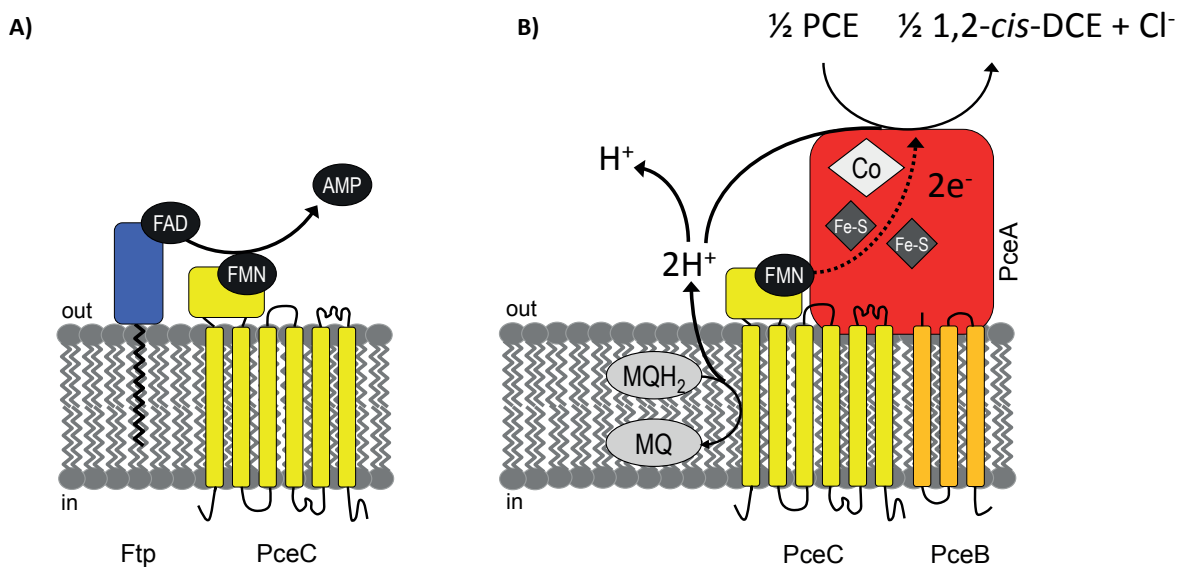


Figure 4.13. Schematic representations of PceC in the cytoplasmic membrane of *D. hafniense*. (A) Possible maturation pathway of PceC (in yellow) with the contribution of Ftp (in blue). (B) Working model of the OHR electron transport chain (accepting half) starting from reduced menaquinones (MQH₂) to PceC (in yellow) and finally to PceA (in red).

Now that it is possible to produce a redox active FMN-binding domain of PceC, it is time to ask the relevant questions of a possible electron transfer to PceA. It is thought that electrons come from the electron-donating part of the respiratory chain and circulate via menaquinones to PceA. Whether PceC is the missing link between the menaquinones and PceA remains to be elucidated (see Figure 4.13 B for a working model).

4.6. References

1. **Backiel, J., O. Juarez, D. V. Zagorevski, Z. Wang, M. J. Nilges, and B. Barquera.** 2008. Covalent binding of flavins to RnfG and RnfD in the Rnf complex from *Vibrio cholerae*. *Biochemistry* **47**:11273-11284.
2. **Barquera, B., L. Ramirez-Silva, J. E. Morgan, and M. J. Nilges.** 2006. A new flavin radical signal in the Na⁺-pumping NADH:quinone oxidoreductase from *Vibrio cholerae*. An EPR/electron nuclear double resonance investigation of the role of the covalently bound flavins in subunits B and C. *J Biol Chem* **281**:36482-36491.
3. **Beck, B. J., and D. M. Downs.** 1998. The *apbE* gene encodes a lipoprotein involved in thiamine synthesis in *Salmonella typhimurium*. *J Bacteriol* **180**:885-891.
4. **Bertsova, Y. V., M. S. Fadeeva, V. A. Kostyrko, M. V. Serebryakova, A. A. Baykov, and A. V. Bogachev.** 2013. Alternative pyrimidine biosynthesis protein ApbE is a flavin transferase catalyzing covalent attachment of FMN to a threonine residue in bacterial flavoproteins. *J Biol Chem* **288**:14276-14286.
5. **Bertsova, Y. V., V. A. Kostyrko, A. A. Baykov, and A. V. Bogachev.** 2014. Localization-controlled specificity of FAD:threonine flavin transferases in *Klebsiella pneumoniae* and its implications for the mechanism of Na(+)-translocating NADH:quinone oxidoreductase. *Biochim Biophys Acta* **1837**:1122-1129.
6. **Boyd, J. M., J. A. Endrizzi, T. L. Hamilton, M. R. Christopherson, D. W. Mulder, D. M. Downs, and J. W. Peters.** 2011. FAD binding by ApbE protein from *Salmonella enterica*: a new class of FAD-binding proteins. *J Bacteriol* **193**:887-895.
7. **Bradford, M. M.** 1976. A rapid and sensitive method for the quantitation of microgram quantities of protein utilizing the principle of protein-dye binding. *Analytical biochemistry* **72**:248-254.
8. **Cox, J., M. Y. Hein, C. A. Lubner, I. Paron, N. Nagaraj, and M. Mann.** 2014. Accurate proteome-wide label-free quantification by delayed normalization and maximal peptide ratio extraction, termed MaxLFQ. *Molecular & cellular proteomics* : **13**:2513-2526.
9. **Deka, R. K., C. A. Brautigam, W. Z. Liu, D. R. Tomchick, and M. V. Norgard.** 2015. Evidence for Posttranslational Protein Flavinylation in the *Syphilis Spirochete Treponema pallidum*: Structural and Biochemical Insights from the Catalytic Core of a Periplasmic Flavin-Trafficking Protein. *mBio* **6**:e00519-00515.
10. **Deka, R. K., C. A. Brautigam, W. Z. Liu, D. R. Tomchick, and M. V. Norgard.** 2016. Molecular insights into the enzymatic diversity of flavin-trafficking protein (Ftp; formerly ApbE) in flavoprotein biogenesis in the bacterial periplasm. *MicrobiologyOpen* **5**:21-38.
11. **Deka, R. K., C. A. Brautigam, W. Z. Liu, D. R. Tomchick, and M. V. Norgard.** 2013. The TP0796 lipoprotein of *Treponema pallidum* is a bimetal-dependent FAD pyrophosphatase with a potential role in flavin homeostasis. *J Biol Chem* **288**:11106-11121.
12. **Duret, A., C. Holliger, and J. Maillard.** 2012. The physiological opportunism of *Desulfitobacterium hafniense* strain TCE1 towards organohalide respiration with tetrachloroethene. *Appl Environ Microbiol* **78**:6121-6127.
13. **Gerritse, J., O. Drzyzga, G. Kloetstra, M. Keijmel, L. P. Wiersum, R. Hutson, M. D. Collins, and J. C. Gottschal.** 1999. Influence of different electron donors and acceptors on dehalorespiration of tetrachloroethene by *Desulfitobacterium frappieri* TCE1. *Appl Environ Microbiol* **65**:5212-5221.
14. **Guyon, L. T., T.; Thuillier, B.; Antoine, R.; Broyer, M.; Boutou, V.; Wolf, JP.; Dugourd, P.** 2008. Femtosecond pump-probe experiments on trapped flavin: Optical control of dissociation. *The Journal of Chemical Physics* **128**:075103-075105.
15. **Hanahan, D., J. Jessee, and F. R. Bloom.** 1991. Plasmid transformation of *Escherichia coli* and other bacteria. *Methods in enzymology* **204**:63-113.
16. **Kern, M., and J. Simon.** 2008. Characterization of the NapGH quinol dehydrogenase complex involved in *Wolinella succinogenes* nitrate respiration. *Mol Microbiol* **69**:1137-1152.

17. **Kruse, T., B. A. van de Pas, A. Atteia, K. Krab, W. R. Hagen, L. Goodwin, P. Chain, S. Boeren, et al.** 2015. Genomic, proteomic, and biochemical analysis of the organohalide respiratory pathway in *Desulfitobacterium dehalogenans*. *J Bacteriol* **197**:893-904.
18. **Larkin, M. A., G. Blackshields, N. P. Brown, R. Chenna, P. A. McGettigan, H. McWilliam, F. Valentin, I. M. Wallace, et al.** 2007. Clustal W and Clustal X version 2.0. *Bioinformatics* **23**:2947-2948.
19. **Mac Nelly, A., M. Kai, A. Svatos, G. Diekert, and T. Schubert.** 2014. Functional heterologous production of reductive dehalogenases from *Desulfitobacterium hafniense* strains. *Appl Environ Microbiol* **80**:4313-4322.
20. **Maillard, J., P. Genevoux, and C. Holliger.** 2011. Redundancy and specificity of multiple trigger factor chaperones in *Desulfitobacteria*. *Microbiology* **157**:2410-2421.
21. **Maillard, J., C. Regeard, and C. Holliger.** 2005. Isolation and characterization of *Tn-Dha1*, a transposon containing the tetrachloroethene reductive dehalogenase of *Desulfitobacterium hafniense* strain TCE1. *Environ Microbiol* **7**:107-117.
22. **Morita, Y., T. Futagami, M. Goto, and K. Furukawa.** 2009. Functional characterization of the trigger factor protein PceT of tetrachloroethene-dechlorinating *Desulfitobacterium hafniense* Y51. *Appl Microbiol Biotechnol* **83**:775-781.
23. **Rupakula, A.** 2010. Purification and characterization of PceC component of the reductive dehalogenase of *Desulfitobacterium* and *Dehalobacter spp.* Master thesis. EPFL, Lausanne.
24. **Rupakula, A., T. Kruse, S. Boeren, C. Holliger, H. Smidt, and J. Maillard.** 2013. The restricted metabolism of the obligate organohalide respiring bacterium *Dehalobacter restrictus*: lessons from tiered functional genomics. *Philosophical transactions of the Royal Society of London. Series B, Biological sciences* **368**:20120325.
25. **Saunders, N. F., E. N. Houben, S. Koefoed, S. de Weert, W. N. Reijnders, H. V. Westerhoff, A. P. De Boer, and R. J. Van Spanning.** 1999. Transcription regulation of the *nir* gene cluster encoding nitrite reductase of *Paracoccus denitrificans* involves NNR and NirI, a novel type of membrane protein. *Mol Microbiol* **34**:24-36.
26. **Smidt, H., M. van Leest, J. van der Oost, and W. M. de Vos.** 2000. Transcriptional regulation of the *cpr* gene cluster in *ortho*-chlorophenol-respiring *Desulfitobacterium dehalogenans*. *J Bacteriol* **182**:5683-5691.
27. **Studier, F. W.** 2014. Stable expression clones and auto-induction for protein production in *E. coli*. *Methods Mol Biol* **1091**:17-32.
28. **Tamura, K., D. Peterson, N. Peterson, G. Stecher, M. Nei, and S. Kumar.** 2011. MEGA5: molecular evolutionary genetics analysis using maximum likelihood, evolutionary distance, and maximum parsimony methods. *Molecular biology and evolution* **28**:2731-2739.
29. **Wunsch, P., and W. G. Zumft.** 2005. Functional domains of NosR, a novel transmembrane iron-sulfur flavoprotein necessary for nitrous oxide respiration. *J Bacteriol* **187**:1992-2001.
30. **Zhang, L., C. Trncik, S. L. Andrade, and O. Einsle.** 2017. The flavinyl transferase ApbE of *Pseudomonas stutzeri* matures the NosR protein required for nitrous oxide reduction. *Biochim Biophys Acta* **1858**:95-102.

Chapter 5

Concluding remarks and
outlook

5. Concluding remarks and outlook

5.1. Functional characterization of two *Sulfurospirillum* spp. competing for tetrachloroethene

A well-established and long-lasting bacterial consortium, named SL2-PCEb, dechlorinates PCE to TCE and *cis*-DCE in a stepwise manner, and harbors two distinct populations of *Sulfurospirillum* spp., namely strains SL2-1 and SL2-2. They show distinct dechlorination potential: strain SL2-1 dechlorinates PCE to TCE only, while strain SL2-2 (selected originally on TCE) kept the potential to dechlorinate both PCE and TCE. The long-term coexistence of both strains raised questions on the nature and details of the interplay and competition between these two populations.

CHAPTERS 2 and 3 of the thesis aimed, therefore, to understand the major factors allowing the long-term coexistence of the two *Sulfurospirillum* populations in the SL2-PCEb consortium. Indications have been obtained from a previous study where a genotyping method has been developed to distinguish both populations on the basis of small differences in the sequence of their respective reductive dehalogenase gene, *pceA_{TCE}* and *pceA_{DCE}*. Indeed, in this work strain SL2-1 cell extract harboring PceA_{TCE} showed a five-fold higher PCE dechlorination activity than strain SL2-2 (4), thus suggesting that the higher turnover rate may be responsible for the maintenance of strain SL2-1 in the consortium. This feature together with the restricted substrate of PceA_{TCE} range further raised interest in the properties of this enzyme. Therefore, the biochemical characterization of PceA_{TCE} was undertaken in **CHAPTER 2**. To this purpose, PceA_{TCE} of strain SL2-1 was purified by chromatography and comparative biochemical analyses of PceA_{TCE} and *S. multivorans* PceA showed that in both cases the corrinoid cofactor, norpseudovitamin B₁₂, is utilized, excluding the possibility that the nature of the corrinoid was the reason for the differences observed. Unfortunately, a full characterization of the enzyme (affinity for PCE, dehalogenation of alternative organohalides) could not be achieved here, as only limited amounts of enzyme were recovered. This was mainly due to the relatively low yield of biomass obtained with the consortium SL2-PCEc harboring strain SL2-1 and also to the loss of protein activity along the three successive chromatography steps. To remediate the former, it would be advantageous

to isolate strain SL2-1 from the consortium which would allow cultivating it in a richer growth medium and improving biomass production. The presence of *Wolinella* sp. in the consortium was shown and isolation attempts have systematically produced colonies of *Wolinella* sp. on solid medium.

Despite the limited amount of purified PceA_{TCE} enzyme obtained here, its comparison with PceA from *S. multivorans* could not clearly show a significantly higher turnover rate, as it has been suggested by the measurement in cell extracts (4). It was decided, therefore, to study population-specific kinetic properties of strain SL2-1 and SL2-2 in order to explain their different physiological behavior and their long-term coexistence in the parental consortium SL2-PCEb. CHAPTER 3 proposed a relatively simple experimental approach to understand the interplay and competition between both *Sulfurospirillum* strains. An extended series of batch cultures of the two strains amended with a large range of PCE concentrations allowed to estimate their respective dechlorination kinetic parameters. While both strains share a similar maximal growth rate around 0.1 h⁻¹, their apparent affinity constant for PCE is significantly different, with values around 6 μM for strain SL2-1 and 35 μM for strain SL2-2. These findings were validated in competition experiments where both populations were mixed at equal population size and cultivate at 6 and 30 μM PCE (aqueous concentration). The observation that both SL2 strains behaved differently in the range of tested PCE concentrations and the differences of nucleotide sequence identity in their *pceA* genes suggest that to survive and compete, strain SL2-1 had adjusted the kinetic properties of its PceA enzyme. Under low substrate concentrations, this strategy gave the opportunity to SL2-1 with an apparent lower *K_s* value for PCE to coexist with strain SL2-2 over long periods of time.

It has been as well observed in this work that the dechlorination and growth of both SL2 strains were clearly inhibited at 200 μM [PCE_{aq}]. This finding prevented to establish simple growth kinetics at a wide range of PCE concentrations. Numerous other studies have reported substrate inhibition by chlorinated compounds and their daughter products, a process called self-inhibition (for a recent review see (27)). Although, it is not always clear whether the inhibition is due to the toxicity of PCE itself or whether it is due to one of its transformation products, here TCE or *cis*-DCE, as both daughter products show higher

solubility in water (8 mM and 79 mM, respectively) than PCE (~1 mM) (5). A previous study has evaluated the inhibition between chlorinated ethenes in anaerobic mixed cultures showing that PCE inhibited TCE dechlorination, while PCE dechlorination was not clearly inhibited by TCE (28). For the simple description of kinetic properties proposed here, the data from cultures with higher concentration than 80 μ M were not considered. However, it would certainly be of a great interest to extend the analysis and data interpretation to higher concentrations by including terms for substrate/product inhibition in order to identify its nature and strength, as proposed earlier (12, 15). However, more experimental data on SL2 growth kinetics would be needed. An alternative for evaluating substrate/product inhibition in SL2 consortia would be to measure the activity of PceA enzymes in cell extracts and establish enzyme kinetics by testing the impact of the dechlorination products.

In complement to this study, the draft genomes of both SL2 strains were obtained by sequencing of the corresponding consortia and genome assembly. Following this analysis, it was proposed that strains SL2-1 and SL2-2 present in the consortia SL2-PCEc and SL2-TCE, respectively, form a new species of *Sulfurospirillum* that was named '*Candidatus Sulfurospirillum diekertiae*'. High sequence similarity suggests that strains SL2-1 and SL2-2 have diverged rather recently from a common ancestor. However, it is not known whether this is the result of the enrichment selection process in the laboratory, although the stepwise dechlorination pattern, reflecting the activity of strain SL2-1, has been recognized early in the process (16).

It was shown that the sequence of PceA_{TCE} showed a high level of 92% identity compared to the PceA of *S. multivorans*, which is known to dechlorinate both PCE and TCE (21). Based on the sequence alignments, a structure model of the PceA_{TCE} enzyme was proposed which revealed eight unique residues in PceA_{TCE} that are different from but consistently conserved in the other three PceA enzymes catalyzing the dechlorination of PCE to *cis*-DCE. The structural features proposed might explain the physiological and biochemical properties of strain SL2-1. A remaining question here is whether there is a link between substrate range reduction and the improvement of substrate affinity in PceA_{TCE} and how single amino acid changes contribute to any of these features.

Similar strain specialization has already been observed. Sequence variations in OHR key enzymes have already been reported with an enrichment culture that reductively dechlorinated chloroform, 1,1,1-trichloroethane and 1,1-dichloroethane, where each of two *Dehalobacter* populations harbor a very similar but distinct enzyme (CfrA and DcrA) with different substrate specificity to chlorinated alkanes (26). It has also been reported that strain differentiation occurred in *Dehalobacter* populations which dechlorinated different dichlorobenzenes isomers (20).

Taken altogether, the studies of microbial OHR community structures and their interplay offer a way to better understand the process occurring at contaminated sites. Laboratory experiments help understanding the selective pressures which possibly act at the genomic level of OHRB. The data presented here on one very simple OHRB community is possibly mimicking what is going on in the environment.

5.2. Reconstitution of PceC flavin domain and its potential role in OHR

In respiratory processes the flow of electrons in the cytoplasmic membrane leads to proton translocation and thus energy conservation. The genetic context of organohalide respiration suggests that different strategies were adopted by phylogenetically diverse OHR bacteria. In *Dehalococcoides mccartyi*, it has been recently reported that the respiratory OHR protein complex has been identified by using two-dimensional BN/SDS-PAGE (14). They found out that the electron transfer chain in *D. mccartyi* is a quinone-independent pathway, but seems to require several membrane-bound protein complexes including one hydrogenase and one member of the large family of complex iron-sulfur molybdoenzymes (CISM). The flow of electrons in the *Firmicutes* among OHRB, such as *Dehalobacter* and *Desulfitobacterium*, is still not elucidated. About 20 years ago, Holliger *et al.* have proposed a tentative scheme of electron transfer involved in OHR of *Dehalobacter restrictus*, including the involvement of one hydrogenase and menaquinones. Experimental data have suggested that an unidentified redox protein must be transferring electrons from menaquinones to the PCE reductive dehalogenase (PceA) (11). The characterization of the genetic context around *pceA* in

Dehalobacter and *Desulfitobacterium* resulted in the identification of the *pceABCT* gene cluster (9, 10, 18). While PceB, and other member of the RdhB family, is predicted to be a membrane anchor, members of the RdhT family have been identified to be a molecular chaperone which helps the folding of RdhA (17, 19). The function of PceC (and more generally RdhC) has so far only been assigned based on sequence homology analysis. Members of the RdhC family (PceC, CprC, DcaC and more) are also encoded in numerous, but not all, *rdh* gene clusters found in the genomes of *Dehalobacter* spp. and *Desulfitobacterium* spp. However, RdhC candidates are not restricted to OHRB members. The survey of RdhC sequences in general protein databases revealed a much higher diversity and broader phylogenetic distribution of this protein family, showing that bacteria not considered as OHRB, such as *Ferrimonas* spp., *Psychromonas* spp., *Vibrio* spp. and *Photobacterium* spp. can harbor also *rdhC* genes, suggesting that a broader use is made of RdhC throughout known and yet to discover OHRB (Appendix 4.5). With its predicted topology and domain architecture, PceC may represent the missing link between the quinone pool of the respiratory chain and the reductive dehalogenase terminal enzyme. However, the membrane nature and high hydrophobicity of the RdhC protein has prevented its heterologous production and biochemical characterization.

Various studies have tried to explain the physiological role of RdhC members in OHR. It started with CprC from *D. dehalogenans*, which has been postulated to act as a membrane-bound regulatory protein as it shared sequence similarity with members of the NosR/NirI family of regulators (25). The sequence similarity is mostly pronounced in the N-terminal region of the protein (one transmembrane α -helix (TMH) and a predicted flavin mononucleotide (FMN) binding domain) and a domain with 5 TMHs including two CXXXCP conserved motifs. However, RdhC proteins are significantly smaller than NosR/NirI proteins, as they lack the C-terminal cytoplasmic domain containing two additional [4Fe-4S] binding motifs which are conserved in NosR and NirI. Transcriptomic analysis of *D. hafniense* strain Y51 has reported that the *pceABCT* gene cluster is constitutively expressed regardless of the presence of chlorinated compounds in growth media. In contrast, *pceC* seemed to be downregulated in culture containing TCE (22). In a recent proteomic study on *D. dehalogenans* with 3-chloro-4-hydroxyphenyl acetate (Cl-OHPA) as electron acceptor, CprC was detected in cells cultivated on Cl-OHPA, while it was not in the cells obtained without

chlorinated compounds (13). Although expected, PceC has not been detected in proteomic analyses of *D. hafniense* strain TCE1 (23) and in *D. restrictus* PER-K23 (24). It is likely, however, that the methodologies used then were not efficient enough to allow extracting highly hydrophobic membrane proteins such as PceC. Overall, it was therefore decided in the present work to reconsider the function of PceC as the putative missing link between menaquinones and PceA in *D. hafniense* strain TCE1.

In **CHAPTER 4**, a preliminary proteomic analysis of soluble and membrane-associated proteins from cells of *D. hafniense* TCE1 allowed to detect for the first time the presence of PceB and PceC. Moreover, they were detected at similar level, suggesting a possible catalytic role of PceC. The FMN-binding domain (FBD) of PceC raised our interest more particularly, since flavins and flavoproteins are known to transfer electrons in redox reactions. A detailed analysis of the alignment of PceC-FBD with characterized flavoproteins harboring covalently-attached FMN cofactors allowed predicting threonine-168 as the conserved amino acid potentially binding FMN in PceC. A proteomic analysis of solubilized membrane proteins from *D. restrictus* cells showed that the expected PceC peptide was carrying a FMN cofactor. Recent studies have demonstrated that flavinylation of flavoprotein, such as NqrB, NqrC, RnfG, RnfD and NosR, occur only with the help of flavin-trafficking proteins (Ftp) (formerly named ApbE) (1-3, 6-8, 29). Ftp has been shown to play a role in hydrolyzing FAD to AMP and FMN in the periplasm of bacteria and in transferring the FMN to a specific threonine residue of FMN-binding enzymes (6). In the present work, the strategy to reconstitute PceC-FBD *in vitro* using urea-denatured PceC-FBD and *E. coli* soluble extract containing Ftp enzymes was successfully performed. The co-expression of PceC-FBD and Ftp1 of *D. hafniense* in *E. coli* was also attempted in a similar fashion as reported by (1, 7), but no reconstitution was observed. In *in vitro* experiments, the Ftp protein was demonstrated to ensure the supply of FMN to PceC-FBD when FAD was provided in the reaction mixture. The FMN-binding domain of PceC could be fully reconstituted and was made completely soluble with this strategy. Mass spectrometry analyses clearly confirmed that threonine-168 as the recipient amino acid for FMN.

The lack of precise function of PceC in OHR still needs to be elucidated. The exact topology of PceC in the cytoplasmic membrane has to be determined in order to elucidate if the FMN-

binding domain of PceC is facing the outside of the cytoplasmic membrane as predicted. An accurate localization of PceC in the membrane has to be performed. Further investigations have to be conducted for the involvement of the FMN-binding domain of PceC in transferring electrons to the reductive dehalogenase. This should be tested in a dedicated *in vitro* assay by using chemically reduced PceC-FBD protein and cell extracts of *D. hafniense* or *D. restrictus*. Cyclic voltammetry has only been attempted here, but seems to be a promising way to understand the redox properties of PceC-FBD. Redox titration of PceC-FBD should also be applied by monitoring the redox state of FMN by UV-visible spectrophotometry. Moreover, one should also address the question of the function of the membrane domain of PceC in accepting electrons from menaquinones and the role of the conserved cysteine motifs. This present work gives new arguments for a possible catalytic role of PceC in organohalide respiration and proposes a new strategy to investigate its possible function in electron transfer to the reductive dehalogenase.

5.3. References

1. **Bertsova, Y. V., M. S. Fadeeva, V. A. Kostyrko, M. V. Serebryakova, A. A. Baykov, and A. V. Bogachev.** 2013. Alternative pyrimidine biosynthesis protein ApbE is a flavin transferase catalyzing covalent attachment of FMN to a threonine residue in bacterial flavoproteins. *J Biol Chem* **288**:14276-14286.
2. **Bertsova, Y. V., V. A. Kostyrko, A. A. Baykov, and A. V. Bogachev.** 2014. Localization-controlled specificity of FAD:threonine flavin transferases in *Klebsiella pneumoniae* and its implications for the mechanism of Na(+)-translocating NADH:quinone oxidoreductase. *Biochim Biophys Acta* **1837**:1122-1129.
3. **Boyd, J. M., J. A. Endrizzi, T. L. Hamilton, M. R. Christopherson, D. W. Mulder, D. M. Downs, and J. W. Peters.** 2011. FAD binding by ApbE protein from *Salmonella enterica*: a new class of FAD-binding proteins. *J Bacteriol* **193**:887-895.
4. **Buttet, G. F., C. Holliger, and J. Maillard.** 2013. Functional genotyping of *Sulfurospirillum* spp. in mixed cultures allowed the identification of a new tetrachloroethene reductive dehalogenase. *Appl Environ Microbiol* **79**:6941-6947.
5. **Chambon, J. C., P. L. Bjerg, C. Scheutz, J. Baelum, R. Jakobsen, and P. J. Binning.** 2013. Review of reactive kinetic models describing reductive dechlorination of chlorinated ethenes in soil and groundwater. *Biotechnol Bioeng* **110**:1-23.
6. **Deka, R. K., C. A. Brautigam, W. Z. Liu, D. R. Tomchick, and M. V. Norgard.** 2015. Evidence for Posttranslational Protein Flavinylation in the *Syphilis Spirochete Treponema pallidum*: Structural and Biochemical Insights from the Catalytic Core of a Periplasmic Flavin-Trafficking Protein. *mBio* **6**:e00519-00515.
7. **Deka, R. K., C. A. Brautigam, W. Z. Liu, D. R. Tomchick, and M. V. Norgard.** 2016. Molecular insights into the enzymatic diversity of flavin-trafficking protein (Ftp; formerly ApbE) in flavoprotein biogenesis in the bacterial periplasm. *MicrobiologyOpen* **5**:21-38.
8. **Deka, R. K., C. A. Brautigam, W. Z. Liu, D. R. Tomchick, and M. V. Norgard.** 2013. The TP0796 lipoprotein of *Treponema pallidum* is a bimetal-dependent FAD pyrophosphatase with a potential role in flavin homeostasis. *J Biol Chem* **288**:11106-11121.
9. **Duret, A., C. Holliger, and J. Maillard.** 2012. The physiological opportunism of *Desulfitobacterium hafniense* strain TCE1 towards organohalide respiration with tetrachloroethene. *Appl Environ Microbiol* **78**:6121-6127.
10. **Futagami, T., T. Yamaguchi, S. Nakayama, M. Goto, and K. Furukawa.** 2006. Effects of chloromethanes on growth of and deletion of the pce gene cluster in dehalorespiring *Desulfitobacterium hafniense* strain Y51. *Appl Environ Microbiol* **72**:5998-6003.
11. **Holliger, C. W., G.; Diekert, G.** 1998. Reductive dechlorination in the energy metabolism of anaerobic bacteria. *FEMS Microbiology* 383-398.
12. **Huang, D., and J. G. Becker.** 2011. Dehalorespiration model that incorporates the self-inhibition and biomass inactivation effects of high tetrachloroethene concentrations. *Environ Sci Technol* **45**:1093-1099.
13. **Kruse, T., B. A. van de Pas, A. Atteia, K. Krab, W. R. Hagen, L. Goodwin, P. Chain, S. Boeren, et al.** 2015. Genomic, proteomic, and biochemical analysis of the organohalide respiratory pathway in *Desulfitobacterium dehalogenans*. *J Bacteriol* **197**:893-904.
14. **Kublik, A., D. Deobald, S. Hartwig, C. L. Schiffmann, A. Andrades, M. von Bergen, R. G. Sawers, and L. Adrian.** 2016. Identification of a multi-protein reductive dehalogenase complex in *Dehalococcoides mccartyi* strain CBDB1 suggests a protein-dependent respiratory electron transport chain obviating quinone involvement. *Environ Microbiol* **18**:3044-3056.
15. **Lai, Y., and J. G. Becker.** 2013. Compounded effects of chlorinated ethene inhibition on ecological interactions and population abundance in a *Dehalococcoides* - *Dehalobacter* coculture. *Environ Sci Technol* **47**:1518-1525.

16. **Maillard, J., M. P. Charnay, C. Regeard, E. Rohrbach-Brandt, K. Rouzeau-Szynalski, P. Rossi, and C. Holliger.** 2011. Reductive dechlorination of tetrachloroethene by a stepwise catalysis of different organohalide respiring bacteria and reductive dehalogenases. *Biodegradation* **22**:949-960.
17. **Maillard, J., P. Genevoux, and C. Holliger.** 2011. Redundancy and specificity of multiple trigger factor chaperones in *Desulfitobacteria*. *Microbiology* **157**:2410-2421.
18. **Maillard, J., C. Regeard, and C. Holliger.** 2005. Isolation and characterization of *Tn-Dha1*, a transposon containing the tetrachloroethene reductive dehalogenase of *Desulfitobacterium hafniense* strain TCE1. *Environ Microbiol* **7**:107-117.
19. **Morita, Y., T. Futagami, M. Goto, and K. Furukawa.** 2009. Functional characterization of the trigger factor protein PceT of tetrachloroethene-dechlorinating *Desulfitobacterium hafniense* Y51. *Appl Microbiol Biotechnol* **83**:775-781.
20. **Nelson, J. L., J. Jiang, and S. H. Zinder.** 2014. Dehalogenation of chlorobenzenes, dichlorotoluenes, and tetrachloroethene by three *Dehalobacter* spp. *Environ Sci Technol* **48**:3776-3782.
21. **Neumann, A., G. Wohlfarth, and G. Diekert.** 1998. Tetrachloroethene dehalogenase from *Dehalospirillum multivorans*: cloning, sequencing of the encoding genes, and expression of the *pceA* gene in *Escherichia coli*. *J Bacteriol* **180**:4140-4145.
22. **Peng, X., S. Yamamoto, A. A. Vertes, G. Keresztes, K. Inatomi, M. Inui, and H. Yukawa.** 2012. Global transcriptome analysis of the tetrachloroethene-dechlorinating bacterium *Desulfitobacterium hafniense* Y51 in the presence of various electron donors and terminal electron acceptors. *J Ind Microbiol Biotechnol* **39**:255-268.
23. **Prat, L., J. Maillard, R. Grimaud, and C. Holliger.** 2011. Physiological adaptation of *Desulfitobacterium hafniense* strain TCE1 to tetrachloroethene respiration. *Appl Environ Microbiol* **77**:3853-3859.
24. **Rupakula, A., T. Kruse, S. Boeren, C. Holliger, H. Smidt, and J. Maillard.** 2013. The restricted metabolism of the obligate organohalide respiring bacterium *Dehalobacter restrictus*: lessons from tiered functional genomics. *Philosophical transactions of the Royal Society of London. Series B, Biological sciences* **368**:20120325.
25. **Smidt, H., M. van Leest, J. van der Oost, and W. M. de Vos.** 2000. Transcriptional regulation of the *cpr* gene cluster in *ortho*-chlorophenol-respiring *Desulfitobacterium dehalogenans*. *J Bacteriol* **182**:5683-5691.
26. **Tang, S., P. H. Wang, S. A. Higgins, F. E. Löffler, and E. A. Edwards.** 2016. Sister *Dehalobacter* Genomes Reveal Specialization in Organohalide Respiration and Recent Strain Differentiation Likely Driven by Chlorinated Substrates. *Front Microbiol* **7**:100.
27. **Wei K., G. A., Chan W. W.M., Richardson R. E., Edwards E. A.** 2016. Electron acceptor interactions between organohalide-respiring bacteria: cross-feeding, competition, and inhibition, p.283-308. *In* L. Adrian and F. E. Löffler (ed.), *Organohalide-Respiring Bacteria*. Springer Berlin Heidelberg.
28. **Yu, S., M. E. Dolan, and L. Semprini.** 2005. Kinetics and inhibition of reductive dechlorination of chlorinated ethylenes by two different mixed cultures. *Environ Sci Technol* **39**:195-205.
29. **Zhang, L., C. Trncik, S. L. Andrade, and O. Einsle.** 2017. The flavinyl transferase ApbE of *Pseudomonas stutzeri* matures the NosR protein required for nitrous oxide reduction. *Biochim Biophys Acta* **1858**:95-102.

Table of content

1.	<u>GENERAL INTRODUCTION</u>	3
1.1.	CHLORINATED ORGANIC CONTAMINATION	3
1.1.1.	NATURAL CHLOROETHENES SOURCES	3
1.1.2.	ANTHROPOGENIC CHLOROETHENES SOURCES	3
1.2.	BIODEGRADATION OF CHLOROETHENES	4
1.3.	ORGANOHALIDE RESPIRATION (OHR)	5
1.4.	OVERVIEW OF KNOWN ORGANOHALIDE-RESPIRING BACTERIA: PHYLOGENETIC AFFILIATION AND CHLORINATED SUBSTRATES SPECIFICITY	6
1.4.1.	THE SL2 ENRICHMENT CULTURE	9
1.5.	DIVERSITY OF REDUCTIVE DEHALOGENASES AND ACCESSORY GENES	9
1.6.	BIOCHEMISTRY OF OHR	11
1.6.1.	REDUCTIVE DEHALOGENASES	11
1.6.2.	THE CORRINOID COFACTOR OF REDUCTIVE DEHALOGENASES	12
1.6.3.	THE OHR ELECTRON TRANSPORT CHAIN	13
1.7.	OBJECTIVES AND OUTLINE OF THE THESIS	15
1.7.1.	OBJECTIVES OF THE THESIS	15
1.7.2.	OUTLINE OF THE THESIS	15
1.8.	REFERENCES	17
2.	<u>CHARACTERIZATION OF AN UNUSUAL <i>SULFUROSPIRILLUM</i> REDUCTIVE DEHALOGENASE DECHLORINATING TETRA-CHLOROETHENE TO TRICHLOROETHENE</u>	29
2.1.	ABSTRACT	29
2.2.	INTRODUCTION	30
2.3.	MATERIAL AND METHODS	32
2.3.1.	BACTERIAL STRAINS AND GROWTH CONDITIONS	32
2.3.2.	PURIFICATION OF THE PCEA _{TCE} REDUCTIVE DEHALOGENASE	32
2.3.3.	SDS-PAGE AND WESTERN BLOT ANALYSIS	33
2.3.4.	REDUCTIVE DEHALOGENASE ACTIVITY ASSAY	34
2.3.5.	COBAMIDE EXTRACTION	35
2.3.6.	MOLECULAR METHODS	35
		129

2.3.7.	ADDITIONAL ANALYTICAL PROCEDURES	39
2.4.	RESULTS AND DISCUSSION	41
2.4.1.	PURIFICATION AND KINETIC PARAMETERS OF THE PCEA _{TCE} ENZYME	41
2.4.2.	PCEA _{TCE} HARBORS NORPSEUDOVITAMIN B ₁₂ AS CORRINOID COFACTOR	45
2.4.3.	RE-ROUTING <i>DE NOVO</i> CORRINOID BIOSYNTHESIS WITH DMB IN THE SL2-PCEC CONSORTIUM	46
2.4.4.	SEQUENCE ALIGNMENTS AND STRUCTURE MODELS OF <i>SULFUROSPIRILLUM</i> PCEA ENZYMES	48
2.5.	CONCLUSIONS	53
2.6.	REFERENCES	54
3.	<u>DECHLORINATION KINETICS GOVERNS THE COMPETITION BETWEEN TWO NEW STRAINS OF THE GENUS <i>SULFUROSPIRILLUM</i></u>	58
3.1.	ABSTRACT	58
3.2.	INTRODUCTION	59
3.3.	MATERIAL AND METHODS	60
3.3.1.	BACTERIAL STRAINS AND GROWTH CONDITIONS	60
3.3.2.	MOLECULAR METHODS	61
3.3.3.	ADDITIONAL ANALYTICAL PROCEDURES	64
3.4.	RESULTS AND DISCUSSION	67
3.4.1.	DRAFT GENOMES OF <i>SULFUROSPIRILLUM</i> SP. STRAINS SL2-1 AND SL2-2 AND DESIGNATION OF A NEW SPECIES	67
3.4.2.	DECHLORINATION AS A MEASURE FOR GROWTH WITH SL2 CONSORTIA	71
3.4.3.	TETRACHLOROETHENE DECHLORINATION KINETIC PARAMETERS OF INDIVIDUAL <i>S. DIEKERTIAE</i> SL2 STRAINS	72
3.4.4.	COMPETITION EXPERIMENTS WITH <i>S. DIEKERTIAE</i> STRAINS SL2-1 AND SL2-2	78
3.5.	CONCLUDING REMARKS AND PERSPECTIVES	80
3.6.	REFERENCES	82
4.	<u>BIOCHEMICAL CHARACTERIZATION OF THE FLAVIN DOMAIN OF PCEC</u>	86
4.1.	ABSTRACT	86
4.2.	INTRODUCTION	87
4.3.	MATERIAL AND METHODS	89
4.3.1.	BACTERIAL STRAINS AND GROWTH CONDITIONS	89
4.3.2.	DNA WORK	89
4.3.3.	PRODUCTION OF RECOMBINANT FTP1 AND FTP2 PROTEINS	92
		130

4.3.4.	PRODUCTION OF RECOMBINANT PCEC-FBD AND VARIANT	92
4.3.5.	FRACTIONATION OF CELL CONTAINING PCEC-FBD INCLUSION BODIES	93
4.3.6.	RECONSTITUTION OF PCEC-FBD PROTEINS	93
4.3.7.	SDS-PAGE GEL STAINING AND IMAGE ANALYSIS	96
4.3.8.	SAMPLE PREPARATION FOR PROTEOME ANALYSIS	96
4.3.9.	MASS SPECTROMETRY ANALYSES OF PCEC-FBD	97
4.3.10.	ADDITIONAL ANALYTICAL PROCEDURES	97
4.4.	RESULTS AND DISCUSSION	99
4.4.1.	DETECTION OF THE MEMBRANE-BOUND REDOX PROTEIN PCEC IN PROTEOMIC ANALYSIS	99
4.4.2.	DETECTION OF THE FMN-BINDING PEPTIDE OF PCEC IN <i>DEHALOBACTER RESTRICTUS</i>	101
4.4.3.	SEQUENCE ANALYSIS OF PCEC AND DIVERSITY OF THE RDHC FAMILY	102
4.4.4.	PRODUCTION OF THE FMN-BINDING DOMAIN OF PCEC (PCEC-FBD)	103
4.4.5.	IDENTIFICATION AND SEQUENCE ANALYSIS OF FLAVIN-TRAFFICKING PROTEINS IN <i>D. HAFNIENSE</i> TCE1 AND <i>D. RESTRICTUS</i> PER-K23	104
4.4.6.	THE FLAVIN-TRANSFERASES OF <i>D. HAFNIENSE</i> CAN FLAVINYLATED PCEC-FBD <i>IN VITRO</i>	105
4.4.7.	THREONINE-168 IS THE SITE FOR COVALENT BINDING OF FMN	110
4.4.8.	MASS SPECTROMETRY ANALYSIS OF RECONSTITUTED PCEC-FBD	112
4.5.	CONCLUDING REMARKS AND PERSPECTIVES	114
4.6.	REFERENCES	116
5.	CONCLUDING REMARKS AND OUTLOOK	121
<hr/>		
5.1.	FUNCTIONAL CHARACTERIZATION OF TWO SULFUROSPIRILLUM SPP. COMPETING FOR TETRACHLOROETHENE	121
5.2.	RECONSTITUTION OF PCEC FLAVIN DOMAIN AND ITS POTENTIAL ROLE IN OHR	124
5.3.	REFERENCES	128

List of Figures

Figure 1.1. Formation of dense non-aqueous phase liquid (DNAPL) and contamination plume following a spillage of chlorinated solvents	4
Figure 1.2. Yearly production of PCE in the U.S.A.	4
Figure 1.3. Sequential reductive dechlorination of PCE to ethene	6
Figure 1.4. Phylogenetic tree of known OHRB based on bacterial 16S rRNA gene sequences	8
Figure 2.1. Structure of cobamides	31
Figure 2.2. Chromatogram of PceA _{TCE} purification on Phenyl-Superose column	43
Figure 2.3. PceA _{TCE} purification protein analysis	44
Figure 2.4. HPLC analysis of corrinoid extracts from purified PceA _{TCE}	45
Figure 2.5. Effect of DMB addition on growth and PCE dechlorination of SL2-PCEc cultures	46
Figure 2.6. HPLC analysis of cobamide extracts from SL2-PCEc cells cultivated without or with amendment of DMB in the medium	47
Figure 2.7. Sequence alignment of <i>Sulfurospirillum</i> spp. PceA enzymes	50
Figure 2.8. Model of the active site PceA _{TCE}	51
Figure 2.9. Detail of the active site of <i>S. multivorans</i> PceA with TCE (PDB 4UR0)	53
Figure 3.1. Quality control and quantification of genomic DNA from the SL2-PCEc consortium	67
Figure 3.2. Average nucleotide identity (ANI) of the draft genomes of strains SL2-1 and SL2-2 in comparison with <i>S. multivorans</i>	69
Figure 3.3. Phylogenetic tree based on the 16S rRNA genes from <i>Sulfurospirillum</i> spp. genomes	70
Figure 3.4. OHR region (partial) comparison of <i>S. diekertiae</i> strains SL2-1 and SL2-2 with <i>S. multivorans</i>	71
Figure 3.5. Direct correlation between chloride release and the <i>Sulfurospirillum rpoB</i> gene copy number in the SL2 consortia	72
Figure 3.6. Dechlorination of <i>S. diekertiae</i> strains at various initial concentrations of PCE	74
Figure 3.7. Dechlorination rate of <i>S. diekertiae</i> SL2 strains as function of aqueous PCE concentration	75
Figure 3.8. Estimation of dechlorination-based kinetic parameters of SL2 strains	77
Figure 3.9. Competition of <i>S. diekertiae</i> strains SL2-1 and SL2-2 for PCE	79
Figure 4.1. SDS-PAGE of <i>D. hafniense</i> strain TCE1 protein samples used for proteomic analysis	99
Figure 4.2. Representation of the predicted membrane topology of PceC and PceB proteins of <i>D. hafniense</i> strain TCE1	100
Figure 4.3. Protein domain architecture comparison of PceC with NosR and NapH	102
	133

Figure 4.4. Sequence alignment of the FMN-binding motif in several flavoproteins biochemically characterized for covalent FMN-binding	103
Figure 4.5. Features of the native PceC protein and the recombinant PceC-FBD protein	104
Figure 4.6. Genetic environment of <i>ftp</i> genes in <i>D. hafniense</i> strain TCE1 and <i>D. restrictus</i>	105
Figure 4.7. <i>In vitro</i> flavinylation attempts of PceC-FBD with and without Ftp1	107
Figure 4.8. PceC-FBD <i>in vitro</i> reconstitution following on-column strategy	108
Figure 4.9. <i>In vitro</i> reconstitution of PceC-FBD by dialysis	109
Figure 4.10. UV-visible absorption spectrophotometry of the flavinylated PceC-FBD as isolated	110
Figure 4.11. <i>In vitro</i> flavinylation of PceC-FBD and the T130V variant	111
Figure 4.12. Fragment map of PceC-FBD showing the unambiguous assignment of Thr129 as the unique FMN-binding residue	113
Figure 4.13. Schematic representations of PceC in the cytoplasmic membrane of <i>D. hafniense</i>	115

List of Tables

Table 2.1. Oligonucleotides used in the work.	40
Table 2.2. Parameters of the quantitative PCR runs targeting the <i>pceA_{TCE}</i> gene	40
Table 2.3. Purification runs of PceA _{TCE}	42
Table 2.4. Amino acid substitutions observed in <i>S. diekertiae</i> PceA _{TCE} in comparison to <i>S. multivorans</i> PceA	50
Table 2.5. Amino acids involved in forming the substrate binding pocket and the substrate channel in <i>S. multivorans</i> PceA and <i>S. diekertiae</i> PceA _{TCE}	52
Table 3.1. PCE concentrations used in this work	60
Table 3.2. Bacterial strains and consortia, and plasmids used in this work	61
Table 3.3. Oligonucleotides used in this study	61
Table 3.4. Parameters of the quantitative PCR runs	62
Table 3.5. Features of the draft genomes of <i>S. diekertiae</i> strains SL2-1 and SL2-2 in comparison with available <i>Sulfurospirillum</i> spp. genomes	68
Table 3.6. Dechlorination-based kinetic parameters of SL2 strains	77
Table 4.1. Bacterial strains and plasmids used in this work	89
Table 4.2. Oligonucleotides used in this study	91
Table 4.3. Stepwise reconstitution mixtures	95
Table 4.4. Software and websites used for bioinformatics analysis	98
Table 4.5. Detection of specific proteins involved in OHR metabolic pathways of <i>D. hafniense</i> strain TCE1	101
Table 4.6. List of samples collected during PceC-FBD reconstitution by dialysis	109

Appendices

Appendices are given with numbers corresponding to the CHAPTERS with which they are associated. The same numbers have been used in the thesis.

Appendix 3.1. Fitting parameters of the dechlorination data of SL2 cultures using the Gompertz model

Culture names are given with the strain (SL2-1 or SL2-2), followed by the initial aqueous concentration of PCE and a code for each replicate (R#). A: asymptote; λ : lag phase (in h); μ_{Cl} : the dechlorination-based growth rate; and SSE: sum of squares due to errors (see Material and Methods for details).

Culture	A	λ	μ_{Cl}	SSE
SL2-1_2-R1	0.60	22.33	0.0038	0.0039
SL2-1_2-R2a	0.28	13.18	0.0120	0.0001
SL2-1_2-R2b	0.45	22.96	0.0044	0.0004
SL2-1_2-R2c	0.83	19.76	0.0099	0.0004
SL2-1_4-R1	1.40	10.54	0.0227	0.0072
SL2-1_4-R2a	0.58	7.80	0.0193	0.0020
SL2-1_4-R2b	0.70	2.32	0.0173	0.0023
SL2-1_4-R2c	1.80	11.58	0.0339	0.0076
SL2-1_6-R1	1.42	13.59	0.0696	0.0011
SL2-1_6-R2a	1.31	26.24	0.0410	0.0010
SL2-1_6-R2b	1.35	14.44	0.0414	0.0012
SL2-1_6-R2c	1.78	3.49	0.0404	0.0128
SL2-1_10-R1	1.44	11.83	0.0805	0.0039
SL2-1_10-R1	1.69	8.46	0.0739	0.1205
SL2-1_10-R2a	1.55	9.59	0.0640	0.0010
SL2-1_10-R2b	1.44	15.80	0.0551	0.0035
SL2-1_10-R2c	1.67	9.52	0.0494	0.0243
SL2-1_20-R1	1.44	10.77	0.0951	0.0002
SL2-1_20-R2	40.00	62.96	0.1863	0.1700
SL2-1_20-R3	1.52	13.96	0.0914	0.0009
SL2-1_20-R4a	1.55	12.84	0.0610	0.1634
SL2-1_20-R4b	1.78	10.55	0.0678	0.0064
SL2-1_20-R4c	1.61	9.20	0.0737	0.0032
SL2-1_20-R5a	1.90	14.20	0.0668	0.0066
SL2-1_20-R5b	1.71	17.71	0.0737	0.0023
SL2-1_20-R5c	2.09	15.73	0.0621	0.0020
SL2-1_30-R1a	1.83	14.84	0.0981	0.0257
SL2-1_30-R1b	2.19	15.85	0.0820	0.0093
SL2-1_30-R1c	2.14	15.02	0.1134	0.0454
SL2-1_40-R1a	1.82	15.04	0.0771	0.0242
SL2-1_40-R1b	1.83	13.89	0.0622	0.0576
SL2-1_40-R1c	2.69	15.91	0.0700	0.0074
SL2-1_40-R2a	2.02	11.24	0.0666	0.0018
SL2-1_40-R2b	1.84	11.01	0.0756	0.0095
SL2-1_40-R2c	1.91	11.74	0.0731	0.0016
SL2-1_50-R1a	2.40	10.56	0.0849	0.1123

SL2-1_50-R1b	2.40	14.94	0.0873	0.0327
SL2-1_50-R1c	2.30	13.63	0.0965	0.0206
SL2-1_100-R1	1.54	8.32	0.0510	0.0138
SL2-1_100-R2a	1.54	13.38	0.0605	0.0034
SL2-1_100-R2b	2.04	12.06	0.0653	0.0046
SL2-1_100-R2c	3.21	18.30	0.0545	0.0314
SL2-1_200-R1	1.46	12.86	0.0532	0.0011
SL2-2_2-R1	1.12	26.68	0.0113	0.0073
SL2-2_10-R1	1.73	11.46	0.0190	0.0497
SL2-2_10-R2a	2.95	23.21	0.0246	0.0442
SL2-2_10-R2b	3.88	28.91	0.0303	0.0369
SL2-2_10-R2c	2.39	19.97	0.0232	0.0353
SL2-2_20-R1	1.87	25.33	0.0308	0.0073
SL2-2_20-R2	1.85	23.21	0.0436	0.0167
SL2-2_20-R3a	1.81	27.82	0.0498	0.0094
SL2-2_20-R3b	2.03	17.91	0.0399	0.0080
SL2-2_20-R3c	2.20	15.56	0.0412	0.0097
SL2-2_30-R1a	1.35	19.46	0.0425	0.0434
SL2-2_30-R1b	1.82	10.74	0.0446	0.0158
SL2-2_30-R1c	1.96	10.83	0.0453	0.0071
SL2-2_40-R1a	2.13	11.64	0.0539	0.0404
SL2-2_40-R1b	2.06	11.29	0.0588	0.0100
SL2-2_40-R1c	2.19	11.01	0.0554	0.0109
SL2-2_50-R1	2.10	14.17	0.0489	0.0552
SL2-2_50-R2a	2.04	12.96	0.0731	0.0224
SL2-2_50-R2b	2.07	15.08	0.0702	0.0200
SL2-2_50-R2c	2.49	15.70	0.0713	0.0054
SL2-2_60-R1a	2.03	10.23	0.0625	0.0275
SL2-2_60-R1b	2.19	9.12	0.0647	0.0204
SL2-2_60-R1c	1.97	10.32	0.0754	0.0140
SL2-2_80-R1a	1.98	9.74	0.0777	0.0105
SL2-2_80-R1b	2.07	10.38	0.0743	0.0054
SL2-2_80-R1c	2.12	9.83	0.0756	0.0161
SL2-2_100-R1	2.03	14.01	0.0686	0.0277
SL2-2_100-R2a	1.91	13.04	0.0598	0.0130
SL2-2_100-R2b	1.97	12.75	0.0738	0.0068
SL2-2_100-R2c	1.91	13.86	0.0719	0.0397
SL2-2_150-R1	2.01	13.45	0.0692	0.0391
SL2-2_200-R1	1.91	25.09	0.0303	0.0059
mixed_6-R1	2.00	1.17	0.0392	0.0883
mixed_6-R2	1.89	2.37	0.0376	0.0357
mixed_6-R3	2.18	0.00	0.0506	0.0849
mixed_30-R1	1.48	15.20	0.0482	0.0034
mixed_30-R2	2.01	14.87	0.0448	0.0039
mixed_30-R3	1.82	15.88	0.0604	0.0140

Appendix 4.1. *Desulfitobacterium hafniense* TCE1 flavin-transferases

D. hafniense Ftp1 (locus DeshaDRAFT_4346)

Secondary structure prediction (HMMTOP)

```
seq  MLQSARLVTI  SNKEGLEIKE  LELLFDKKKC  GRKKLSFVAV  ALITLGLLTA  50
pred  IIIIIIIIIII  IIIIIIIIIII  IIIIiiiiiii  iiiHHHHHHH  HHHHHHHHHH

seq  CNGKPVQQEE  VKKFESTDIA  MGTVISQRFV  GDNGQAAIDA  ALEKIKSLEA  100
pred  Hoooooooo  oooooo0000  0000000000  0000000000  0000000000

seq  LLTFNAPGGD  VNKLNDYAGK  QSVELQPETL  LVLKESQEVA  ELSGGAFDVT  150
pred  0000000000  0000000000  0000000000  0000000000  0000000000

seq  VGPIVKSWSGI  GTDNARIPSE  TELKELLPLV  NYKNLLIEGN  TAYLKQAGQM  200
pred  0000000000  0000000000  0000000000  0000000000  0000000000

seq  VDLGGIAKGY  AGDAAIEVYK  KQGITSAFIN  LGGNVVTLGT  KPDGSSWTVG  250
pred  0000000000  0000000000  0000000000  0000000000  0000000000

seq  VRNPRPAGEE  DQIVGMITVA  DKAVVTAGDD  QRYFEVDGVR  YHHILNPHTG  300
pred  0000000000  0000000000  0000000000  0000000000  0000000000

seq  YPAQSDLMSV  TLVTDSSLLA  DALDTAVYIL  GLEKGREMLE  NYGGVEAVFI  350
pred  0000000000  0000000000  0000000000  0000000000  0000000000

seq  TRDKKIYVTD  GLKDSFEFFD  ESKEYEFVKD  380
pred  0000000000  0000000000  0000000000
```

The predicted lipid-binding cysteine is indicated in yellow.

Sequence of the recombinant Ftp1 (Ftp1₅₁₋₃₈₀)

```
MNGKPVQQEEVKKFESTDIAMGTVISQRFVGDNGQAAIDAALEKIKSLEALLTFNAPGGD
VNKLNDYAGKQSVELQPETLLVLKESQEVAELSGGAFDVTVGPIVKSWSGIGTDNARIPSE
TELKELLPLVNYKNLLIEGNTAYLKQAGQMVDLGGIAKGYAGDAAIEVYKKQGITSAFIN
LGGNVVTLGTPDGSSWTGVRNPRPAGEEDQIVGMITVADKAVVTAGDDQRYFEVDGVR
YHHILNPHTGYPAQSDLMSVTLVTDSSLLADALDTAVYILGLEKGREMLENYGGVEAVFI
TRDKKIYVTDGLKDSFEFFDESKEYEFVKDLESGKETAAAKFERQHMDSTSAA
```

The following modifications in the recombinant protein are indicated in bold:

- The initial transmembrane α -helix was removed
- The protein starts with a methionine that replaces the original conserved cysteine
- A stretch of 22 amino acid containing the S•tag™ (underlined) to improve solubility

D. hafniense Ftp2 (locus DeshaDRAFT_4351)

Secondary structure prediction (HMMTOP)

```
seq  MQNLRPSSFK  SRLLVMLICV  CLSFSLVGL  SAETKVKEFE  PVVETTFLMG  50
pred  Iiiiiiii  iiHHHHHHH  HHHHHHHHH  HHoooooooo  oooooooooo

seq  TVAKITIIYDE  IKDNEIFQRV  FDRLTDIEQR  MTINDDYPNS  EIIQLNKASG  100
pred  OOOOOOOOO  OOOOOOOOO  OOOOOOOOO  OOOOOOOOO  OOOOOOOOO

seq  KEFVKINPDT  FYVLEKAKYL  AELSQGKFDI  TVGPIVKLWN  IGSDNARVPG  150
pred  OOOOOOOOO  OOOOOOOOO  OOOOOOOOO  OOOOOOOOO  OOOOOOOOO

seq  IDEINKKLPL  VDYHNLILDK  DNSSAKLNQE  GMVVDLGAIA  KGAADEAVK  200
pred  OOOOOOOOO  OOOOOOOOO  OOOOOOOOO  OOOOOOOOO  OOOOOOOOO

seq  ILKEAGIEHA  IVNLGGNIVA  MNTKLDGSLW  RLGLQDPYEI  RGKSMGVVLL  250
pred  OOOOOOOOO  OOOOOOOOO  OOOOOOOOO  OOOOOOOOO  OOOOOOOOO

seq  NDQTMVSSGT  YERYFEEGGK  VYHHLIDPDT  GYPGENGLIS  VSIITKESIN  300
pred  OOOOOOOOO  OOOOOOOOO  OOOOOOOOO  OOOOOOOOO  OOOOOOOOO

seq  ADGLSTGTFL  LGLEEGMKMI  EKIPDTEAIF  ITADKKVYVT  SGINSSNFEI  350
pred  OOOOOOOOO  OOOOOOOOO  OOOOOOOOO  OOOOOOOOO  OOOOOOOOO

seq  TNPDYHLQTT  PSPEK  366
pred  OOOOOOOOO  OOOOOO
```

The predicted lipid-binding cysteine is indicated in yellow.

Sequence of the recombinant Ftp2 (Ftp2₂₉₋₃₆₆)

MLSSAETKVKEFE P V V E T T F L M G T V A K I T I Y D E I K D N E I F Q R V F D R L T D I E Q R M T I N D D Y P
N S E I I Q L N K A S G K E F V K I N P D T F Y V L E K A K Y L A E L S Q G K F D I T V G P I V K L W N I G S D N A R V
P G I D E I N K K L P L V D Y H N L I L D K D N S S A K L N Q E G M V V D L G A I A K G Y A A D E A V K I L K E A G I E
H A I V N L G G N I V A M N T K L D G S L W R L G L Q D P Y E I R G K S M G V V L L N D Q T M V S S G T Y E R Y F E E G
G K V Y H H L I D P D T G Y P G E N G L I S V S I I T K E S I N A D G L S T G T F L L G L E E G M K M I E K I P D T E A
I F I T A D K K V Y V T S G I N S S N F E I T N P D Y H L Q T T P S P E S K **LESGKETAAAKFERQHMSSTS**
AA

The following modifications in the recombinant protein are indicated in bold:

- The initial transmembrane α -helix was removed
- The protein starts with a methionine that replaces the original conserved cysteine
- A stretch of 22 amino acid containing the S•tagTM (underlined) to improve solubility

Appendix 4.2. Proteomic analysis of *D. hafniense* strain TCE1

Sample preparation (performed by the PCF laboratory, EPFL)

Samples were prepared as described under paragraph 4.2.8.1 and then were treated as following: samples were then digested as previously described in (2). Briefly, aliquots of lysates were mixed with 200 μ L of 8 M urea in Microcon devices YM-10 or YM-3 (Millipore). The device was centrifuged at 14,000 $\times g$ at 20 °C for 40 min. All following centrifugation steps were performed applying the same conditions allowing maximal concentration. The concentrate was diluted with 200 μ L of 8 M urea in 0.1 M Tris-HCl, pH 8.5 and the device was centrifuged. Subsequently, 100 μ L of 0.05 M iodoacetamide in 8 M urea in 0.1 M Tris-HCl, pH 8.5 were added to the concentrate followed by centrifugation. The resulting concentrate was diluted with 100 μ L 8 M urea in 0.1 M Tris-HCl, pH 7.9 and concentrated again. This step was repeated 2 times, and the concentrate was subjected to proteolytic digestion. The digests were collected by centrifugation, and the filter device was rinsed with 50 μ L 0.5 M NaCl and centrifuged. Detailed instructions for performing FASP are described in (2). The combined filtrates were desalted on MILI-SPE Extraction disk cartridge (C18-SD); 7 mm per 3 ml (Millipore).

The peptide content was estimated by UV light spectral density at 280 nm using an extinctions coefficient of 1.1 of 0.1% (g/L) solution that was calculated on the basis of the frequency of tryptophan and tyrosine (the main UV light-absorbing amino acids at 280 nm).

LC-MS-MS analysis (performed by the PCF laboratory, EPFL)

Liquid chromatography tandem mass spectrometry (LC-MS/MS) analysis was performed according to the protocol developed by the Protein Core Facilities (PCF; EPFL, Lausanne, Switzerland), as previously described (1). Each SAX fraction was resuspended in 2% acetonitrile containing 0.1% formic acid for LC-MS/MS injections. Reverse phase separations were performed on a Dionex Ultimate 3000 RSLC nano-UPLC system (Thermo Fisher Scientific) connected on line with an Orbitrap Elite Mass Spectrometer (Thermo Fisher Scientific) piloted with Xcalibur (version 2.1) and Tune (version 2.5.5). A homemade nano-ESI source and a noise reduction system (Active Background Ion Reduction Device) were used to generate stable spray. Samples were trapped for 10 min at a flow rate of 3 μ L/min in 0.1% TFA on a homemade capillary pre-column (Magic AQ C18; 3 μ m to 200 Å; 2 cm x 100 μ m inner diameter) and then separated on a C18 tip-capillary column (Nikkyo Technos Co; Magic AQ C18; 3 μ m to 100 Å; 15 cm x 75 μ m inner diameter) at 250 nL/min. A long and shallow gradient (235 min) was performed ranging first from 99% A (2% acetonitrile, 0.1% formic acid) to 23% B (90% acetonitrile, 0.1% formic acid) in 130 min, then up to 42% B in 60 additional min, and finally up to 80% B in 35 min. Samples were analyzed in data-dependent acquisition mode with a dynamic exclusion of 40 s and a relative mass window of 10 ppm. The 20 most intense parent ions from each MS survey scan (m/z 300–1800) were selected and fragmented by collision-induced dissociation into the linear ion trap. Orbitrap MS survey scan resolution was set at 60'000 (at 400 m/z), and fragments were acquired at low resolution in centroid mode. The filling time in MS mode was set at 200 ms with a limitation of 1106 ions, whereas the filling time for fragments recording was set at 100 ms with a limitation of 1104 ions. Singly charged ions were excluded, and a threshold of 500 counts was applied to trigger the fragmentation. Source spray voltage was set at 1.9 kV, and capillary temperature at 200°C. During fragmentation, an activation Q value of 0.25 was used, and normalized collision energy was set at 35% for 10 ms.

Appendix 4.3. Mass spectrometry analyses of PceC-FBD

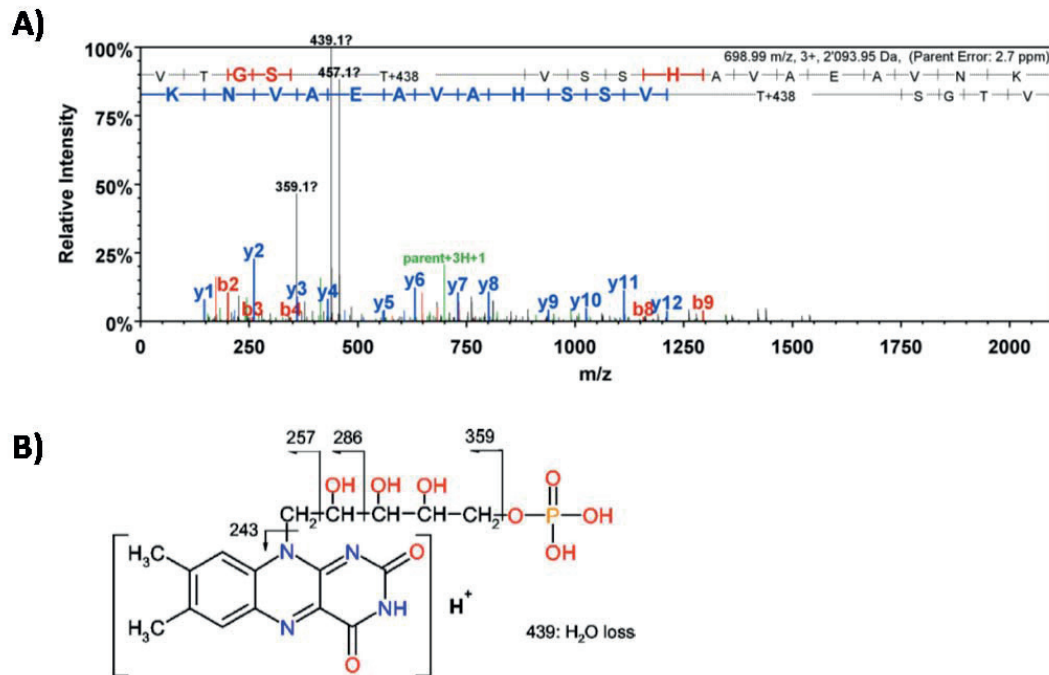
Mass spectrometry analysis of intact PceC-FBD proteins (performed by the ISIC Mass spectrometry facility, EPFL)

The analysis of intact PceC-FBD and its T168V variant were done with the following apparatus: Orbitrap QExactive HF interfaced with a Dionex UPLC-Ultimate-3000 system. LC separation was performed with a C4-column (Waters), 1 x 150 mm, using a gradient of A (H₂O-HCOOH 0.1%) and B (CH₃CN-HCOOH 0.1%) as mobile phases. A full MS scan run was acquired in the range 400-2000 *m/z* using a high-resolution scan of 60 K and averaging of 10 μ scans.

Top-down analysis of fragmented PceC-FBD protein (performed by the ISIC Mass spectrometry facility, EPFL)

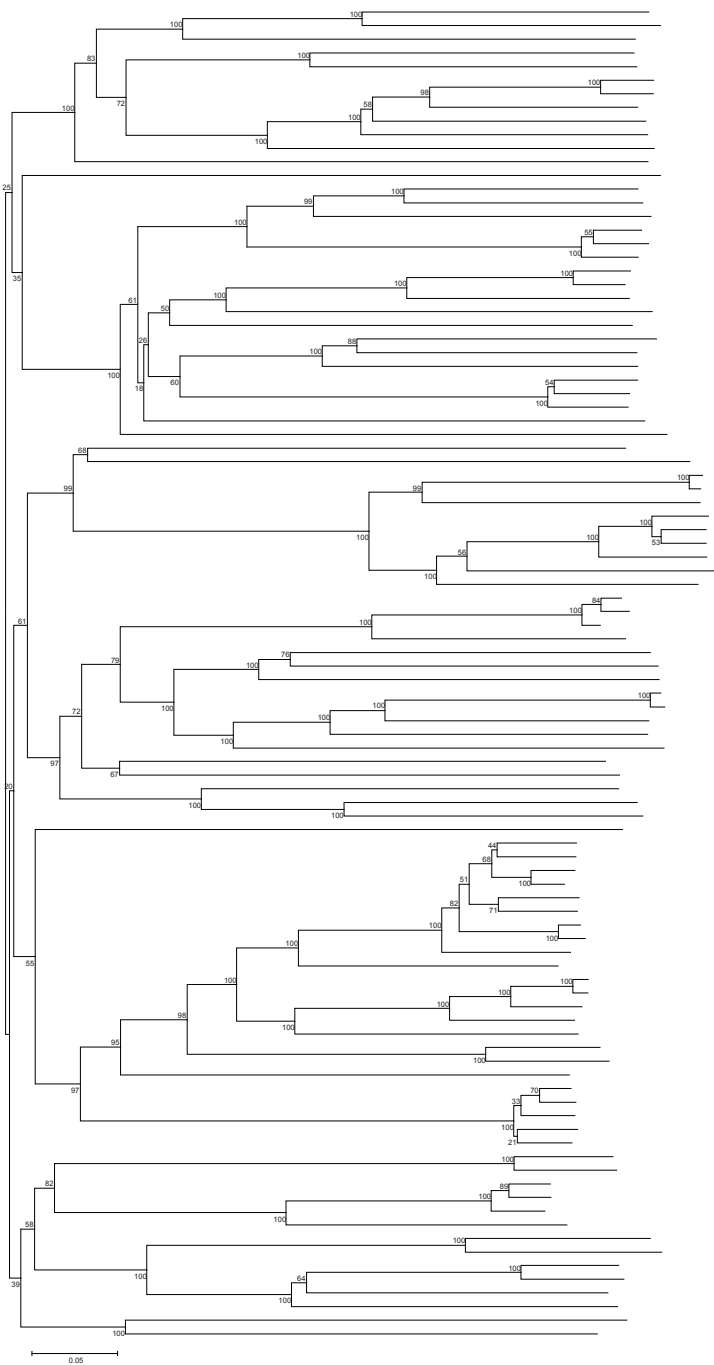
Then to detect predicted FMN-binding internal fragments, a full MS scan run was acquired using a high-resolution scan of 140 K. Then HCD fragmentation was performed using a mass selection window of 200 Th centered on the *m/z* 915.8 ion (charge state +21) with collision energy of 10 eV. A total of 10 consecutive LC experiments were acquired for the PceC-FBD protein sample. In parallel with a standard .raw file containing only mass spectra, the time-domain signals (transients) were acquired using a commercial built-in high-performance data acquisition systems, the FMS Booster X1, developed by SpectroSwiss (EPFL Innovation Park, Switzerland). The spectra/transients were summed across all LC-MS/MS runs, processed with absorption mode FT, the mass spectra were recalibrated and baseline corrected to generate an accurate peak list (using Peak-by-Peak software) in a *mzxml* format. High resolution HCD mass spectra of the protein (19 kDa) were analyzed with MASH-Suite Pro and ProSight Lite v1.3 software. In parallel, our in-house developed free-access ChemInfo.org algorithms was used for predicting and matching the experimental tandem spectra to theoretical fragment ions, in particular internal fragment ions. For processing, up to 9 protons was allowed, 3 groups (C₁₇H₂₁N₄O₉P, C₁₇H₁₉N₄O₈P or nothing) tested with a comparison zone of -1.5 to 6.5 around the monoisotopic theoretical peak. The minimum similarity allowed was set to 85%.

Appendix 4.4. Mass spectrometry analysis of the FMN-binding peptide of *D. restrictus* PceC



A SDS solubilized membrane fraction obtained from *D. restrictus* biomass was analysed by MS analysis and revealed a peptide mass of 2093.95 Da which matched with the theoretical mass of the corresponding peptide carrying the FMN on a threonine residue (monoisotopic mass of 2094.15 Da). A) Mass spectra of trapped protonated FMN (m/z 457), B) The protonated FMN (m/z 457) molecule showing branching points for major photofragments and their m/z value

Appendix 4.5. Sequence likelihood analysis of 98 RdhC representatives and their distribution in major OHR bacteria.



Representative	1	2	3	4	5
<i>Fer.ful</i> .WP_028110583.1					
<i>Fer.kyo</i> .WP_028113301.1					
<i>Psy.oss</i> .WP_019615531.1					
<i>Fer.kyo</i> .WP_051252770.1					
<i>Fer.kyo</i> .WP_051252377.1					
<i>Vib.sco</i> .ANS87102.1					
<i>Vib.sco</i> .ANU38885.1					
<i>Vib.vul</i> .WP_045614048.1					
<i>Pho.aqu</i> .WP_047880183.1					
<i>Pho.aph</i> .WP_047876354.1					
<i>Vib.sp</i> .RC588.WP_003555742.1					
<i>Desv.sp</i> .JC271.WP_066851901.1					
<i>Phy.sp</i> .SM23-30.KPK75298.1					
<i>Dehg.alk</i> .KT847646.1					1
<i>Dehg.sp</i> .WBC2.WP_046737509.1					1
<i>Dehg.lyk</i> .WP_013218780.1					1
<i>Dehc.mcc</i> .WP_012882709.1				4*	
<i>Dehc.mcc</i> .WP_010937267.1				2*	
<i>Dehc.mcc</i> .WP_015407347.1				7*	
<i>Dehc.mcc</i> .WP_058292278.1				2*	
<i>Dehc.mcc</i> .WP_041330356.1				2*	
<i>Dehc.mcc</i> .WP_011308839.1				4*	
<i>Dehc.mcc</i> .WP_041381170.1				2*	
<i>Dehc.sp</i> .WP_012882531.1				7*	
<i>Dehg.alk</i> .WP_058438349.1					1
<i>Dehg.sp</i> .WBC2.WP_046737513.1					1
<i>Dehg.lyk</i> .WP_013218776.1					1
<i>Dehc.mcc</i> .CG1.AII58599.1				4*	
<i>Dehc.mcc</i> .CBDB1.CA83695.1				7*	
<i>Dehc.sp</i> .E1.WP_019223070.1				2*	
<i>Dehc.mcc</i> .WP_041330571.1				1*	
<i>Dehg.sp</i> .WBC2.AK652960.1					1
<i>Pep.sp</i> .BICA1-8.KJS88162.1					
<i>Geo.kv</i> .WP_012470906.1					
<i>Des.haf</i> .WP_041272478.1		2	1	6	
<i>Des.dic</i> .WP_015261905.1		2			
<i>Dehb.sp</i> .E1.WP_019223070.1		2			
<i>Dehb.res</i> .WP_025205947.1		2	1		
<i>Dehb.res</i> .WP_025205935.1		2	1		
<i>Dehb.sp</i> .UNSWDHB.WP_021315547.1		1			
<i>Dehb.sp</i> .FTH1.WP_020493163.1		1			
<i>Dehb.sp</i> .FTH1.WP_034382578.1		1			
<i>Des.haf</i> .WP_018307566.1				2	
<i>Des.haf</i> .WP_005814565.1				3*	
<i>Des.haf</i> .WP_018213029.1				3*	
<i>Des.haf</i> .WP_018307239.1				2	
<i>Des.deh</i> .WP_014793758.1				2	
<i>Dehb.sp</i> .FTH1.WP_020491520.1		1			
<i>Dehb.sp</i> .FTH1.WP_020492855.1		1			
<i>Des.haf</i> .WP_04E85222.1				2	
<i>Des.haf</i> .WP_058491209.1				3*	
<i>Des.haf</i> .WP_015945114.1				2	
<i>Des.deh</i> .WP_014795330.1				2	
<i>Dess.sp</i> .HMP52.WP_034598538.1					
<i>Bac.mas</i> .WP_034293334.1					
<i>Des.haf</i> .WP_018308519.1				1	
<i>Clo.sp</i> .BRH-c20a.KJ523348.1					
<i>Moo.gly</i> .WP_054936000.1					
<i>Gra.sp</i> .BRH-c7a.KUO60295.1				1	
<i>Des.deh</i> .WP_014792041.1					
<i>Clo.sp</i> .PH28.KKM11604.1					
<i>Dehb.sp</i> .UNSWDHB.E0B20153.1		3			
<i>Dehb.sp</i> .WP_025205302.1		1	1		
<i>Dehb.sp</i> .FTH1.WP_020493240.1		1	1		
<i>Dehb.sp</i> .WP_025205299.1		1	1		
<i>Dehb.sp</i> .WP_015044407.1		1			
<i>Dehb.sp</i> .WP_015044416.1		1			
<i>Dehb.sp</i> .FTH1.WP_020492097.1		2			
<i>Dehb.sp</i> .1cCB1.WP_068883723.1		1			
<i>Dehb.sp</i> .E1.WP_019223030.1		1			
<i>Dehb.res</i> .WP_051408109.1		1	1		
<i>Dehb.sp</i> .DCA.WP_015043245.1		1			
<i>Dehb.sp</i> .CF.WP_015046255.1		1			
<i>Dehb.sp</i> .UNSWDHB.WP_021315090.1		1			
<i>Dehb.res</i> .WP_025205282.1		1	1		
<i>Gra.sp</i> .BRH-c7a.KUO60932.1				2	
<i>Des.deh</i> .WP_014793608.1				3*	
<i>Des.haf</i> .WP_005809550.1				3*	
<i>Dess.ori</i> .WP_014188100.1					
<i>Dehb.sp</i> .FTH1.WP_026156195.1		2			
<i>Dehb.sp</i> .DCA.WP_015043196.1		2			
<i>Dehb.sp</i> .E1.WP_019225851.1		1			
<i>Dehb.res</i> .WP_025205906.1		1	1	2	
<i>Dehb.sp</i> .UNSWDHB.WP_021315310.1		1	1		
<i>Dehb.res</i> .WP_025205944.1		1	1		
<i>Dehb.sp</i> .FTH1.WP_020493218.1		1	1		
<i>Dehb.sp</i> .UNSWDHB.WP_021315178.1		2			
<i>Dehb.sp</i> .FTH1.WP_020491078.1		1	1		
<i>Dehb.res</i> .WP_025205912.1		1			
<i>Des.haf</i> .WP_015942953.1				2	
<i>Des.haf</i> .CDX01553.1				2	
<i>Dehb.sp</i> .FTH1.WP_020492150.1		1			
<i>Des.deh</i> .AAD44543.2				2	
<i>Des.haf</i> .WP_015942995.1				2	
<i>Dehb.sp</i> .FTH1.WP_020492142.1		1			
<i>Des.haf</i> .WP_015942978.1				1	
<i>Desi.alk</i> .WP_069642403.1				1	
<i>Desi.alk</i> .WP_051534041.1				1	
Total	40	10	36	44	7

1. *Dehalobacter* spp.; 2. *Dehalobacter restrictus* PER-K23; 3. *Desulfitobacterium* spp.; 4. *Dehalococcoides* spp.; 5. *Dehalogenimonas* spp. (see Supplementary material for detail annotation of sequences).

Appendix 4.6. Primary sequence alignment of the Ftp enzyme active sites

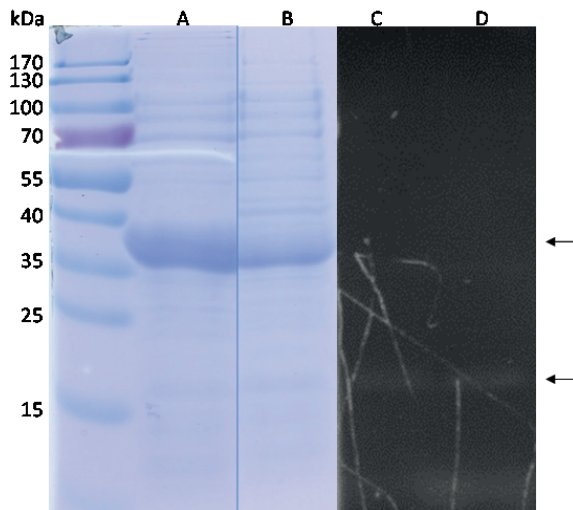
```

Ftp1_Dha  ....TFN....DLGGIAKGYAGD....TAGDDQRY....YHHILNPHTG....DSSLLADALDTAVYI....
Ftp2_Dha  ....TIN....DLGAIAKGYAAD....SSGTYERY....YHHLIDPDTG....KESINADGLSTGTFL....
Ftp_Dr    ....NKF....DLGAIAKGYAVS....TSGNYERF....YSHILDPRTG....ENPIMADALATAAFV....
Ftp_Tp    ....SAN....DLGAIAKGYLAD....TSGAYERF....YHHIIDPVTG....PRSTDADALATACFV....
Ftp_Td    ....NAN....DLGGIAKGYAAD....TSGNYERF....YHHIFDSKTG....ESSTLADALSTSSYV....
Ftp_Lm    ....KIN....DLGAIAKGYITD....TSGIYERY....YHHLDPKTG....KKSIDGDGLSTATFS....
Ftp_Ef    ....TVN....DLGAIAKGYITD....TSGIYERY....YHHLFDRETG....DKSIDGDGLSTAVFS....
Ftp_Hd    ....STY....DLSSIAKGYGVD....TSGNYRNY....LSHIDPKAL....PTSMTADGLSTGLFV....
Ftp_So    ....STY....DLSSIAKGYGVD....TSGDYRNY....FTHIDPRTG....NECMTADGFATAMMV....
Ftp_Ab    ....STY....DLSSIAKGYAVD....TSGDYRNY....FSHIDPRTG....KSAMIADGLATAMTV....
Ftp_Ec    ....STY....DLSTVGEYAAD....TSGSYRNY....LSHVIDPQTG....PTALEADAWDTGLMV....

```

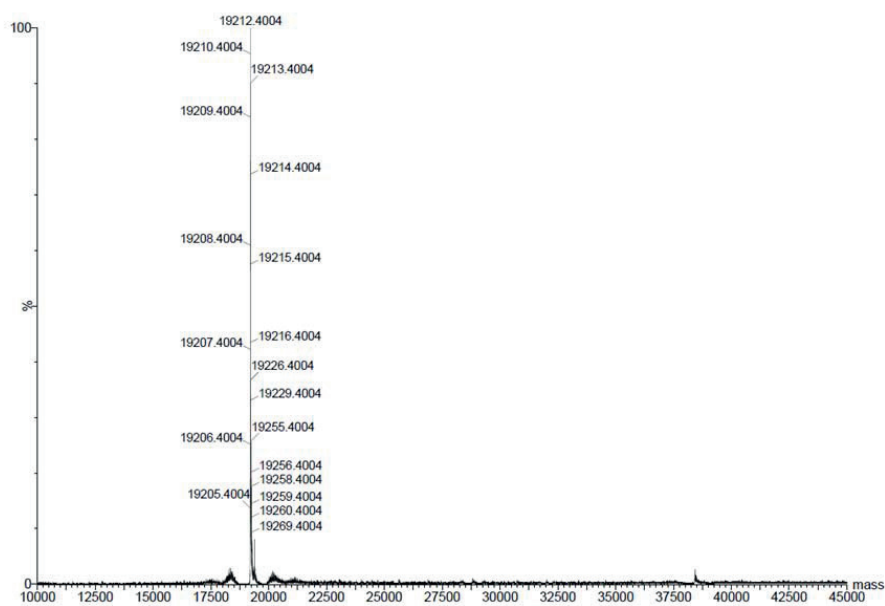
The active site residues are highlighted in colors. Ftp indicated in blue are the Mg²⁺-dependent FAD pyrophosphatases (class I), and in orange the FAD-binding enzymes (class II). Red amino acids are the residues involved in either metal or FAD binding; underlined are the critical residues that bind to the isoalloxazine ring of FAD, which is a tyrosine residue in the FAD-binding Ftp enzymes. Ftp1_Dha, *D. hafniense* TCE1 (DeshaDRAFT_4346); Ftp2_Dh, *D. hafniense* TCE1 (DeshaDRAFT_4351); Ftp_Dr, *D. restrictus* PER-K23 (AHF09382); Ftp_Tp, *T. pallidum* (WP_010882241); Ftp_Td, *T. denticola* (WP_002680621); Ftp_Lm, (WP_003726729); Ftp_Ef, *E. faecalis* (WP_048948427); Ftp_Hd, *H. ducreyi*(WP_041603359); Ftp_So, *S. oneidensis*(WP_011071353); Ftp_Ab, *A. borkumensis* (OJH07441); Ftp_Ec, *E. coli* (4XGX_B).

Appendix 4.7. *In vitro* flavinylation of PceC-FBD in solution with Ftp1 (A, C) and Ftp2 (B, D).



The samples collected after incubation in reconstitution mixture were analyzed by SDS-PAGE followed by A, B) Coomassie staining, and C, D) UV illumination. The arrows on the right side refer to the expected positions of Ftp proteins (~37 kDa) and PceC protein (~19 kDa).

Appendix 4.8. MS/MS spectrum of reconstituted PceC-FBD with FMN



A mass of 19'212.4 Da was found as dominant in the MS spectrum of the reconstituted PceC-FBD protein in its intact form. See CHAPTER 4 (section 4.4.7.1) for details. This analysis was done by L. Menin (ISIC, EPFL).

Appendix 4.9. Bottom-up mass spectrometry of reconstituted PceC-FBD

Glu-C digestion (24 h)

MGQSVDYKGI IQKNVLGVIS IEKMMGNQHA YKIDT*AQGRF YAVCDSAIGY
QSKVEAMTIV NEKGLIEKVI ITKQGETPVF FERLTDQKYF DGFQGLAIKE
PIYLGAYGY SGYLGSIKT*N NYIDT*VT*GST* VSSHAAVEAV NKGNSYLSGQ
FFNTQWANPY DLLEHHHHHH

The main binding site of FMN is in the G92-E138 region. Because non-FMN peptides in the region S45-E55 were clearly identified (S46-E55), the FMN-peptide T35-E55 is probably very minor. It remains 4 possible binding sites for FMN on the G92-E138 part (indicated by *).

Trypsin digestion (6 h)

MGQSVDYKGI IQKNVLGVIS IEKMMGNQHA YKIDTAQGRF YAVCDSAIGY ||
QSKVEAMTIV NEKGLIEKVI ITKQGETPVF FERLTDQKYF DGFQGLAIKE
PIYLGAYGY SGYLGSIKTN NYIDTVTGST VSSHAAVEAV NKGNSYLSGQ |
FFNTQWANPY DLLEHHHHHH

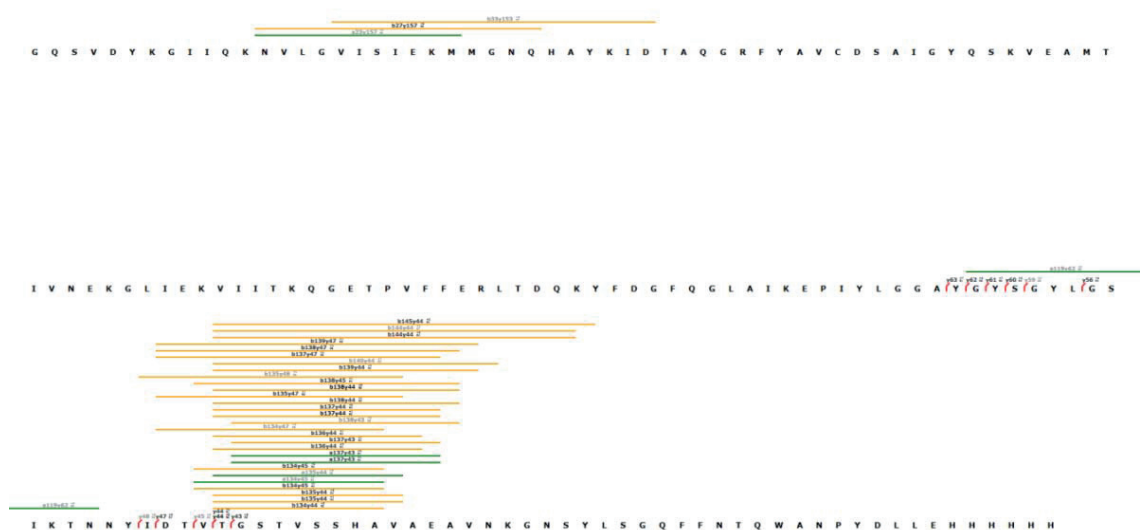
Two possible binding sites for FMN : region I T119-K142 ; region II : F40-K63.

Appendix 4.10. Top-down mass spectrometry analysis of PceC-FBD

The MS/MS spectra generated after multiplexing and advanced FTMS data analysis framework was deconvoluted using MASH Suite Pro and the ions mass list was imported in ProSight Lite. The FMN group (C₁₇H₁₉N₄O₈P) was placed on different threonine positions, looking at the number of b and y fragment ions assigned. The Graphical fragment map showing the best results, i.e. the position of FMN leading to the highest number of fragment ions assigned and identified for the PceC-FBD protein, is displayed on Figure 4.12. A total of 37 b-ion fragments could be assigned with an average mass error of 1 ppm but none of them contained the FMN group. Regarding the C-terminal end of the protein, 32 y-ions were assigned with an average mass tolerance of 1.1 ppm, among them the first 21 y-ions do not have the FMN adduct. The last unmodified y-ions is y₃₉, whereas the first FMN y-ion is y₄₃. This result demonstrate that the FMN adduct is most probably located in the string of the 4 residues GST₁₂₉V in the protein.

In order to confirm the FMN localization on the Thr₁₂₉ of the protein, the in-house ms-cheminfo.org algorithm was used to assign internal fragments and detect FMN-internal fragments in the region of the threonine. None of the commercial software allows assignment of MS/MS internal fragments in an intact protein.

(A) Graphical fragment map showing results for the FMN-binding domain of PceC-FBD

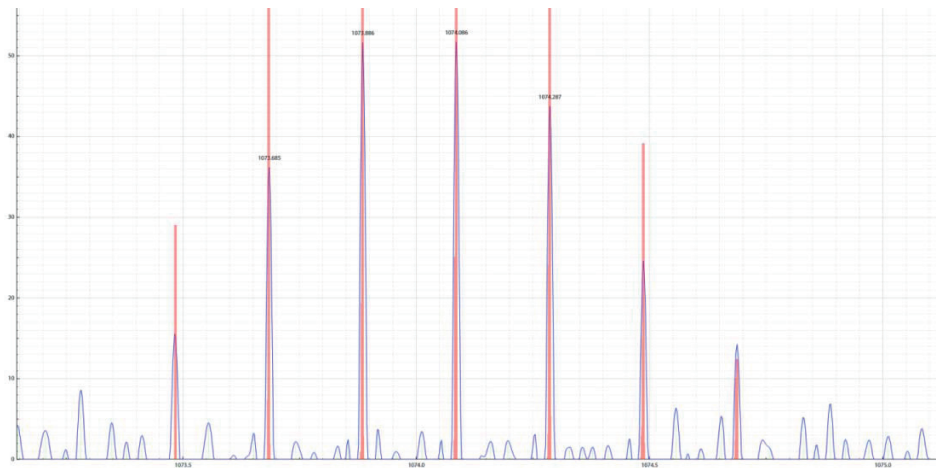


The graphics only displays internal fragment ions bearing the FMN (C₁₇H₁₉N₄O₉P) group, and identified with a similarity score >85%.

A total of 33 FMN-internal fragment ions could be assigned with a similarity score > 85%. Figure A shows the graphical fragment map restricted to internal fragment ions bearing the FMN (C₁₇H₁₉N₄O₉P) group and identified with a similarity score > 85%. The majority of FMN-internal fragments found is located in the same region (region II) and include Thr₁₂₉. The other region (I) located in the N-terminal part of the protein has only 3 fragment ions found with good similarity scores. Because a threonine is not present in the sequence involved and because no FMN-b ions could be detected in the N-terminal part of the protein, the binding site region of FMN is certainly in region II. The smallest FMN-internal fragment ions found are b₁₃₇y₄₄ and b₁₃₄y₄₄, with high

similarity scores between experimental data and theoretical, respectively 96% and 5%. The first modified y-ion identified was the FMN-y44 fragment, assigned with a similarity score of 96% (**Figure B**).

(B) MS/MS spectra of the FMN-binding domain of PceC, focused on the fragment ion y44-FMN at m/z 1073.48 (z=5)



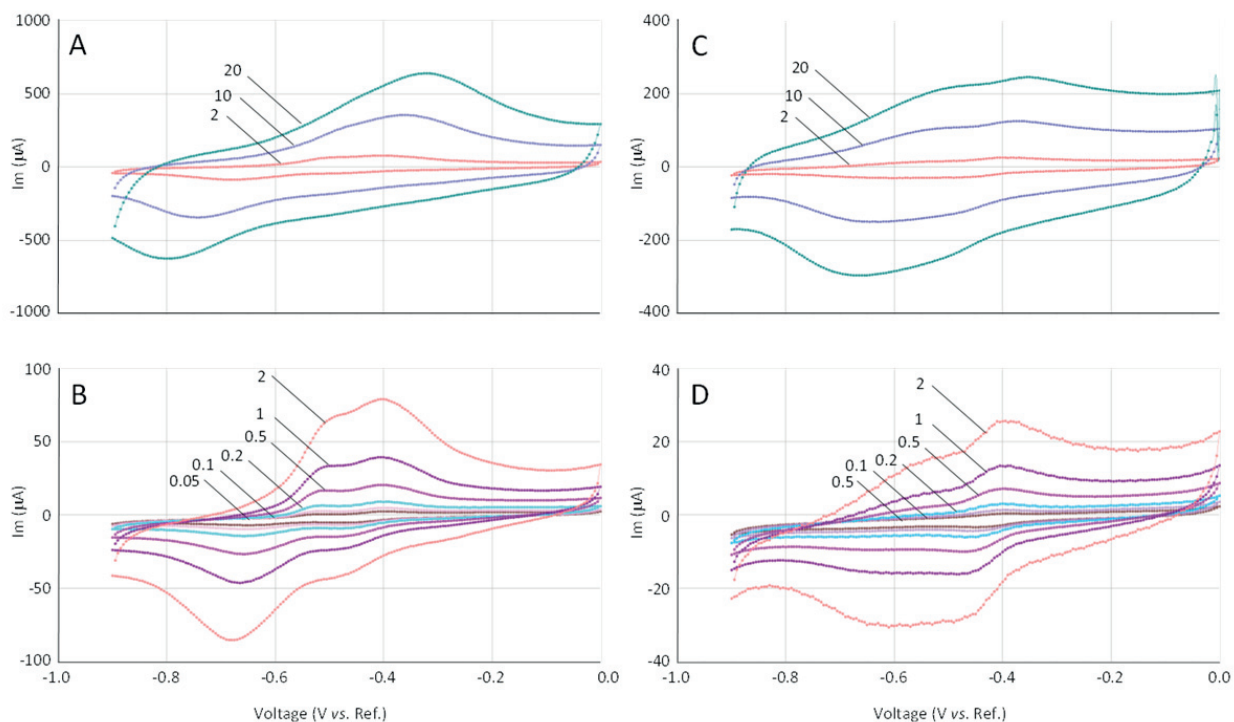
The isotopic pattern of the theoretical fragment ion FMN-y44 (red) matches the experimental spectra (blue) with a similarity score of 96%. Fragment ion y44 represent the first C-terminal fragment of PceC-FBD with FMN.

Appendix 4.11. Preliminary cyclic voltammetry analysis of PceC-FBD

Electrochemical procedures

Cyclic voltammetry (CV) experiments were conducted in collaboration with M. Schreier (LPI, EPFL) with a computer-controlled Eco Chemie Autolab PGSTAT 100 instrument with an ADC fast scan generator. All voltammetric experiments were conducted under a helium atmosphere to avoid complications of reduced flavins reacting with dissolved molecular oxygen. The working electrode was a 1-mm-diameter silver disk that was polished frequently with 1 μm and 0.5 μm alumina powder and used in conjunction with a Pt-wire counter electrode and a Ag/AgCl reference electrode. A buffer solution was prepared with 50 mM Tris-HCl and 150 mM NaCl at pH 7.2 in deionized water. FMN was then added to this buffered solution to form a 0.2 mM reference solution. All voltammetric experiments were conducted at RT.

Preliminary data



Cyclic voltammograms FMN and PceC-FBD.

Free FMN (A, B) and reconstituted PceC-FBD (C, D) were analyzed by cyclic voltammetry. Cyclic voltammograms were recorded at variable scan rate (0.1-20 V/s, as indicated) with silver, Ag/AgCl, Pt as working, reference, and counter electrodes, respectively. The potential is defined versus Ag/AgCl.

Additional references

1. **Chopra, T., R. Hamelin, F. Armand, D. Chiappe, M. Moniatte, and J. D. McKinney.** 2014. Quantitative mass spectrometry reveals plasticity of metabolic networks in *Mycobacterium smegmatis*. *Molecular & cellular proteomics* :**13**:3014-3028.
2. **Wisniewski, J. R., A. Zougman, N. Nagaraj, and M. Mann.** 2009. Universal sample preparation method for proteome analysis. *Nat Methods* **6**:359-362.

Private address:

Rte des Channes 19
CH-1076 Ferlens
E-mail: geraldine.buttet@epfl.ch

Professional address:

Laboratory for Environmental Biotechnology (LBE)
ENAC IIE LBE
Ecole Polytechnique Fédérale de Lausanne (EPFL)
Building CH – Station 6
CH-1015 Lausanne
Tel : +41 21 693 47 30

Professional Experience

-
- Sept 2012 – March 2017 **Research Assistant**, Laboratory for Environmental Biotechnology, EPFL, Lausanne, Switzerland
- Biochemical characterization of the organohalide respiration process in chloroethene-dechlorinating bacteria
- Sept 2011 – June 2012 **Master research**, Laboratory for Environmental Biotechnology, EPFL, Lausanne, Switzerland
- Functional diversity of reductive dehalogenases in a bacterial consortium degrading chloroethenes
- Dec 2009 – Jul 2010 **Scientist Assistant**, Laboratory of Chemical Ecology, UNINE, Neuchâtel, Switzerland
- Breeding of *Diabrotica virgifera virgifera* larvae
- June 2007 - August 2007 **Eco-volunteer**, Ekko Brasil, Island of Santa Catharina, Brazil
- Technical participation in the study of the distribution of *Lontra longicaudis*
- 2003 – 2007 **Manager services**, Groupe Mutuel, Lausanne
- Sept – Oct. 2003 **Manager services**, SUPRA, Lausanne
- 2001 – 2002 **Manager services third pillar**, Winterthur-Life, Lausanne

Education

-
- 2017 **EPFL – Lausanne, Switzerland**
Ph.D. in environmental biotechnology
- 2012 **University of Lausanne and Neuchâtel – Lausanne and Neuchâtel, Switzerland**
Degree awarded: Master in Biogeosciences
- 2010 **University of Neuchâtel – Neuchâtel, Switzerland**
Degree awarded: B.S. in Biology
- 2006 **Gymnase of « La Cité », Lausanne**
Certificate of the complementary exams (Passerelle Dubs, night school)
- 2003 **Professional school of commerce, Lausanne**
Professional maturity commercial
- 2000 **Professional school of commerce, Lausanne**
CFC of commercial apprenticeship (learning to the prefecture of Oron)

Collaborations

-
- 2012-2014 **Alice Badin**, Hydrogeology and Geothermy Centre, University of Neuchâtel.
Multiple dual C-Cl isotope patterns associated with reductive dechlorination of tetrachloroethene.
- 2012-2016 **Cindy Kunze, Sebastian Keller, Tobias Goris and Torsten Schubert**, Institute for Microbiology, University of Jena, Germany.
Characterization of PceA_{TCE}

2016-2017 **Alexandra Murray**, Department of Environmental Engineering, Water Resources Engineering, DTU, Denmark
Modelization and data analysis.

Teaching and supervising expertise

Swiss Federal Institute of Technology (EPFL), Lausanne, Switzerland.

2012-2016 Assistant in microbiology lectures (Prof. C. Holliger)
2012-2016 Assistant in practical classes of microbiology
2012-2016 Supervisor of several lab technician apprentices
2016 Supervision of 5-months bachelor project student Mélissa Burion from HES-SO, Sion
Project title: Affinity of two *Sulfurospirillum* populations for tetrachloroethene

Conference talks

- 2016 **Buttet G.**, Holliger C., Maillard J., Competition of two *Sulfurospirillum* populations for tetrachloroethene. Swiss Society for Molecular Microbiology, Bern, Switzerland.
- 2015 **Buttet G.**, Hamelin R., Armand F., Holliger C., Maillard J., *Desulfitobacterium hafniense* TCE1 membrane proteomics. Bacterial Electron Transfer Processes and their Regulation, Vimeiro, Portugal.
- 2014 **Buttet G.**, Kunze C., Schubert T., Diekert G., Holliger C., Maillard J., Functional characterization of a new tetrachloroethene reductive dehalogenase of *Sulfurospirillum* spp. identified in mixed cultures. DehaloCon, Jena, Germany

Conference posters

- 2016 **Buttet G.**, Holliger C., Maillard J., **Competition of two *Sulfurospirillum* populations for tetrachloroethene.** Swiss Society for Molecular Microbiology, Bern, Switzerland.
- 2015 **Buttet G.**, Hamelin R., Holliger C., Maillard J., ***Desulfitobacterium hafniense* TCE1 membrane proteomics.** Swiss Society for Molecular Microbiology, Lugano, Switzerland.
- 2015 **Buttet G.**, Hamelin R., Armand F., Holliger C., Maillard J., ***Desulfitobacterium hafniense* TCE1 membrane proteomics.** Bacterial Electron Transfer Processes and their Regulation, Vimeiro, Portugal.
- 2014 **Buttet G.**, Kunze C., Keller S., Schubert T., Holliger C., Maillard J., **Functional diversity of reductive dehalogenases in a bacterial consortium degrading chloroethenes.** Swiss Society for Molecular Microbiology, Granges-Paccot, Switzerland.
- 2014 Badin A., **Buttet G.**, Maillard J., Holliger C. & Hunkeler D, **Anaerobic reductive dechlorination of tetrachloroethene: how can dual Carbon-Chlorine isotopic measurements help elucidating which mechanism underlies the reaction?** European Geosciences Union, Vienna, Austria
- 2014 **Buttet G.**, Kunze C., Schubert T., Diekert G., Holliger C., Maillard J., **Functional characterization of a new tetrachloroethene reductive dehalogenase of *Sulfurospirillum* spp. identified in mixed cultures,** DehaloCon, Jena, Germany
- 2013 Badin A., **Buttet G.**, Maillard J., Holliger C. & Hunkeler D, **Carbon and chlorine isotopic analysis in tetrachloroethene : application to fingerprinting and understanding of anaerobic dechlorination,** Geochemical Society, Sopot, Poland
- 2013 **Buttet G.**, Badin A., Holliger C., Maillard J., **Functional genotyping of *Sulfurospirillum* spp. mixed cultures allowed the identification of a new tetrachloroethene reductive dehalogenase.** Swiss Society for Molecular Microbiology, Interlaken, Switzerland

- 2013 **Buttet G.**, Holliger C., Maillard J., **Functional genotyping of *Sulfurospirillum* spp. in mixed cultures allowed the identification of a new tetrachloroethene reductive dehalogenase.** Swiss Microbial Ecology Meeting, Murten, Switzerland
- 2013 **Buttet G.**, Kunze C., Badin A., Holliger C., Maillard J., **Functional genotyping of *Sulfurospirillum* spp. in mixed cultures allowed the identification of a new tetrachloroethene reductive dehalogenase.** Federation of European Microbiological Societies, Leipzig, Germany
- 2012 **Buttet G.**, Holliger C., Maillard J., **Functional diversity of reductive dehalogenases in a bacterial consortium degrading chloroethenes.** Swiss Society for Molecular Microbiology, St-Gallen, Switzerland
- 2012 **Buttet G.**, Holliger C., Maillard J., **Functional diversity of reductive dehalogenases in a bacterial consortium degrading chloroethenes.** Swiss Molecular Microbiology Meeting, Villars-sur-Ollon, Switzerland

Publications

- 2013 **Buttet G.**, Holliger C., Maillard J., **Functional genotyping of *Sulfurospirillum* spp. in a mixed cultures allowed the identification of a new tetrachloroethene reductive dehalogenase.** Appl Environ Microbiol 2013, 79 (22), 6941-7.
- 2014 Badin A., **Buttet G.**, Maillard J., Holliger C., Hunkeler D., **Multiple dual C-Cl isotope patterns associated with reductive dechlorination of tetrachloroethene.** Environ Sci Technol. 2014, 48 (16), 9179-86.

References

Dr. Christof Holliger, Full Professor

Ecole Polytechnique Fédérale de Lausanne (EPFL), ENAC IIE LBE
Station 6
CH-1015 Lausanne, Switzerland
+41 21 693 4722
christof.holliger@epfl.ch

Dr. Julien Maillard, Research Associate

Ecole Polytechnique Fédérale de Lausanne (EPFL), ENAC IIE LBE
Station 6
CH-1015 Lausanne, Switzerland
+41 21 693 4730
julien.maillard@epfl.ch